UNIVERSITÀ
DEGLI STUDI
DI PADOVA

Administrative unit: University of Padova

Department: **Land, Environment, Agriculture and Forestry (TESAF)**

PhD Program: **Land, Environment, Resources and Health (LERH)**

Batch: XXXVI

Towards a Greener Wood Industry: Exploring Natural Tannin–Based Resins for Sustainable Engineered Wood Products

PhD Program Coordinator: Prof. Marco Borga

Supervisor: Prof.ssa Michela Zanetti

Co–Supervisor: Prof. Gianluca Tondi

PhD candidate: Emanuele Cesprini

UNIVERSITÀ
DEGLI STUDI
DI PADOVA

Sede Amministrativa: Università degli Studi di Padova

Dipartimento Territorio e Sistemi Agro–Forestali (TESAF)

CORSO DI DOTTORATO DI RICERCA: **Land, Environment, Resources, Health (LERH)**

Ciclo: XXXVI

Verso un'industria del legno più verde: Esplorazione delle resine naturali a base di tannino per prodotti in legno ingegnerizzati sostenibili

PhD Program Coordinator: Prof. Marco Borga

Supervisor: Prof.ssa Michela Zanetti

Co–Supervisor: Prof. Gianluca Tondi

PhD candidate: Emanuele Cesprini

Table of contents

List of abbreviations

ATR	Attenuated total reflectance	LCI	Life cycle inventory
CFF	Chicken feather fiber	LCIA	Life cycle impacts analysis
CLT	Cross laminated timber	LDF	Low density fibreboard
CO	Carbon monoxide	LDH	Layered double hydroxide
CO_2	Carbon dioxide	LPF	Lignin phenol formaldehyde
Da	Dalton	LR	Leaching resistance
DAD	Diode array detector	LS	Lignosulfonate
DoC	Degree of compression	LULUCF	Land use, land use change and forest
ER	Ethanol residue	LVL	Laminated veneer lumber
EU	European union	PF	Phenol formaldehyde
EWP	Engineered wood products	PFA	Polyfurfuryl alcohol
FA	Furfuryl alcohol	MC	Moisture content
FTIR	Fourier-transform infrared spectroscopy	MDF	Medium density fibreboard
GHG	Greenhouse gas	MF	Melamine formaldehyde
GWP	Global warming potental	MOE	Modulus of elasticity
HBS	Brinell Surface Hardness	MUF	Melamine urea formaldehyde
HDF	High density fibreboard	NMR	Nuclear magnetic resonance
HDME	Hexanediamine	OSB	Orientated Strand Board
HEFA	N,N-bis(2-hydroxyethyl) fatty amide	PEGDE	(Poly)-ethylene glycol diglycidyl ether
HPLC	High Performance Liquid Chromatography	PF	Phenol formaldehyde
HRSEC	High-resolution size-exclusion chromatography	PFA	Polyfurfuryl alcohol
HWP	Harvested wood products	pMDI	Poly methylene diphenyl diisocyanate
IB	Internal bond	PP	Polypropylene
IPCC	Intergovernmental Panel on Climate Change	PS	Polysaccharide content
ISSO	International Organisation for Standardization	PSA	Pressure sensitive adhesive
LCA	Life cycle assessment	PUR	Polyurethane

List of abbreviations

RID	Refractive index detector	TFS	Tannin furfuryl alcohol formulation
RQ	Research question		
RS	Regenerated silk	TGA	Thermogravimetric analysis
SC	Solid content	TMA	Thermomechanical analysis
SD	Standard deviation	TPC	Total phenolic content
SM	Soy meal	TRIS	Tris(hydroxymethyl)nitromethane
SPI	Soy protein isolates	TSS	Tensile shear strength
TA	Tannin acid	UF	Urea formaldehyde
TCD	Thermal conductivity detector	UV	Ultraviolet light
LVL	Laminated veneer lumber	5-HMF	5-hydroxy-methylfurfural
TCT	Total condensed tannins		

List of Tables, Figures and Equations

1. Introduction

Tables:

Figures:

3. Material and methods

Tables:

4. Results

4.1 Synthesis and characterization of tannin–based polymers.

(1) Development of Quebracho (Schinopsis balansae) Tannin–Based Thermoset Resins

Tables:

Figures:

Equations:

4.2 Application of biobased tannin polymers to produce wood–based materials.

(1) Quebracho–Based Wood Preservatives: Effect of Concentration and Hardener on Timber Properties

Tables:

Figures:

8. Leaching resistance of timber–impregnated samples in function of the concentration of hexamine. The symbol “ * ” indicates the outliers of the tests performed.

Equations:

1. Wet retention

2. Dry retention

3. Leaching resistance

(2) Renewable Tannin–Based Adhesive from Quebracho Extract and Furfural for Particleboards

Tables:

1. Total phenolic content, total condensed tannins, antioxidant capacity, and polysaccharide fraction of quebracho Fintan 737 industrial tannin extract.

2. Density and thickness values of particleboards glued with 15% tannin in function of the pressing parameters.

3. Physical and mechanical outcomes from the optimization of process parameters at 160 °C.

Figures:

1. (a) Cold pre–pressed wood particles mat glued with 15% of quebracho–furfural adhesives (b) Particleboards with 32 × 32 × 1 cm size pressed at different glue amounts (c) Panel cutting section for samples manufacturing used for physical and mechanical analysis.

2. Viscosity of 45% tannin−water solutions at pH = 8 with (black) and without (red) furfural hardener.

3. Density box char plot in function of pressing time and temperature. The whiskers represent scores outside the middle 50%, the median is represented by the line inside the box, while lower and upper quartiles are, respectively, the inferior and the bottom end of the box. Possible outsiders are indicated by asterisks.

4. Density profile for particleboards manufactured at different pressing times (7, 9, 11 min) and temperatures (160, 180, 200 °C).

5. Influence of pressing parameter on (a) Internal Bond, (b) Modulus of elasticity, (c) Modulus of rupture. The whiskers represent scores outside the middle 50%, the median is represented by the line inside the box, while lower and upper quartiles are, respectively, the inferior and the bottom end of the box. Possible outsiders are indicated by asterisks.

6. Thickness swelling after 24 h of the produced particleboards in function of the pressing parameters.

7. Scanning electron microscopy images of particleboard glued with 15% of adhesive formulation. Different magnifications of the same representative area are proposed: (A) 1000× (B) 2000×. Red arrows identify the wooden matrix; green arrows identify the tannin–furfural adhesive.

(3) Quebracho Tannin Bio–Based Adhesives for Plywood

Tables:

1. Number of test specimen for the physical and mechanical properties testing of Quebracho tannin–furfural bonded five layered beech plywood.

2. Results of statistical significance for one–way ANOVA.

Figures:

1. Viscosity of a 65% tannin furfural formulation.

2. ATR–FTIR of Quebracho tannin furfural formulations at room temperature (black) and cured at 100 °C (red).

3. Possible product from Quebracho tannin and furfural reaction.

4. (a) Density grouped by time and temperature. Dots and stars within the box plot indicate outliers and (b) density profile for the 5–layers plywood glued for 15 min with Quebracho tannin– furfural adhesives at different temperature.

5. (a) Mean thickness and (b) mean degree of compression (DoC) of five layered Quebracho tannin furfural bonded plywood. The brackets within the figure indicate the interval ± 1 standard deviation (SD).

6. Influence of press time and press temperature of five layered Quebracho Tannin furfural bonded beech plywood on (a) Modulus of elasticity (MOE) and (b) Modulus of rupture (MOR). The top of the column indicates the means and the bars within the figure represent the standard deviation (SD).

7. Stress–deformation behaviour of selected samples for 15 min press time and three different temperatures.

8. Dry state tensile shear strength for the 5–layered Quebracho tannin bonded plywood. The brackets within the columns of the figure indicate the standard deviation.

(4) Bio–Based Tannin–Furanic–Silk Adhesives: Applications in Plywood and Chemical Cross–linking Mechanisms

Table:

Table 1. Relative content of each component within the final formulations.

Figures:

1. A: Dry and 24h wet shear strength of reference panels (TSF–0) and TFS samples synthesized at different wt% of RS. B: Modulus of elasticity (MOE) and modulus of rupture (MOR) of reference panels (TFS–0) and TFS samples synthesized at different wt% of RS. C: Scanning electron microscopy images of TFS–0, TSF–20 and of TFS–0', TSF–20' samples, at different magnifications (e. g. x100 and x 1000, respectively).

2. Non–isothermal and isothermal (see the inset) mechanical analysis of TSF–0 and TFS samples synthesized at different wt% of RS.

3. 13C–NMR spectra of: furfuryl alcohol (PFA, black curve), regenerated silk (RS, red curve), polyfurfuryl alcohol– regenerated silk (PFA–RS, brown), quebracho tannin (T, green curve) and quebracho polyfurfuryl alcohol–regenerated silk–quebracho tannin (PFA–RS–T, blue curve).

4. ATR–FT–IR spectra of: furfuryl alcohol (PFA, black curve), regenerated silk (RS, red curve), polyfurfuryl alcohol–regenerated silk (PFA–RS, brown), quebracho tannin (T, green curve) and quebracho polyfurfuryl alcohol–regenerated silk–quebracho tannin (PFA–RS–T, blue curve).

5. Average FTIR spectra of surface samples of polyfurfuryl alcohol–quebracho tannin (PFA–T, red curve) and polyfurfuryl alcohol–regenerated silk–quebracho tannin (PFA–RS–T, light blue curve).

Schemes:

1. A: Principal mechanism of reaction of furfuryl alcohol polymerization. B: Diels Alder reaction mechanism involved in the polymerization of furfuryl alcohol.

2. A: possible carbocation formation in a primary alcohol of the silk protein structure and interaction with nucleophilic centres. B: schematic representation and possible interaction of a tannin–alcohol furfuryl co–polymer and silk.

4.3 Life cycle assessment of protein counterpart involved in the tannin–based adhesive formulation.

(1) Assessing the Environmental Impact of Silk Protein Production for Bio–Based Materials: A Life Cycle Assessment Study

Tables:

1. Cultivation practices of one hectare of mulberry orchard.

2. Consumption related to the worm growth process for the production of one dry kg of silk cocoons.

3. Inventory analysis of the main substances contributing to the impacts for the production of 1 kg of silk cocoons for the main processes involved. The rows in the table in reference to "remaining substances" refer to the application of a 5% Cut–off.

4. LCA results for the Base Case and Alternative Scenarios. Scenario 1 includes chipping of wood waste and sale of wood chips in the Italian market; Scenario 2 includes using wood chips to dry the cocoons and sale of the leftover wood chips.

Figures:

1. Overview of silk environmental friendly silk supply chain and the alternative uses of silk proteins.

2. Detailed schematic representation of the silk cocoon rearing divided into the two main subprocess: background (Mulberry orchard) and foreground (Silk cocoon rearing). The numerical values of the inputs are related to 1 kg of dry silk cocoons production.

4.4 Chemical investigation of polyphenolic wood extractive.

(1) Chemical characterization of cherry (Prunus avium) extract in comparison with commercial mimosa and chestnut tannins

Tables:

Figures:

Supplementary information

Annex 1

Annex 2

Summary

Nowadays, the transition toward renewable resources is crucial for addressing environmental challenges. Wood material, known for its versatility and sustainability, offers a durable and recyclable alternative to finite fossil resources. The wood industry is a significant adhesive consumer, and can drive eco–friendly policies by adopting environmentally conscious solutions. In this context the objective of the current study is to investigate a range of natural resins tailored for the production of engineered wood products, offering sustainable alternatives to conventional synthetic resins. The research has begun with a preliminary study of different tannin–based resins, proposing different hardeners and studying the physical and chemical characteristics of the resins, and thus the most promising formulations suitable for our study's objectives have been identified. Hence, the most interesting formulations have been applied in the production of engineered wood products. Specifically, a tannin–hexamine resin has been used to impregnate various wood species, showing that low percentages of the hardener (<5%) are sufficient to increase the mechanical properties of the wood. Instead, furans–tannin resins have been utilized for the production of plywood and particleboards. Although acceptable results have been shown for applications in dry environments, limitations for wet purposes have been reported. In this direction, a protein counterpart, silk fibroin, within a promising tannin–based formulation has been proposed to improve moisture tolerance. The results have shown how low amounts of silk fibroin lead to a substantial increase in mechanical properties, also in a humid environment. Finally, in a general perspective of sustainable development and in cooperation with the producers of the silk cocoons, an environmental impact analysis carried out with the Life Cycle Assessment methodology, has been developed. This environmental impact study aimed to revitalize the Italian industry of silk production, while also providing a comparative analysis with similar studies performed in different international contexts. Those researches consistently highlight silk as having the highest environmental impact among fibre–based materials. However, sustainable and non–intensive agricultural practices involved within the Italian supply chain have demonstrated a reduced environmental impact compared to intensive methods. However, specific hotspots in the supply chain have been identified and reported in order to enhance the overall sustainability in the process. In conclusion, this research provides a comprehensive exploration of tannin-based resins, utilizing a commercial extract as a polyphenolic matrix.

Riassunto

Nell'attuale contesto, la transizione verso risorse rinnovabili è essenziale per affrontare le sfide ambientali. Il legno, noto per la sua versatilità e sostenibilità, emerge come un'alternativa promettente alle risorse fossili. Tuttavia, anche il settore del legno richiede politiche più sostenibili, soprattutto riguardo agli adesivi utilizzati per l'incollaggio dei principali prodotti legnosi. In questo contesto, l'obiettivo del presente studio è quello di analizzare una gamma di adesivi naturali, adatti alla produzione di prodotti legnosi ingegnerizzati, che offrano alternative sostenibili agli adesivi sintetici convenzionali. La ricerca ha preso avvio con uno studio preliminare focalizzato su diverse formulazioni adesive a base di tannino, le quali includevano diversi indurenti. Durante questa fase, sono state esaminate approfonditamente le caratteristiche fisiche e chimiche degli adesivi al fine di identificare le formulazioni più promettenti. Le composizioni più intriganti sono state successivamente impiegate nella produzione di prodotti in legno ingegnerizzato. In particolare, una formulazione adesiva a base di tannino–esammina è stata utilizzata per impregnare diverse specie legnose, dimostrando che anche basse percentuali di indurente (esammina<5%) sono sufficienti ad aumentare le proprietà meccaniche del legno. Successivamente, delle formulazioni adesive furano–tanniche sono state utilizzate per la produzione di compensati e pannelli truciolari. Sebbene siano stati ottenuti risultati accettabili per applicazioni in ambiente secco, le formulazioni adesivi non sono adatte per applicazioni in ambiente umido. Al fine di ovviare a questo problema e aumentare la tolleranza all’acqua delle formulazioni, è stato studiato un additivo proteico, la fibroina di seta, inserita in una promettente formulazione a base di tannino e alcool furfurilico. I risultati hanno mostrato come piccole quantità di fibroina portino a un sostanziale aumento delle proprietà meccaniche anche in ambiente umido. Infine, in una prospettiva generale di sviluppo sostenibile, in collaborazione con i produttori di proteine della seta, è stata sviluppata un'analisi dell'impatto ambientale, utilizzando la metodologia Life Cycle Assesment. Questo studio mira a rilanciare l'industria italiana della produzione di seta, fornendo al contempo un'analisi comparativa con studi simili condotti in diversi contesti internazionali. Questi studi evidenziano come la seta abbia il più alto impatto ambientale tra le diverse fibre tessili, sintetiche e naturali. Le pratiche agricole italiane, sostenibili e non intensive, hanno però dimostrato un impatto ambientale ridotto rispetto ai metodi intensivi di riferimento, evidenziando quindi un vantaggio ambientale per la filiera studiata. Grazie allo studio di impatto ambientale, è stato possibile identificare i punti critici della filiera di produzione, al fine di migliorare la sostenibilità complessiva del processo. Concludendo, questo lavoro di ricerca offre una visione approfondita degli adesivi a base di tannino, utilizzando un estratto commerciale come matrice polifenolica.

1. Introduction

1.1 Forests as a Climate Change Mitigation Solution

The Paris agreement highlights the urgent need to intensify efforts to mitigate climate change and transition toward a carbon–neutral society. Globally, the goal of the Paris Agreement is to limit the increase in average temperature to below 2°C, with a target of achieving an even stricter target of 1.5 °C [1], also reiterated during the COP28 conference held in Dubai at the end of 2023. The Intergovernmental Panel on Climate Change (IPCC) has widely recognised the vital role of global forests in the carbon cycle and the mitigation of climate change, particularly through afforestation and reforestation programmes [2],[4], within the land use, land use change, and forest (LULUCF). Forests are undeniably crucial in the long–term objective of achieving a balance between CO_2 emissions from human activities and the natural removal of the gas by the second half of this century. In alignment with this objective, the Paris Agreement calls on the participating parties to actively protect and improve the capacity of natural reservoirs and sinks for greenhouse gases [1]. Forests play a critical role in sequestering carbon by capturing carbon dioxide from the atmosphere and storing it within their biomass through the photosynthesis process. Depending on their unique characteristics and utilisation, they can assume various roles within the carbon cycle. Indeed, they may function as net carbon sinks, absorbing more carbon than they emit, or, conversely, as net carbon emitters, releasing more carbon than they sequester, depending on how forests are managed and harvested. Currently, approximately one third of anthropogenic CO_2 emissions are removed by terrestrial ecosystems, mainly forests [5]. However, since many countries are not making sufficient progress in controlling carbon emissions [6], there is a growing emphasis on monitoring and managing carbon emissions and removals related to LULUCF [7]. Furthermore, the increasing demand for timber and biomass, especially for bioenergy purposes [8], together with the ageing structure of forests, could pose a significant risk to the carbon sink in the European Union (EU). The ability of forests to absorb and sequester carbon is under threat, and there is growing concern over its diminishing capacity. As mentioned above, forests must play a dual role in addressing climate change: (i) they contribute to the mitigation of climate change by capturing carbon from the atmosphere, and (ii) storing it in trees and soil [9],[10]. Simultaneously, the use of harvested wood products (HWP) instead of more carbon–intensive materials could lead to substitution benefits in various economic sectors [11]. Indeed, timber harvesting can be seen as a transition of carbon from the carbon pool to the harvested wood products [11]. Whether there is a short–term trade–off between increasing wood harvesting and maintaining a larger net carbon sink, it depends on regional contexts, such as local climate conditions [12],[13], forest plantation management strategies[14],[15], tree species [16],[17], and wood product types and their life cycle activities (eg manufacturing processes, use phase, substitution benefits, and end of life) [18],[19]. In this direction, various scenarios have highlighted the effectiveness of wood products in mitigating climate change by increasing the time that CO_2 is kept out of the atmosphere [20],[21]. For example, models of young forests in California, which are subjected to a high fire risk, have forecasted several benefits of increasing biofuel and mass timber production (CLT, Glulam) [15]. Furthermore, Zhang et al. [22] highlighted the importance of strategically considering sustainable wood products as a valid nature–based solution to meet global wood products demand, which is growing rapidly [23], and mitigate climate change by replacing carbon–intensive construction materials such as concrete and steel [24],[25]. In contrast, if all harvested timber is directly utilized as wood fuel, carbon dioxide emissions from wood consumption will overcome the emissions from the chosen non–renewable energy sources [21]. Although forest management policies and organisation depend heavily on various factors, as described above, the importance of HPWs is crucial in order to keep carbon stored as timber or wood–based product. Therefore, the next introductory chapter provides an analysis of the main engineered wood products (EWPs), their evolution, and the main challenges to consider for their sustainable development.

1.2 Engineered wood products

The term engineered wood products (EWPs) includes different composites manufactured by binding different timber fractions (e.g. lamellas, veneer, strands, flakes, particle, fibers) with adhesives to obtain homogeneous single elements of desired dimensions. These products become substitutes for solid wood in the furniture and construction industries [26], due to several advantages, such as the use of smaller fractions, the use of waste wood from other processing, the reduction of defects, the increase in homogeneity, the increases in tailored properties, and the possibility of making products of different shapes and dimensions [27]. These feature make the EWPs increasingly present for a wide range of applications [27]. The EWPs can be categorized based on their intended use, whether they are meant for structural or non–structural purposes, their suitability for exterior or interior applications, and the materials involved, which can range from fibreboards to laminated beams. The main EWPs products are, therefore, described below.

Laminated beam (glulam): a multilayer flat–pressed timber beam with thick wooden boards that form the layers is used for external structural applications and glued with cold–setting polyurethane (PUR) or melamine urea formaldehyde (MUF), or even with phenol–resorcinol–formaldehyde (PUR) resins. Individual wooden boards are glued to the required length to form the beam with finger joints glued with one of the same three adhesives as above. The density range ranges from 420 to 750 $\mathrm{kg \cdot m^{-3}}$.

Cross laminated timber panel (CLT): it is made up of thick multilayer wooden boards arranged in alternating sheets, creating a cross–sectional pattern for enhanced strength and stability. The unique orthogonal laminar structure of this material enables its versatile application as a full–scale wall and floor component, while also serving as a linear timber member capable of bearing loads both in–plane and out–of–plane. It is important to note that certain parameters, including bonding pressure, amount and the type of applied adhesive, moisture content of adherends, and other factors, have been informed by insights gained from working with glulam. The density falls in the range of 380–420 $\mathrm{kg \cdot m^{-3}}$. Similar structural adhesives used for glulam are applied, even if more urea formaldehyde (UF) is used due to the more common indoor use.

Laminated Veneer Lumber (LVL): in this composite veneer slices of softwood, typically spruce of 3.2 mm thickness, are accurately selected and dried. Seven to twenty–five layers of veneers are then glued together with the grain parallel to each other with hot press processing by applying waterproof adhesives, usually phenolic resins. These products may reach total thickness of 75 mm and they are usually involved for outdoor purposes as roof beams or other structural applications.

Plywood: A flat hot–pressed wood panel composed of orientated wood veneers bonded by hot pressing using thermosetting adhesives. In contrast to LVL, for the plywood the wood grains of the veneer are 90° from each other in the adjacent layers, resulting in a solid panel. Depending on the final use, the density can range from 460 to 680 $\mathrm{kg \cdot m^{-3}}$.

Orientated Strand Board (OSB): A flat hot–pressed three–layer wood composite panel composed of orientated wood wafers bonded by hot pressing using thermosetting adhesives. The thin wafers have the same direction within the same layer and 90° with respect to the adjacent layer, leading to a panel suitable for structural applications. The lower surface area of wafers compared to other panel types like particleboards, yields less adhesive to bond (4–5 %).

Introduction

Particleboard: Flat hot–pressed wood composite panel composed of randomly orientated wood chips bonded by hot pressing using thermosetting adhesives. The density is generally 650–700 kg m^{-3} and resin solid content is between 6% and 12% on dry wood.

Low, Medium, and High–Density Fibreboard (LDF, MDF, HDF): a flat, hot–pressed composite panel composed of wood fibres obtained by thermomechanical pulping and mainly bonded with traditional urea–formaldehyde adhesive thermosetting adhesive. These three types of fibreboards differ primarily in their density levels, affecting their weight, strength, and intended applications. LDF is lighter with a density range between 320–480 kg · m^{-3}, and suitable for more niche applications; MDF provides a good balance of density (750–800 kg · m^{-3}) for versatile applications, and HDF is the densest, offering strength for demanding applications, with a density value between 800–1450 kg m^{-3}.

Hardboard: A flat pressed wood composite panel composed of randomly orientated wood fibres obtained by thermomechanical pulping of wood and traditionally bonded without any adhesive only by hot pressing that induced the flow of the lignin component of the fibres due to the very high density (900–1100 kg · m^{-3}). Nowadays, the panels could contain a small amount of the main synthetic adhesive (2–3%) to improve the properties.

The discussion of wood composites inevitably leads to the consideration of polymeric binders that play a pivotal role in binding the different wood fractions. The evolution of wood composites closely mirrors the progress in adhesive manufacturing. With the ongoing advancements and refinements of chemical binders employed as adhesives, wood composites are steadily enhancing their properties, positioning bonded wood as a crucial material that in some important case is structural (e.g. Glulam, CLT, and LVL). Creating a high–quality wood composite involves merging two essential technologies: Appropriate selection of the wooden matrix and application of a performing adhesive as reinforcement to guarantee the required properties of the composite. Expertise in formulation, engineering, and process means development in composite manufacturing, and hence, producing more bio–based products with higher performance, facilitating the end–of–life strategies for waste recovery and disposal.

1.3 Overview of the different types of adhesives present in the market

The term "adhesive" encompasses a broad range of materials, each of which serves the common function of bonding separate substrates. Despite this shared purpose, adhesives operate through various mechanisms with different specifications. In an adhesive joint, a polymeric substance is connected to the substrate through chemical bonds, physicochemical attractions, and mechanical interlocking. The application method of this polymer is crucial because of its chemical composition, as it determines the conditions and industrial uses. It also influences factors such as the spread of the adhesive and the contact area, significantly affecting the strength of the adhesive. The various mechanisms of adhesive hardening are summarised in Table 1.

Table 1. Overview of the principal mechanisms of adhesive hardening [28].

Type	**Mechanism of hardening**	**Example of compounds**
Solution / dispersion	Evaporation of solvent	Polyvinil acetates, polyurethanes, acrylates, rubber
Hot melt	Cooling	Polyamides, saturated polyester
1–Component	External impulse (i.e. temperature, UV–light, moisture)	Polyurethanes, silanes, cyanoacrylates, phenol formaldehyde, urea formaldehyde, melamine formaldehyde),acrylates
2–Component	Mixing of component	Epoxides, polyurethanes, methacrylates
Pressure sensitive adhesives	Retain tackiness	Acrylates, rubber

The use of adhesives that require the evaporation of the solvent to produce the bonded joint is becoming less and less common because of the possible problems of dispersion of the latter into the environment. However, the use of water as a carrier is a viable alternative [29]. On the other hand, the class of hot melt resins has the advantage of a short bonding time. These resins are poured over the joint and cross–linked by cooling [29]. Hot–melt adhesives typically consist of thermoplastic polymers, including polyamides, saturated polyesters, and ethylene–vinyl acetate copolymers, but they do not find wide application in wood products. Finally, there are the adhesives (prepolymers) that are applied before the final polymer structure is achieved. Bonding is achieved through a cross–linking reaction of the components. As shown in Table 1, the reaction can occur in a single–component mixture or in a 2–component resin, where the substances are mixed just before application. The initiation of the cross–linking reaction leading to the formation of the adhesive joint is typically induced by an external stimulus. For example, condensation resins of phenol–formaldehyde, urea–formaldehyde, or melamine–formaldehyde adhesives initiate the cross–linking process under elevated temperatures. On the other hand, one–component polyurethane resins need moisture as an agent to start polymerization. In the case of acrylates, their curing process is facilitated by exposure to ultraviolet (UV) light. This UV light activates a photo initiator compound, initiating a radical polymerisation reaction in the acrylate adhesive.

Epoxides and polyurethanes are two of the most important examples of two–component adhesives, whose polymerisation occurs through addition reaction. However, it is important to emphasise that the classes of adhesives described before cannot be always separated entirely. Still, the different properties of individual components are often exploited to create hybrid classes and achieve superior cohesion and durability. For example, pressure–sensitive adhesives (PSA) are often based on acrylates, rubbers, and UV–curing polymers and are used in adhesive tapes and labels [30]. Although the types of reactions and classes of adhesives are several, condensation thermosetting resins dominate the wood products market, and therefore the principal compounds are described below.

1.3.1 Principal synthetic adhesives for wood products

Synthetic adhesives continue to dominate the wood composite market. Below, the most current wood adhesives are briefly listed.

Urea–formaldehyde (UF)

Urea–formaldehyde (UF) adhesives are market leaders in wood composites used for furniture and a wide variety of other applications. An approximate 11 million tons per year of these wood adhesives are used worldwide [31]. They are obtained by the condensation reaction between urea and formaldehyde. The structure of the resin is reported in Figure 1. In 2006, the International Agency for Research on Cancer (IARC) revised the classification of formaldehyde, upgrading it from a "probable human carcinogen" (Group 2A) to a "carcinogenic to humans" (Group 1). This reclassification was intended to encourage producers to minimise formaldehyde emissions to mitigate potential health risks [32].

Due to stringent regulations on formaldehyde emissions, production technology has advanced a great deal in recent decades, for example, decreasing the formaldehyde/other component ratio [33]. UF adhesives were typically produced with an initial mole ratio of formaldehyde (F) to urea (U) of 2.0 to 4.0 [32]. Given that urea has four reactive sites, it theoretically allows for the use of higher initial F/U mole ratios, extending up to 4.0. Nowadays, to decrease the formaldehyde emissions, the F/U ratio has to be set between 1 and 1.3 [32]. However, a lower F/U molar ratio resulting in poor performance of UF resins. In this direction, other ways to limit formaldehyde emissions can be achieved by varying pressing parameters [34], such as time or temperature, by adding scavengers, such as tannins, lignin and wheat flour [31],[35] or finally post wood surface treatments [36]. However, despite disadvantages such as lack of outdoor weather resistance and presence of formaldehyde, they are still difficult to replace due to their relatively low cost, excellent adhesion performance, and ease of handling [29].

Melamine–Formaldehyde (MF) and Melamine–Urea–Formaldehyde (MUF)

Melamine–formaldehyde (MF) resins, categorized as amino plastic resins, stand out as rigid and robust thermosetting polymers. Their notable qualities include high moisture resistance, thermal stability, scratch resistance, abrasion resistance, boil resistance, flame retardancy, and a smooth and transparent surface. These features make MF resins widely applicable in diverse industrial uses. MF are expensive products, so they are marketed as melamine–urea–formaldehyde (MUF) resins. There are mainly two products: (i) mUF, UF resins with only 2–5% melamine, which are nothing more than improved UF resins for interior use, this also being a method to decrease the formaldehyde emission of an UF [33]; (ii) MUF adhesives for exterior and semi–exterior use containing 30% to 40% melamine [29]. The schematic representation is shown in Figure 1.

Phenol–Formaldehyde (PF)

Phenol–formaldehyde (PF) adhesives are, by volume, the second most important wood composite adhesive, with up to 3 million tons of per year being used around the world [31]. They are used mainly for OSB and marine plywood with high resistance to weathering, and therefore they are used outdoors. However, at the beginning they reported slower cure at higher temperatures than MUF adhesives. Nonetheless, considerable research into these resins, and PF resins are now commercially available, as they cure at the same rate as MUF resins [29]. The repetitive unit is reported in Figure 1.

Phenol–resorcinol–formaldehyde (PRF)

This class of adhesives differs from the previous ones in that they belong to the class of cold–curing adhesives. Resorcinol is an expensive reagent, and therefore production is limited to about 30 thousand tons per year. However, they are used for laminated wood, finger joints and similar products at room temperature. In addition, they are binders for all–round, weather–resistant composites [29]. However, this class of adhesives is no longer commonly used. In Figure 1 is reported the schematic representation of PRF resin.

Polymeric isocyanate (pMDI)

Concern about formaldehyde vapour emission levels from UF adhesives has brought isocyanate adhesives to the forefront, because no formaldehyde is added. For wood composites, the isocyanate used is 4,4–diphenylmethane polymer diisocyanate (pMDI). pMDI offers high performance in significantly lower proportions than UF, MUF, and PF for bonding wood composites [37]. It is, however, more expensive than the other three main formaldehyde–based adhesives, which somewhat offsets the advantage of being needed in lower proportions. In addition, it has recently been under pressure from stringent environmental regulations as a result of its vapour and relative toxicity. Thus, one use in which it has a particular advantage is mixing, in smaller proportions, with any of the three formaldehyde–based adhesives to improve their performance. The pMDI unit is shown in Figure 1.

One–Component Polyurethanes (PURs)

The PURs of one component are the main competitor of PRF adhesives for the same types of applications. The main advantage is their remarkable ease of handling. No mixing or addition of hardeners is required. On the other hand, their main disadvantage is in the structure itself, as they are prone to breakage of bonded joints subject to temperature–dependent creep and sliding. They are relatively expensive, but not less than their PRF competitors [31]. The representation of PUR resin is shown in Figure 1.

As mentioned above, one of the main issues related to the use of synthetic adhesives is the high use of formaldehyde, recognised as a probable carcinogen [38]. Its use has been limited with the decrease in the molar ratio of urea to formaldehyde and the adoption of safer application methods. mUF resin or MUF resin with a higher percentage of melamine is increasingly used in the wood industry to meet formaldehyde emission limits and strength requirements, especially for structural application in a wet environment [39]. However, melamine is limited due to its high price. Although pMDI adhesives boast a formaldehyde–free composition and exhibit desirable traits like swift hardening and excellent resistance to atmospheric elements, it is essential to note their origin from fossil resources. Furthermore, increased safety measures are imperative during production due to the toxicity associated with isocyanate [40]. In addition, isocyanate–based residues have a high nitrogen content that could compromise a possible energy recovery of production waste [41].

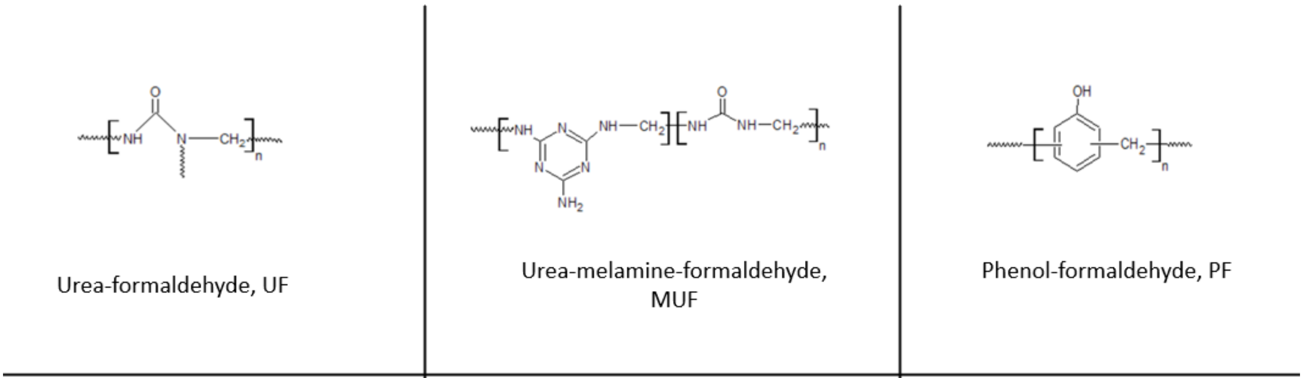

Urea-formaldehyde, UF

Urea-melamine-formaldehyde, MUF

Phenol-formaldehyde, PF

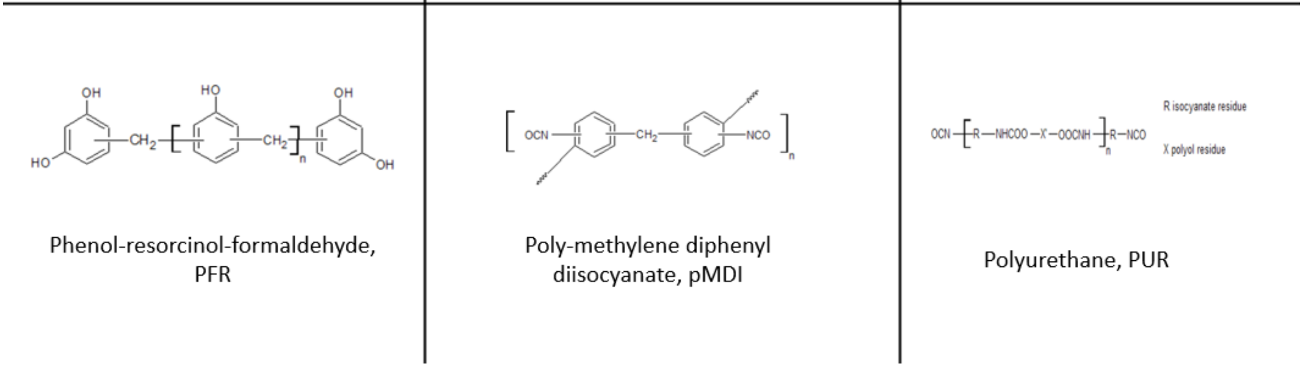

Phenol-resorcinol-formaldehyde, PFR

Poly-methylene diphenyl diisocyanate, pMDI

Polyurethane, PUR

Figure 1. Schematic representation of repetitive units of the main synthetic resins discussed above.

The interconnected environmental and human concerns, coupled with the imperative to shift away from non–renewable resources, are closely tied to the ecological challenges facing our planet. This has prompted a heightened focus on renewable resources as a means of discovering more environmentally friendly alternatives to existing synthetic adhesives.

1.4 Bio adhesives for wood products: state–of–the–art

For decades, unrestrained consumption of resources combined with a lack of conservation and recycling policies have caused serious environmental problems. To rebalance the current condition, new policy lines must be taken. New plans, such as the circular economy, are the basis for environmental policies, which push industries and consumers from a linear economy system 'take–make–dispose', with high waste production, towards a programme of prevention of consumption and recycling of the materials used [42],[43]. Considering the need to create alternatives to the current construction market and that wood products are the major users of adhesives, representing over 65% by volume of all adhesives used in the world [44], an important response to new environmental policies can be given by finding new "green" solutions in the production of adhesives. In recent years, significant strides have been made in the realm of bio adhesive research, advocating for the utilisation of natural constituents such as proteins, carbohydrates, and polyphenols, including lignin and tannin. These elements serve as fundamental building blocks for the development of natural resins specifically designed for wood bonding applications.

1.4.1 The main natural resources of bio–adhesives production in the field of wood composites

Proteins

Proteins, which are derived predominantly from the mechanical or solvent extraction of oils such as soy, palm, canola, cottonseed, and sunflower, constitute significant markets in various industrial applications. Furthermore, in Europe, proteins extracted from wheat gluten, a by–product of bioethanol production, are widely accessible [45]. Other proteins, including zein extracted from maize seeds, casein derived from milk and animal blood, and proteins obtained from feathers, find various industrial applications [46], starting as energy sources for animal food [47] to a new platform for the development of bioplastics [48]. Soybeans, which represent around 52% of global oil production, undergo a comprehensive processing cycle to produce soybean meal. This meal, with a protein content ranging from 44% to 50%, becomes a valuable raw material for the production of various derivatives such as soy flour, soy protein concentrates and soy protein isolates (SPI). Protein adhesive properties are intricately influenced by their structural complexity, which arises from the 3D arrangement of amino acid monomers to form macromolecules [49]. Although soy protein has been extensively studied for its application as wood adhesives, other protein sources such as canola, wheat gluten, zein, casein, pea, mussel, whey, and cottonseed exhibit unique adhesive properties based on their amino acid composition. For example, mussel proteins offer high tolerance to water, although their cost has prompted researchers to explore the modification of soy proteins to mimic these desirable qualities [50]. Wheat gluten, obtained as a by–product of starch production and through direct extraction from wheat flour, has become a noteworthy protein source for various applications. Comprising glutenin and gliadin, wheat gluten is characterised by its hydrophobic nature and dispersibility in alkali and acid. Its study, along with investigations into hydrolysed gluten proteins, contributes to the expanding repertoire of wood adhesives, improving the diversity and versatility of the options available in the field [45],[51].

Starches

Starch, a complex polysaccharide derived from the seeds, roots, and leaves of plants, plays a pivotal role as the primary energy storage unit in various plant species. Abundantly found in corn, wheat, potatoes, rice, tapioca, and sago, pure starch is insoluble in cold water [52]. However, through dry roasting in the presence of an acid catalyst, it transforms into soluble dextrin's, which are soluble in water, and the viscosity of the dextrin solution is easier to adjust than that of starches. Composed of glucose units linked by glycosidic bonds, starch manifests itself in two fractions: linear helical amylose and the branched amylopectin. Together, they form semicrystalline granules, whose size and shape vary between plant species [52]. Native starch adhesives, inherently highly hydrophilic with poor water resistance and relatively low bond strength, require significant modifications for applications in the wood industry [53]. These modifications encompass chemical approaches such as oxidation, esterification, and etherification, as well as physical, enzymatic, and genetic methods [52]. One of the challenges associated with starch adhesives is their high viscosity, which results from the entanglement of high molecular weight macromolecules. To address this problem, strategies involve reducing the number of entanglements per chain by adding small molecules to swell the polymer network. Alternatively, shear refinement can be used, where molecules orient themselves under flow conditions, thus decreasing the entanglements in polymer melts [54]. These modifications not only enhance the adhesive properties of starch but also make it more versatile and suitable for a wide array of industrial applications.

Lignins

Historically, lignin, derived primarily as a byproduct of the pulping process, has often been relegated to a low value status, finding utility as fuel in the recovery boilers of pulp and paper mills. Its structural diversity, which ranges from nearly native to highly degraded forms, requires strategic modifications and crosslinking to improve the adhesive properties crucial for applications in wood bonding [55],[56]. Lignin is broadly classified into two main categories: sulphur–containing lignin (kraft and lignosulfonate lignin) and non–sulphur biorefinery lignin (derived from processes such as soda, organosolv, steam explosion, hydrolysis, diluted acid, pyrolytic, high pressure refining, and ammonia–fibre–expansion lignin) [57]. The chemical changes that occur during the processing to obtain lignin underscore their distinct properties and potential applications. Lignin is a complex polymer composed of three monomers: coniferyl alcohol, synapyl alcohol, and p–coumaryl alcohol, linked through ether and carbon–carbon linkages. It results in three different units known as guaiacyl units (G type), syringyl units (S–type) and p–hydroxylphenol propane units (p–H type), and exhibits major chemical functional groups such as hydroxyl, methoxyl, carbonyl, and carboxyl groups [7]. There are significant differences in the properties and water solubility of lignin derived from different processes. Sulphur–free extraction processes, such as alkaline processes, produce lignin of higher quality as a result of milder treatments, whereas detailed structural information for many types of biorefinery lignin remains elusive. Kraft lignin, for example, exhibits insolubility in water and solvent, except in highly alkaline environments (pH > 11), while soda and organosolv lignin are essentially insoluble in water insoluble [59]. Lignosulfonates, on the other hand, are water–soluble in the presence of a suitable counterion [60]. With the anticipated growth in the biomass–to–biofuel and biomass–to–sugar conversion industries, biorefinery lignin is poised to become more readily available. Researchers are exploring oxidative pathways to convert biorefinery lignin into valuable platform chemicals, which offer the potential for subsequent transformation into adhesives, as described in a review by Ma et al. [61].

Tannins

Tannins, which are naturally present in various parts of the plant such as bark, wood, leaves, and fruits, play a versatile role in industrial applications, notably in the production of inks, textile dyes, leather tanning, and corrosion inhibitors. Although tannins are widespread in plant species, extraction is economically viable only from specific sources such as pine, quebracho, oak, chestnut, wattle, eucalyptus, myrtle, maple, birch, and willow [62]. Tannins are divided into two principal classes, condensed and hydrolysable, with different chemical structures and, consequently, different properties. The structure of the former consists of flavonoid oligomers with a variable degree of polymerisation [63]. Units are usually linked C4 to C6 or C4 to C8 to form various length chains depending on the type of tannin. Hydrolysable tannins are simple esters of gallic acid that are categorised according to the products obtained after hydrolysis: gallic tannins (composed of gallic acid and glucose) and ellagic tannins (composed of diaryl units and glucose) [64]. The family of condensed tannins offers the opportunity to undergo electrophilic addition of aldehydes, which opens the opportunity to produce cross–linking; this is a key for the production of adhesives. This higher reactivity compared to that of hydrolysable tannins allows the formation of more stable three–dimensional polymeric structures. These distinctions in the types of tannin offer a spectrum of possibilities for various industrial applications.

1.4.2 Development of bio adhesives

Partial replacement of synthetic–based adhesive systems

An early step in the transition to greater sustainability and a detachment from non–renewable resources has seen the incorporation of bioresources within major synthetic resins, with more or less satisfactory results. For example, the substitution of synthetic resin portions with soy protein has demonstrated a tendency to lower resin reactivity and increase viscosity compared to fully synthetic adhesives. Furthermore, the introduction of soy protein as a modifier in UF resin does not result in a reduction in formaldehyde emissions [65]. In fact, the cross–linking reaction between soy protein and formaldehyde is frequently reversible, especially unless an excess of formaldehyde is employed. Soy adhesive that does not undergo copolymerisation remains soluble in water after curing and is susceptible to moisture. However, when contrasting the properties of 100% soy adhesives, an improvement was observed by blending cost–effective soy flour with synthetic adhesives such as MUF and UF. Similarly, natural starch in its original form lacks the adhesive bonding strength required for effective wood bonding. Research efforts in starch adhesives have been comparatively limited compared to those in other biobased adhesives. Recent investigations focus mainly on the use of starch as a replacement or extension of solid wood dispersion adhesives, with the aim of improving viscosity and reducing material costs [66]. The focus on starch adhesive studies in wood bonding has been on various formulations, including corn starch in starch/polyvinyl alcohol [67], starch/isocyanates [68], and starch/tannin adhesives [54]. Studies have shown a tendency to increase the thermal stability of adhesives without decreasing the mechanical properties, as long as the amount of starch remains in the range of 10%–20%. Chemically, tannins and lignin are similar, and they have been successfully used as partial replacements for phenol in PF resins, due to their similar chemical nature. According to Danielson and Simonson [69], a substitution of 50% phenol with Kraft lignin in PF resin yields favourable results in terms of resin viscosity, storage stability, and bonding capacity. However, this replacement requires an increase in pressing time of 30%. Similarly, the ethanol residue (ER), the by–product arising from the production of lignocellulosic ethanol, leads to optimal results when 30% and 50% of the phenol are replaced, resulting in the production of exterior grade plywood that meets the relevant Chinese standards [70]. Akhtar et al. [71] have explored lignosulfonate (LS) as a replacement phenol in PF resin, achieving relatively high replacement levels of up to 50% by weight, increasing both thermal properties and altered flow behaviour. Generally, alkaline, dealkaline, sulfonate lignin and technical lignin liquefied in acid phenol solution might be used to produce PF resins [72]. Tannins, in parallel to lignin, because of their phenolic structure, enable a high similarity in behaviour with the main synthetic resins. An amount of tannin has been added to synthetic UF resin up to 50% by dry weight [73], obtaining similar results compared to the UF sample. Similarly, tropical hardwood plywood was glued using Mangium tannin combined with paraformaldehyde, demonstrating suitable strength for interior applications. However, to optimise its efficacy for outdoor applications, a refined formulation was developed by incorporating copolymerisation with PF and resol during the condensation process [74]. An alternative formulation for bonding was tested using Mangium tannin and paraformaldehyde, supplemented with a low molecular weight phenol–formaldehyde counterpart. This modification proved effective in enhancing the shear strength of the plywood, increasing it from 0.96 to 1.43 MPa after a 72–hour boiling test. The resulting adhesive is deemed suitable for both interior and exterior grade plywood applications [75]. In this direction, resorcinol–tannin–formaldehyde resins have been developed industrially as adhesives for glulam and finger joints achieving the mechanical properties required by standards [76]. Additionally, elevating the tannin content in the adhesive system is directly correlated with a reduction in formaldehyde emissions. Nevertheless, the drawback of incorporating high concentrations of tannin into PF resins is an increase in viscosity and a decrease in pot life. This is attributed to the increased reactivity of tannins compared to phenol in the presence of formaldehyde [77].

Total replacement of synthetic–based adhesives systems

Research has evolved from the attempt to introduce renewable percentages into commercial synthetic resins to the pursuit of developing entirely renewable formulations over time. As anticipated earlier, the harnessing of renewable resources such as proteins and carbohydrates requires a process of physical or chemical modification to yield materials endowed with properties suitable for specific applications. For proteins to serve as adhesives, denaturation is essential to expose more polar groups, enhancing solubility and promoting bonding through hydrogen interactions. Denaturation refers to a modification that alters the secondary, tertiary, or quaternary structure of a protein without disrupting covalent bonds. This process unfolds the protein, exposing hydrophilic groups for modification reactions. Denaturation can be induced by heat, exposure to acid or alkali, organic solvents, detergents, or urea. In particular, research on SPIs underscores the significant influence of detergent concentration and pH values on adhesive strength [78]. Furthermore, the response of proteins to modifications and additives varies according to their source. For example, in a study by Cheng et al. [79], it was observed that the anionic charge, such as glutamic acid, acetic, and butyric acid, positively influenced the adhesive properties of the cotton seed protein. On the contrary, no notable improvement was detected in soy protein adhesive formulations with the same modifiers. Another finding suggests that, after alkali modification, the adhesive properties and water resistance of soy protein isolates exceed those of wheat gluten protein [80]. Similarly, starch, which is initially insoluble in water, faces challenges in adhesive applications because of precipitation caused by extensive hydrogen bonding forces. This crystallisation issue during drying reduces the contact area and compromises adhesion. Gelatinization, achieved by water heating, disrupts the crystalline particles of starch chains, forming a paste with dissolved amylose and starch granule fragments. Various modifications, including acid treatment, alkali treatment, derivatization, oxidation, and enzyme treatment, aim to open tightly bound starch granules [81]. In specific studies, such as those by Wang et al. [82], up to two hours of acid hydrolysis was found to improve grafting reactions and reduce steric obstruction, inhibit retrograde of starch molecules, and improve the overall characteristics of starch–based wood adhesives. Although lignin, as previously discussed, exhibits more affine chemical properties for its incorporation within synthetic resins, modifications are necessary for the production of lignin–only adhesives to achieve satisfactory results. Popular chemical modification methods for lignin are methylolation or hydroxymethylation, phenolation, and demethylation. In this direction, Alonso et al. [83] conducted a study on various LS samples, observing that softwood lignin exhibited superior characteristics for methylolation compared to hardwood. This difference was attributed to the higher number of aromatic protons present in the structure of softwood lignosulfonates. The reactivity of lignin in methylolation is also influenced by pulping parameters such as pH, temperature, and pressure [84]. This modified form of lignin has demonstrated an increase in reactivity compared to unmodified lignin. Similarly, phenolated organosolv LPF resins outperform resins with unmodified lignin, showing an improved hardening time [85]. On the other hand, although various chemical modifications, such as acylation, esterification, methylolation, and etherification, have also been proposed for condensed tannins [86], these compounds enjoy good inherent reactivity, allowing them to be used as is for the production of adhesives for wood composites. For example, commercial applications of tannin–formaldehyde already exist, and several reviews on the use of tannin as a wood adhesive can be found in the literature [77],[80]. However, some recommendations were recently discussed and published in a review [87]. As can be seen, tannins often offer good intrinsic reactivity, but high molecular weight leads to high viscosity and consequently low solid content within the final resin. Simple modifications, such as by adding small molecules, such as acetic, maleic anhydride, or caustic soda, might make these materials suitable for use in the formulation of adhesive resins. Briefly, tannin extract solids undergo a process with mechanical stirring at 80–82°C. Initially, 3% anhydride is added, followed by a gradual increase in temperature to 90–92°C over for 45 minutes. Subsequently, 25–30% NaOH solution is slowly introduced over 15 minutes to achieve a pH near 8. The mixture is stirred at 90–92°C for 3 hours, resulting in a natural pH drop to 7.2–7.5. After cooling, acetic acid or NaOH is used to adjust the pH to 6.7–6.9 for optimal pH [87].

Utilisation of condensed tannins as a fundamental building block for wood adhesives in the realm of EWPs is due to their captivating chemical properties and the practicality they offer in industrial applications. The intriguing characteristics of condensed tannins, such as their polyphenolic nature and their ability to form robust cross–linked structures, make them ideal candidates for developing adhesive resins. These compounds possess a unique capacity to interact with various substrates, including wood, leading to enhanced adhesion properties. Furthermore, the relatively straightforward processing requirements and the environmentally friendly nature of tannins align with the growing demand for sustainable and eco–friendly materials in the field of bio resins. The following chapter delves deeper into the chemistry of condensed tannins, exploring their molecular structure, reactivity, and the specific mechanisms that make them well–suited for the development of advanced wood adhesives.

Through a comprehensive examination, the main objective of the current doctoral dissertation is to elucidate the pivotal role that tannins play in advancing the field of engineered wood products, paving the way for innovative and sustainable adhesive solutions. Indeed, upon meticulous scrutiny of primary bioresources for bio-adhesive development, tannins emerged as optimal starting material. This choice stems from their inherent chemical properties, which will be elucidated in the next sub-chapter.

1.5 Condensed tannins

1.5.1 Chemistry and extraction process

As mentioned above, economically viable tannin extraction is feasible only from a limited number of plant species that possess a substantial tannin content. Notable examples include wattle (mimosa), various species of pine, quebracho, oak, chestnut, eucalyptus, myrtle, maple, birch, and willow. Condensed tannins exhibit an intricate chemical composition, consisting of hydroxylated C15 flavonoid units that bond with each other at various sites. These tannins consist of complex phenolic compounds with high molar masses, ranging from 500 to 20,000 Da [88], and show an origin from polyhydroxy–flavan–3–ol oligomers, predominantly linked by C–C bonds between the A rings of flavanol units and the pyran rings of others. The basic structures of condensed or polyflavonoid tannins are: ring A: resorcinol or phloroglucinol ring B: pyrogallol, catechol [89]. In the commercially employed tannin extracted from mimosa, the prevailing flavonoid structure is prorobinetinidin, characterised by a resorcinolic A–ring and a pyrogallic B ring. Figure 2 and Table 2 illustrate the four primary structures of condensed flavonoid tannins.

Table 2. The main chemical composition of condensed flavonoid tannins.

Flavonoid type	**A–ring**	**B–ring**	**Tannin type**
Prodelphinidin	Phloroglucin	Pyrogallol	Pine
Procyanidin	Phloroglucin	Catechin	Pine
Prorobinetinidin	Resocinol	Pyrogallol	Mimosa
Profisetinidin	Resocinol	Catechin	Quebracho

Condensed tannins distinguish themselves among hydrolysable compounds by exhibiting a notable decrease in formaldehyde emission levels. This reduction is attributed to its increased reactivity with formaldehyde, coupled with the presence of catechol groups. Consequently, condensed tannins have emerged as extensively studied precursors for wood adhesives on a global scale, commanding a higher market value compared to hydrolysable tannins. In fact, they make up more than 90% of the global production of commercial tannins, with approximately 200,000 tons of production.

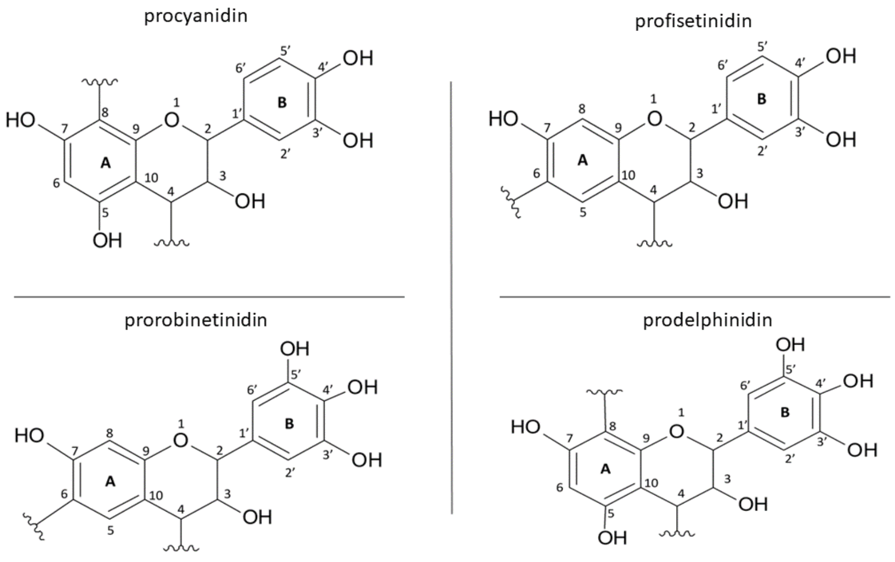

Figure 2. The main structure of tannin flavonoid units.

The extraction of various plants is often hindered by low and economically unviable yields. Efficiency depends on factors such as plant species, type of solvent, and extraction method [90]. Traditional water–based extraction is common, which is advantageous because of its straightforward process, high effectiveness, and broad applicability. To increase the quality of the extract, decreasing the presence of impurities such as sugars and polymeric carbohydrates, some chemicals might be added during the extraction process. Specifically, industrial processes involve the addition of a catalytic amount of sodium sulfite or bisulfite [91], sodium hydroxide or sodium carbonate [93], and alcohols [93]. In fact, tannins are highly polymerised substances and can be associated with other constituents, such as carbohydrates [94]. Although reducing viscosity and allowing higher extract concentrations could be achieved by selectively eliminating polymeric carbohydrates, the implementation of purification processes, such as micro– and ultrafiltration [95],[96], or acid precipitation followed by filtration or centrifugation [97], has been hampered by prohibitive costs, and in large–scale industrial production, tannin extracts are typically marketed as spray dried powders, foregoing purification steps. Alternative methods to manage viscosity involve optimising extraction conditions to minimise non tannin substances, chemically degrading polymeric carbohydrates, disrupting hydrogen bonds with bond breakers such as urea, or modifying the extract acetic anhydride or NaOH. Furthermore, extraction parameters, including time and temperature, significantly influence yield and quality, and are especially chosen based on the raw material. In addition, newer methods, such as microwave and ultrasound–assisted extraction, as well as those using compressed fluids or Shoxhlet with supercritical CO_2, offer alternative approaches to improve efficiency [98],[99].

1.5.2 Tannin–based adhesive systems

Polycondensation reactions involving tannins and aldehydes have found widespread application. Tannin–formaldehyde adhesives, a result of such reactions, have been successfully commercialized for the production of wood–based composites and are in long–term use in certain countries [100]. However, due to the emission limitations of formaldehyde, a compound classified as a carcinogen (Group 1) [32], several alternatives have been proposed in order to restrain its use as crosslinker. As previously discussed, condensed tannins have been incorporated into commercial resins at the outset to reduce the reliance on synthetic components, enhance reactivity, and mitigate formaldehyde emissions. The primary investigations in this realm are summarized in Table 3.

Table3. Overview of the main studies that investigate the incorporation of various condensed tannins within synthetic resins for wood adhesive applications.

Wood species	**Adhesive application specifications**				
Tannins extracted from wood timber					
	Extraction yield (%)	Synthetic resin	Percentage of addition (%)	Applications and specifications.	Results
Quebracho (Schinopsis balansae and S. lorentzii) [101], [102]	40	PF	6	Particleboard	Satisfy exterior grade EN 314. Low formaldehyde emissions.
Tannins extracted from bark					
Wattle or mimosa (Acacia mearnsii) [103].	22–48	PF	12.5	Particleboard	Internal bond= 0.23 – 0.39 MPa
Mangium (Acacia mangium) [104], [74], [75]	11	PF	/	Plywood	Shear strength= 1.43 MPa (72–hours boiling test)
Spruce (Picea abies) [75].	7–25	PF	60–80	Plywood	Percentages above 20% decrease properties below standard limits.
Mangrove (Rhizophora mangle L.) [105],[106]	19–27	PF–resol	20	Plywood	Bond strength similar to commercial PF resins.
Pinus radiata [98], [107]	8–23	UF	/	Particleboard	Increased tolerance to the moisture content of glued wood particles.
Larch (Larix gmelini) [108], [109].	10	PF	60	Particleboard	Suitable for industrial exterior applications.
Barbatimao [110], [111].	15–37	UF	25–75	OSB	The interior grade requisites were reach at 25:75, UF:T.
Eucalyptus [112], [113].	7–11	PF	10–50	Fiber composites	Mechanical properties comparable to PF resins
Other source for condensed tannins					
Grape pomace [114], [115].	/	75%	F(5)–PMDI(20)	Particleboard	Internal bond= 0.26 – 0.36 MPa.

Subsequentially, in the pursuit of creating entirely tannin–based wood adhesives with minimal emissions, various cross–linking agents have been employed in order to achieve properties comparable with those of tannin–formaldehyde resins. As a non–toxic alternative to traditional aldehydes, glyoxal is suggested for use as a hardener in condensed tannins [116]. Although glyoxal exhibits a behaviour similar to that of formaldehyde, its performance as an adhesive is compromised due to extended pressing times. This is attributed to a portion of glyoxal activating the aromatic ring, leading to incomplete cross–linking, leaving the second carbonyl group unreacted after an electrophilic substitution, a reaction that occurs at the main reactive centres reported in Figure 3 [117]. Other aldehydes such as acetaldehyde, propionaldehyde, n–butyraldehyde, and isobutyraldehyde have been studied but low degree or polymerisation have been highlighted [118],[119]. The rapid increase in molecule sizes during cross–linking results in distances between reactive sites that are too extensive for a straightforward methylene bridge. Cross–linking agents with higher molecular sizes than formaldehyde prove to be more effective in bridging these gaps between reactive flavonoid sites. Viable longer chain cross–linkers include ethyleneglycol–diglycidyl ether, which belongs to the epoxy class compounds, which has been reacted with pine tannin [120]. In the realm of tannin–based adhesives, the interaction with hexamethylenetetramine is particularly intriguing, serving as a non–aldehyde yielding hardener under alkaline conditions [121]. Remarkably, hexamine has been shown to not to break down into formaldehyde and ammonia in the presence of reactive condensed tannin [122]. As a result, hexamine–containing adhesives exhibit minimal formaldehyde emissions, restricted only to those arising from the wood heating process. Diphenylmethane diisocyanate, better known as pMDI, is an aromatic diisocyanate and has also been proposed for the cross–linking of condensed tannins [123]. Particleboard panels bonded with condensed tannin extracted from pine bark and pMDI show similar internal cohesion to those in which formaldehyde is used as a hardener, in both dry and wet environments [124]. A novel approach to substitute the use of expensive and hazardous isocyanates involves initiating the process with the reaction between tannin and dimethyl carbonate. Subsequently, the addition of a diamine, such as hexamethylenediamine, culminates in the formation of a resin based on urethane [125]. Methylolated nitroparaffins, including the cost–effective tris(hydroxymethyl)nitromethane (TRIS), effectively serve as cross–linking agents for tannin adhesives. By substituting other hardeners proportionally, TRIS has demonstrated the ability to reduce formaldehyde emissions and extend the pot life of tannin adhesives [126]. However, it is noteworthy that TRIS requires significantly higher curing temperatures compared to alternative hardeners. Among the different types of hardeners of particular interest are the furan class of molecules, which are bio derivates obtained from the dehydration of agricultural and forest waste from hemicelluloses [127]. The most prominent compounds in this class are furfural and furfuryl alcohol [119], with the latter can lead to the production of copolymers due to its ability to self–polymerize in an acidic environment [128]. Alternative curing agents, including fatty amides derived from vegetable oils, have been used as crosslinkers for tannin adhesives. For instance, Patel et al. [129] specifically investigated the efficacy of N,N–bis(2–hydroxyethyl) fatty amide (HEFA) derived from Karanja oil and rice bran oil as cross–linking agents for tannins.

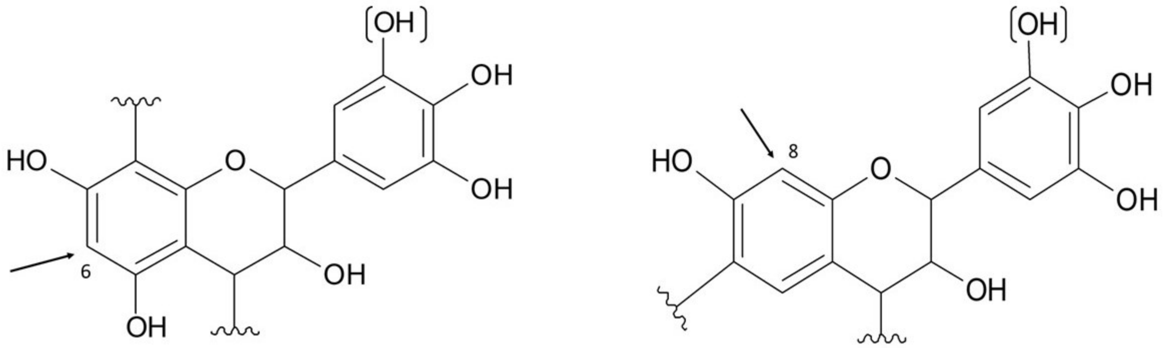

Figure 3. Principal reactive sites of flavonoids.

The main known cross–linkers and their application for wood products are therefore reported in Table 4 to summarize their applications and to have an overview of results.

Table 4. Overview of the main studies that investigate the reaction of condensed tannins within different hardeners for wood adhesive applications.

Hardeners	Tannin	Adhesive specification	Hardener concentration (%)	Adhesive amount	Wood products	Pressing details	Results
Aldehyde compounds							
Formaldehyde	Red Pine (Pinus Brutia) [124].	Solid content: 40%; pH: 6.12, Gel time: 52 sec; Viscosity: 339 cP.	8	0.019 – 0.024 g·cm^{-2}	2–layers veneer (3 x 25x 115mm)	4 min, 140°C	Bond strength: Dry= 4.66 MPa Wet= 1.89 MPa
	Several Tannin sources [130].	Solid content: 40%, pH:7.1, 7.7, 6.6, 7.7, 8.5, 8.6, 10.3	10	10%	1–layer particleboard, target density: 700 kg·m^{-3}	155 sec·mm^{-2}, 195°C	Internal bond dry= 0.76 (pine), 0.91 (pine), 0.91 (pecan nut), 0.52 (mimosa); 0.93 (mimosa), blows (quebracho), 0.43 (quebracho) MPa
	Pine (Pinus maritimus) : BIOLANDES (1)	(1) Solid content: 46.1%; pH: 4.5; Viscosity: 14.000 cP; Gelt time: 45’’	5	10%	1–layer particleboard target density: 700 kg·m^{-3}	7.5 min, 195°C	(1) Internal bond dry= 0.43 MPa
	Pine (Pinus maritimus) : DRT (2) [131]	2) Solid content: 45.3%; pH: 3.5; Viscosity: 9.9000 cP; Gel time: 52’’					(2) Internal bond dry= 0.60 MPa
	Mimosa [126]	pH: 8	7	9%	1–layer particleboar, target density: 704 kg · m^{-3}	10 sec·mm^{-2}, 190–195 °C	Internal bond: Dry= 0.80 MPa Wet= 0.19 MPa
	Quebracho [126]	pH: 9.5	/	250 g · cm^{-2}	5–layers plywood	6 minutes, 120°C	Breaking load= 1.73 MPa, wood failure > 80%
Glyoxal	Red Pine (Pinus Brutia) [124]	Solid content: 40%; pH: 5.49, Gel time: 461 s; Viscosity: 152 cP	12	0.019 – 0.024 g · cm^{-2}	Fagus orientalis two layers veneer (3 x 25x 115mm)	4 min, 140°C	Bond strength: Dry= 3.5 MPa Wet= 0.14 MPa
	Pine (Pinus maritimus), BIOLANDES (1) [131]	(1)Solid content: 44.3, 43.2; pH: 4.5, 6.5; Viscosity: 10.200, 15.215 cP; Gelt time: 2’44’’, 1’38’’	9	10%	1–layer particleboar, target density: 700 kg·m^{-3}	7.5 min, 195°C	(1) Internal bond dry= 0.16 MPa, 0.22 MPa
	Pine (Pinus maritimus) : DRT (2) [131]	(2) Solid content: 44.2; 42.7; pH: 3.5, 5.3; Viscosity: 10.600, 91.000 cP; Gel time: 44.2; 42.7					(2) Internal bond dry= 0.3 MPa, 0.51 MPa
	Pine (Pinus radiata) [132].	Solid content: 45%; pH: 8, 9.5; Gel time: 60’’	9	12%	1–layer particleboard	7.5 min, 190–195°C	Internal bond dry= 0.44 MPa
Glutaraldehyde	Mimosa (Acacia Mearnsii) [119].	/	/	/	/	/	The compound lead to low degree of polymerization.
Other aldehydes: acetaldehyde, propionaldehyde, n–butyraldehyde, isobutyraldehyde	Pine and wattle [118]	/	/	/	/	/	No stable polymers have been highlighted.
Furanic molecules							
Furfural	Mimosa (Acacia Mearnsii) [119].	Solid content: 33.3%; pH: 2, 4.5, 7, 9	25, 37.5	Not applied	Not applied	Not applied	Furfural produces solids from pH 4.5 to 9.0. The higher the pH, the lower the curing temperature observed.
Furfuryl alcohol (FA)	Mimosa (Acacia Mearnsii) [119].	Solid content: 33.3%; pH: 2, (4.5)	12.5, 25	Not applied	Not applied	Not applied	The furfuryl alcohol only produces polymers at pH 2.
	Mimosa (Acacia mearnsii) tannin [133]	pH: 11, 10, 8; Gel time: 260 – 600’’	100, 50	10%	1–layer particleboard	7.5 min, 190–195 °C	Internal bond, pH10, 50%FA = 0.34 MPa
	Pine (Pinus radiata) [133]	pH: 8; Gel time: 110 – 150’’	50, 75				Internal bond 50%FA= 0.35 MPa Internal bond 75%FA= 0.40 MPa
	Mimosa (Acacia mearnsii) [134]	Solid content: 60%	40	10 %	1–layer particleboard	6 min, 180 °C	Internal bond dry= 0.15 MPa
5–hydroxy–methylfurfural (5–HMF)	Pine [135]	Solid content: 42%; pH: 6.5, 9.5; Gel time: 142’’, 38’’	20	10%	1–layer particleboar, Density: 679, 693 kg · m^{-3}	7.5 min, 220°C	Internal bond dry= 0.299, 0.152 MPa

Hardeners	Tannin	Adhesive specification	Hardener concentration (%)	Adhesive amount	Wood products	Pressing details	Results
Maleic anhydride	Mimosa (Acacia Mearnsii) [119]	Solid content: 33.3%; pH: 2, 4.5	12.5 to 50	/	/	/	Elastic solid similar to the glyoxal.
Other hardeners							
Hexamine	Red Pine (Pinus Brutia) [124]	Solid content: 44.89; pH: 6.75; Gel time: 248’’; Viscosity: 204 cP	5	0.019 to 0.024 g·cm^{-2}	Fagus orientalis veneer(3 x 25x 115mm)	4 min, 140°C	Bond strength Dry= 3.7 MPa Wet=0.26 MPa
	Maritime pine : BIOLANDES (1) [131]	(1)Solid content= 43.5; 42.3 pH= 4.5, 6.5; Viscosity= 20.000, 30.000 cP; Gel time= 2’44’’, 1’38’’	10	10%	1–layer particleboar, target density: 700 kg · m^{-3}	7.5 min, 195°C	(1)Internal bond dry= 0.16 MPa; 0.19 MPa
	Maritime pine : DRT (2)	(2) Solid content: 43.9, 42.8, pH: 3.5, 5.3, Viscosity: 2.050, 4150 cP; Gel time: 39’’, 35’’					(2) Internal bond dry= 0.38 MPa ; 0.23 MPa
	Mimosa–O (1) [136]	Solid content: 45%; pH: 9	5	7%	1–layer particleboard, target density: 880 kg · m^{-3}	330 sec, 180 °C	Internal bond dry= 0.58 MPa
	Mimosa–T (2) [136]	Solid content: 45%; pH: 10	5; 10; 15			380 sec, 180°C	Internal bond dry= 0.95, 0.71, 0.78 MPa
Hexanediamine (HDME)	Bayberry tannin [137]	Solid content: 30%; pH: 9, Viscosity: 2635, 2218, 1779, 1541, 1013, 830 mPa · s	15, 20, 25, 30, 35	240 g · cm^{-2}	Plywood	5 min, 200°C	25% of HDME is needed to satisfy the shear strength standards for both dry and wet tests.
(Poly)–ethylene glycol diglycidyl ether (PEGDE)	Pinus radiata [123].	Solid content: 40%; pH: 4, 7, 10	5	/	/	/	Alkaline pH accelerates the processes. Comparable behaviour with formaldehyde system highlighted.
Tris(hydroxymethyl)nitromethane (TRIS)	Quebracho [126]	pH: 9.5	12 (1), 12 + 3 of silica (2)	9%	1–layer particleboard, target density: 704 kg · m^{-3}	15 s·mm^{-2}, 190–195 °C	(1)Internal bond dry = 0.7 MPa Internal bond wet= / (2) Internal bond dry= 0.8 MPa; Internal bond wet= 0.23 MPa
	Mimosa [126]						(1)Internal bond dry = 0.8 MPa; Internal bond wet= 0.20 MPa (2) Internal bond dry= 0.8 MPa; Internal bond wet= 0.21 MPa
	Quebracho [126]	pH: 9.5	6, 8, 10	250 g · cm^{-2}	5–layers plywood	6 min, 120°C	Breaking load= 0.9, 1.7, 2.1 MPa, wood failure > 80%
Diphenylmethane diisocyanate (pMDI)	Red pine Pinus Brutia) [124]	Solid content: 44.71; pH: 5.93; Gel time: 387’’, Viscosity: 278 cP	10%	0.019 to 0.024 g · cm^{-2}	Fagus orientalis veneer (3 x 25x 115mm)	4 min, 140°C	Bond strength: Dry= 2.8 MPa, Wet=1.2 MPa
	Pine [138]	Solid content: 37%; pH= 4.6 (natural) Viscosity: 1000 mPa	20, 10 of formaldehyde	/	3–layers plywood of (1)beech and (2)poplar	5 min at specific pressure of 1.18 N · mm^{-2}	(1)Shear strength dry= 1.34MPa; Shear strength wet= 1.16 MPa (2) Shear strength dry= 1.58MPa; Shear strength wet= 1.13MPa

1.6 Life Cycle Assessment

The assessment of the environmental impact of novel materials within a market context is intrinsically linked to the physical and mechanical characteristics of the product, and, therefore, to its production process. Indeed, in contemporary society, the synergy between material properties and environmental impacts is of paramount importance. Keeping this in consideration, a thorough study was conducted to analyse the environmental impact of one of the formulations developed over the years. Additionally, the study proposed its integration and comparison within the realm of adhesives, encompassing both synthetic and natural resins. As previously discussed, wood products might play a pivotal role in fostering a sustainable environment by seamlessly integrating material and energy flows across various sectors, particularly within the construction, forestry, energy, and industrial domains. This integration not only promotes eco–friendly practices, but also contributes to the overall development of a sustainable ecosystem. Growing concern about the environmental effects of the production and use of goods and how they are disposed of at the end of their life has led to a growing interest in sustainably manufactured wood–based products. Long–term sustainable development is a crucial concern in many countries, leading to regulations regarding the impact of products during their life cycle, including efforts to create effective reverse logistics strategies to manage post–use materials. A better understanding of the environmental impacts of materials and processes associated with manufacturing sectors, including wood, is vital to driving sustainable market processes. Life cycle assessment (LCA) is a tool for assessing the environmental impact of a system (process, product or service), considering its entire life cycle "from cradle to grave" or part of it. That is why LCA is considering a global (“life cycle”) approach that should contribute to sustainability decision making [139]. LCA consists of 4 phases: (i) definition of the goals and scope definition; (ii) life cycle inventory analysis (LCI); (iii) life cycle impacts analysis (LCIA); and (iv) interpretation of the results [140],[141]. LCA studies aim to identify the most important contributors to environmental impacts, allowing efforts to reduce those impacts. The end–of–life management of wood–based products is an essential factor in energy and GHG balances.

The LCA methodology has been applied to a wide range of processes and sectors. Regarding the wood industry, numerous studies have been conducted to investigate the environmental performance of wood products for various uses, starting with the impact of wood harvesting and supply chain [142]–[145] to studies that consider different types of engineered wood production [146]–[148]. Environmental impact analysis is of great importance, as also underlined by European directives, as Product Environmental Footprint (PEF) [149] to unite analysis methods and offer immediate comparisons between different studies. Wood material is a viable alternative to non–renewable materials, both in the structural and non–structural fields. As stated above, wood and adhesives are inseparable from each other. However, there are still not many studies in the bibliography on comparing the environmental impact of wood products assembled with synthetic and bio adhesives, or at least not for all the natural product alternatives that can be used to produce bio adhesives. For instance, Yang and Rosentrater [150] compared the impact of 1kg of the two leading synthetic resins on the market, UF and PF, which reported greenhouse gas emissions in a range of 2.04 kg CO_2 eq. kg^{-1} for UF and 2.88 kg CO_2 eq. kg^{-1} for PF. McDevitt and Grigsby [151] had conducted a study comparing the LCA of bio and petrochemical adhesive used in MDF production. The bio adhesive formulation was calculated theoretically to achieve the equivalent performance of UF synthetic resin, considering the components that have demonstrated applicability in the field of adhesives. The study reports a 22% higher environmental impact to produce petroleum–based adhesives when one square meter of MDF is considered as functional unit. Again, Yang and Rosentrater [152] reported a more in–depth study in which a specific adhesive was selected. The central unit of the (bio) Pressure Sensitive Adhesive PSA adhesive can be produced from renewable resources (soya) or petroleum. PSA produced from bio–glycerol showed an environmental impact 40% lower than that of glycerol derived from petrol, taking 1 kg of produced adhesive as functional unit. The impact of using soy protein to prepare 1 kg of adhesive has also been studied and compared with UF MUF and PF resins by Ana Arias et al. [153]. The study provided a broad overview of the different impact factors resulting from the production of soy flour or soybean by proposing the use of the main cross–linkers that have been proposed in the literature. Taking soybean as raw material, the soy–based bio adhesives showed better environmental profiles that were better than those of UF and PF, even if compared to MUF, which is the fossil resin with the best environmental friendly profile.

Furthermore, the study revealed that bio–based alternatives pose a reduced potential risk to human health. The toxicity levels, encompassing both carcinogenic and non–carcinogenic aspects, were found to be markedly lower compared to UF and PF resins—widely employed in the wood panel production industry. Thus, the use of renewable substances seems to produce adhesives with a favourable impact on the environment and human health.

In the dynamic field of bio adhesive and wood products, achieving optimal sustainability remains a continual challenge. As advancements progress, intense research is imperative for developing high–performance and eco–friendly solutions. LCA methodology plays a pivotal role by systematically evaluating the environmental impacts throughout the product lifecycle. This approach guides informed decision–making, steering the industry toward the creation of bio adhesives and wood products that excel in both performance and sustainability.

References of Introduction

1. Paris Agreement to the United Nations Framework Convention on Climate Change, Dec. 12, 2015, T.I.A.S. No. 16–1104.

2. Daigneault, A.; Baker, J. S.; Guo, J.; Lauri, P.; Favero, A.; Forsell, N.; Johnston, C.; Ohrel, S. B.; Sohngen, B. How the Future of the Global Forest Sink Depends on Timber Demand, Forest Management, and Carbon Policies. *Glob. Environ. Chang.* **2022**, *76*, 102582. https://doi.org/10.1016/j.gloenvcha.2022.102582.

3. Lauri, P.; Forsell, N.; Korosuo, A.; Havlík, P.; Obersteiner, M.; Nordin, A. Impact of the 2 °C Target on Global Woody Biomass Use. *For. Policy Econ.* **2017**, *83*, 121–130. https://doi.org/10.1016/j.forpol.2017.07.005.

4. Domke, G. M.; Oswalt, S. N.; Walters, B. F.; Morin, R. S. Tree Planting Has the Potential to Increase Carbon Sequestration Capacity of Forests in the United States. *Proc. Natl. Acad. Sci. U. S. A.* **2020**, *117* (40), 24649–24651. https://doi.org/10.1073/pnas.2010840117.

5. Romppanen, S. The LULUCF Regulation : The New Role of Land and Forests in the EU Climate and Policy Framework. *J. Energy Nat. Resour. Law* **2020**. https://doi.org/10.1080/02646811.2020.1756622.

6. Climate Action Tracker, ‘Global Update: Governments Still Showing Little Sign of Acting on Climate Crisis https://climateactiontracker.org/publications/governments–still–not–acting–on–climate–crisis/ (accessed 2023 –10 –09).

7. Nabuurs, G.; Delacote, P.; Ellison, D.; Hanewinkel, M.; Lindner, M.; Nesbit, M.; Ollikainen, M.; Savaresi, A. *A New Role for Forests and the Forest Sector in the EU Post–2020 Climate Targets. From Science to Policy 2.*; 2015. https://doi.org/https://doi.org/10.36333/fs02.

8. European Environment Agency. *Trends and Projections in Europe 2018. Tracking Progress towards Europe’s Climate and Energy Targets*; 2018. https://doi.org/10.2800/931891.

9. Soimakallio, S.; Böttcher, H.; Niemi, J.; Mosley, F.; Turunen, S.; Hennenberg, K. J.; Reise, J.; Fehrenbach, H. Closing an Open Balance: The Impact of Increased Tree Harvest on Forest Carbon. *GCB Bioenergy* **2022**, *14* (8), 989–1000. https://doi.org/10.1111/gcbb.12981.

10. Nabuurs, G.; Delacote, P.; Ellison, D.; Hanewinkel, M.; Hetemäki, L.; Lindner, M. By 2050 the Mitigation Effects of EU Forests Could Nearly Double through Climate Smart Forestry. *Forests* **2017**, *8* (12), 484. https://doi.org/https://doi.org/10.3390/f8120484.

11. Sathre, R.; Connor, J. O. Meta–Analysis of Greenhouse Gas Displacement Factors of Wood Product Substitution. *Environ. Sci. Policy* **2010**, *13* (2), 104–114. https://doi.org/10.1016/j.envsci.2009.12.005.

12. Forster, E. J.; Healey, J. R.; Dymond, C.; Styles, D. Commercial Afforestation Can Deliver Effective Climate Change Mitigation under Multiple Decarbonisation Pathways. *Nat. Commun.* **2021**, *12* (1), 1–12. https://doi.org/10.1038/s41467–021–24084–x.

13. Lewis, S. L.; Wheeler, C. E.; Mitchard, E. T. A.; Koch, A. Restoring Natural Forests Is the Best Way to Remove Atmospheric Carbon. *Nature* **2019**, *568* (7750), 25–28. https://doi.org/10.1038/d41586–019–01026–8.

14. Law, B. E.; Hudiburg, T. W.; Berner, L. T.; Kent, J. J.; Buotte, P. C.; Harmon, M. E. Land Use Strategies to Mitigate Climate Change in Carbon Dense Temperate Forests. *Proc. Natl. Acad. Sci. U. S. A.* **2018**, *115* (14), 3663–3668. https://doi.org/10.1073/pnas.1720064115.

15. Cabiyo, B.; Fried, J. S.; Collins, B. M.; Stewart, W.; Wong, J.; Sanchez, D. L. Innovative Wood Use Can Enable Carbon–Beneficial Forest Management in California. *Proc. Natl. Acad. Sci. U. S. A.* **2021**, *118* (49), e2019073118. https://doi.org/10.1073/pnas.2019073118.

16. Naudts, K.; Chen, Y.; McGrath, M. J.; Ryder, J.; Valade, A.; Otto, J.; Luyssaert, S. Europe's Forest Management Did Not Mitigate Climate Warming. *Science (80–.).* **2016**, *351* (6273), 597–601.

17. Osuri, A. M.; Gopal, A.; Raman, T. R. S.; Defries, R.; Cook–Patton, S. C.; Naeem, S. Greater Stability of Carbon Capture in Species–Rich Natural Forests Compared to Species–Poor Plantations. *Environ. Res. Lett.* **2020**, *15*, 034011. https://doi.org/10.1088/1748–9326/ab5f75.

18. Oliver, C. D.; Nassar, N. T.; Lippke, B. R.; McCarter, J. B. Carbon, Fossil Fuel, and Biodiversity Mitigation With Wood and Forests. *J. Sustain. For.* **2014**, *33* (3), 248–275. https://doi.org/10.1080/10549811.2013.839386.

19. Hudiburg, T. W.; Law, B. E.; Moomaw, W. R.; Harmon, M. E.; Stenzel, J. E. Meeting GHG Reduction Targets Requires Accounting for All Forest Sector Emissions. *Environ. Res. Lett.* **2019**, *14* (9). https://doi.org/10.1088/1748–9326/ab28bb.

20. Iordan, C. M.; Hu, X.; Arvesen, A.; Kauppi, P.; Cherubini, F. Contribution of Forest Wood Products to Negative Emissions: Historical Comparative Analysis from 1960 to 2015 in Norway, Sweden and Finland. *Carbon Balance Manag.* **2018**, *13* (1). https://doi.org/10.1186/s13021–018–0101–9.

21. Butarbutar, T.; Köhl, M.; Neupane, P. R. Harvested Wood Products and REDD+: Looking beyond the Forest Border. *Carbon Balance Manag.* **2016**, *11* (1). https://doi.org/10.1186/s13021–016–0046–9.

22. Zhanga, B.; Lan, K.; Harris, T.; Ashton, M.; Yao, Y. Climate–Smart Forestry through Innovative Wood Products and Commercial Afforestation and Reforestation on Marginal Land. *Environ. Sci. Ecol.* **2023**, *120* (23), e2221840120. https://doi.org/https://doi.org/10.1073/pnas.2221840120.

23. UNECE/FAO. *"Chapter 1 Economic Overview and Policies" in Forest Products–Annual Market Review 2020–2021*; 2021.

24. Pei, S.; van de Lindt, J. W.; Popovski, M.; Berman, J. W.; Dolan, J. D.; Ricles, J.; Sause, R.; Blomgren, H.; Rammer, D. R. Cross–Laminated Timber for Seismic Regions: Progress and Challenges for Research and Implementation. *J. Struct. Eng.* **2016**, *142* (4), 1–11. https://doi.org/10.1061/(asce)st.1943–541x.0001192.

25. D'Amico, B.; Pomponi, F.; Hart, J. Global Potential for Material Substitution in Building Construction: The Case of Cross Laminated Timber. *J. Clean. Prod.* **2021**, *279*, 123487. https://doi.org/10.1016/j.jclepro.2020.123487.

26. Araújo, C. K. de C.; Salvador, R.; Piekarski, C. M.; Sokulski, C. C.; de Francisco, A. C.; Camargo, S. K. de C. A. Circular Economy Practices on Wood Panels: A Bibliographic Analysis. *Sustain.* **2019**, *11* (4), 1–21. https://doi.org/10.3390/su11041057.

27. Ansell, M. P. Wood Composites. In *Handbook of Wood Chemistry and Wood Composites*; 2005; pp 281–301. https://doi.org/10.1016/C2014–0–02700–1.

28. Heinrich, L. A. Future Opportunities for Bio–Based Adhesives–Advantages beyond Renewability. *Green Chem.* **2019**, *21* (8), 1866–1888. https://doi.org/10.1039/c8gc03746a.

29. Dunky, M. Adhesives in the Wood Industry. In *Handbook of Adhesive Technology, Third Edition*; 2003; pp 223–262. https://doi.org/10.1201/9781315120942.

30. Vendamme, R.; Schüwer, N.; Eevers, W. Recent Synthetic Approaches and Emerging Bio–Inspired Strategies for the Development of Sustainable Pressure–Sensitive Adhesives Derived from Renewable Building Blocks. *J. Appl. Polym. Sci.* **2014**, *131* (17), 8379–8394. https://doi.org/10.1002/app.40669.

31. Pizzi, A.; Papadopoulos, A. N.; Policardi, F. Wood Composites and Their Polymer Binders. *Polymers (Basel).* **2020**, *12* (5). https://doi.org/10.3390/POLYM12051115.

32. Science, W. M.; Kristak, L.; Antov, P.; Bekhta, P. Recent Progress in Ultra–Low Formaldehyde Emitting Adhesive Systems and Formaldehyde Scavengers in Wood–Based Panels : A Review. *Wood Mater. Sci. Eng.* **2023**, *18* (2), 763–782. https://doi.org/10.1080/17480272.2022.2056080.

33. Paiva, N. T.; Henriques, A.; Cruz, P.; Ferra, J.; Carvalho, L. Production of Melamine Fortified Urea–Formaldehyde Resins with Low Formaldehyde Emission. *J. Appl. Polym. Sci.* **2012**, *124*, 2311–2317.

34. Petinarakis, J. H.; Kavvouras, P. K. Technological Factors Affecting the Emission of Formaldehyde from Particleboards. *Wood Res.* **2006**, *51* (1), 31–40.

35. Moubarik, A.; Allal, A.; Pizzi, A. P. Characterization of a Formaldehyde–Free Cornstarch–Tannin Wood Adhesive for Interior Plywood Journal: *Eur. J. Wood Wood Prod.* **2010**, *68* (4), 427–433. https://doi.org/10.1007/s00107–009–0379–0.

36. Bekhta, P.; Sedliačik, J.; Jones, D. Effect of Short–Term Thermomechanical Densification of Wood Veneers on the Properties of Birch Plywood. *Eur. J. Wood Wood Prod.* **2018**, *76* (2), 549–562. https://doi.org/10.1007/s00107–017–1233–4.

37. Pizzi. Wood Adhesives: Chemistry and Technology. *Marcel Dekker New York, NY, USA* **1983**.

38. Swenberg, J. A.; Moeller, B. C.; Lu, K.; Rager, J. E.; Fry, R. C.; Starr, T. B. Formaldehyde Carcinogenicity Research: 30 Years and Counting for Mode of Action, Epidemiology, and Cancerrisk Assessment. *Toxicol. Pathol.* **2012**, *00*, 1–9. https://doi.org/10.1177/0192623312466459.

39. Lei, H.; Frazier, C. E. Curing Behavior of Melamine–Urea–Formaldehyde (MUF) Resin Adhesive. *Int. J. Adhes. Adhes.* **2015**, *62*, 40–44. https://doi.org/10.1016/j.ijadhadh.2015.06.013.

40. Hemmilä, V.; Adamopoulos, S.; Karlsson, O.; Kumar, A. Development of Sustainable Bio–Adhesives for Engineered Wood Panels–A Review. *R. Soc. Chem.* **2017**, *7* (61), 38604–38630. https://doi.org/10.1039/c7ra06598a.

41. Cesprini, E.; Resente, G.; Causin, V.; Urso, T.; Cavalli, R.; Zanetti, M. Energy Recovery of Glued Wood Waste – A Review. *Fuel* **2020**, *262*, 116520.

https://doi.org/10.1016/j.fuel.2019.116520.

42. Wilts, H.; Brien, M. O. A Policy Mix for Resource Efficiency in the EU : Key Instruments , Challenges and Research Needs. *Ecol. Econ.* **2019**, *155*, 59–69. https://doi.org/10.1016/j.ecolecon.2018.05.004.

43. Domenech, T.; Bahn–walkowiak, B. Transition towards a Resource Efficient Circular Economy in Europe: Policy Lesson from the EU and the Members States. *Ecol. Econ.* **2017**, *155*, 7–19. https://doi.org/10.1016/j.ecolecon.2017.11.001.

44. Pizzi, A. Wood Products and Green Chemistry. *Ann. For. Sci.* **2016**, *73* (1), 185–203. https://doi.org/10.1007/s13595–014–0448–3.

45. Nordqvist, P.; Nordgren, N.; Khabbaz, F.; Malmström, E. Plant Proteins as Wood Adhesives : Bonding Performance at the Macro– and Nanoscale. *Ind. Crop. Prod.* **2013**, *44*, 246–252. https://doi.org/10.1016/j.indcrop.2012.11.021.

46. Patel, A. R.; Velikov, K. P. Zein as a Source of Functional Colloidal Nano– and Microstructures. *Curr. Opin. Colloid Interface Sci.* **2014**, *19* (5), 450–458. https://doi.org/10.1016/j.cocis.2014.08.001.

47. Bernard, J. K. Feed Concentrates : Oilseed and Oilseed Meals. In *Reference Module in Food Science*; 2016; pp 349–355. https://doi.org/10.1016/B978–0–08–100596–5.00756–3.

48. Jaski, A. C.; Schmitz, F.; Horta, R. P.; Cadorin, L.; Silva, B.; Andreaus, J.; Paes, M. C.; Riegel–Vidotti, I.; Zimmermann, L. Zein – a Plant–Based Material of Growing Importance: New Perspectives for Innovative Uses. *Ind. Crops Prod.* **2022**, *186*, 115250. https://doi.org/10.1016/j.indcrop.2022.115250.

49. Qi, G.; Li, N.; Wang, D.; Sun, X. S. Physicochemical Properties of Soy Protein Adhesives Obtained by In Situ Sodium Bisulfite Modification During Acid Precipitation. **2012**, 301–312. https://doi.org/10.1007/s11746–011–1909–6.

50. Ou, X.; Xue, B.; Lao, Y.; Wutthinitikornkit, Y.; Tian, R.; Zou, A.; Yang, L.; Wang, W.; Cao, Y.; Li, J. Structure and Sequence Features of Mussel Adhesive Protein Lead to Its Salt–Tolerant Adhesion Ability. **2020**, *6*, 1–12.

51. Lei, H.; Pizzi, A.; Navarrete, P.; Rigolet, S.; Redl, A.; Wagner, A. Gluten Protein Adhesives for Wood Panels. **2010**, *24*, 1583–1596. https://doi.org/10.1163/016942410X500963.

52. Masina, N.; Choonara, Y. E.; Kumar, P.; Toit, L. C.; Govender, M.; Indermun, S.; Pillay, V. A Review of the Chemical Modification Techniques of Starch. *Carbohydr. Polym.* **2016**. https://doi.org/10.1016/j.carbpol.2016.09.094.

53. Amico, S. D.; Hrabalova, M.; Müller, U.; Berghofer, E. Bonding of Spruce Wood with Wheat Flour Glue — Effect of Press Temperature on the Adhesive Bond Strength. **2010**, *31*, 255–260. https://doi.org/10.1016/j.indcrop.2009.11.001.

54. Moubarik, A.; Causse, N.; Poumadere, T.; Allal, A. Shear Refinement of Formaldehyde–Free Corn Starch and Mimosa Tannin (Acacia Mearnsii) Wood Adhesives. *J. Adhes. Sci. Technol.* **2011**, *2*, 1–13. https://doi.org/10.1163/016942411X576176.

55. Glasser, W. G. About Making Lignin Great Again—Some Lessons From the Past. *Front. Chem.* **2019**, *7*, 1–17. https://doi.org/10.3389/fchem.2019.00565.

56. Ghaffar, S. H.; Fan, M. Lignin in Straw and Its Applications as an Adhesive. *Int. J. Adhes. Adhes.* **2014**, *48*, 92–101. https://doi.org/10.1016/j.ijadhadh.2013.09.001.

57. Mansouri, N. El; Salvad, J. Structural Characterization of Technical Lignins for the Production of Adhesives : Application to Lignosulfonate , Kraft , Soda–Anthraquinone , Organosolv and Ethanol Process Lignins. **2006**, *24*, 8–16. https://doi.org/10.1016/j.indcrop.2005.10.002.

58. Tejado, A.; Peña, C.; Labidi, J.; Echeverria, J. M.; Mondragon, I. Physico–Chemical Characterization of Lignins from Different Sources for Use in Phenol–Formaldehyde Resin Synthesis. *Bioresour. Technol.* **2007**, *98* (8), 1655–1663. https://doi.org/10.1016/j.biortech.2006.05.042.

59. Lora, J. H.; Glasser, W. G. Recent Industrial Applications of Lignin : A Sustainable Alternative to Nonrenewable Materials. **2002**, *10* (April).

60. Widsten, P.; Kandelbauer, A. Adhesion Improvement of Lignocellulosic Products by Enzymatic Pre–Treatment. **2008**, *26*, 379–386. https://doi.org/10.1016/j.biotechadv.2008.04.003.

61. Ma, R.; Xu, Y.; Zhang, X. Catalytic Oxidation of Biorefinery Lignin to Value–Added Chemicals to Support Sustainable Biofuel Production. **2014**, 1–29. https://doi.org/10.1002/cssc.201402503.

62. Bisanda, E. T. N.; Ogola, W. O.; Tesha, J. V. Characterisation of Tannin Resin Blends for Particle Board Applications. *Cem. Concr. Compos.* **2003**, *25* (6), 593–598. https://doi.org/10.1016/S0958–9465(02)00072–0.

63. Drewes, S.; Roux, D. Condensed Tannins. 15. Interrelationships of Flavonoid Components in Wattle–Bark Extract. *Biochem. J.* **1963**, *87* (1), 167–172. https://doi.org/10.1042/bj0870167.

64. Pizzi, A. Tannins: Prospectives and Actual Industrial Applications. *Biomolecules* **2019**, *9*, 344. https://doi.org/10.3390/biom9080344.

65. Lorenz, L.; Conner, A.; Christiansen, A. The Effect of Soy Protein Additions on the Reactivity and Formaldehyde Emission of UF Adhesive Resins. **1999**, *49* (3), 73–78.

66. Ferdosian, F.; Pan, Z.; Gao, G.; Zhao, B. Bio–Based Adhesives and Evaluation for Wood Composites Application. *Polymers (Basel).* **2017**, *9* (2). https://doi.org/10.3390/polym9020070.

67. Imam, S. H.; Mao, L.; Diego, S.; Chen, L.; Greene, R. V. Wood Adhesive from Crosslinked Poly (Vinyl Alcohol) and Partially Gelatinized Starch : Preparation and Properties. *Starch/Stärke* **1999**, *51* (6), 225–229.

68. Qiao, Z.; Gu, J.; Lv, S.; Cao, J.; Tan, H.; Zhang, Y. Preparation and Properties of Normal Temperature Cured Starch–Based Wood Adhesive. *BioResources* **2016**, *11* (2), 4839–4849. https://doi.org/10.15376/biores.11.2.4839–4849.

69. Danielson, B.; Simonson, R. Journal of Adhesion Science and Kraft Lignin in Phenol Formaldehyde Resin . Part 1 . Partial Replacement of Phenol by Kraft Lignin in Phenol Formaldehyde Adhesives for Plywood. *J. Adhes. Sci. Technol.* **1998**, *12* (9), 923–939. https://doi.org/10.1163/156856198X00542.

70. Zhang, W.; Ma, Y.; Wang, C.; Li, S.; Zhang, M.; Chu, F. Preparation and Properties of Lignin – Phenol – Formaldehyde Resins Based on Different Biorefinery Residues of Agricultural

Biomass. *Ind. Crop. Prod.* **2013**, *43*, 326–333. https://doi.org/10.1016/j.indcrop.2012.07.037.

71. Akhtar, T.; Lutfullah, G.; Ullah, Z. Lignonsulfonate–Phenolformaldehyrde Adhesive: A Potential Binder for Wood Panel Industries. *J. Chem. Soc. Pakistan* **2011**, *33(4)*, 535–538.

72. Wei, J.; Wei, C.; Su, L.; Fu, J.; Lv, J. Synergistic Reinforcement of Phenol–Formaldehyde Resin Composites by Poly (Hexanedithiol)/ Graphene Oxide. *J. Mater. Sci. Chem. Eng.* **2015**, *3*, 56–70. https://doi.org/http://dx.doi.org/10.4236/msce.2015.38009.

73. Pizzi, A. P. Industrial Application of Wattle Tannin/Urea–Formaldehyde Fortified Starch Adhesives for Damp–Proof Corrugated Cardboard. *Holzforsch. und Holzverwertung* **1979**, *6*, 131–133.

74. Hoong, Y. B.; Paridah, M. T.; Luqman, C. A.; Koh, M. P.; Loh, Y. F. Fortification of Sulfited Tannin from the Bark of Acacia Mangium with Phenol – Formaldehyde for Use as Plywood Adhesive. **2009**, *30*, 416–421. https://doi.org/10.1016/j.indcrop.2009.07.012.

75. Tahir, P.; Halip, J. A.; Lee, S. H. Tannin–Based Bioresin as Adhesives. In *Lignocellulose for Future Bioeconomy*; 2019; pp 109–133. https://doi.org/10.1016/B978–0–12–816354–2.00007–4.

76. Pizzi, A.; Roux, D. G. The Chemistry and Development of Tannin–Based Weather–Proof and Boil–Proof Cold–Setting and Fast–Setting Adhesives for Wood. *J. Appl. Polym. Sci.* **1978**, *22* (7), 1945–1954.

77. Pizzi, A. Polyflavonoid Tannins Self– Condensation Adhesives For. **2009**, *85* (2–3), 57–68. https://doi.org/10.1080/00218460902781917.

78. Wang, Y.; Wang, D.; Sun, X. S. Thermal Properties and Adhesiveness of Soy Protein Modified with Cationic Detergent. **2005**, *82* (5), 357–363.

79. Cheng, H. N.; Ford, C.; Dowd, M. K.; He, Z. Use of Additives to Enhance the Properties of Cottonseed Protein as Wood Adhesives. *Int. J. Adhes. Adhes.* **2016**, *68*, 156–160. https://doi.org/10.1016/j.ijadhadh.2016.02.012.

80. Nordqvist, P.; Khabbaz, F.; Malmstr, E. Comparing Bond Strength and Water Resistance of Alkali–Modified Soy Protein Isolate and Wheat Gluten Adhesives. **2010**, *30*, 72–79. https://doi.org/10.1016/j.ijadhadh.2009.09.002.

81. Nie, Y. of different duration of acid hydrolisi on the properties starch based wood adhesive. pdfna.; Tian, X.; Liu, Y.; Wu, K.; Wang, J. Research on Starch– g –Polyvinyl Acetate and Epoxy Resin–Modified Corn Starch Adhesive. *Polym. Compos.* **2013**, 87. https://doi.org/10.1002/pc.

82. Wang, A. Y.; Xiong, H.; Wang, Z.; Chen, L. Effects of Different Durations of Acid Hydrolysis on the Properties of Starch–Based Wood Adhesive. *Int. J. Biol. Macromol.* **2017**, *103*, 819–828. https://doi.org/10.1016/j.ijbiomac.2017.05.102.

83. Alonso, M. V; Rodrı, J. J.; Oliet, M.; Rodrı, F. Characterization and Structural Modification of Ammonic Lignosulfonate by Methylolation. **2001**, 2661–2668. https://doi.org/10.1002/app.2119.

84. Benar, P.; Gonçalves, A. R.; Mandelli, D.; Schuchardt, U. Eucalyptus Organosolv Lignins: Study of the Hydroxymethylation and Use in Resols. *Bioresour. Technol.* **1999**, *68* (1), 11–16. https://doi.org/10.1016/S0960–8524(98)00076–5.

85. Cetin, N. S.; Ozmen, N. Use of Organosolv Lignin in Phenol – Formaldehyde Resins for Particleboard Production I . Organosolv Lignin Modified Resins. **2002**, *22*, 477–480.

86. Zhang, T.; Yu, C.; Yu, M.; Huang, Y.; Tan, J.; Zhang, M.; Zhu, X. Multifunctional Tannin Extract–Based Epoxy Ts Derived from Waste Bark as a Highly Toughening and Strengthening Agent for Epoxy Resin. *Ind. Crop. Prod.* **2022**, *176*, 114255. https://doi.org/10.1016/j.indcrop.2021.114255.

87. Pizzi, A.; Inrae, E. A.; Aiguillettes, B. Little Secrets for the Successful Industrial Use of Tannin Adhesives : A Review. **2023**. https://doi.org/10.32604/jrm.2023.030930.

88. Özacar, M.; Soykan, C.; Şengil, I. A. Studies on Synthesis, Characterization, and Metal Adsorption of Mimosa and Valonia Tannin Resins. *J. Appl. Polym. Sci.* **2006**, *102* (1), 786–797. https://doi.org/10.1002/app.23944.

89. Pizzi, A. Natural Phenolic Adhesives I: Tannin. In *Handbook of adhesive technology 2*; Marcel Dekker Madison, Ed.; 2003; pp 573–589.

90. Chatterjee, A.; Rakshit, A.; Singh, N. N. Strategies for the Determination of Bioactive Phenols in Plants, Fruit and Vegetables. *J. Chromatogr. A* **2003**, *1000*, 657–691. https://doi.org/10.1007/978–3–642–33965–3_2.

91. Sealy–Fisher, V. J.; Pizzi, A. Increased Pine Tannins Extraction and Wood Adhesives Development by Phlobaphenes Minimization. *Holz als Roh– und Werkst.* **1992**, *50* (5), 212–220. https://doi.org/10.1007/BF02663290.

92. Vázquez, G.; Antorrena, A.; Parajó, J. C. Selection of Operational Conditions in Alkaline Lixiviation of Pinus Pinaster Bark. *Holz als Roh– und Werkst.* **1986**, *44* (11), 415–418. https://doi.org/10.1007/BF02609635.

93. Arbenz, A.; Avérous, L. Chemical Modification of Tannins to Elaborate Aromatic Biobased Macromolecular Architectures. *Green Chem.* **2015**, *17* (5), 2626–2646. https://doi.org/10.1039/c5gc00282f.

94. Pizzi, A. Tannin–Based Adhesives. *J. Macromol. Sci. Part C* **1980**, *C18* (2), 247–315.

95. Yazaki, Y.; Hillis, W. E. Molecular Size Distribution of Radiata Pine Bark Extracts and Its Effect on Properties. *Holzforschung* **1980**, *34* (4), 125–130. https://doi.org/10.1515/hfsg.1980.34.4.125.

96. Martinez, S. Inhibitory Mechanism of Mimosa Tannin Using Molecular Modeling and Substitutional Adsorption Isotherms. *Mater. Chem. Phys.* **2003**, *77* (1), 97–102. https://doi.org/10.1016/S0254–0584(01)00569–7.

97. Vázquez, G.; Antorrena, G.; Parajó, J. C.; Francisco, J. L. Preparation of Wood Adhesives by Polycondensation of Phenolic Acids from Pinus Pinaster Bark with Resoles. *Holz als Roh– und Werkst.* **1989**, *47* (12), 491–494. https://doi.org/10.1007/BF02613031.

98. Aspé, E.; Fernández, K. The Effect of Different Extraction Techniques on Extraction Yield, Total Phenolic, and Anti–Radical Capacity of Extracts from Pinus Radiata Bark. *Ind. Crops Prod.* **2011**, *34* (1), 838–844. https://doi.org/10.1016/j.indcrop.2011.02.002.

99. Dhawale, P. V.; Vineeth, S. K.; Gadhave, R. V.; Fatima M. J., J.; Supekar, M. V.; Thakur, V. K.; Raghavan, P. Tannin as a Renewable Raw Material for Adhesive Applications: A Review.

Mater. Adv. **2022**. https://doi.org/10.1039/d1ma00841b.

100. Valenzuela, J.; Von Leyser, E.; Pizzi, A.; Westermeyer, C.; Gorrini, B. Industrial Production of Pine Tannin–Bonded Particleboard and MDF. *Eur. J. Wood Wood Prod.* **2012**, *70* (5), 735–740. https://doi.org/10.1007/s00107–012–0610–2.

101. Trosa, A.; Mondovi, S. M.; Pizzi, A. Stability and Performance of Tannin–Accelerated PF Resins for Plywood. **2000**, *55* (1997), 1997.

102. Moubarik, A.; Pizzi, A.; Allal, A.; Charrier, F.; Charrier, B. Cornstarch and Tannin in Phenol–Formaldehyde Resins for Plywood Production. *Ind. Crops Prod.* **2009**, *30* (2), 188–193. https://doi.org/10.1016/j.indcrop.2009.03.005.

103. El–Sayed, E. S.; El–Sakhawy, M.; Kamel, S.; El–Gendy, A.; Abou–Zeid, R. E. Eco–Friendly Mimosa Tannin Adhesive System for Bagasse Particleboard Fabrication. *Egypt.J.Chem* **2019**, *65* (5), 1–12. https://doi.org/10.21608/ejchem.2018.5413.1479.

104. Sylvi, D.; Ismed, I.; Merlin, S. Characteristics of Mangium (Acacia Mangium) Bark Extract with Some Extraction Time and Its Application to Cotton Fabric Dyeing. *EKSAKTA* **2022**, *23* (04), 329–342. https://doi.org/https://doi.org/10.24036/eksakta/vol23–iss04/362.

105. Sowunmi, S.; Ebewele, R. O.; Conner, A. H.; River, B. H. Fortified Mangrove Tannin–Based Plywood Adhesive. *J. Appl. Polym. Sci.* **1996**, *62* (3), 577–584. https://doi.org/10.1002/(sici)1097–4628(19961017)62:3<577::aid–app15>3.3.co;2–x.

106. Irman, N.; Abd Latif, N. H.; Brosse, N.; Gambier, F.; Syamani, F. A.; Hussin, M. H. Preparation and Characterization of Formaldehyde–Free Wood Adhesive from Mangrove Bark Tannin. *Int. J. Adhes. Adhes.* **2022**, *114*, 103094. https://doi.org/10.1016/j.ijadhadh.2022.103094.

107. Pizzi, A.; Valenzuela, J.; Westermeyer, C. Low Formaldehyde Emission, Fast Pres– Sing, Pine and Pecan Tannin Adhesives for Exterior Particleboard. *Holz Roh. Werkst.* **1994**, *52*, 311–315.

108. Lu, Y.; Shi, Q. Larch Tannin Adhesive for Particleboard. *Holz Roh. Werkst.* **1995**, *53*, 17–19.

109. Wang, W.; Zhang, W.; Li, J. Reactivity of Larch and Valonia Tannins in Synthesis of Tannin–Formaldehyde Resins. *BioResources* **2016**, *11*, 2256–2268. https://doi.org/10.15376/biores.11.1.2256–2268.

110. Santos, S. C.; Costa, W. F.; Ribeiro, J. P.; Guimarães, D. O.; Ferri, P. H.; Ferreira, H. D.; Seraphin, J. C. Tannin Composition of Barbatimão Species. *Fitoterapia* **2002**, *73* (4), 292–299. https://doi.org/10.1016/S0367–326X(02)00081–3.

111. Carvalho, A. G.; Mori, F. A.; Mendes, R. F.; Zanuncio, A. J. V.; Silva, M. G. da; Mendes, L. M.; De Oliveira Mori, C. L. . Use of Tannin Adhesive from Stryphnodendron Adstringens (Mart.) Coville in the Production of OSB Panels. *Eur. J. Wood Prod.* **2014**, *72*, 425–432.

112. Sartori, C. J.; Mota, G. S.; Miranda, I.; Mori, F. A.; Pereira, H. Tannin Extraction and Characterization of Polar Extracts from the Barks of Two Eucalyptus Urophylla Hybrids. *BioResources* **2019**, *13* (3), 4820–4831. https://doi.org/10.15376/biores.13.3.4820–4831.

113. Hussein, A. S.; Ibrahim, K. I.; Abdulla, K. . Tannin–Phenol Formaldehyde Resins as Binders for Cellulosic Fibers: Mechanical Properties. *Nat. Resour.* **2011**, *2*, 98–101.

114. Ping, L.; Pizzi, A.; Guo, Z. D.; Brosse, N. Condensed Tannins Extraction from Grape Pomace: Characterization and Utilization as Wood Adhesives for Wood Particleboard. *Ind. Crop. Prod.*

2011, *34* (1), 907–914. https://doi.org/https://doi.org/10.1016/j.indcrop.2011.02.009.

115. Ping, L.; Pizzi, A.; Guo, Z. D.; Brosse, N. Condensed Tannins from Grape Pomace: Characterization by FTIR and MALDI TOF and Production of Environment Friendly Wood Adhesive. *Ind. Crop. Prod.* **2012**, *40*, 13–20. https://doi.org/https://doi.org/10.1016/j.indcrop.2012.02.039.

116. Ballerini, A.; Despres, A.; Pizzi, A. Non–Toxic, Zero Emission Tannin–Glyoxal Adhesives for Wood Panels. *Holz als Rohund Werkst.* **2005**, *63* (6), 477–478. https://doi.org/https://doi.org/10.1007/s00107–005–0048–x.

117. Dunky, M. Wood Adhesives Based on Natural Resources: A Critical Review: Part III. Tannin– and Lignin–Based Adhesives. *Prog. Adhes. Adhes. Vol. 6* **2021**, *6*, 383–530. https://doi.org/10.1002/9781119846703.ch10.

118. Rossouw, D. du T.; Pizzi, A.; McGillivray, G. The Kinetics of Condensation of Phenolic Polyflavonoid Tannins With Aldehydes. *J. Polym. Sci. A1.* **1980**, *18* (12), 3323–3343. https://doi.org/10.1002/pol.1980.170181201.

119. Tondi, G. Tannin–Based Copolymer Resins: Synthesis and Characterization by Solid State 13C NMR and FT–IR Spectroscopy. *Polymers (Basel).* **2017**, *9* (6). https://doi.org/10.3390/polym9060223.

120. Soto, R.; Freer, J.; Baeza, J. Evidence of Chemical Reactions between Di– and Poly–Glycidyl Ether Resins and Tannins Isolated from Pinus Radiata D. Don Bark. *Bioresour. Technol.* **2005**, *96* (1), 95–101. https://doi.org/10.1016/j.biortech.2003.05.006.

121. Pizzi, A. Hardening Mechanism of Tannin Adhesives with Hexamine. *Eur. J. Wood Wood Ind.* **1994**, *52*, 229–229. https://doi.org/10.1007/BF02619098.

122. Vázquez, G.; Santos, J.; Freire, M. S.; Antorrena, G.; González–Álvarez, J. DSC and DMA Study of Chestnut Shell Tannins for Their Application as Wood Adhesives without Formaldehyde Emission. *J. Therm. Anal. Calorim.* **2012**, *108* (2), 605–611. https://doi.org/10.1007/s10973–011–2138–9.

123. Valenzuela, J.; Westermeyer, C. Non–Emulsifiable, Water–Based, Mixed Diisocyanate Adhesive Systems for Exterior Plywood : Part II. Theory Application and Industrial Results. *Holzforschung* **1993**, *47* (1), 68–71. https://doi.org/10.1515/hfsg.1993.47.1.68.

124. Gonultas, O. Properties of Pine Bark Tannin–Based Adhesive Produced with Various Hardeners. *BioResources* **2018**, *13* (4), 9066–9078. https://doi.org/10.15376/BIORES.13.4.9066–9078.

125. Thébault, M.; Pizzi, A.; Essawy, H. A.; Barhoum, A.; Van Assche, G. Isocyanate Free Condensed Tannin–Based Polyurethanes. *Eur. Polym. J.* **2015**, *67*, 513–526. https://doi.org/10.1016/j.eurpolymj.2014.10.022.

126. Trosa, A.; Pizzi, A. A No–Aldehyde Emission Hardener for Tannin–Based Wood Adhesives for Exterior Panels. *Holz als Roh – und Werkst.* **2001**, *59* (4), 266–271. https://doi.org/10.1007/s001070100200.

127. Gandini, A. Polymers from Renewable Resources: A Challenge for the Future of Macromolecular Materials. *Macromolecules* **2008**, *41* (24), 9491–9504. https://doi.org/10.1021/ma801735u.

128. Tondi, G.; Cefarin, N.; Sepperer, T.; D'Amico, F.; Berger, R. J. F.; Musso, M.; Birarda, G.; Reyer, A.; Schnabel, T.; Vaccari, L. Understanding the Polymerization of Polyfurfuryl Alcohol: Ring Opening and Diels–Alder Reactions. *Polymers (Basel).* **2019**, *11* (12), 1–15. https://doi.org/10.3390/polym11122126.

129. Patel, D. S.; Toliwal, S. D.; Patel, J. V. Eco–Friendly Adhesives Based on Tannin and N,N–Bis(2–Hydroxy–Ethyl) Fatty Amides (HEFAs) from Non–Traditional Oils for Wood Bonding. *J. Adhes. Sci. Technol.* **2012**, *26* (18–19), 2217–2227. https://doi.org/10.1163/156856111X610144.

130. Pizzi, A.; Stephanou, A. Fast vs. Slow–Reacting Non–Modified Tannin Extracts for Exterior Particleboard Adhesives. **1994**, *52*, 218–222. https://doi.org/https://doi.org/10.1007/BF02619095.

131. Navarrete, P.; Pizzi, A.; Pasch, H.; Rode, K.; Delmotte, L. Characterization of Two Maritime Pine Tannins as Wood Adhesives. *J. Adhes. Sci. Technol.* **2013**, *27* (22), 2462–2479. https://doi.org/10.1080/01694243.2013.787515.

132. A., B.; Despres, A.; A. Pizzi. Non–Toxic, Zero Emission Tannin–Glyoxal Adhesives for Wood Panels. *Holz Roh. Werkst.* **2005**, *63*, 477–478.

133. Hani, U.; Abdullah, B. Tannin–Furfuryl Alcohol Wood Panel Adhesives without Formaldehyde. **2013**, 71:131–132. https://doi.org/10.1007/s00107–012–0629–4.

134. Luckeneder, P.; Gavino, J.; Kuchernig, R.; Petutschnigg, A.; Tondi, G. Sustainable Phenolic Fractions as Basis for Furfuryl Alcohol–Based Co–Polymers and Their Use as Wood Adhesives. *Polymers (Basel).* **2016**, *8* (11), 396. https://doi.org/10.3390/polym8110396.

135. Santiago–Medina, F. J.; Pizzi, A.; Abdalla, S. Hydroxymethylfurfural Hardening of Pine Tannin Wood Adhesives. *J. Renew. Mater.* **2017**, *5*, 435–447. https://doi.org/10.7569/JRM.2017.634166.

136. Pichelin, F.; Nakatani, M.; Pizzi, A.; Wieland, S.; Despres, A.; Rigolet, S. Structural Beams from Thick Wood Panels Bonded Industrially with Formaldehyde–Free Tannin Adhesives. *For. Prod. J.* **2006**, *56* (5), 31–36.

137. Xu, G.; Zhang, Q.; Xi, X.; Lei, H.; Cao, M.; Du, G.; Wu, Z. Tannin–Based Wood Adhesive with Good Water Resistance Crosslinked by Hexanediamine. *Int. J. Biol. Macromol.* **2023**, *234*, 123644. https://doi.org/10.1016/j.ijbiomac.2023.123644.

138. Zhou, X.; Pizzi, A. Pine Tannin Based Adhesive Mixes for Plywood. *Int. Wood Prod. J.* **2014**, *5* (1), 27–32. https://doi.org/10.1179/2042645313Y.0000000043.

139. Bauman, H.; Tillman, A. The Hitch Hiker´s Guide to LCA – An Orientation in LCA Methodology and Application. *Int. J. Life Cycle Assess.* **2004**, *11* (2), 142–142. https://doi.org/10.1065/lca2006.02.008.

140. British Standards. BSI Standards Publication Environmental Management — Life Cycle Assessment — Principles and Framework BS EN ISO 14040:2006+A1:2020. *Br. Stand.* **2006**.

141. British Standards. BSI Standards Publication Environmental Management — Life Cycle Assessment — Principles and Framework BS EN ISO 14044:2006+A2:2020. *Br. Stand.* **2006**.

142. Chen, J.; Ter–Mikaelian, M. T.; Yang, H.; Colombo, S. J. Assessing the Greenhouse Gas Effects of Harvested Wood Products Manufactured from Managed Forests in Canada. *Forestry* **2018**,

91 (2), 193–205. https://doi.org/10.1093/forestry/cpx056.

143. Sahoo, K.; Bergman, R.; Alanya–Rosenbaum, S.; Gu, H.; Liang, S. Life Cycle Assessment of Forest–Based Products: A Review. *Sustain.* **2019**, *11* (17), 1–30. https://doi.org/10.3390/su11174722.

144. Pierobon, F.; Zanetti, M.; Grigolato, S.; Sgarbossa, A.; Anfodillo, T.; Cavalli, R. Life Cycle Environmental Impact of Firewood Production – A Case Study in Italy. *Appl. Energy* **2015**, *150*, 185–195. https://doi.org/10.1016/j.apenergy.2015.04.033.

145. Sgarbossa, A.; Boschiero, M.; Pierobon, F.; Cavalli, R.; Zanetti, M. Comparative Life Cycle Assessment of Bioenergy Production from Differentwood Pellet Supply Chains. *Forests* **2020**, *11*, 1127. https://doi.org/10.3390/f11111127.

146. Chen, C. X.; Pierobon, F.; Ganguly, I. Life Cycle Assessment (LCA) of Cross–Laminated Timber (CLT) Produced in Western Washington: The Role of Logistics and Wood Species Mix. *Sustain.* **2019**, *11* (5). https://doi.org/10.3390/su11051278.

147. Corradini, G.; Pierobon, F.; Zanetti, M. Product Environmental Footprint of a Cross–Laminated Timber System: A Case Study in Italy. **2019**, *24* (5), 975–988. https://doi.org/10.1007/s11367–018–1541–x.

148. Pierobon, F.; Huang, M.; Simonen, K.; Ganguly, I. Environmental Benefits of Using Hybrid CLT Structure in Midrise Non–Residential Construction: An LCA Based Comparative Case Study in the U.S. Pacific Northwest. *J. Build. Eng.* **2019**, *26*, 100862. https://doi.org/10.1016/j.jobe.2019.100862.

149. European Commission–Joint Research Center. COMMISSION RECOMMENDATION (EU) 2021/2279 of 15 December 2021 on the Use of the Environmental Footprint Methods to Measure and Communicate the Life Cycle Environmental Performance of Products and Organisations. *Off. J. Eur. Union L 471/1* **2021**.

150. Yang, M.; Rosentrater, K. A. Life Cycle Assessment of Urea–Formaldehyde Adhesive and Phenol–Formaldehyde Adhesives. *Environ. Process.* **2020**, *7* (2), 553–561. https://doi.org/10.1007/s40710–020–00432–9.

151. McDevitt, J. E.; Grigsby, W. J. Life Cycle Assessment of Bio– and Petro–Chemical Adhesives Used in Fiberboard Production. *J. Polym. Environ.* **2014**, *22* (4), 537–544. https://doi.org/10.1007/s10924–014–0677–4.

152. Yang, M.; Rosentrater, K. A. Life Cycle Assessment and Techno–Economic Analysis of Pressure Sensitive Bio–Adhesive Production. *Energies* **2019**, *12* (23). https://doi.org/10.3390/en12234502.

153. Arias, A.; González–García, S.; Feijoo, G.; Moreira, M. T. Environmental Benefits of Soy–Based Bio–Adhesives as an Alternative to Formaldehyde–Based Options. *Environ. Sci. Pollut. Res.* **2021**, 29781–29794. https://doi.org/10.1007/s11356–021–12766–4.

2. Objective and thesis structure

In the contemporary context, it is imperative to prioritise our key concerns, particularly in the efficient utilisation of Earth's resources. Despite the fact that numerous resources are not fully harnessed, there exists a significant opportunity to elevate the value of wood products as an innovative renewable material. Indeed, the overarching objective of this research project was to develop a wood bio adhesive for EWPs that demonstrates physical and mechanical characteristics comparable with the corresponding commercially available synthetic resins, in order to obtain products that are less and less dependent on non–renewable resources.

The three-year research endeavour unfolded along a logical trajectory, anchored in the exploration of three main research questions (RQs) that served as a guiding thread throughout the study. The specific inquiries are detailed below:

1. RQ (1): Which natural resource holds the most promise features for the development of bioplastics intended for wood adhesive applications?
2. RQ (2): Do the formulated natural adhesives exhibit properties suitable for their intended applications, and how can those formulations be further optimized?
3. RQ (3): What environmental advantages are associated with utilizing natural resources in the production of wood adhesives?

In order to reply to RQ (1) an extended bibliographic research has been done at the beginning of the route, and as extensively described in the introductory chapter, , tannins have been selected due to their distinguished and intrinsic features which can be exploited to develop of bio adhesive for wood products. In this direction, the second most abundant commercial condensed tannin extract, due to its outstanding extraction yields, and known as quebracho (*Schinopsis balansae* Engl.), has been chosen as a starting resource for the research. This dark brown powder is chemically classified as condensed tannin, exhibiting a substantial phenolic content and a higher concentration of low–molecular–mass sugars compared to mimosa tannin. Consequently, a valuable reactivity is anticipated. The research project is therefore primarily focused on formulating adhesive resins using the industrially extract, named Fintan 737, supplied by the respected manufacturer SilvaTeam (Mondovì, CN, Italy). The extract has been slightly modified for adhesive application during the extraction process in order to increase its properties for adhesive purposes. Fintan 737 serves as an ideal industrial case study, allowing the extending of previously established findings with pine and spruce extracts, both condensed tannins, which are possible important resources. It should be noted that these alternatives are not currently available at the industrial level. This choice broadens the scope of the investigation, contributing to a comprehensive understanding of quebracho tannins and their potential as a building block in bio adhesive formulations.

The part related to the research outcomes (Chapter 4) has mainly divided into as many subchapters, shortly described underneath and each one containing one or more scientific articles published in indexed journals. The first subchapter (4.1), named “Synthesis and characterization of tannin–based polymers”, reports the systematic study of different hardeners for the production of tannin–based resins. The study aimed to comprehend the chemical and physical attributes of the developed resins, providing a comprehensive overview of various hardeners essential for the evolution of a polymer matrix.

The subsequent subchapter (4.2), titled “Application of bio–based tannin polymers to produce wood based materials”, aims to investigate the application of the most interesting resins studied in the previous chapter for the production of EWPs in order to reply to the RQ (2). Subsequentially, the next subchapter (4.3) delves into an assessment of the environmental impact of the silkworm cocoon production process in order to respond to RQ (3). The chapter is tiled as “Life cycle assessment of silk protein used in the tannin–based adhesive formulation”. Specifically, this research aims to investigate the environmental impact of the primary protein component of silkworm cocoons, which has been utilized as an additive in tannin developed formulation. This is the only study not yet published in an indexed journal.

Finally, in the last subchapter of results (4.4) a detailed account is provided for the physicochemical characterization of a polyphenolic extract with an initially unknown composition, which has been titled "Chemical investigation of wood polyphenolic extract".

3. Materials and methods

This chapter provides a concise summary of the materials and methods employed to investigate the objectives outlined in the "Objectives and thesis structure." More comprehensive details can be found in the scientific papers that make up this thesis.

Materials and chemicals

Quebracho tannin extract (*Schinopsis balansae* Engl), named Fintan 737B was kindly provided by the company Silva team (S. Michele Mondovì, CN, Italy) and involved as polyphenolic matrix to develop tannin based polymers. For the synthesis of wood adhesives, the hardening process employed a range of chemical reagents. Hexamethylenetetramine (hexamine), glyoxal, formaldehyde, and maleic anhydride were procured by Alfa–Aesar (Thermofisher, Waltham, MA, US), whereas furfural and furfuryl alcohol were supplied by International Furan Chemical IFC (Rotterdam, NL). Debarked cherry (*Prunus avium L.*) wood were provided by Silva Team (San Michele Mondovì, Italy) and used to extract cherry tannin for its chemical investigation. Industrial tannin powders of chestnut (*Castanea sativa* Mill.) and mimosa (*Acacia mearnsii* De Wild.) were supplied by Saviolife (Viadana, MN, Italy) and Silva Team (S. Michele Mondovì, CN, Italy) respectively, and were used as benchmark respectively for hydrolysable and condensed tannin. Sulphuric acid and sodium hydroxide were purchased by Alfa–Aesar (Thermofisher, Waltham, MA, US) and use to adjust the pH of the solutions. Other chemicals used during the research are briefly listed. High purity (≥99%) ethanol, sodium carbonate, sodium acetate trihydrate, acetic acid, 2,4,5–tripyridyl–s–triazine, HCl, ferric chloride, ammonium formate, pectin, and dextran were purchased from Sigma–Aldrich (St. Louis, MO, USA). Folin–Ciocalteu's phenol reagent and vanillin were purchased by Merck (Darmstadt, Germany). While sodium hydrogen carbonate, calcium chloride, and formic acid were supplied by Alfa Aesar (Thermo Fisher, Waltham, MA, USA). Lowest grade Bombyx mori silk cocoons was provided by a local research center (CREA–AA, Padova, Italy).

Methods

Synthesis of adhesive

Quebracho–tannin water solutions were prepared at different concentrations by weight, underwent vigorous stirring for homogeneity. Different pH and different hardener concentration were studied in order to obtain the best conditions for reaction reactions. Each particular reaction is later described in detail.

Adhesive characterization

Comprehensive characterization of the adhesive resins was achieved through a series of physical, mechanical, thermal, optical, spectroscopic and chemical analysis aiming to establish a thorough profile for each adhesive. The key findings of these primary tests are outlined below, while detailed technical information is provided in subsequent chapters of the thesis.

Physical–mechanical investigations

The gel time was measured by placing a certain amount of adhesive solution in a test tube and exposing it to 100 °C in an oil bath, and gelation times were recorded using a stopwatch, while the viscosity was analyzed with Rheometer Kinexus Lab from Malvern Panalytical (Malvern, UK). The leaching tests were conducted on tannin polymers cross–linked at 100 °C for 24 hours, and the calculation of the insoluble, hence crosslinked, component was carried out for all investigated resins.

Thermal investigation

Thermomechanical analysis of tannin resins was performed through TMA/SDTA840 Mettler Toledo instrument by both exothermic and non–exothermic methods. While, SDT 2960, Simultaneous DSC–TGA, TA instrument was used to measure the thermogram of cured samples.

Optical investigations

The morphological characterization of the adhesives was performed by scanning electron analysis with FEI Quanta scanning electron microscopy (variable pressure environmental E/SEM). While, a mechanically focused upright microscope (Leica DM4B) was used for wood slice observation.

Spectroscopic investigation

Solid–state 13C NMR experiments of the tannin cured and leached polymers were performed on a Bruker AVANCE NEO 400 MHz NMR spectrometer using a 4 mm CP–MAS probe. Fourier transform infrared (FTIR) spectra measurements were performed with several equipment's: (i) Nicolet, NEXUS, B70, FT–IR instrument and (ii) A Frontier FT–MIR from Perkin Elmer (Waltham, MA, USA), both equipped with an ATR accessory with a diamond crystal and (iii) Alpha (Bruker Optics) spectrometer equipped with a Platinum ATR module. FTIR hyperspectral images were acquired by using a bidimensional 64x64 pixels focal plane array (FPA) coupled to a VIS–IR microscope Hyperion 3000

(Bruker Optics, Billerica, US) and with a VERTEX 70v in–vacuum interferometer (Bruker Optics, Billerica, US) through a 15x Cassegrain objective–condenser pair in transmission mode.

Chemical investigations

The tannin powders were chemically characterized following several methods, described below. Determination of total phenolic content (TPC) was performed using the Folin–Ciocalteu assay, while the transformation of condensed tannin into anthocyanidols under the presence of sulphuric acid and vanillin allowed to calculate the concentration of total condensed tannins (TCT). Furthermore, FRAP assay was performed for determination of the extracts' antioxidant capacity. The quantity and molecular distribution of polysaccharides were determined by analyzing extracts from tannin powders using High–Resolution Size Exclusion Chromatography (HRSEC). Finally, the atomic composition of Carbon, Hydrogen, Nitrogen, Sulphur of the tannin powders was investigated with eager Xperience software.

Engineered wood products production

Various tannin–based adhesives have been employed in the manufacturing of EWPs, with their preparation methods outlined below.

- Wood samples of four distinct wood species: Norway spruce (*Picea abies* (L) Karst.), pine (*Pinus* supp.), white poplar (*Populus alba* L.), and European beech (*Fagus sylvatica* L.) were sourced from local sawmills. The samples, measuring 50×15×15 mm^3, were used for impregnation tests.
- A laboratory plowshare mixer (ETM–WHB75m) was used to mix the wood particles with the resin mixture and then used for particleboards production. The glued chips were evenly distributed in a 32 x 32 cm mold. The panels were then pressed at a density target of 650 kg · m^{-3} and a final thickness of 1 cm with a Höfer (Taiskirchen, Austria) HLOP 280 laboratory press.
- The plywood consisted of both of five and three layered 90° crosswise oriented 2.2 mm thick beech (*Fagus sylvatica* L.) veneer plies. Adhesive application was carried out manually by weighing the required adhesive per glue line with a KERN ITB 35K1IP device (Balingen–Frommern, Germany).

Physical and mechanical properties of EWPs

The physical and mechanical tests carried out its manufactured wood products are shown in Table 1.

Table 1. Determination of physical and mechanical properties according to the specific standard.

	Impregnated Wood	**Reference standard**	**Partcileboard**	**Reference standard**	**Plywood**	**Reference standard**
Physical and optical properties	Leaching resistance	/	Density	EN 323	Density	EN 323
			Density profile	/	Density profile	/
	Optical analysis	/	Thickness swelling	EN 317	Degree of compression (DoC)	/
			SEM analysis	/		
Mechanical properties	Modulus of elasticity (MOE)	EN 13061	Internal bond (IB)	EN 314	Dry and wet shear strength (TSS)	EN 314
	Modulus of rupture (MOR)		Modulus of elasticity (MOE)	EN 310	Modulus of elasticity (MOE)	EN 310
	Brinell Surface hardness(HBS)	EN 1534	Modulus of rupture (MOR)		Modulus of rupture (MOR)	

Statistical analysis

All laboratory tests and related analyses were performed for at least three repetitions in order to achieve statistical significance. Statistical tests were conducted based on the data distribution specific to each experiment. Utilizing both Origin Pro and R Studio software, the analyses for each experiment are elaborated upon in the following sections, providing details on the tests employed.

4. Results

4.1 Synthesis and characterization of tannin–based polymers.

4.1.1 Development of Quebracho (*Schinopsis balansae*) Tannin–Based Thermoset Resins

Emanuele Cesprini, Primož Šket, Valerio Causin, Michela Zanetti and Gianluca Tondi

This chapter has published as:

Cesprini E., Šket P., Causin V., Zanetti M. and Tondi G. Development of Quebracho (*Schinopsis balansae*) Tannin–Based Thermoset Resins Polymers (2021); 13 (24), 4412; https://doi.org/10.3390/polym13244412.

Abstract

One of the major challenges currently in the field of material science is finding natural alternatives to the high–performing plastics developed in the last century. Consumers trust synthetic products for their excellent properties, but they are becoming aware of their impact on the planet. One of the most attractive precursors for natural polymers is tannin extracts and in particular condensed tannins. Quebracho (*Schinopsis balansae*) extract is one of the few industrially available flavonoids and can be exploited as a building block for thermoset resins due to its phenol–like reactivity. The aim of this study was to systematically investigate different hardeners and evaluate the water resistance, thermal behaviour, and chemical structure of the quebracho tannin–based polymers in order to understand their suitability as adhesives. It was observed that around 80% of the extract is resistant to leaching when 5% of formaldehyde or hexamine or 10% of glyoxal or furfural are added. Additionally, furfuryl alcohol guarantees high leaching resistance, but only at higher proportions (20%). The quebracho–based formulations showed specific thermal behaviour during hardening and higher degradation resistance than the extract. Finally, these polymers undergo similar chemistry to those of mimosa, with exclusive reactivity of the A–ring of the flavonoid.

Introduction

In a context of growing interest in sustainable products and a circular economy, the need for high–performing bio–based solutions is rising exponentially [1],[2]. In particular, bioplastics are an attractive alternative, because they have the potential to combine the high performance we are used to having with a lower environmental impact compared to oil–based synthetic resins [3],[4]. Among the main natural resources of particular interest as building blocks for thermosetting resins, condensed tannins are one of the most attractive alternatives due to their availability and their phenol–like chemistry [5],[6]. These polyphenols are industrially extracted from mimosa (*Acacia mearnsii*) and quebracho (*Schinopsis balansae*) for several applications, especially in the leather tannery row [7],[8], in oenology [9],[10], as antitumor and anti–oncogenic activities in pharmaceutical and medical applications [11],[12], for thermal valorisation [13],[14], and water remediation [15],[16]. As previously mentioned, these extracts were proved to crosslink with several hardeners, exploiting their phenol–like chemistry. In the study of Pizzi et al., as well as in that of Yurtsever and Sengil, stable polymers were formed by the reaction between quebracho and formaldehyde [17],[18]. This flavonoid substrate was also used for the preparation of wood preservatives and adhesives for bio–based composites in combination with hexamine [19]–[21]. Quebracho's chemistry was also exploited for the preparation of insulating foams, where furfuryl alcohol was applied as comonomer [22],[23]. Another attractive reaction of Quebracho flavonoids occurs with dimethyl carbonate and hexamine, where Thébault et al. were able to produce urethane without the use of isocyanate [24],[25]. Further successful exploitation of quebracho was the blending with commercial phenol–formaldehyde (PF) resins [26]. Here, the role of the condensed tannin was useful not only in decreasing the synthetic part but also in enhancing the physical properties and containing the formaldehyde emissions of the resulting resin [27]. Despite the number of studies performed, a systematic assessment of the polymerization parameters has not yet been presented [28].

In our work, industrially available quebracho extracts are proposed as building blocks for thermoset resins. Several curing agents were selected: formaldehyde, hexamine, glyoxal, maleic anhydride, furfural, and furfuryl alcohol. The effects of pH and hardener concentration in the curing process were investigated, and the resulting polymers were characterized for their leaching resistance, thermomechanical (TMA), and thermal (TGA) behaviour as well as for their chemical structure (FT–ATR and solid–state 13C–NMR). Therefore, this research provides an overview of the properties of quebracho tannin–based sustainable polymers and the most suitable conditions for their synthesis.

Experimental

Chemicals and reagents

Quebracho tannin extract (Fintan 737B) was kindly provided by the company Silva team (S. Michele Mondovì, CN, Italy) while furfuryl alcohol and furfural were provided by International Furan Chemical IFC (Rotterdam, NL). Hexamethylenetetramine (hexamine), glyoxal, formaldehyde so as sulphuric acid and sodium hydroxide were purchased by Alfa–Aesar (Thermofisher, Waltham, MA, US).

Methods

Adhesive preparation and hardening

Quebracho–tannin water solutions were prepared at 50% by weight under vigorous stirring. The pH of the homogeneous solution (pH =6.7) was modified to 2, 4, 6, 8 by adding 33% wt. solutions of sulphuric acid and sodium hydroxide. Subsequently, 5g of the tannin solution were introduced into plastic test tubes and added of 1, 2.5, 5, 10, 15 % of hardener based on solid tannin. The test tubes were then tightly screwed and exposed at 100 ± 5°C for 24h to cure. The solid obtained was removed and grinded with a mortar obtaining a fine powder which was stabilized 24 h at room temperature. Table 1 summarizes the experimental design of this study.

Table 1. Summary of the different hardeners studied by varying their concentrations and pH.

Hardeners	**Amount**	**pH**
Formaldehyde (37%)	2.5%, 5%, 10%, 15%	2, 4, 6, 8
Glyoxal (40%)	2.5%, 5%, 10%, 15%	2, 4, 6, 8
Hexamine (33%)	1%, 2.5%, 5%, 10%, 15%	2, 4, 6, 8
Furfural	2.5%, 5%, 10% ,15%, 30%	2, 4, 6, 8
Furfuryl alcohol	5%, 10%, 15%, 20%, 30%	2, 4, 6, 8
Maleic anhydride (50%)	5%, 10%, and 15%	2, 4, 6, 8

Leaching test

The test consisted in keeping 1 g of dried tannin polymer powder in 50 ml of deionized water under magnetic stirring for 1 hr. The solution was then filtered (paper filter 125 µm) and the leaching resistance was calculated by weighing the dried filtered material according to the following formula:

$$Leaching\ Resistance\ (\%) = \frac{\text{Weight after leaching}}{\text{Weight before leaching}} * 100 \tag{1}$$

Thermal Mechanical Analysis (TMA)

Thermomechanical analysis was carried out with TMA/SDTA840 Mettler Toledo instrument with equipped with a three–point bending probe. The samples were prepared by applying about 20 mg of tannin–based formulations (before curing) between two beech wood plies (15mm x 5mm x 1.5mm). Non–isothermal method was applied, a 10°C/min heating rate was set and a cycle of 0.1/0.5 N force was applied on the specimens, with each force cycle of 12 s (6 s/6 s) has been set up. Through the relationship between force and deflection the Young's modulus MOE is calculated for each tested case. The equation used to calculate the modulus of elasticity is shown below:

$$MOE = [\frac{L^3}{(4bh^3)}][\frac{\Delta F}{\Delta f}] \tag{2}$$

Where L is length, b the wide and h the height of the samples. F is the force applied and f the deflection due to the applied load.

Thermogravimetric analysis (TGA)

SDT 2960, Simultaneous DSC–TGA, TA instrument was used to measure the thermogram of cured samples applying 10 °C min^{-1} heating rate from 30°C up to 800°C. The weight loss of the samples was recorded as a function of temperature. The tests were carried out under N_2 flow inert environment.

13C NMR Spectroscopy

Solid–state NMR experiments of the tannin cured and leached polymers (with 15% hardener) were performed on a Bruker AVANCE NEO 400 MHz NMR spectrometer using a 4 mm CP–MAS probe. The sample spinning frequency was 15 kHz. The 1H–13C CP–MAS NMR experiments consisted of excitation of protons with p/2 pulse of 3.5 ms, CP block of 2 ms, and signal acquisition with high–power proton decoupling. A total of ca. 2,000 to 15,000 scans were accumulated with the repetition delay of 5 s. The chemical shifts were referenced externally using adamantine.

ATR FT–IR Spectroscopy

The same samples analysed by 13C–NMR were analysed with the Nicolet, NEXUS, B70, FT–IR instrument, equipped with an ATR accessory with a diamond crystal. The spectra were acquired with 32 scans from 4500 to 600 cm^{-1}, and the region between 1800 to 600 cm^{-1} was reported and discussed.

Data analysis

The data obtained from the TMA, TGA analysis and the FT–ATR spectra were elaborated using OriginPro 8.5.0 SR1 software.

Results and discussion

The hardening tests performed adding different crosslinkers have shown that it is possible to produce several polymers of quebracho. The only crosslinker that gave rise to limited curing was maleic anhydride, and it will not be further treated in this article. According to the reaction mechanism proposed by Tondi [29], maleic anhydride crosslinks mimosa tannin through its –OH in position C3. This suggests that this position for quebracho is less frequently hydroxylated or less sterically accessible due to the higher branching and the pyrogallic B–ring. The solid adducts obtained by curing the quebracho extract formulations with formaldehyde, hexamine, furfural, and furfuryl alcohol at various pH underwent a leaching procedure, and the leaching resistances are reported in Figure 1.

Most of the solid polymers tested registered leaching resistance > 70% at different pHs. Formaldehyde, glyoxal and furfural produced water–resistant polymers at every pH, however formaldehyde reached 80 ±1% at pH 4; glyoxal reached 76 ±1% at pH 2 and furfural reached 84 ±1% at pH 8. Hexamine and furfuryl alcohol cured the quebracho extract at high (6,8) and low (2,4) pHs respectively. These findings are in line with the ones observed for the mimosa tannin extract polymers because the leaching resistance observed were also higher than 70% but the major difference was the more suitable pH for the different crosslinkers [16]. Considering the most successful pH for every hardener, the leaching resistance was monitored adding different amount of hardeners. In Figure 2 the leaching resistance trend is reported for the five crosslinkers. The graph generally depicts an increase in leaching resistance by increasing the amount of hardener; however, not all the crosslinkers present the same behavior.

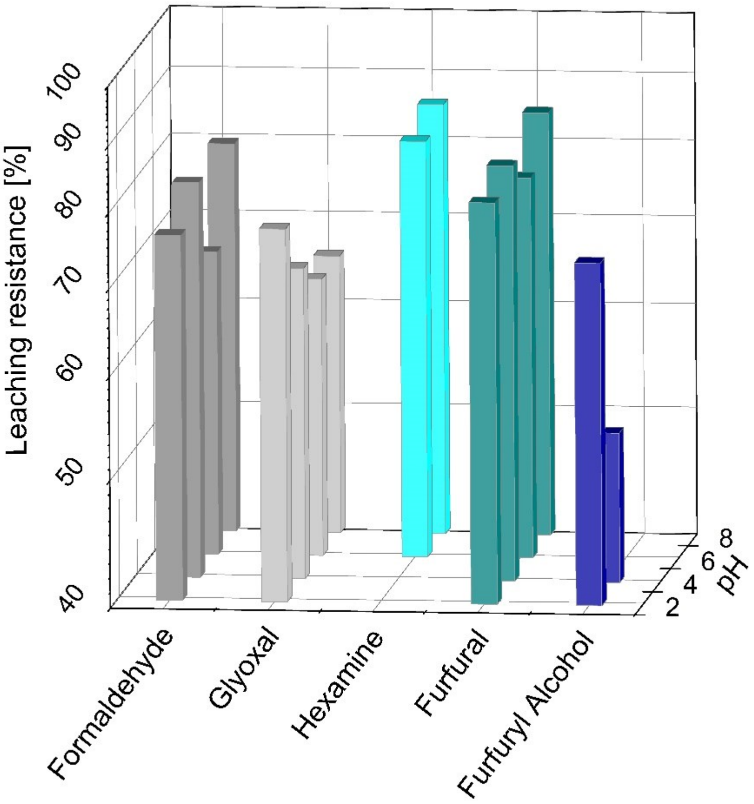

Figure 1. Leaching resistances of quebracho tannin formulations cured with 15% of formaldehyde, glyoxal, hexamine, furfural, and furfuryl alcohol at pH 2, 4, 6, and 8.

Formaldehyde, glyoxal, and hexamine reached a plateau of leaching resistance at around 5% of crosslinker, which suggests that, with 5% of hardener, the activation is complete; the addition of further hardener does not affect the leaching resistance, and around 20% of extract will be leached out. Conversely, furfural and furfuryl alcohol increase their leaching resistance, constantly reaching values over 85% when 30% of hardener is added. This behavior is due to the capacity of furanic monomers to self–polymerize [30],[31], involving a structural tightening that also keeps the less reactive fractions of the tannin extract embedded in the network. However, it was observed that, with 10% hardener, furfural reached over 80% leaching resistance, while furfuryl alcohol did not even reach 70%, lowering its applicative interest. In order to understand and compare the reactivity of the different hardeners, a concentration of 15% was selected to monitor the behavior of the formulations as a function of the temperature through TMA and TGA.

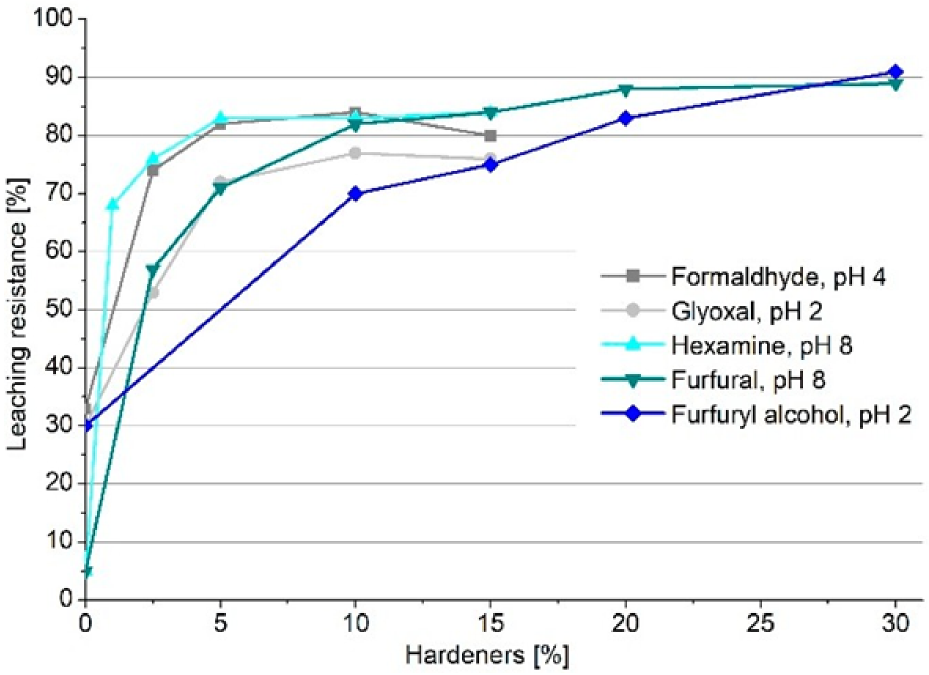

Figure 2. Leaching resistance of quebracho tannin polymers as a function of the amount of crosslinker.

In Figure 3, the thermomechanical behavior of the quebracho–hardener formulations is reported.

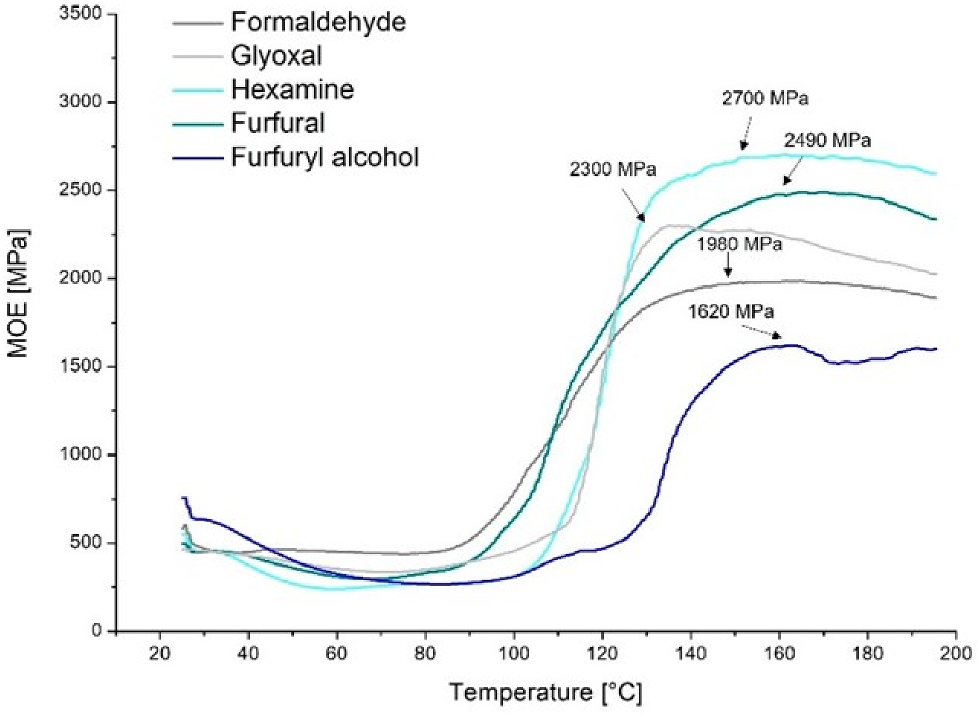

Figure 3. Thermomechanical analysis of the quebracho–crosslinker formulations.

The TMA confirms that the temperature increase involves an increase in stiffness, meaning that the formulations cure. Most of the measured formulations start their hardening at around 80 °C, and they reach maximum curing at 160 °C. MOE is defined as the ratio of strain and deflection. The TMA instrument applies constant strain during the temperature rise and registers the deflections; therefore, a lower deflection implies an increase in rigidity (MOE), to be attributed to the curing process, which tightens the polymer network. The highest value was reached by hexamine (2700 MPa), suggesting higher structural tightening and hence a higher crosslinking degree. This stiffness is reached in only 50 °C (from 100 to 150 °C), highlighting the outstanding curing rate (high slope) for hexamine to combine with the quebracho tannin formulations. A similar curing rate was observed for glyoxal, which also reached a high rigidity (MOE= 2300 MPa). Glyoxal started the curing slightly later (at around 110 °C) and showed faster joint degradation shortly after reaching the maximum at around 130 °C. This behavior was also observed by Navarrete et al. [32]. This means that glyoxal starts curing later, increasing the stiffness similarly to hexamine, but the produced polymer suffers higher temperatures more than that with hexamine. As expected from the leaching resistance tests, furfural increases the rigidity of the adduct stepwise (gentler slope), reaching high values of MOE (2490 MPa). Here, the curing starts at around 80 °C and increases until 160 °C, with a variable slope, accelerating at around 105 °C. The higher MOE is in line with the higher leaching resistance of this formulation (at 15% hardener). Surprisingly, the formulation with formaldehyde registered relatively contained MOE (1980 MPa), which indicates a more elastic behavior when the polymer is cured. This could be explained by the evaporation of the excess of hardener, which also explains the earlier start at 80 °C. Furfuryl alcohol recorded the lowest value of MOE, reaching only 1620 MPa, suggesting incomplete polymerization. Additionally, this assumption fits well with the leaching resistance experiments, where a higher amount of hardener would be needed (30%) to completely cure the formulation. Further, the curing occurs in two separate steps (110 °C and 130 °C), meaning that this hardener reacts with itself and with the flavonoids at different stages.

Table 2 highlights how the amount of hexamine affects the curing process of the formulations, reporting the initial curing temperature, the curing rate, and the maximum MOE registered in TMA experiments.

Table 2. Starting temperature (T_i), curing rate and maximum Young's modulus (MOE max) for quebracho formulations at different amount of hexamine.

Hexamine [%]	**T_i [°C]**	**Curing rate [MPa/°C]**	**MOE_{max} [MPa]**
1	78	20 ±0.3	2780
2.5	81	27 ±0.3	2590
5	84	37 ±0.5	2570
10	88	42 ±0.5	2960
15	93	50 ±0.7	2700

Firstly, it is possible to observe that initial curing temperature and amount of hardener are proportional. This seems to be due to the increase in viscosity of tannin solutions when hexamine is added, which is in line with the study of Moubarik et al. [33] that reported increasing viscosity for hexamine–added tannin solutions. The curing rate is expressed as the slope of the central part of the sigmoid of the thermogram, and it shows that higher amounts of hardener involve faster curing of the resin, although this kinetic does not affect the water resistance of the polymer. Finally, it has to be considered that the amount of hardener does not significantly affect the maximum elastic modulus, meaning that the final rigidity of the cured polymer is almost independent of the amount of hexamine added.

Once the polymers are synthesized, it was possible to observe their degradation when the temperature increased up to 800 °C in order to evaluate the behavior of the polymer during possible processing at high temperature. In Figure 4, the TGA of the five polymers is presented:

Thermogravimetric analysis provides information about the degradation due to in– creasing heat. Three main regions could be identified during the rise of temperature for all samples, and the weight loss percentage is reported in Figure 4. The first one (25–130 °C) characterizes mainly loss of water absorbed and traces of volatile compounds such as CO and CO_2. The second region (135–600 °C) is typical of the degradation of later chains of the tannin and decomposition of hardeners, with the cleavage of C–C bonds forming CH_4, CO, or CO_2 [34],[35]. In particular, two main events occur for a tannin degradation: the first, at around 260 °C, corresponds to decarboxylation, and the other one at, around 600 °C, corresponds to oxidation of high–carbon residues [36]. The last region between 600 and 800 °C is characterized by the decomposition of natural structures of tannins, in particular the disruption of the polyphenolic structure (rings A and B) [35]. Overall, it can be observed that the thermal degradation of the quebracho cured polymers is similar for all hardeners and presents a constant degradation pattern involving an acceleration between 250 and 300 °C for all polymers. This is different from what was observed for the quebracho powder, which degrades faster starting from 150–200 °C. This might suggest that the networking established after curing facilitates the initial rearrangement of the aromatic molecules during pyrolysis [37], involving the need for more energy before starting the linear degradation. Comparing the behavior of tannin resins with industrial resins (PF), this does not show any substantial differences in temperature resistance [38] but rather increases its resistance when added to an industrial resin (UF) [39]. This is a further detail that suggests the establishment of a real polymer network of the quebracho–hardener adducts.

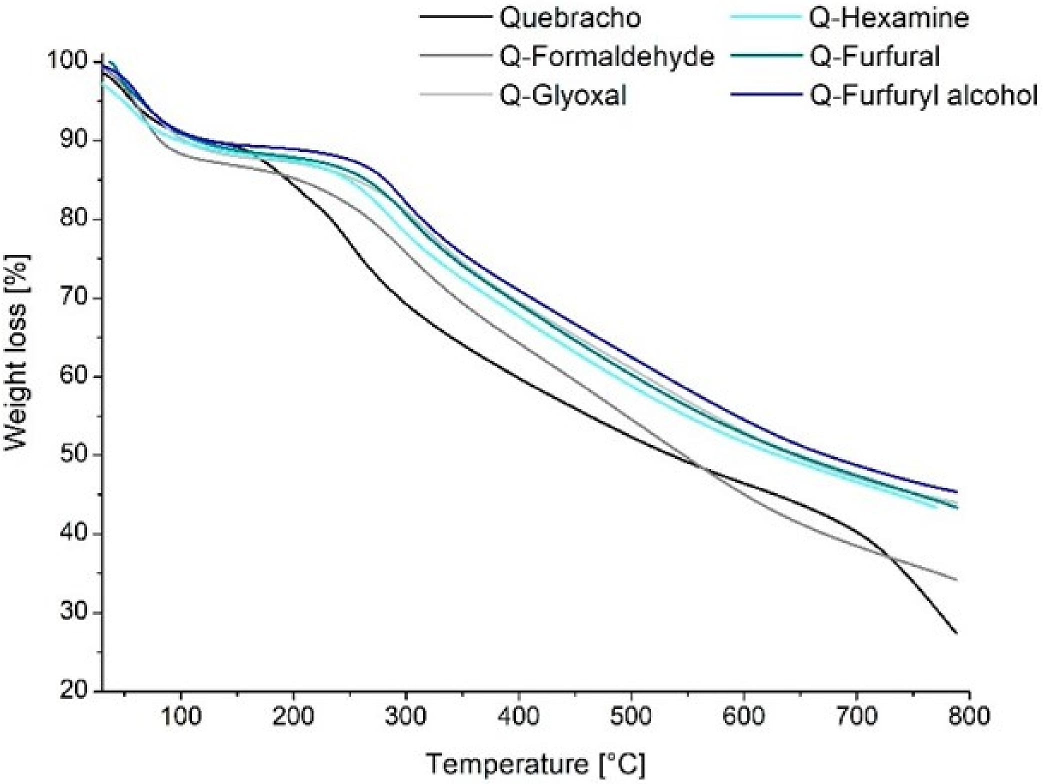

Figure 4. Thermogravimetric analysis of the quebracho–crosslinked polymers.

In order to shed further light on the polymerization process, two chemical investigations of the cured polymers after leaching were also considered: 13C–NMR (Figure 5) and FT–IR.

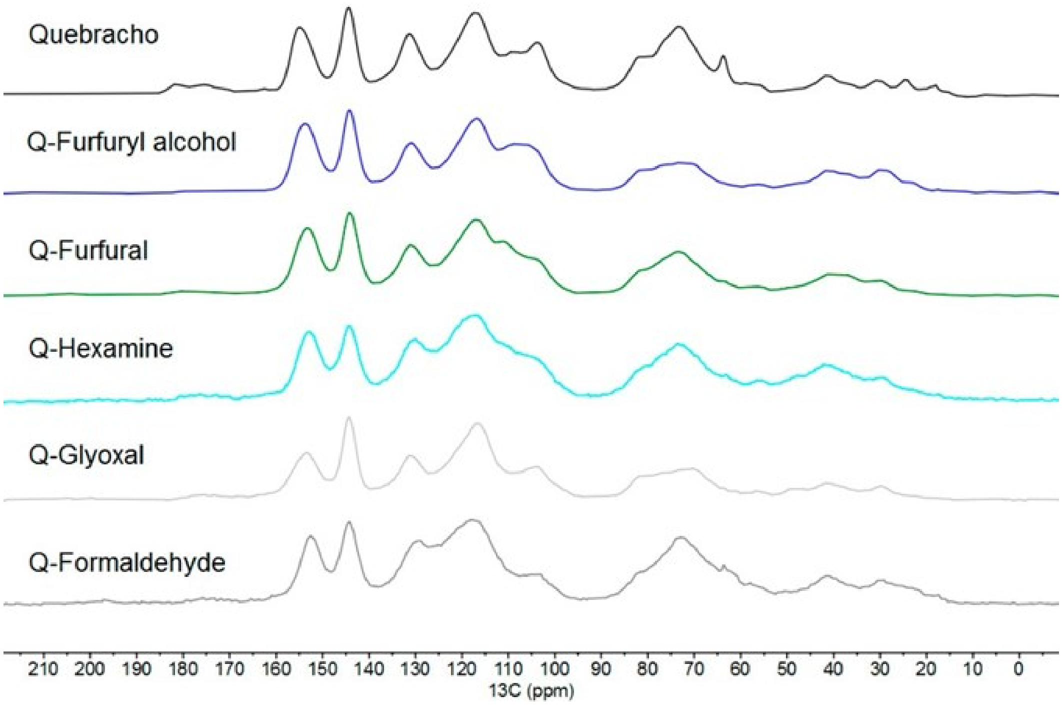

Figure 5. Solid–state 13C–NMR spectra of quebracho extract and its five polymers.

Following the findings of the previous study of Tondi [29] with the polymers of mimosa tannin extracts, it is possible to observe that the major difference between quebracho and mimosa extract is the inverted area of the signals at 105 and 120 ppm.

The quebracho extract presents major absorption at around 120 ppm, while the mimosa extract showed higher absorption at 105 ppm. These two absorptions are related to the –C8 position of A and B (C2′, C5′, and C6′) rings, respectively, suggesting that quebracho has lower –OH groups in the A–ring (resorcinol–like) and/or more substituted (branched), while the B–ring also has lower OH groups, suggesting a catechol–like ring [40]. Figure 6 shows the dominant flavonoid structure of quebracho extract.

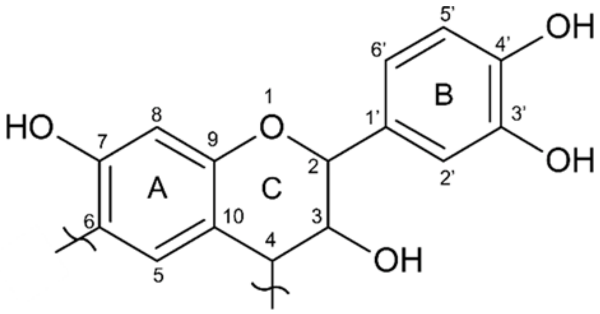

Figure 6. Model structure of the main flavonoid component of quebracho (Profisetinidin).

The fact that quebracho extract has lower signal intensity at around 105 ppm com– plicates the evaluation of further crosslinking; however, it can be observed that this band significantly decreases for all polymers except for the furfuryl alcohol (here, the CH of fu– rans overlap). This means that the number of free C8 positions in the A–rings decrease, and hence, they are substituted by the activating hardeners when cured. Conversely, despite the higher number of free C in the catechol B–ring, they do not decrease for any hardener, suggesting that, in quebracho, activation and, therefore, polymerization through the B–ring do not occur. This observation is also in line with the chemistry of phenol: in case of the pyrogallic nature of the B–ring, the OH groups in positions 3′ and 5′ activate the 2′ and 6′ positions, and only the OH group in position 4′ is inhibitory; conversely, in quebracho, the catechol has vicinal OH groups in positions 3′ and 4′ that do not activate the positions 2′, 5′, and 6′. Another observation to be highlighted is that the overall shape of the spectra of the cured polymers appears broader than that of quebracho extract, suggesting an increase in molecular dimension.

Finally, the ATR FT–IR spectrum of the leached polymer powders was collected, and it is reported in Figure 7. A major observation can be made in the region between 1800 and 600 cm^{-1}. The signal at 1550 cm^{-1} in the C=C aromatic stretching region disappears for every polymerized powder. This vibration is unique for quebracho and can be attributed to the C6 free position in the repeating unit connected C4–C8. The band at 1510 cm^{-1} disappears for hexamine, and this occurs when the π electrons can be delocalized in three–dimensional networks, or alternatively, the band shifts to 1600 cm^{-1} into a bulky signal of aromatics where symmetric and asymmetric vibrations absorb at the same wavenumber. The bands at 1400 cm^{-1} and at 1030 cm^{-1} decrease for most of the polymers, and they can be attributed to C–H bending, asymmetrical and symmetrical, respectively. These highlight an increase in steric hindrance that restrains some vibrations of the polymer. In this context, the disappearance of the signal at 970 cm^{-1} due to out–of–plane C–H bending is also logical. This signal remains only in the furfuryl alcohol polymer, strengthening the idea that some of the flavonoids are just “caged” into the furanic network.

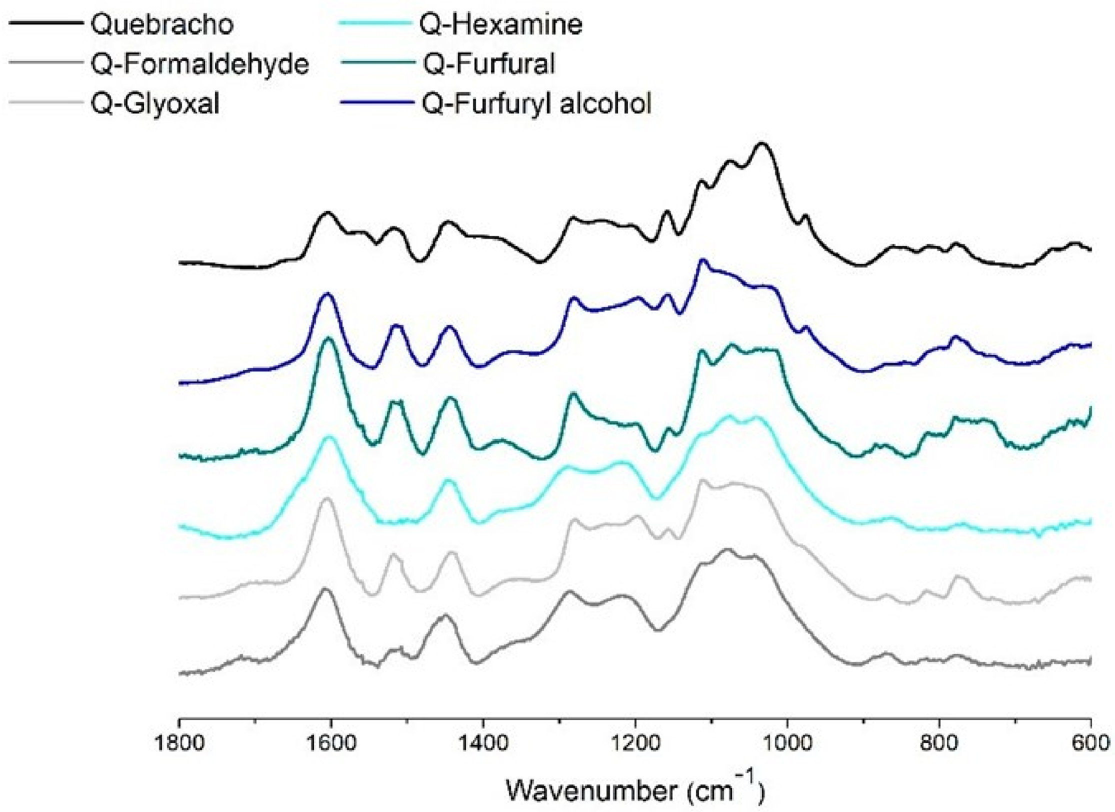

Figure 7. ATR FT–IR spectra of quebracho extract and its five polymers.

Conclusions

Quebracho tannin extract can be successfully polymerized with five hardeners: formaldehyde, hexamine, glyoxal, furfural, and furfuryl alcohol. The leaching resistance of these polymers reaches values of around 80%, suggesting that part of the extract does not take part in the curing process and can be removed easily. The hardeners used cured with different kinetics: hexamine and glyoxal cured quickly in a one–step process, and furfural cured more stepwise. The produced polymers show enhanced thermal resistance compared to the quebracho extract, because the networking facilitates the rearrangement during pyrolysis. The polymerization of the formulations was also spectroscopically proven. Quebracho polymers are connected exclusively through the A–ring with every hardener, and the crosslinking products are similar to those occurring with the mimosa extract. Evidence of structure tightening can be seen in both spectroscopies, including band broadening and a decrease in C–H bending vibrations. The quebracho tannin–based formulations developed in this study can be proposed as alternative thermosetting polymers to replace phenolic resins in adhesives, coatings, insulation materials, and other molded products of the construction.

Reference

1. Lewandowski, I.; Bahrs, E.; Dahmen, N.; Hirth, T.; Rausch, T.; Weidtmann, A. Biobased value chains for a growing bioeconomy. GCB Bioenergy **2019**, 11, 4–8.

2. Tondi, G.; Schnabel, T. Bio–based polymers for engineered green materials. Polym. Basel. **2020**, 12, 775.

3. Philp, J.C.; Ritchie, R.J.; Guy, K. Biobased plastics in a bioeconomy. Trends Biotechnol. **2013**, 31, 65–67.

4. Confente, I.; Scarpi, D.; Russo, I. Marketing a new generation of bio–plastics products for a circular economy: The role of green self–identity, self–congruity, and perceived value. J. Bus. Res. **2020**, 112, 431–439.

5. Pizzi, A. Condensed tannins for adhesives. Ind. Eng. Chem. Prod. Res. Dev. **1982**, 21, 359–369.

6. Roux, D.G. Recent advances in the chemistry and chemical utilization of the natural condensed tannins. Phytochemistry **1972**, 11, 1219–1230.

7. Pizzi, A.; Simon, C.; George, B.; Perrin, D.; Triboulot, M.C. Tannin antioxidant characteristics in leather versus leather light stability: Models. J. Appl. Polym. Sci. **2004**, 91, 1030–1040.

8. Sreeram, K.J.; Ramasami, T. Sustaining tanning process through conservation, recovery and better utilization of chromium. Resour.Conserv. Recycl. **2003**, 38, 185–212.

9. Parker, M.; Smith, P.A.; Birse, M.; Francis, I.L.; Kwiatkowski, M.J.; Lattey, K.A.; Liebich, B.; Herderich, M.J.B. The effect of post–ferment additions of grape derived tannin on Shiraz wine sensory properties and phenolic composition. Aust. J. Grape Wine Res. **2007**, 13, 30–37.

10. Jones–Moore, H.R.; Jelley, R.E.; Marangon, M.; Fedrizzi, B. The interactions of wine polysaccharides with aroma compounds, tannins, and proteins, and their importance to winemaking. Food Hydrocoll. **2021**, 123, 107150.

11. Kashiwada, Y.; Nonaka, G.I.; Nishioka, I.; Chang, J.J.; Lee, K.H. Antitumors agents, 1290 . Tannins and related compounds as selective cytotoxic agents. J. Nat. Prod. **1992**, 55, 1033–1043.

12. Valentini, L.; Ceccarini, M.R.; Verdejo, R.; Tondi, G.; Beccari, T. Stretchable, Bio–Compatible, Antioxidant and Self–Powering Adhesives from Soluble Silk Fibroin and Vegetal Polyphenols Exfoliated Graphite. Nanomaterials **2021**, 11, 2352.

13. Gaugler, M.; Grigsby,W.J. Thermal degradation of condensed tannins from radiata pine bark. J. Wood Chem. Technol. **2009**, 29, 305–321.

14. Zanetti, M.; Cesprini, E.; Marangon, M.; Szscurek, A.; Tondi, G. Thermal valorization and elemental composition of industrial tannin extracts. Fuel **2021**, 289, 119907.

15. Heredia, J.B.; Martín, J.S. Removing heavy metals from polluted surface water with a tannin–based flocculant agent. J. Hazard. Mater. **2009**, 165, 1215–1218.

16. Bacelo, H.; Vieira, B.R.C.; Santos, S.C.R.; Boaventura, R.A.R.; Botelho, C.M.S. Recovery and valorization of tannins from a forest waste as an adsorbent for antimony uptake. J. Clean. Prod. **2018**, 198, 1324–1335.

17. Pizzi, A. The chemistry and development of tannin/urea–formaldehyde condensates for exterior wood adhesives. J. Appl. Polym. Sci. **1979**, 23, 2777–2792.

18. Yurtsever, M.; ¸Sengil, I.A. Biosorption of Pb (II) ions by modified quebracho tannin resin. J. Hazard Mater. **2009**, 163, 58–64.

19. Thevenon, M.F.; Tondi, G.; Pizzi, A. High performance tannin resin–boron wood preservatives for outdoor end–uses. Eur. J. Wood Wood Prod. **2009**, 67, 89–93.

20. Nicollin, A.; Kueny, R.; Toniazzo, L.; Pizzi, A. High density biocomposite from natural fibers and tannin resin. J. Adhes. Sci. Technol. **2012**, 26, 1537–1545.

21. Kain, G.; Güttler, V.; Lienbacher, B.; Barbu, M.C.; Petutschnigg, A.; Richter, K.; Tondi, G. Effects of different flavonoid extracts in optimizing tannin–glued bark insulation boards. Wood Fiber Sci. **2015**, 47, 258–269.

22. Martinez de Yuso, A.; Lagel, M.C.; Pizzi, A.; Fierro, V.; Celzard, A. Structure and properties of rigid foams derived from quebracho tannin. Mater. Des. **2014**, 63, 208–212.

23. Tondi, G.; Pizzi, A. Tannin–based rigid foams: Characterization and modification. Ind. Crops Prod. **2009**, 29, 356–363.

24. Thébault, M.; Pizzi, A.; Essawy, H.A.; Barhoum, A.; Van Assche, G. Isocyanate free condensed tannin–based polyurethanes. Eur. Polym. J. **2015**, 67, 513–526.

25. Thébault, M.; Pizzi, A.; Santiago–Medina, F.J.; Al–Marzouki, F.M.; Abdalla, S. Isocyanate–free polyurethanes by coreaction of condensed tannins with aminated tannins. J. Renew. Mater. **2017**, 5, 21–29.

26. Moubarik, A.; Pizzi, A.; Allal, A.; Charrier, F.; Charrier, B. Cornstarch and tannin in phenol–formaldehyde resins for plywood production. Ind. Crops Prod. **2009**, 30, 188–193.

27. Solt, P.; Konnerth, J.; Gindl–Altmutter, W.; Kantner, W.; Moser, J.; Mitter, R.; van Herwijnen, H.W.G. Technological performance of formaldehyde–free adhesive alternatives for particleboard industry. Int. J. Adhes. Adhes. **2019**, 94, 99–131.

28. Vera, M.; Urbano, B.F. Tannin polymerization: An overview. Polym. Chem. **2021**, 12, 4272–4290.

29. Tondi, G. Tannin–Based copolymer resins: Synthesis and characterization by solid state 13C NMR and FT–IR spectroscopy. Polym. Basel **2017**, 9, 223.

30. McKillip,W.J. Chemistry of furan polymers. Adhes. Renew. Resour. **1989**, 408–423.

31. Tondi, G.; Cefarin, N.; Sepperer, T.; D'Amico, F.; Berger, R.J.; Musso, M.; Birarda, G.; Reyer, A.; Schnabel, T.; Vaccari, L. Understanding the polymerization of polyfurfuryl alcohol: Ring opening and diels–alder reactions. Polymers **2019**, 11, 2126.

32. Navarrete, P.; Pizzi, A.; Pasch, H.; Rode, K.; Delmotte, L. Characterization of two maritime pine tannins as wood adhesives. J. Adhes. Sci. Technol. **2013**, 27, 2462–2479.

33. Moubarik, A.; Charrier, B.; Alla0l, A.; Charrier, F.; Pizzi, A. Development and optimization of a new formaldehyde–free cornstarch and tannin wood adhesive. Eur. J. Wood Wood Prod. **2009**, 68, 167–177.

34. Zhang, W.; Yang, X.; Li, C.; Liang, M.; Lu, C.; Deng, Y. Mechanochemical activation of cellulose and its thermoplastic polyvinyl alcohol ecocomposites with enhanced physicochemical properties. Carbohydr. Polym. **2011**, 83, 257–263.

35. Konai, N.; Raidandi, D.; Pizzi, A.; Girods, P.; Lagel, M.C.; Kple, M. Thermogravimetric analysis of anningre tannin resin. Madera. Cienc. Tecnol. **2016**, 18, 245–252.

36. Garro Galvez, J.M.; Riedl, B.; Conner, A.H. Analytical Studies on Tara Tannins. Holzforschung **1997**, 51, 235–243.

37. Tondi, G.; Pizzi, A.; Pasch, H.; Celzard, A. Structure degradation.; conservation and rearrangement in the carbonisation of polyflavonoid tannin/furanic rigid foams—A MALDI–TOF investigation. Polym. Degrad. Stab. **2008**, 93, 968–975.

38. Zhao, Y.; Yan, N.; Feng, M.W. Thermal degradation characteristics of phenol–formaldehyde resins derived from beetle infested pine barks. Thermochim. Acta **2013**, 555, 46–52.

39. Zanetti, M.; Causin, V.; Saini, R.; Cardin, A.; Cavalli, R. Effect of tannin on increasing UF adhesive performance at high temperature investigated by TMA and TGA analysis. Eur. J. Wood Wood Prod. **2014**, 72, 385–392.

40. Pizzi, A. Advanced Wood Adhesives Technology, 1st ed.; CRC Press: New York, NY, USA, 1994; p. 289.

4.2 Application of biobased tannin polymers to produce wood–based materials.

Following an examination of the chemical–physical characteristics of tannin polymers cross–linked with various hardeners, the investigation progressed to the utilization of these resins in the production of engineered wood products. This phase involved the consideration of three distinct hardeners: hexamine, furfural, and furfuryl alcohol. This chapter delineates the application of these polymers within the domain of wood products. Specifically, the initial study focuses on assessing the efficacy of tannin–hexamine polymers for impregnating diverse wood species, with the aim of discerning potential enhancements in mechanical properties.

Subsequent to the preliminary investigations, the examination delved into two compounds categorized as furan molecules: furfural and furfural alcohol. These molecules, sourced from agricultural and forestry biomass waste, were systematically explored for their applicability in the production of plywood and particleboard. Notably, each study culminated in publications within scientific journals.

Those works have published as :

- Cesprini E., Baccini R., Urso T., Zanetti M., Tondi G. Quebracho–Based Wood Preservatives: Effect of Concentration and Hardener on Timber Properties. Coatings **2022**, 12(5), 568; https://doi.org/10.3390/coatings12050568.
- Cesprini E., Causin V. , De Iseppi V., Zanetti M., Marangon M., Barbu M.C., Tondi G. Renewable Tannin–Based Adhesive from Quebracho Extract and Furfural for Particleboards. Forests. **2022**, 13(11), 1781. https://doi.org/10.3390/f13111781
- Jorda J., Cesprini E., Barbu M.C., Tondi G., Zanetti M., Kràl P. Quebracho Tannin Bio–Based Adhesives for Plywood. Polymers. **2022**, 14(11), 2257. https://doi.org/10.3390/polym14112257
- Cesprini E., Jorda J., Paolantoni M., Valentini L., Šket P., Causin V., Bedolla D.E., Zanetti M., and Tondi G. Bio–Based Tannin–Furanic–Silk Adhesives: Applications in Plywood and Chemical Cross–linking Mechanisms. ACS Appl. Polym. Mater. **2023**, 5, 4468−4476. https://doi.org/10.1021/acsapm.3c00539

4.2.1 Quebracho–Based Wood Preservatives: Effect of Concentration and Hardener on Timber Properties

Emanuele Cesprini, Riccardo Baccini, Tiziana Urso, Michela Zanetti and Gianluca Tondi

Abstract

Tannin polyphenols are produced by plants to protect themselves against natural decay. It is expected that impregnating low–durable timber with tannin extracts of more durable species such as quebracho (*Schinopsis balansae*) will enhance the durability of the specimens. This biomimetic approach combined with the in situ polymerization of quebracho–hexamine formulations can be a valid alternative to synthetic wood preservatives. In this work, we aim to evaluate the impregnation mechanism as well as the impact of tannin and hardener concentration on the mechanical and leaching resistance properties of treated wood. Compression resistance, surface hardness and leaching resistance of four different common non–durable wood species: spruce (*Picea abies*), pine (*Pinus* spp.), poplar (*Populus alba*) and beech (*Fagus sylvatica*) impregnated with different concentrations of extract and hexamine are presented. The results show that the mechanical properties of tannin–impregnated timber are enhanced, especially for timber with lower densities. Tannin and hardener concentrations tendentially do not contribute significantly to further increase MOE (modulus of elasticity), MOR (modulus of rupture) and Brinell hardness. Similar results are also obtained when the specimens are tested against leaching: tannin is significantly more water–resistant when cured with hexamine, but higher amounts of hardener do not further improve its water resistance. These findings suggest that quebracho tannin–hexamine formulations are already effective at low concentrations (5 to 10% extract with 2.5 to 5% hexamine).

Introduction

Although the major worry of these years is the pandemic situation, we are all aware that climate change is already happening and its consequences will be dramatic for the life on our planet [1],[2]. After the Paris Agreement, the reduction of CO_2 emissions became a must for many countries, and a more sustainable use of the resources is yet required [3]. It is expected that bioresources will soon replace most of the fossil derivatives, and the wood production chain, which is already registering important growths, will further expand [4]. Timber is and will be a fundamental source of energy and materials, and its correct exploitation will be the key for the future of our species [5]. For these reasons, it will be important to sustainably extend the service life and the applicability of timber by increasing its durability and its mechanical performance. Succeeding in this purpose will involve a decrease in concrete and plastics in the building sector with a consequent reduction in carbon footprint [6]. The use of tannins for improving wood durability has been known for decades [7]. This approach is an example of biomimicry because tannins, which are naturally produced by superior plants to protect against biotic and abiotic decay, are infiltrated into the wood structure of low–durable timber species [8,9]. The use of tannin formulations for the protection of wood would be a real break– through in the industry of protective coatings and impregnation chemicals because the market is at present still dominated by synthetic polymers such as polyacrylates and polyurethanes [10],[11] and by heavy–metal solutions based on copper and chromium [12],[13]. The first studies performed by applying tannin extracts as wood preservatives showed an interesting increase in durability against fungi, but their solubility hindered their use as preservatives for moist environments and outdoors [14],[15]. In the 1970s it was discovered that condensed tannins undergo similar polymerization chemistry to phenolics [16],[17]. In particular, it was observed that hexamine was able to establish stable networks in an alkaline environment when combined with mimosa extracts to produce bio–based adhesives [18],[19]. The tannin–hexamine polymer produced is stable and highly water–resistant because it is characterized by nitrogen–containing bridges which connect flavonoid units through methylene anchorage [20]. Recently, tannin–based formulations were fixed in wood through in situ polymerization, producing timber samples with extended resistance against mechanical stress, leaching, fire and biologic attacks [21]–[24]. Despite the attractive properties achieved by mimosa tannin–treated timber, also by modifying the formulations, resistance against weathering is still the major drawback hindering the long–term exposure outdoors [25]. This is principally due to the rigid network produced by the mimosa extract, which breaks after several dimension changes in wood exposed to weathering [26].

The second–most abundant, commercially condensed tannin extract, due to its out– standing extraction yields [27], is quebracho (*Schinopsii balancae*). This dark–brown powder belongs chemically to the condensed tannin [28], and it presents high phenolic content [29] and also higher amounts of low–molecular–mass sugars than mimosa [30]; therefore, it is expected that they could facilitate the interaction with wood in their use as a preservative. In this study we aimed to impregnate different low–durable wood species such as spruce (*Picea abies*), pine (*Pinus spp*.), poplar (*Populus alba*), and beech (*Fagus sylvatica*) with a commercial extract of quebracho tannin extract in order to understand the impregnation mechanisms and the retentions. Furthermore, the mechanical properties and the leaching resistances will be observed after the addition of different concentrations of tannin and hexamine (used as hardener).

Materials and Methods

Materials

Wood pieces of 50×15×15 mm^3 of 4 different wood species were obtained from local sawmills: Norway spruce (*Picea abies*), pine (*Pinus spp.*), white poplar (*Populus alba*) and European beech (*Fagus sylvatica*). Fintan 373b commercial tannin of quebracho (*Schinopsis balancae*) was kindly provided by Silvateam (S.Michele Mondovì, Italy). The pH of a 40% water solution of the extract was 6.7. Sodium hydroxide and hexamine (hexamethylenetetramine) were purchased from AlfaAesar (Thermofisher, Waltham, MA, USA).

Preparation of the Tannin–Based Formulations

Solutions of concentrations of 5%, 10%, 15% and 20% of quebracho extract were obtained by quickly adding deionized water to the quebracho extract and then adding NaOH (33%) until the pH was 8. Hexamine was added to the tannin formulations in different proportions by weight of tannin extracts, specifically 2.5%, 5.0%, 7.5% and 10%.

Wood Impregnation

Dry samples of different wood species were placed into a 2 L beaker, divided by plastic nets in order to avoid surface contact between samples. A load was put on top to avoid floating. The tannin solution was then added, and the whole system was transferred into a desiccator. Air was removed from the samples by applying a vacuum of 100 mBar in the desiccator for 30 min. Then, the system was slowly brought to atmospheric pressure again and the wood specimens were left dipping in the tannin solution for 24 h. Finally, the impregnated specimens were recovered from the tannin bath and wiped with blotting paper. The wet retention (R_{wet}) of the samples was calculated according to the following formula:

$$R_{wet}\,[g] = W_{wet}\,[g] - W_0\,[g] \tag{1}$$

where W_0 and W_{wet} are the weight before and after impregnation, respectively.

Then, the impregnated wood samples were oven–dried at 102 ±2 °C for an additional 24 h. This heating stage allowed the tannin–hexamine formulation to in situ polymerize, enhancing the mechanical properties of the specimens.

The dry retention (R_{dry}) was calculated according to the following formula:

$$R_{dry}\,[g] = W_{dry}\,[g] - W_0\,[g] \tag{2}$$

where W_{dry} is the weight of the impregnated sample after drying.

Each test involved the repetition of 8 samples which were conditioned before characterization.

Microscopic Analysis

Sample Preparation

Spruce and beech micro cuts were obtained with a Leica CM1950 cryostat working at around 30 °C. Finally, 5 × 30 mm^2 slices of 15–20 µm thickness were obtained with a rotary microtome.

Optical Apparatus

A mechanically focused upright microscope (Leica DM4B) was used for slice observation. The instrument mounted transmitted light LED illumination with BF, PH, DF, and POL transmitted light contrast methods and fully automated fluorescence axis. The microscope was coupled to a Leica DMC4500 5 megapixels Sony CCD–ICX282 digital camera. The sensor allowed 2560 × 1920/3.4 µm × 3.4 µm resolution and 8.7 mm × 6.5 mm scanning area.

Mechanical Tests

The mechanical analyses were performed with a Galdabini Quasar 25 universal testing machine on 50 15 15 mm^2 stabilized samples. The appliance is composed of a rigid double–column system with a maximum capacity of 25 kN. The execution of the tests and the monitoring of the results were controlled using Labtest software (Galdabini, Cardano al Campo, Italy).

Compression Resistance Test

The stabilized samples were compressed along the grain according to the ISO13061–2 [31]. Compression rate of 2 mm · min^{-1} and maximum load (MOR) and modulus of elasticity (MOE) in compression were registered. Every experiment was repeated for at least 8 specimens.

Brinell Surface Hardness

Surface hardness tests (HBS) were performed on both radial and tangential faces. This test was carried out according to EN 1534 [32]. For the spruce, pine and poplar (soft), the spherical indenter was used at a rate of 25 N · s^{-1} up to a maximum load of 48 N, while for beech (hard), a rate of 120 N·s^{-1} up to a maximum load of 980 N was applied. For both methods, the test time once the maximum load was reached was 30 s. Through the calculation of orthogonal diagonals derived from the spherical imprint, hardness values were calculated and expressed according to the Brinell scale. Every test was repeated at least 8 times.

Resistance

The leaching process was carried out by dipping 8 impregnated specimens in around 20 mL of deionized water per sample (24 samples in 500 mL), and applying 10 min of 100 mbar pressure, and then keeping them under water for 3 h. The leached samples were removed from the bath and exposed to 103 °C for 24 h. The final weight of the leached sample was registered (W_{leach}), and the leaching resistance (L.R. %) was calculated according to the following formula:

$$\text{L.R. [\%]} = 1 - \frac{W_{dry} - W_{leach}}{R_{dry}} x100 \qquad (3)$$

Statistical Analysis

As the data are not normally distributed, a non–parametric test was chosen in order to compare the dependent variables. In particular, the Kruskal and post hoc Dunn tests were selected. The software used was RStudio Team (2021) [33].

Results

The influence of the tannin concentration for wood impregnation was initially assessed using spruce and beech as examples of coniferous and deciduous wood, respectively. An amount of 5% tannin weight of hexamine was used as a hardener (Section 3.1). The second part of the study was dedicated to understanding the effect of the amount of crosslinker on the mechanical properties of four wood species (Section 3.2).

Influence of Tannin Concentration on Impregnation

Wet and dry retention of the specimens impregnated with different concentrations of tannin are reported in Table 1. It can be observed that by raising the tannin concentration, the amount of solution which impregnates the sample decreases (wet retention), while the amount of tannin inserted in wood is higher (dry retention).

Table 1. Solution and tannin uptake for different concentrations of tannin–water solution for spruce (*Picea abies*) and beech (*Fagus sylvatica*).

Tannin [%]	**Spruce**		**Beech**	
	R_{wet} [g]	**R_{dry} [g]**	**R_{wet} [g]**	**R_{dry} [g]**
5	6.70	0.23	6.99	0.24
10	5.72	0.38	6.43	0.41
15	4.64	0.51	5.43	0.58
20	4.18	0.54	6.19	0.80

In the case of spruce, the wet retention drastically decreases while the dry retention increases by a factor of 2.35. In particular, there is no significant dry retention increase between 15% and 20% of tannin solution, suggesting that the higher viscosity decreases the penetration and the tannin accumulates on the surface. Conversely, beech wet retentions remain almost constant, and the dry retentions increase by a factor of 3.33. This means that the solution penetrates beech independently of the tannin concentration and hence the dry retention increases with the concentration of the formulation. These results show that the wood permeability is correlated with the species: while beech is easy to impregnate, spruce is generally hard [34].

Anatomic observations were performed in the two wooden structures to understand the different absorption mechanisms for spruce and beech.

Optical Analysis

Figure 1 shows the core cut of impregnated spruce (a) and beech (b) specimens. The tannin seems to be completely penetrated in the beech specimens while a partial penetration from the grains is visible in spruce.

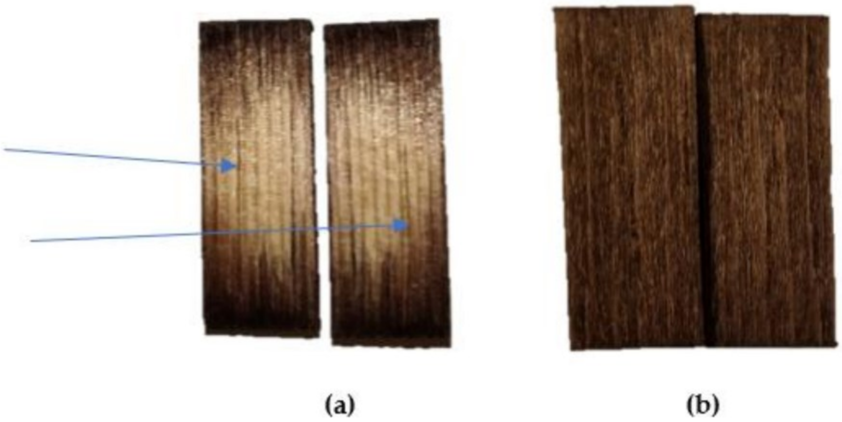

Figure 1. (**a**) Longitudinal section of spruce (*Picea abies*) sample impregnated with 10% of tannin water solution. (**b**) Longitudinal section of beech sample impregnated with 10% of tannin water solution.

Wood cell pore sizes depend on species, radial position and environmental factors. Generally, the diameter of beech vessels is around 50 µm [35], while the mean tracheid diameter (latewood and earlywood) in spruce is around 30 µm [36]. Considering the conduction elements, the hardwood vessel cells are in open contact with each other, establishing a sort of tube which allows the longitudinal conduction, whereas softwood tracheids are connected only through bordered pits. Indeed, water flow in spruce occurs through bordered pits which generally close when they dry. Eventually, the narrower diameter of lumina tracheids, coupled with the resistance of the pit membrane, reduces the flow in softwood, resulting in a difficulty to impregnate. It can also be observed that the darker longitudinal traits in Figure 1a (blue arrows) are large resiniferous ducts into which the impregnating agent easily penetrates. The preferred penetration paths for the two species can be better highlighted at higher magnifications (Figures 2 and 3).

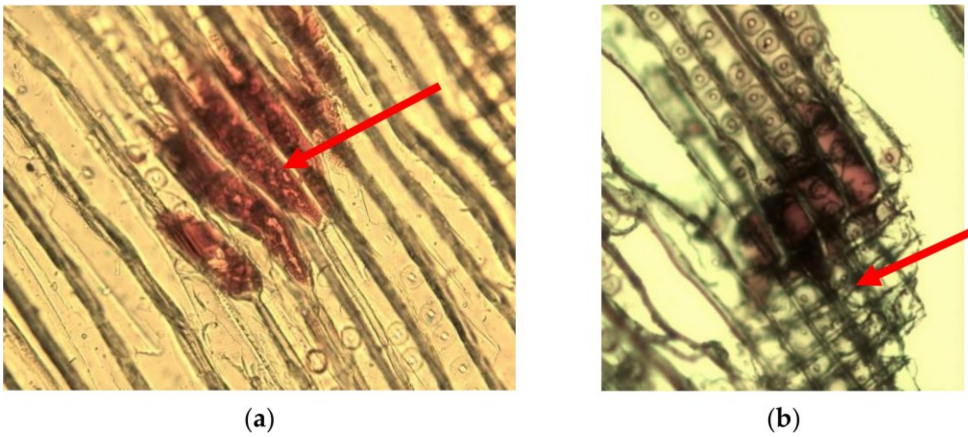

Figure 2. (a) Spruce (*Picea abies*) with 5% tannin solution 400×. Tannin solution accumulated at the ends of tracheids; (b) Tannin solution does not enter in rays (radial parenchyma cells, uncolored).

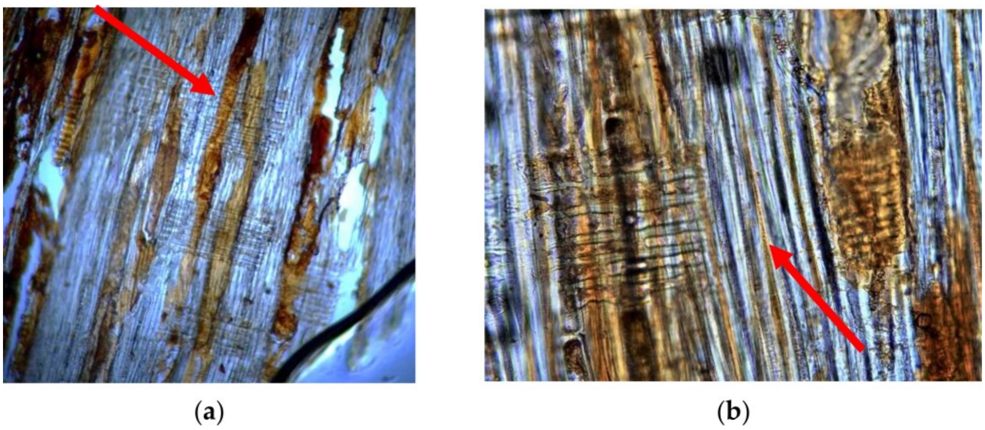

Figure 3. Beech (*Fagus sylvatica*) wood impregnated with 10% of tannin solution. (a) Tannin solution in vessels, 100×; (b) Few narrow fiber tracheids contain a small amount of tannin solution, 400×.

Figure 2a shows that the tannin solution flows in a non–linear way from one tracheid to another, passing through the bordered pits in spruce samples. The cell walls appear to be the same color, which suggests that the tannin solution accumulates in the cell lumen and does not infiltrate into the cell wall. Additionally, the solution flows until it reaches the bottom of the tracheids, where it appears to form granular masses on the inner surface of the cell wall (red arrow). The rays (radial parenchyma cells) do not appear to contain the tannin solution. However, in the spruce there are also radial tracheids, which can allow a contained radial flow of the solution (Figure 2b).

The preferred impregnation route for beech are the vessels, and in a smaller amount the fiber tracheids. The tannin solution concentrates mainly in the vessels (Figure 3a), (red arrow) while in the parenchymatic tissue, the tannin solution seems absent (Figure 3a,b). These observations confirm that the impregnation of spruce is harder and less homogeneous than that of beech due to the structural differences between coniferous and deciduous trees [36].

Mechanical Properties

In Figure 4, the stress vs. strain behavior for impregnated spruce (Figure 4a) and beech (Figure 4b) is reported. For both wood species, the presence of tannin–hexamine solutions enhances the maxi–mum compression resistance, but the concentration of tannin does not significantly affect the performances. In the case of spruce, the presence of tannin–hexamine polymers renders the specimens initially weaker, but then the elastic region lasts longer with the consequent increase in maximal load. Conversely, the increase in tannin concentration contributes to produce stiffer specimens, with no improvement in its modulus of rupture. The impregnation of beech simply extends the elastic region and consequently its maximum load. A higher concentration of tannin only extends the plastic deformation before collapsing.

Hardness also shows improvement after impregnation. While spruce samples have an average hardness of 1.78, the hardness of impregnated samples is between 2.56 and 2.74, independently on the concentration; beech has an average hardness of 3.48, with its impregnated samples between 3.57 and 3.72. The increase in hardness for spruce is around 50%, while for beech it is just 5%.

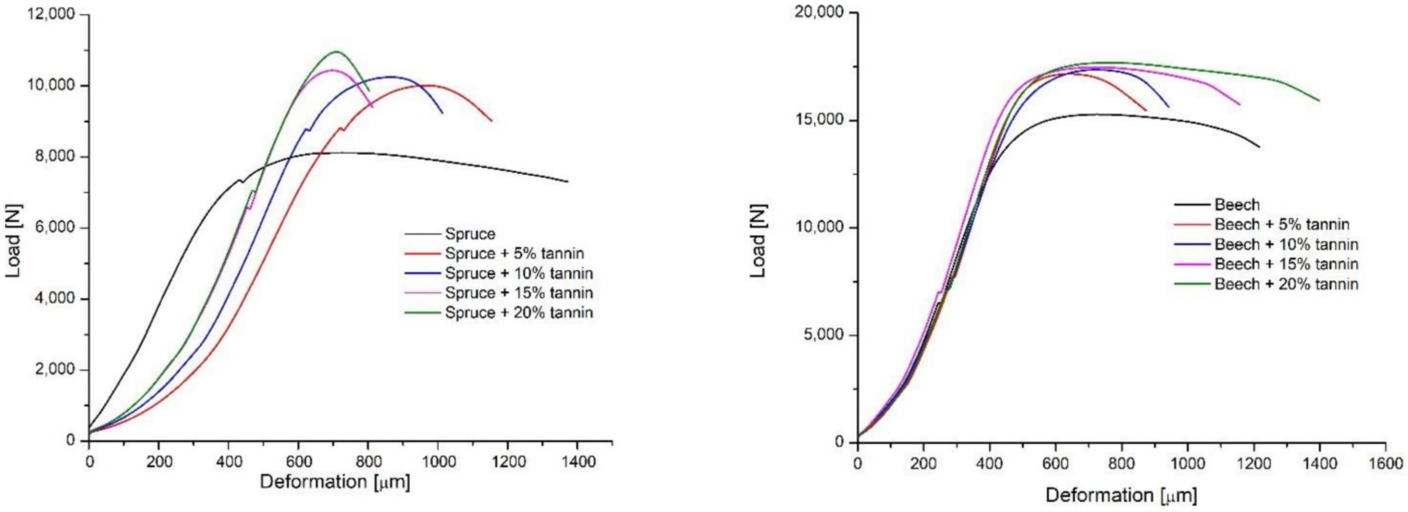

(a) (b)

Figure 4. Compression resistance behavior of spruce **(a)** and beech **(b)** treated with different concentrations of tannin–hexamine solutions.

Influence of Hexamine Amount on Impregnation

Once the effects of tannin concentration were defined, the influence of the hexamine was investigated in terms of retention, mechanical properties and leaching resistance by keeping the tannin concentration fixed at 10%. In this second part, poplar and pine are included in the study.

Wet and dry retentions of tannin–hexamine formulations with different concentration of hardener are shown in the Table 2 for the four wood species.

Table 2. Wet and dry retentions for different wood species treated with 10% quebracho tannin solutions with different hexamine concentrations.

	Wood Species							
	Beech^1		**Poplar^2**		**Spruce^3**		**Pine^4**	
(%)	**R_{wet}**	**R_{dry}**	**R_{wet}**	**R_{dry}**	**R_{wet}**	**R_{dry}**	**R_{wet}**	**R_{dry}**
2.5^a	5.71	0.48	6.14	0.49	6.53	0.48	3.45	0.25
5^b	4.98	0.33	6.27	0.50	6.88	0.50	3.59	0.29
7.5^c	5.93	0.40	6.16	0.47	6.38	0.44	4.26	0.29
10^d	4.68	0.30	6.40	0.48	6.56	0.46	3.78	0.26

**The numbers and letters used for species and cross–linking concentration, respectively, identify statistically significant differences in the following tables.*

The increase in hardener concentration does not seem to affect the wet and dry retentions. The *p*–values of 0.7383 and 0.2914 are registered for solution and tannin penetration. A strong effect on wet, and consequently on dry, retention is due to the wood species. In particular, pine was harder to impregnate, while no significant difference was observed for poplar and spruce (*p*–value > 0.05).

Mechanical Properties

The impregnated samples with 10% tannin and hardened with different amounts of hexamine (2.5%, 5.0%, 7.5%, 10.0% *w/w* related to tannin) were tested to understand the influence of the amount of hexamine in terms of modulus of elasticity (MOE) and modulus of rupture (MOR) on compression and Brinell hardness (HB).

The graphic in Figure 5 reports the MOE for the four species untreated (0%) and impregnated with 10% tannin and variable amounts of hexamine (2.5%, 5%, 7.5% and 10%).

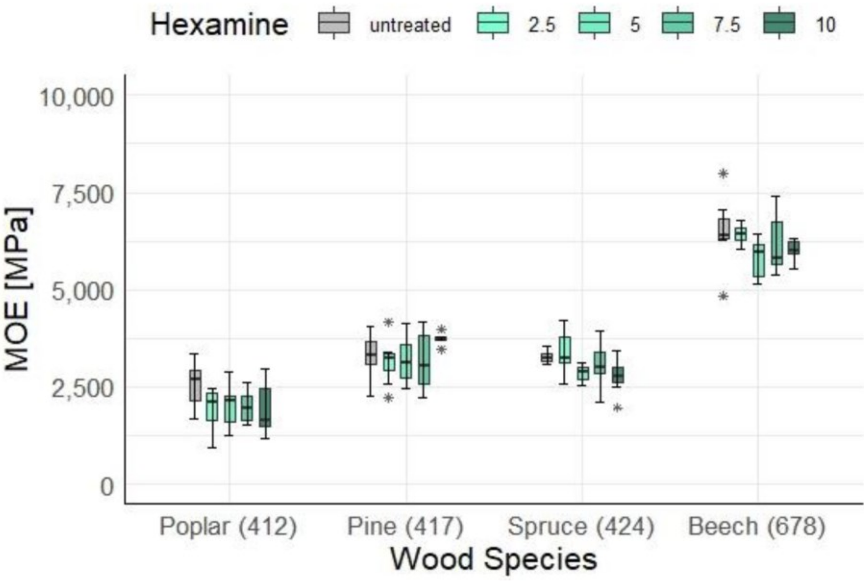

Figure 5. Boxplot chart of modulus of elasticity for different wood species at various hexamine amounts. The symbol " * " indicates the outliers of the tests performed.

From this plot, it is possible to highlight that the impregnation with tannin formulation does not affect the MOE of the samples (*p*–value 0.7758). Statistical differences were observed between species, except for spruce and pine that register an average of 3064 and 3300 MPa (Table 3). Although the MOE was not affected by the treatment, MOR results were enhanced after impregnation (Figure 6).

Table 3. Kruskal and post hoc Dunn tests for MOE, MOR and HB as a function of wood species and amount of hexamine.

	MOE		p–Value > 0.05	MOR		p–Value > 0.05	HB		p–Value > 0.05
Hexamine	χ	1.8	a × b × c × d	χ	18.0	a × b × c × d	χ	17.4	untreated–a; a–b; a–c; b × c × d
	p–value	0.8		p–value	1×10^{-3}		p–value	1×10^{-3}	
Wood species	χ	115.0	3–4	χ	108.2	3–4	χ	88.4	2–3; 2–4; 3–4
	p–value	2×10^{-16}		p–value	2×10^{-16}		p–value	2×10^{-16}	

In particular, the correlation between hexamine concentration and MOR shows a *p*–value of $1 \cdot 10^{-3}$, confirming a significant difference following impregnation (Table 3). The Dunn's test returned a significant difference (<0.05) between the non–impregnated samples and the specimens treated with a hexamine content of 2.5% or more in the solutions, but no difference was found between the different concentrations of hardener used.

From Figure 6, it can be seen that spruce and beech significantly increase their MOR, even when a contained concentration of hexamine is applied. In poplar, a direct proportionality between the amount of crosslinker and MOR was observed, which could be due to the limited mechanical performances of the untreated wood.

To complete the mechanical properties, the surface hardness of the untreated and tannin–hexamine–treated specimens is summarized in Figure 7.

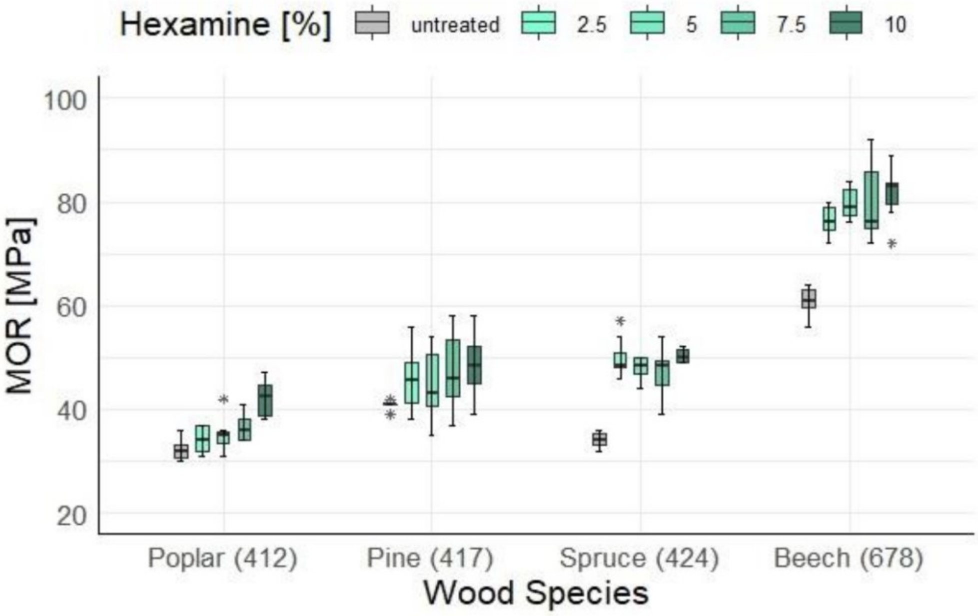

Figure 6. Boxplot chart of modulus of rupture for different wood species at various hexamine amounts. The symbol “ * ” indicates the outliers of the tests performed.

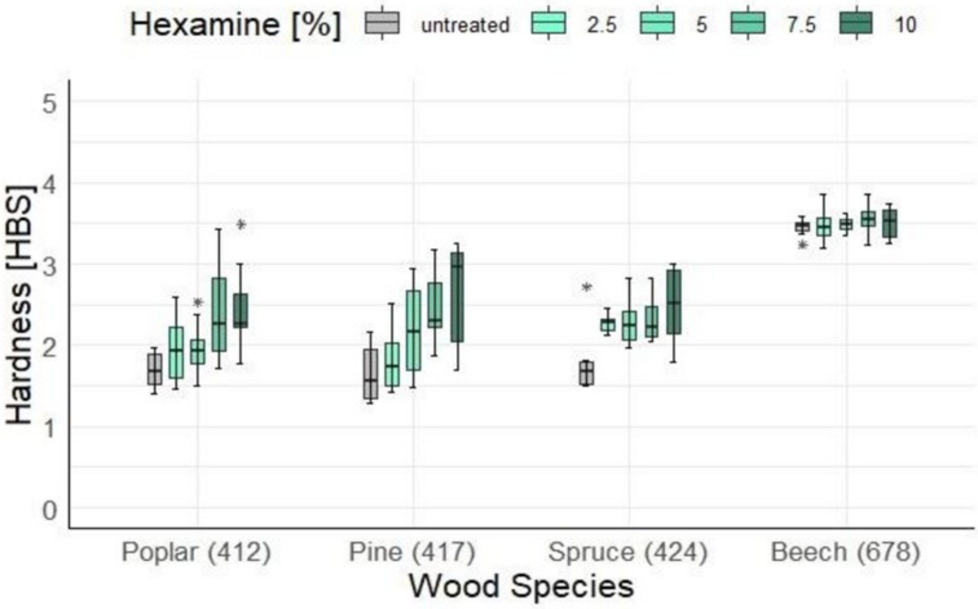

Figure 7. Boxplot chart of Brinell surface hardness for different wood species at various hexamine amounts. The symbol “ * ” indicates the outliers of the tests performed.

In this experiment, a significantly higher hardness was observed for beech. It clearly appears that the beech surface hardness is not affected by any tannin treatment.

Conversely, the surface hardness of the weaker species is positively influenced by the impregnation and by the amount of hexamine applied. Significant differences between the amount of hardener and HBS is reported by Kruskal test with a *p*–value of 1×10^{-3} (Table 3).

Leaching Resistance

The leaching resistance of the quebracho–tannin impregnated samples is presented in Figure 8. It can be seen that the presence of hexamine significantly increases the leaching resistance of the polymer. This can be observed for every timber species, and the increase can be quantified as between 20% and 30%. Even though slightly higher leaching resistance is observed when 10% of hardener is applied, the concentration of hexamine does not show statistically significative consequences on the leaching resistance (Table 4). A further observation indicates that softwoods show major leaching compared with hardwoods. This is because the hindered penetration involves the deposition of higher amounts of polymer in the surface layer; therefore, the proportion of tannin polymer that contacts water will be higher.

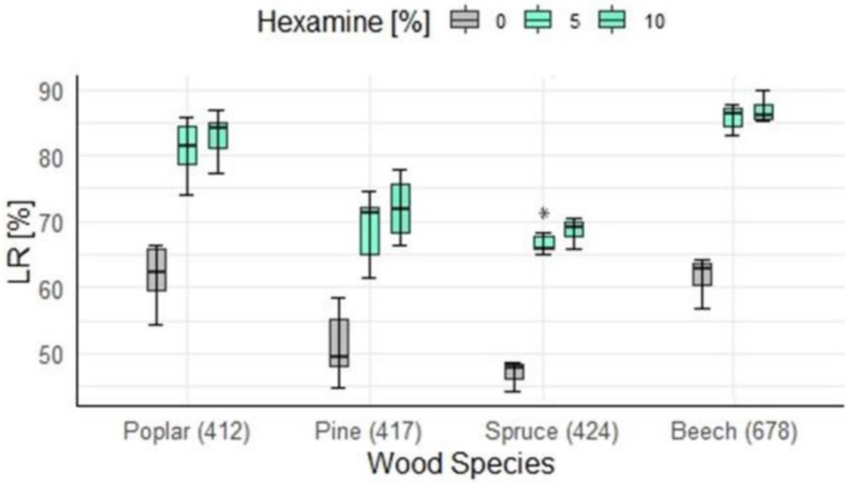

Figure 8. Leaching resistance of timber–impregnated samples in function of the concentration of hexamine. The symbol " * " indicates the outliers of the tests performed

Table 4. Kruskal and post hoc Dunn tests for leaching resistance as a function of wood species and amount of hexamine.

	LR		**p–Value > 0.05**
Hexamine	χ	43.9	5–10
	p–value	2×10^{-10}	
Wood Species	χ	19.0	1–2; 3–4
	p–value	2×10^{-4}	

Discussion

The presence of in situ crosslinked tannin–based polymers improves the mechanical properties of the impregnated wood samples. This finding was expected and already observed by other researchers with non–polar waxes as well as with thermoset resins [37]–[40]. However, this enhancement depends on the wood species, the mechanical tests performed and the amount of hardeners. Considering that the dry retention is almost independent from the amount of hardener and from the wood species (except pine), it is possible to summarize that:

- While spruce, pine and poplar have similar mechanical behavior, beech registers higher MOE, MOR and hardness, independently, on the impregnation. As expected, the wood species and the density are key for the mechanical properties of specimens [41]. In other words, due to lower density, poplar mechanical properties are more similar to that of spruce and pine, despite it taxonomically belonging to hardwood [42].
- The presence of a tannin–hexamine network embedded in the wood structure con– tributes to the enhancement of the mechanical properties of spruce and beech, although the concentration of tannin does not affect the intensity of this improvement. In the case of spruce, the presence of tannin polymer is significantly more important, involving a 30% increase in MOR and 50% in HBS against the 15% in MOR and 5% in HBS registered for beech. This is due to the lower density of spruce and the higher concentration of tannin on the surface.

- The MOE is not significantly affected by the presence of different amounts of hexamine. Conversely, MOR and hardness improve when more hardener is applied. The importance of hexamine is more significant for timber species at lower density. This suggests that the tannin polymer supports the wood structure when the elastic region expires, meaning that when the deformation becomes irreversible, the tannin network contributes to maintaining the wood structure before collapsing. Brinell hardness enhancement is especially contained for beech, because the easy penetration in the inner part of the wood dilutes the polymer accumulation on the surface.
- Hexamine also has a dominant impact at low concentration for MOR of spruce and beech; otherwise, its increase only slightly affects the property of the impregnated timber. This suggests that contained amounts of hexamine are already sufficient to create most of the supporting network of tannin [43]. However, using higher amounts brings further advantages that could be considered, especially for increasing the hardness of low–density species. This contained effect of polymerization with higher amounts of hexamine was unexpected. Other scientists applied hexamine to phenol–formaldehyde and pyrocatechol resins and observed that higher concentrations involved an increase in networking [44],[45].
- The leaching resistance highlights that, as expected, the presence of hexamine significantly contributes to increasing the water resistance of the flavonoid–based network for every wood species tested [19],[20]. However, the increase in concentration does not involve significant water resistance improvements. This confirms the observation of the previous point that for this property also, the excess of hexamine does not significantly contribute to strengthening the polymer network.

These quebracho tannin–based wood preservatives are almost completely bio–based products presenting enhanced mechanical and water resistance properties. Despite these interesting properties, these products cannot be easily compared with other promising bio–based preservatives. However, compared with a study of Barbero–Lopez et al. [46], quebracho tannin–hexamine registered retention between 20 and 70 kg · m^{-3}, which is in line with other tannin quebracho (Colatan GT10) and pine oil measurements of the study, especially considering that we impregnated the wood without extra external pressure. Mechanical enhancement registered was contained, compared with that observed by Noel et al. [47], who treated wood with lactic acid polymer. However, the retentions and the polymerization conditions considered were higher [47].

Furthermore, more consistent comparisons will be addressed when the efficacy of these formulations are tested against biologic attacks.

Conclusions

In this work, the impregnation of different wood species with quebracho–tannin formulations was observed. We found that the concentration of the impregnating solution affects the wet retention of spruce, while beech is easier to penetrate. This was due to the transportation tissues of the two species. While the beech structure can be easily accessed from broad vessels, spruce was hindered by most of the tracheids that presented closed bordered pits. The presence of quebracho tannin networked with hexamine embedded in the structure contributes to enhance the mechanical properties of timber, especially the modulus of rupture and the surface hardness of the samples with lower density. An increased concentration of tannin and hexamine in the impregnating solution did not involve significant enhancement, suggesting that for improving mechanical properties and leaching resistance, 10% quebracho tannin formulations containing 2.5–5% of hexamine (w/w. tannin) are already sufficient [48]. These novel formulations will be tested for their biological and weathering resistance to understand their efficacy as wood preservatives and their position in the market. At present, the major limitation is the more contained yet still important leaching sensibility that could be reduced by crosslinking the polymer at higher temperatures.

References

1. Raj, A.; Jhariya, M.K.; Yadav, D.K.; Banerjee, A. (Eds.) Climate Change and Agroforestry Systems: Adaptation and Mitigation Strategies; CRC Press: Boca Raton, FL, USA, **2020**.

2. Prendin, A.L.; Normand, S.; Carrer, M.; Bjerregaard Pedersen, N.; Matthiesen, H.; Westergaard–Nielsen, A.; Hollesen, J. Influences of summer warming and nutrient availability on Salix glauca L. growth in Greenland along an ice to sea gradient. Sci. Rep. **2022**, 12, 3077.

3. United Nations. Paris Agreement to the United Nations Framework Convention on Climate Change; T.I.A.S. No. 16–1104; United Nations: San Francisco, CA, USA, **2015**.

4. Hildebrandt, J.; Hagemann, N.; Thrän, D. The contribution of wood–based construction materials for leveraging a low carbon building sector in Europe. Sustain. Cities Soc. **2017**, 34, 405–418.

5. Budzinski, M.; Bezama, A.; Thrän, D. Estimating the potentials for reducing the impacts on climate change by increasing the cascade use and extending the lifetime of wood products in Germany. Resour. Conserv. Recycl. X **2020**, 6, 100034.

6.Hill, C.; Hughes, M.; Gudsell, D. Environmental impact of wood modification. Coatings. **2021**, 11, 366.

7. Laks, P.E.; McKaig, P.A.; Hemingway, R.W. Flavonoid biocides: Wood preservatives based on condensed tannins. Holzforschung, **1988**, 42, 299–306.

8. Quideau, S.; Deffieux, D.; Douat–Casassus, C.; Pouységu, L. Plant polyphenols: Chemical properties, biological activities, and synthesis. Angew. Chem. Int. **2011**, 50, 586–621.

9.Peng, Y.; Wang, Y.; Zhang, R.; Wang, W.; Cao, J. Improvement of wood against UV weathering and decay by using plant origin substances: Tannin acid and tung oil. Ind. Crops Prod. **2021**, 168, 113606.

10. Wang, J.; Wu, H.; Liu, R.; Long, L.; Xu, J.; Chen, M.; Qiu, H. Preparation of a fast water–based UV cured polyurethane–acrylate wood coating and the effect of coating amount on the surface properties of oak (Quercus alba L.). Polymers **2019**, 11, 1414.

11. Sow, C.; Riedl, B.; Blanchet, P. UV–waterborne polyurethane–acrylate nanocomposite coatings containing alumina and silica nanoparticles for wood: Mechanical, optical, and thermal properties assessment. J. Coat. Technol. Res. **2011**, 8, 211–221.

12. Noll, M.; Buettner, C.; Lasota, S. Copper containing wood preservatives shifted bacterial and fungal community compositions in pine sapwood in two field sites. Int. Biodeterior. Biodegrad. **2019**, 142, 26–35.

13. Shukla, S.R.; Zhang, J.; Kamdem, D.P. Pressure treatment of rubberwood (Heavea brasiliensis) with waterborne micronized copper azole: Effects on retention, copper leaching, decay resistance and mechanical properties. Constr. Build. Mater. **2019**, 216, 576–587.

14. Yamaguchi, H.; Okuda, K.I. Chemically modified tannin and tannin–copper complexes as wood preservatives. Holzforschung. **1998**, 52, 596–602.

15. Sen, S.; Tascioglu, C.; Tırak, K. Fixation, leachability, and decay resistance of wood treated with some commercial extracts and wood preservative salts. Int. Biodeterior. Biodegrad. **2009**, 63, 135–141.

16. Pizzi, A.; Scharfetter, H.O. The chemistry and development of tannin–based adhesives for exterior plywood. J. Appl. Polym. Sci. **1978**, 22, 1745–1761.

17. Pizzi, A. Tannin–based adhesives. J. Macromol. Sci. Rev. Macromol. Chem. 1980, 18, 247–315.

18. Pizzi, A.; Tekely, P. Mechanism of polyphenolic tannin resin hardening by hexamethylenetetramine: CP–MAS 13C–NMR. J. Appl. Polym. Sci. **1995**, 56, 1645–1650.

19. Pichelin, F.; Kamoun, C.; Pizzi, A. Hexamine hardener behaviour: Effects on wood glueing, tannin and other wood adhesives. Holz Als Roh–Und Werkst. **1999**, 57, 305–317.

20. Tondi, G. Tannin–based copolymer resins: Synthesis and characterization by solid state 13C NMR and FT–IR spectroscopy. Polymers **2017**, 9, 223.

21. Thevenon, M.F.; Tondi, G.; Pizzi, A. High performance tannin resin–boron wood preservatives for outdoor end–uses. Eur. J. Wood Wood Prod. **2009**, 67, 89–93.

22. Tondi, G.; Wieland, S.; Wimmer, T.; Thévenon, M.F.; Pizzi, A.; Petutschnigg, A. Tannin–boron preservatives for wood buildings: Mechanical and fire properties. Eur. J. Wood Wood Prod. **2012**, 70, 689–696.

23. Tondi, G.; Palanti, S.; Wieland, S.; Thevenon, M.F.; Petutschnigg, A.; Schnabel, T. Durability of tannin–boron–treated timber. BioResources **2012**, 7, 5138–5151.

24. Sommerauer, L.; Thevenon, M.F.; Petutschnigg, A.; Tondi, G. Effect of hardening parameters of wood preservatives based on tannin copolymers. Holzforschung **2019**, 73, 457–467.

25. Hu, J.; Thevenon, M.F.; Palanti, S.; Tondi, G. Tannin–caprolactam and Tannin–PEG formulations as outdoor wood preservatives: Biological properties. Ann. For. Sci. **2017**, 74, 1–9.

26. Tondi, G.; Schnabel, T.; Wieland, S.; Petutschnigg, A. Surface properties of tannin treated wood during natural and artificial weathering. Int. Wood Prod. J. **2013**, 4, 150–157.

27. Kryn, J.M. Quebracho, Quebracho Colorado, Quebracho Macho: Schinopsis Lorentzii Engl. and Schinopsis balansae Engl., Family Anacardiaceae; U.S. Department of Agriculture: Washington, DC, USA, 1954.

28. Tondi, G.; Petutschnigg, A. Middle infrared (ATR FT–MIR) characterization of industrial tannin extracts. Ind. Crops Prod. **2015**, 65, 422–428.

29. Auad, P.; Spier, F.; Gutterres, M. Vegetable tannin composition and its association with the leather tanning effect. Chem. Eng. Commun. **2020**, 207, 722–732.

30. Kirby, K.S.; White, T. Minor constituents of Quebracho tannin extract. Biochem. J. **1995**, 60, 582.

31. International Organization for Standardization. Physical and Mechanical Properties of Wood—Test Methods for Small Clear Wood Specimens—Part 2: Determination of Density for Physical and

Mechanical Tests; ISO 13061–2:2014; International Organization for Standardization: Geneva, Switzerland, **2014**.

32. EN 1534. Wood Flooring–Determination of Resistance to Indentation–Test Method; National Standards Authority of Ireland: Dublin, Ireland, **2010**.

33. RStudio. Integrated Development Environment for R; RStudio PBC: Boston, MA, USA. Available online: http://www.rstudio.com/ (accessed on 7 March 2022).

34. Tarmian, A.; Zahedi Tajrishi, I.; Oladi, R.; Efhamisisi, D. Treatability of wood for pressure treatment processes: A literature review. Eur. J. Wood Wood Prod. **2020**, 78, 635–660.

35. Wagenführ, R. Anatomie des Holzes. Leinfelden–Echterdingen; DRW–Verlag Weinbrenner GmbH & Co.: Leinfelden–Echterdingen, Germany, **1999**.

36. Irbe, I.; Sable, I.; Noldi, G.; Grinfelds, U.; Jansons, A.; Treimanis, A.; Koch, G. Wood and tracheid properties of Norway Spruce (Picea abies (L.) Karst) clones Grown on former agricultural land in Latvia. Balt. For. **2015**, 21, 114–123.

37. Esteves, B.; Nunes, L.; Domingos, I.; Pereira, H. Improvement of termite resistance, dimensional stability and mechanical properties of pine wood by paraffin impregnation. Eur. J. Wood Wood Prod. **2014**, 72, 609–615.

38. Dong, Y.; Yan, Y.; Wang, K.; Li, J.; Zhang, S.; Xia, C.; Cai, L. Improvement of water resistance, dimensional stability, and mechanical properties of poplar wood by rosin impregnation. Eur. J. Wood Wood Prod. **2016**, 74, 177–184.

39. Gindl, W.; Müller, U.; Teischinger, A. Transverse compression strength and fracture of spruce wood modified by melamine– formaldehyde impregnation of cell walls. Wood Fiber Sci. **2003**, 35, 239–246.

40. Xie, Y.; Fu, Q.; Wang, Q.; Xiao, Z.; Militz, H. Effects of chemical modification on the mechanical properties of wood. Eur. J. Wood Wood Prod. **2013**, 71, 401–416.

41. Reinprecht, L. Wood Deterioration, Protection and Maintenance; John Wiley & Sons: Hoboken, NJ, USA, **2016**.

42. Zhang, S.Y. Wood specific gravity–mechanical property relationship at species level. Wood Sci. Technol. **1997**, 31, 181–191.

43. Kretschmann, D. Mechanical properties of wood. In Wood Handbook: Wood as an Engineering Material; Centennial Edition; General Technical Report FPL; GTR–190; Department of Agriculture, Forest Service, Forest Products Laboratory: Madison, WI, USA, **2010**; Chapter 5; pp. 5.1–5.46.

44. Singh, A.; Yadav, R.K.; Srivastava, A. Synthesis of resole–type phenolic beads from phenol and formaldehyde by suspension polymerization technique. J. Appl. Polym. Sci. **2009**, 112, 1005–1011.

45. Yadav, U.S.; Kumar, H.; Mahto, V. Experimental investigation of partially hydrolyzed polyacrylamide–hexamine–pyrocatechol polymer gel for permeability modification. J. Sol–Gel Sci. Technol. **2020**, 94, 335–346.

46. Barbero–López, A.; Akkanen, J.; Lappalainen, R.; Peräniemi, S.; Haapala, A. Bio–based wood preservatives: Their efficiency, leaching and ecotoxicity compared to a commercial wood preservative. Sci. Total Environ. **2021**, 753, 142013.

47. Noël, M.; Mougel, E.; Fredon, E.; Masson, D.; Masson, E. Lactic acid/wood–based composite material. Part 2: Physical and mechanical performance. Bioresour. Technol. **2009**, 100, 4717–4722.

48. Cesprini, E.; Šket, P.; Causin, V.; Zanetti, M.; Tondi, G. Development of Quebracho (Schinopsis balansae) Tannin–Based Thermoset Resins. Polymers **2021**, 13, 4412.

4.2.2 Renewable Tannin–Based Adhesive from Quebracho Extract and Furfural for Particleboards

Emanuele Cesprini, Valerio Causin, Alberto De Iseppi, Michela Zanetti, Matteo Marangon, Marius Catalin Barbu and Gianluca Tondi

Abstract

With increasing concerns about the production of sustainable materials, the field of wood– based materials still offers a critical challenge. Indeed, a close dependence on petroleum derivatives is still required, involving high consumption of non–renewable and toxic chemicals in the assembly of wooden parts. Herein, the aim of this research was to evaluate the potentiality of an entirely renewable tannin–based adhesive for particleboard production. Industrial quebracho (*Schinopsis balansae*) tannin powder was selected as a raw material and analyzed in terms of polyphenols, polysaccharides, and the total condensed amount. Furfural was proposed as a bio–sourced hardener to establish crosslinking between the flavonoid units and hence produce a resin. This formulation was analyzed in terms of viscosity and curing time and then applied to laboratory–scale single–layer particleboard production. The density, mechanical properties, and thickness swelling of the panels were investigated at different glue ratios and pressing conditions. It was observed that time has a higher impact than temperature on the internal bond, and panels pressed at 160 °C for a longer pressing time (>7 min) performed better than the boards obtained at a higher temperature. The registered values at 160 °C for 11 min of pressing of internal bond (0.37 MPa) and modulus of elasticity (1417 MPa) met the required standards for P1 panels according to European norms EN 312 (2010). Conversely, the modulus of rupture (4.9 MPa) did not satisfy the requirements suggesting the need for the use of additive or post–treatments. Considering the results achieved, quebracho–furfural adhesives are an interesting base for bio–based adhesive formulations.

Introduction

The world wood composites market has been increasing over the last decades with– out registering any drops until 2010, and recording a production of 420.3 million m^3 in 2017 [1]. Furthermore, since wood products enhance the carbon sink forest capacity by increasing the time that CO_2 is kept out of the atmosphere, a further increase in the wood product market to around 658.1 million m^3 by 2027 is foreseen [2]. In order to lead this large market to be more sustainable, new challenges for faster curing and lower formaldehyde emissions adhesives, as well as the inclusion of recycled material in the boards, have already been proposed [1],[3]–[5]. However, engineered wood products heavily depend upon large amounts of synthetic derivates during the assembly process (~50 million tons of adhesives), despite academia and industry making strong research efforts to get sustainable alternatives in recent decades [6]–[8]. Despite their environmental and human health threats, formaldehyde–based resins still dominate the wood adhesives markets (~95%) due to their excellent bonding performance and contained costs [9],[10]. Nevertheless, the future scarcity of oil derivates and the related price increase, together with the increased concern for the environment by governments, continue to drive research toward more competitive green solutions. Within the wood–based material market, particleboard production accounts for half of the European wood product demand [11], covering a large share of adhesive consumption.

Before the rapid growth in the 1950s of synthetic derivatives, several bioresources were exploited, including polysaccharides, which are now re–purposed through implementations or modifications. For instance, Ningsi et al. extracted chitin from shrimp shells and converted it to chitosan, applying it as raw material for particleboard adhesives. The mechanical properties of these panels satisfied the requirements for the P2 panel type [12]. Starch extracted from palm oil was crosslinked with epichlorohydrin and applied to gluing rubberwood particleboards. In addition, in this study, the mechanical properties satisfied the standards for dry state requirements [13]. Among renewable resources, proteins of both animal and plant origin provided good potentialities, and several studies pointed to the revaluation of protein–based adhesives [14–16]. In particular, soy was deeply investigated and proposed for particleboards meeting the P2 requirements [17]–[19].

Moreover, similar results were obtained for formaldehyde–free adhesives consisting of soy flour, polyethyleneimine, and maleic anhydride, which were investigated for three layer particleboard [20]. Due to the relevant protein and carbohydrate requests from the food and medicine sectors, the market is looking for non–food alternatives in order to avoid ethical conflicts. In this context, lignin plays a key role due to its great abundance and its polyphenolic nature [21],[22]. Chen et al.

[23] and El Mansouri et al. [24], for instance, exploited modified lignin for particleboard manufacturing, obtaining boards respecting the EN 312 (2010) for P2 requirements. In addition, magnesium sulfonate lignin added with a low amount of isocyanate was applied to obtain stable formaldehyde–free boards [25]. In order to limit the use of hazardous substances such as isocyanates as much as possible, appealing alternatives are proposed by exploiting the polyphenolic character of lignin. Thus, strong urethane bonds are proposed without the use of isocyanates [26]. Even though intensive lignin valorization research is ongoing [27],[28], some drawbacks still limit industrial applications due to its high heterogeneity and low reactivity and solubility [29],[30].

These disadvantages of lignin do not frequently occur for polyphenolic tannins, which are the fourth most abundant biomass–extracted compounds right after cellulose, hemicellulose, and lignin [31]. Thus, as natural substitutes for synthetic resins, they are one of the most attractive candidates [32],[33]. As in the case of lignin, new lines of research focus on the creation of urethane bonds without using toxic reagents and report promising results [34]. The copolymerization of tannin and urea–formaldehyde showed improved properties of particleboards, increasing the moisture resistance and decreasing the formaldehyde emissions [35]. Several types of hardeners have been proposed for tannin crosslinking [36],[37], but a limited part of these formulations was investigated for particleboard production. Indeed, the major scientific works reported the combination of condensed tannins with formaldehyde and hexamine [38]. For instance, Anris et al. [39] and Valenzuela et al. [40] highlighted the good stability of tannin–hexamine formulation for fiber– and particleboard production. Alternative aldehydes, such as glyoxal, were pro– posed to replace formaldehyde, categorized as carcinogenic. Tannin–glyoxal resins reached an internal bond above 0.4 MPa [41]. In order to increase the sustainability of adhesive formulations, the use of bio–renewable hardeners is a viable path. Luckeneder et al. proposed furfuryl alcohol as a furanic derivate to produce engineered wood products, achieving the standard limit for P2 panel classification [42].

Materials and Methods

Materials

Quebracho tannin extract (Fintan 737B) was supplied by the company Silvateam (S. Michele Mondovì, Cuneo, Italy), and furfural (99%) was provided by International Furan Chemical IFC (Rotterdam, The Netherlands). Sodium hydroxide was purchased by Alfa Aesar (Thermo Fisher, Waltham, MA, USA). High purity (≥99%) ethanol, sodium carbonate, sulfuric acid, sodium acetate trihydrate, acetic acid, 2,4,5–tripyridyl–s–triazine, HCl, ferric chloride, ammonium formate, pectin, and dextran were purchased from Sigma–Aldrich (St. Louis, MO, USA). Folin–Ciocalteu's phenol reagent and vanillin were purchased from Merck (Darmstadt, Germany). Finally, the entirely recycled mixed wood species particles for industrial particleboard productions were provided by Fantoni spa (Osoppo, Udine, Italy).

Characterization of the Quebracho Extract

100 mg of tannin powder was dissolved in 5 mL of EtOH/H_2O (80/20) and left under mechanical stirring for 30 min at 25 °C. The sample was then centrifuged for 15 min at 4°C and 10,000 rpm to remove the insoluble fraction. The obtained extract was employed in the quantification of total polyphenols and condensed tannins.

The determination of total phenolic content (TPC) was performed using the Folin– Ciocalteu assay [45]. Briefly, 1 mL of diluted tannin extract, 1 mL of Folin reagent (diluted 1:10 with deionized water), and 0.8 mL of sodium carbonate solution at 7.5% were mixed. The solution was left in the dark at 40 °C for 30 min before the absorbance at 765 nm was measured. Each measurement was repeated three times. A serial dilution of gallic acid was used to create the calibration curve, and the results were expressed as $\mu gGAE \cdot mg^{-1}$.

The transformation of condensed tannins into anthocyanins using sulfuric acid and vanillin led to calculating the concentration of total condensed tannins (TCT) [46]. To sum up, 50 µL of the ethanol tannin solution was mixed with 2 mL of 4% methanol vanillin solution and 450 µL concentrated sulfuric acid. After 15 min, the absorbance was read at 527 nm, and the results were expressed as a relative ratio of equivalent catechin ($\mu gCE \cdot mg^{-1}$).

HRSEC was used for the quantification of the total polysaccharides and for the determination of their molecular weight distribution [47]. In brief, 1 mg of sample was dis– solved in 1 mL of mobile phase (50 mmol/L aqueous solution ammonium formate) and sterile filtered (0.22 µm acetate cellulose filters, Millipore, Burlington, MA, USA) directly into HPLC glass vials. Then, 10 µL were injected into the chromatographic system with an Agilent 1260 series II quaternary pump LC (Agilent Technologies, Santa Clara, CA, USA) equipped with both DAD and RID detectors. Samples were kept at 4 °C before injection in a temperature–controlled auto–sampler. The separation was carried out at 20 °C with a gel permeation HPLC column (PL–Aquagel–OH 40, Agilent). The mobile phase was applied at a constant flow of 0.6 mL/min for 35 min, and the temperature of the RID cell was kept at 35 °C.

Adhesive Preparation and Characterization

Quebracho tannin water solution was prepared at 45% *w/w* at room temperature un– der vigorous mechanical agitation. Once a homogenous solution was obtained, furfural was added to the solution at 10% with respect to the solid amount of tannin. The pH of the solution was adjusted from 6.7 to 8 by sodium hydroxide addition. The gel time was measured by placing 5.0 g of adhesive solution in a test tube and exposing it to 100 °C in a water bath. The transition from liquid to a no longer workable viscous solution was observed, and gelation times were recorded using a stopwatch [48]. The test was repeated three times. The viscosity of the solution was analyzed with a Kinexus Lab rheometer from Malvern Panalytical (Malvern, UK). A cone–shaped geometry spindle with a diameter of 4 cm was used, and the gap between the plates was set at 0.15 mm. The experiment was conducted at 25 °C with a share rate between 10 s^{-1} to 300 s^{-1}.

Particleboard Production

A laboratory plowshare mixer (ETM–WHB75m) was used to mix the wood particles with the resin mixture. In the first step, the wood chips were put into the plowshare mixer, and then the adhesive was gradually added during vigorous mixing (approx. 100 rounds/min) for 1 min. The glued chips were evenly distributed in a 32x32 cm mold (Figure 1a). The panels were then pressed at a density target of 650 $kg \cdot m^{-3}$ and a final thickness of 1 cm with a Höfer (Taiskirchen, Austria) HLOP 280 laboratory press. Three pressing times (7, 9, 11 min) and temperatures (160, 180, 200 °C) at 15% gluing on dry wood particles were selected and initially investigated according to the typical particleboard reaction conditions. Subsequently, those parameters were optimized according to the results obtained. Specifically, lower temperature (140 °C), adhesive amount (10%), and longer pressing time (13 min) were tried. Afterward, the boards were stored at 25 °C and 65% humidity (Figure 1b), cut out of the side layers, and then the samples were prepared (Figure 1c).

(a) (b) (c)

Figure 1. (a) Cold pre–pressed wood particles mat glued with 15% of quebracho–furfural adhesives (b) Particleboards with 32 × 32 × 1 cm size pressed at different glue amounts (c) Panel cutting section for samples manufacturing used for physical and mechanical analysis.

Particleboard Testing

The density was calculated according to EN 323:2005 [49] for samples 1–10, while the density profile was measured with a DENSE–LAB X (EWS, Hameln, Germany) for specimens 1, 4, 5, 8, 9. Furthermore, the same specimens were analyzed for internal bond (IB) according to EN 319 [50], while modulus of rupture (MOR) and modulus of elasticity (MOE) were determined according to EN 310 [51] for samples A, B, C. Finally, the specimens 2, 3, 6, 7, 10 were tested for water absorption and thickness swelling following EN 3017 [52]. SEM analysis was performed with FEI Quanta scanning electron microscopy (variable pressure environmental E/SEM) for the morphological characterization of particleboards. The instrument was equipped with a tungsten filament for electron pro– duction, SED and LFD detectors for Everhart–Thornley, and large field secondary electrons, respectively, BSED/GAD for backscattered electrons, and EDX (EDAX Element– C2B) for X–ray detection. The image acquisitions were carried out in low vacuum at 20 kV.

Statistical Analysis

Analysis of variance (ANOVA) evaluated the significance of the difference between factors and levels. The means were compared using the Tukey multi–range test to identify which groups were significantly different at a 95% confidence level. Statistical analysis was performed using RStudio Team (2021)) [53].

Results and Discussion

Industrial Quebracho Extract Chemical Analysis

The chemical characterization enabled us to understand the tannin composition and thus obtain suitable information for further possible optimizations for the extraction process. The total phenolic content (TPC), total condensed tannins (TCT), and polysaccharide content (PS) of the extract are reported in Table 1.

Table 1. Total phenolic content, total condensed tannins, antioxidant capacity, and polysaccharide fraction of quebracho Fintan 737 industrial tannin extract.

Extract	**TPC (µg GAE·mg^{-1})**	**TCT (µg CE·mg^{-1})**	**PS (mg·L^{-1})**
Quebracho	646 ± 18	304 ± 65	552 ± 103

The measured values were similar to those previously reported for mimosa tannin extract [46],[54]. The nature and extraction process may affect the reactivity of the polyphenols, influencing the effectiveness of the electrophilic substitution reactions involved with aldehyde based–hardeners. For instance, the presence of impurities, such as proteins or carbohydrates, and the establishment of non–covalent interactions, such as hydrogen bonds, hydrophobic interactions, and π–π stacking, should decrease the number of free positions on the aromatic ring [55]. In this view, the quebracho extract shows a moderate polysaccharide content [54],[56], registering a value of 552 mg·L^{-1}. Hence, the good purity combined with a high TCT/TPC ratio (0.47) promotes the quebracho industrial extract as an attractive polyphenol resource for the production of bio–resins [57].

Adhesive Characterization

The physical parameters of the adhesive were investigated in order to determine the processability of the resin. The resistance of the tannin–based adhesives to shear stress is expressed according to the physical parameter of viscosity expressed in mPa s and reported in Figure 2. A Non–Newtonian character was observed for the tannin–water formulation at pH = 8 (red curve). Conversely, the addition of furfural involved a lower drop when the shear stress increased (black curve) and lower viscosity due to its liquid character at room temperature. It has to be considered that the theoretical solid content of the resin without furfural is lower (45.0%) than that with furfural (47.4%), but because furfural is a liquid at room temperature, the viscosity of the tannin–furfural formulation was significantly lower.

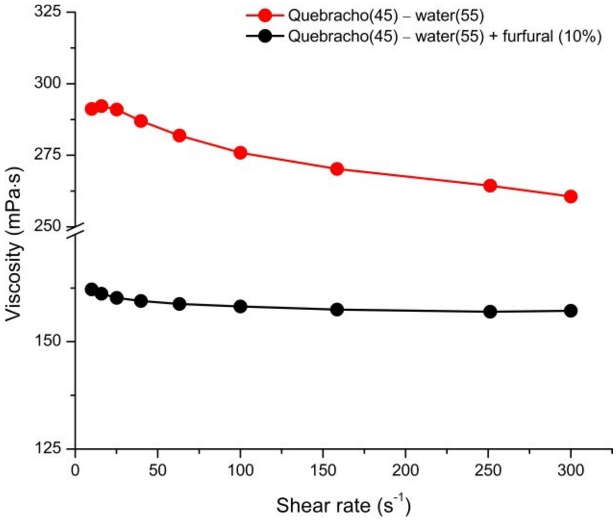

Figure 2. Viscosity of 45% tannin–water solutions at pH = 8 with (black) and without (red) furfural hardener.

Furthermore, the reactivity of the resin was monitored using the gel time test performed at 100 °C. The registered value of 304 (±27)s was higher compared to that of commercial urea–formaldehyde (UF) (127 s), suggesting the need for a longer pressing time [58]. On the other hand, phenol–formaldehyde resins presented slower kinetics than UFs, recording a gel time five times higher [59]. Previous research showed that the addition of condensed tannins to PF led to 30% faster crosslinking [48]. This means that the polyphenolic characteristics of tannin, added to bio–based furfural hardener, could be an attractive alternative to phenol–based synthetic resins due to the reactivity and the sustainability of its reagents.

Particleboard Characterization

Density Profile

Density is one of the major physical parameters influencing the mechanical proper– ties of wood composites. Considering the prefixed density target of 650 kg·m^{-3}, the registered values reported in Table 2 are slightly higher, and a certain correlation between density and pressing time (*p*–value = 0.0661) was observed. Conversely, no correlation (*p*– value = 0.3194) with temperature was highlighted, as is visible in Figure 3. The higher values recorded were presumably correlated to the achieved board thicknesses, which were lower than the targeted 10 mm. Indeed, the pre–pressing at 9 mm could have caused the thickness decrease because of the rigidity of tannin–furanic adhesives [60], which did not allow the expected spring–back. Furthermore, the density profiles reported in Figure 4 show that 7 min at 160 °C reveals an irregular profile, with a sharp decrease in the middle (4–6 mm) due to the too–mild reaction conditions. As soon as the conditions became tougher, the typical "U–shape" [60] profile was observable, and in particular, the profiles recorded at 9 min all temperatures showed an "arc–shape." When too harsh conditions were applied, the core density decreased again. Thus, given that density was mostly affected by the pressing time showing irregular profiles, especially at 7 min, longer times will probably be necessary to guarantee the panel stability.

Table 2. Density and thickness values of particleboards glued with 15% tannin in function of the pressing parameters.

Temperature (°C)	**Time (min)**	**Density ($kg \cdot m^{-3}$)**		**Thickness (mm)**	
		Mean	**SD**	**Mean**	**SD**
	7	663	21	10.1	0.19
160	9	692	55	9.6	0.09
	11	701	46	9.3	0.08
	7	659	40	9.4	0.10
180	9	687	29	9.6	0.13
	11	698	40	9.3	0.05
	7	696	37	9.4	0.07
200	9	713	52	9.3	0.07
	11	685	39	9.5	0.10

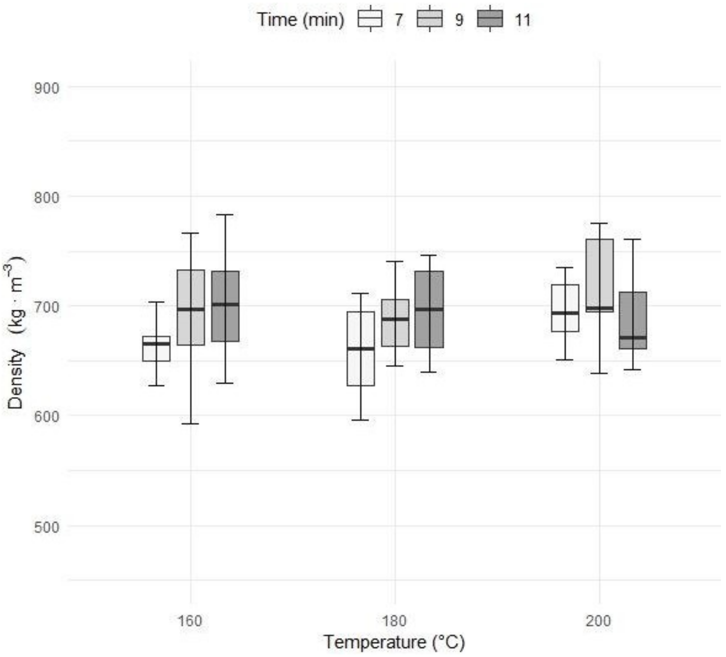

Figure 3. Density box char plot in function of pressing time and temperature. The whiskers represent scores outside the middle 50%, the median is represented by the line inside the box, while lower and upper quartiles are, respectively, the inferior and the bottom end of the box. Possible outsiders are indicated by asterisks.

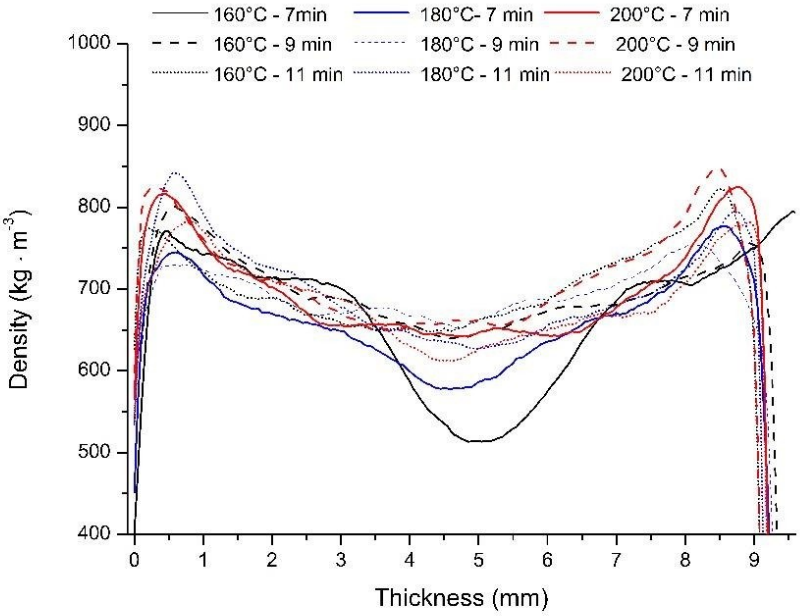

Figure 4. Density profile for particleboards manufactured at different pressing times (7, 9, 11 min) and temperatures (160, 180, 200 °C).

Mechanical Properties

Internal bond (IB), modulus of elasticity (MOE), and modulus of rupture (MOR) were studied to understand the mechanical behaviour of the boards (Figure 5).

Internal bond is often considered one of the more significant mechanical properties of particleboards. It was observed that, on the one hand, a high direct correlation between pressing time and internal bond was observed, reporting a p–value equal to $2 \cdot 10^{-16}$, as represented in Figure 5a. On the other hand, the pressing temperature showed a limited influence on the final value of cohesion, showing a p–value equal to 0.685, while a combination of both press parameters significantly affected the final internal bond value (*p*– value = $1.37 \cdot 10^{-10}$). It can be observed that increasing the temperature allowed for reducing the pressing time, reaching a similar final value of internal cohesion. The boards pressed at 160 °C for 9 and 11 min were characterized by the highest value of an internal bond (0.32 MPa and 0.37 MPa, respectively), exceeding the P1 limit standard requirement of 0.28 MPa for general purposes. The results of the bending tests are reported in Figure 5b,c. MOE resulted in parameters unaffected by a reaction, recording a *p*–value of 0.906 and 0.430 for pressing time and temperature, respectively.

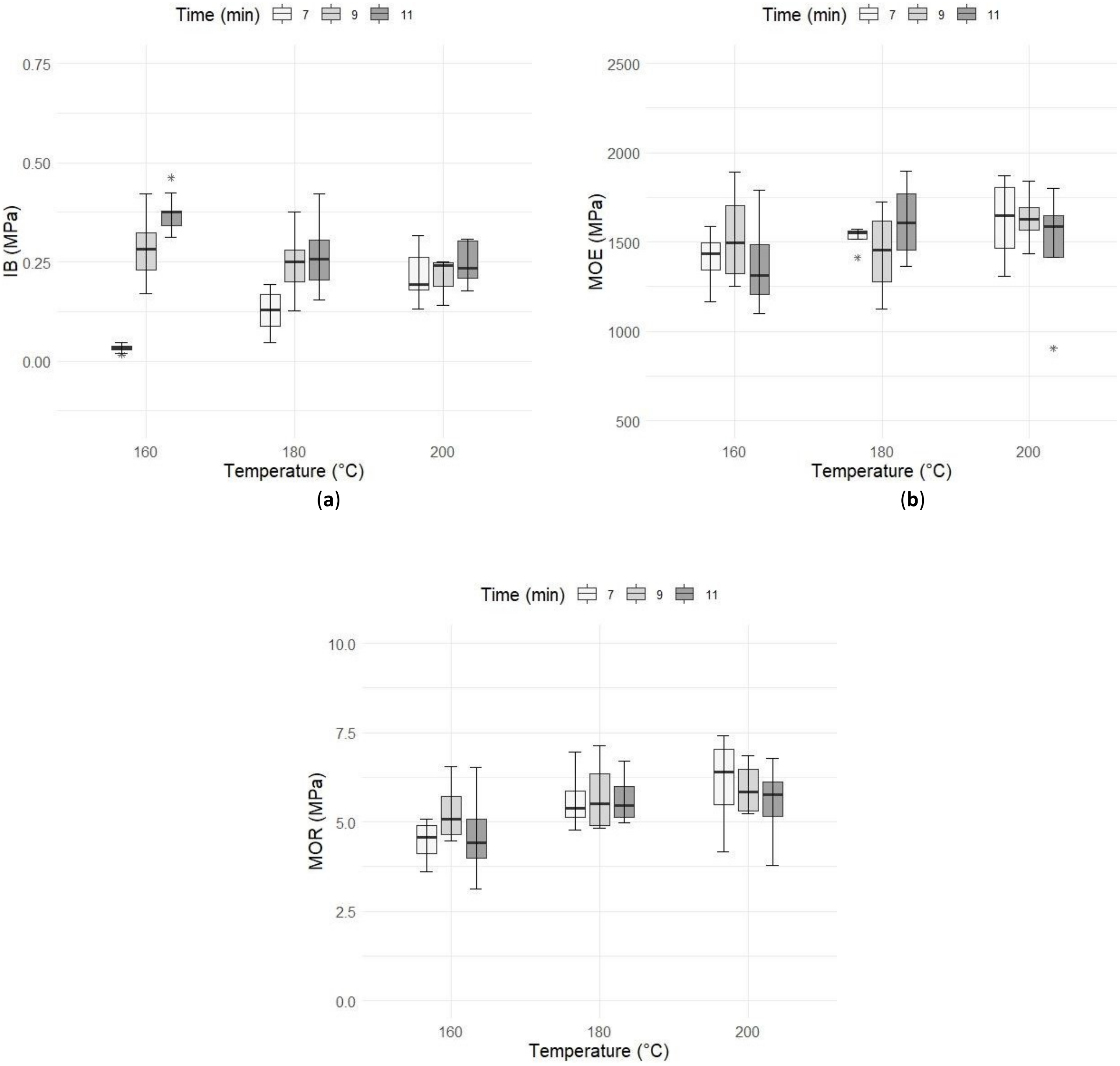

(a)

(b)

(c)

Figure 5. Influence of pressing parameter on (a) Internal Bond, (b) Modulus of elasticity, (c) Modulus of rupture. The whiskers represent scores outside the middle 50%, the median is represented by the line inside the box, while lower and upper quartiles are, respectively, the inferior and the bottom end of the box. Possible outsiders are indicated by asterisks.

Meanwhile, a slightly significative correlation between MOR and temperature was found (*p*–value 0.0491) and using a post hoc Tukey test, a significative difference between 160 and 200 °C was highlighted. Although no standard minimum MOE value was given for P1 general dry applications, the values of MOR obtained were moderately lower than the standard requirements for boards, with thickness ranging between 6 and 13 mm [61]. However, these bending properties can both be significantly improved by coating with melamine–impregnated paper, which is a common praxis in modern furniture.

Thickness Swelling

Thickness swelling was also investigated, and the results are presented in Figure 6. The panels pressed at milder conditions (160 °C, 7 min) did not resist the dipping in water for 24 h, while all the other combinations resisted the test. However, thickness swelling was significantly influenced by pressing temperature (*p*–value = 0.045) as well as by pressing time (*p*–value < 0.01). Indeed, harsher reaction conditions involved panels with lower water affinity, and also for this feature, pressing time plays a major role. Observing the thickness swelling behavior from 160 °C to 200 °C for 11 min of pressing, a decrease in swelling of around 30% was detected. Although an increase in reaction parameters led to a low water affinity, the registered values did not satisfy the requirement for wet application, and additional treatments would be necessary to increase the moisture resistance properties of the particleboard.

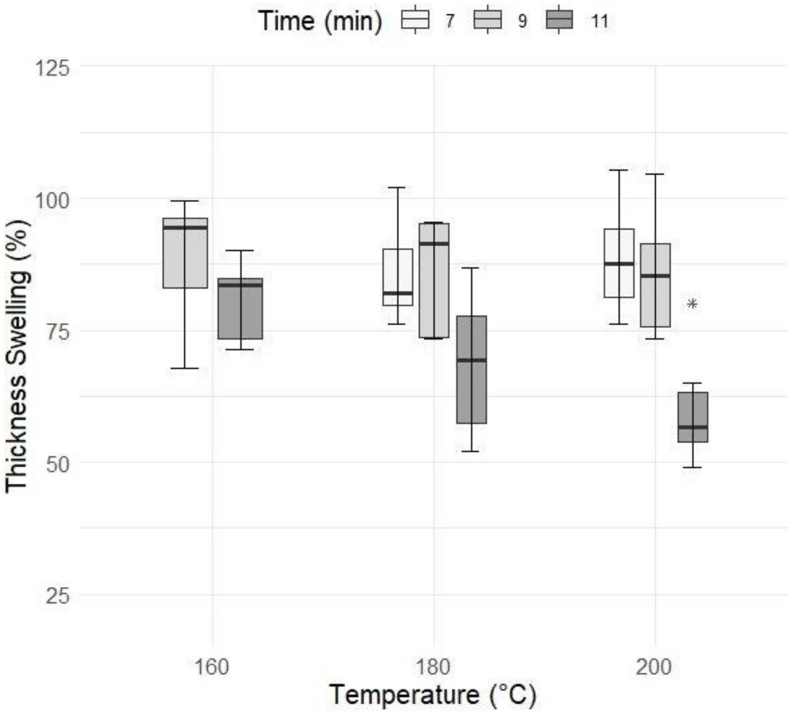

Figure 6. Thickness swelling after 24 h of the produced particleboards in function of the pressing parameters.

SEM Analysis

In order to investigate the morphological features of the produced particleboard, a representative section was selected for SEM analysis and reported in Figure 7.

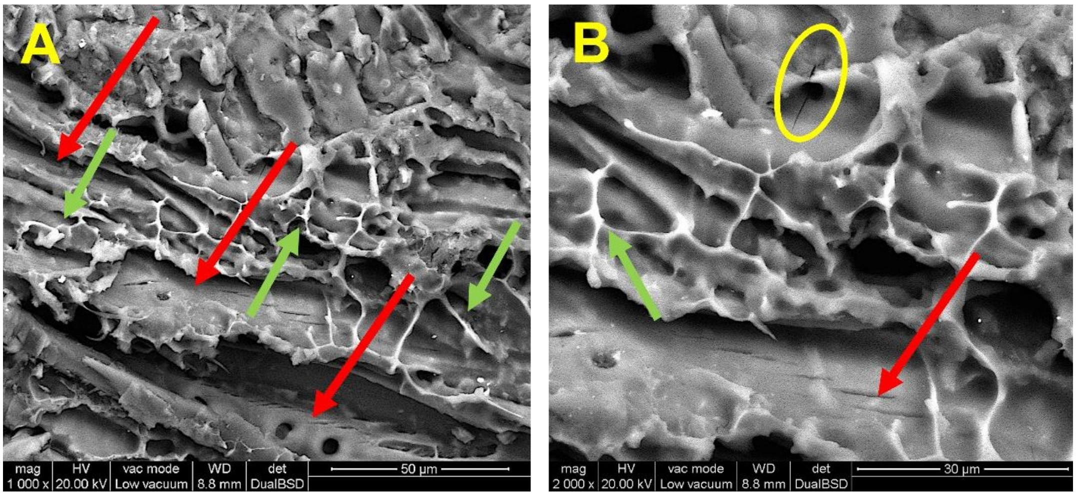

Figure 7. Scanning electron microscopy images of particleboard glued with 15% of adhesive formulation. Different magnifications of the same representative area are proposed: (A) 1000× (B) 2000×. Red arrows identify the wooden matrix; green arrows identify the tannin–furfural adhesive.

Although the fibers in the wood matrix were not easy to identify, the SEM images allowed us to observe: (i) the wood fiber structure, constituted of parallel fibers (red arrows), and (ii) the adhesive distributed in a networked morphology, which accumulated in the white areas (green arrows). Notwithstanding the presence of visible pits, this microscopic analysis suggests a relatively homogenous distribution of the adhesive within the woody matrix. At a higher magnification (Figure 7b), the presence of sharp breaks (yellow area), which can be due to the rigidity of the furanic adhesive, can also be noticed.

Optimization of Pressing Parameters

Further investigations extending the processing conditions were also performed. In particular, we tried to consider extended conditions such as temperature (140 °C), pressing time (13 min), and adhesive amount (10%). The results of these tests are summarized in Table 3, where they are compared with the reference measurement (in bold) and the most promising series at 160 °C with the lower pressing time (in italics).

Table 3. Physical and mechanical outcomes from the optimization of process parameters at 160 °C.

Samples			IB	MOE	MOR	T–Swelling
***Temperature* (°C)**	***Pressing time* (min)**	***Adhesive Amount* (%)**	**(MPa)**	**(MPa)**	**(MPa)**	**(%)**
140	11	15	0.16	1453	4.8	82
160	13	15	0.35	1560	5.5	77
160	11	10	0.31	1083	5.5	82
160	**11**	**15**	**0.37**	**1417**	**4.9**	**80**
160	*9*	*15*	*0.32*	*1542*	*5.3*	*90*
160	*7*	*15*	*0.03*	*1417*	*4.5*	*n.a.*

According to what was observed in the literature [62], the pressing temperature is a fundamental parameter also for tannin–furfural bonded particleboard. The panels produced at 140 °C showed less than half the internal bond of the reference formulation, clearly highlighting the need for a higher temperature (>140 °C). Extending the pressing time to 13 min did not lead to a substantial increase of internal bond, but the panels improved their bending strength MOE and MOR by 10%, but still did not completely meet the required standards. Further, a slightly lower tendency to absorb water was recorded. This observation further highlights the importance of the pressing time for the properties of the tannin–furfural panels because of the contained reactivity of this bio–based adhesive. We also tested the performance of the boards using less adhesive (10% in place of 15%), and it led to a reduction in board elasticity, registering a lower MOE (around 30%). However, no considerable differences were found for IB and MOR. In addition, the high thickness swelling was related to the adhesive itself and not influenced by its amount, and no substantial differences were found for thickness swelling. To sum up, the increase in pressing temperature and time mainly affected the internal cohesion of the boards. Under more severe conditions, the diffusion of water in the wood was favored, and consequently, the resin was able to penetrate easily into the voids (mechanical interlocking) [63]. Furthermore, at higher temperatures, a chemical change in the woody substrate is promoted, such as the overcoming of the glass transition of lignin and the breaking of hydrogen bonds, which allows chemical interlocking, too.

On the other hand, MOR and MOE are slightly affected by the pressing parameters. In fact, those properties are mostly influenced by the nature of the resin itself and the size and geometry of the wood particles [64],[65].

However, a literature comparison between bio–sourced adhesives is not simple due to the broad system of variables. A general overview is presented below and compared to the presented formulation. In particleboard with a density of 650 kg·m^{-3} bonded by oxidized base lignin resin, the authors registered an internal cohesion strength of 0.10 MPa, while the modulus of elasticity and modulus of rupture were respectively 1847 and 8.1 MPa. Adding different amounts of isocyanate from 1 to 3%, increases of up to 0.40, 2900, and 15 MPa, respectively, were observed [25].

When a mixture of corn starch and mimosa tannin was applied at 22% for a three– layer laboratory scale particleboard pressed for 7 min at 200 °C, this led to IB, MOR, and MOE of 0.98, 10.36, and 2220 MPa, respectively [66]. In another study, bio–based dextrin adhesive was synthesized and applied to particleboard production [67]. Despite a pressing time of 30 min, low–quality mechanical properties are reached, recording an MOE, MOR, and IB of 915, 5.68, and 0.11 MPa.

Additionally, chestnut tannin extract crosslinked with different hardeners was considered an adhesive [68]. Here the boards were pressed at 195 °C for 7.5 min and registered a final dry IB of 0.4–0.6 MPa, and a wet IB of 0.06–0.15 MPa. Mechanical properties are not as sensitive as water resistance for particleboards glued with bio–based adhesives. Moisture and water resistance can be considered the main drawback of bio–based adhesives, which often limit the application to dry conditions only.

For instance, Zhao et al. applied a tannin–sucrose formulation to the production of particleboard, registering a thickness swelling of around 30% [69]. Slightly higher values were registered by Ghary and Pizzi [70] using a soy flour–tannin–based adhesive. Casein–based adhesives were used to glue other agroforestry resources for boards [71], and in this case, values between 18 and 53% of thickness swelling were measured. However, the quebracho–furfural resin has been shown to be more stable for gluing particleboard than plywood, regardless of process parameters [43]. A final consideration is that the use of recycled particles was observed to lead to a significant reduction of mechanical properties[72]. In this study, a decrease of 38% for IB, 28% for MOR, and 18% for MOE, was observed using UF adhesives.

In this context, the quebracho–furfural formulation presented in this work offers com– parable mechanical properties to other bio–sourced adhesives. Internal bonds of 0.37 MPa satisfy the European standard for a P1 panel type, and an increase in density allows an enhancement of cohesion, thus broadening the potential fields of application [23]. Like the vast majority of natural–based resins, the presented resin does not offer sufficient moisture resistance, requiring the addition of some reinforcing component such as other phenolics (PFs, RFs) or isocyanates. It has to be considered that the industrial conditions for particleboard production consist of higher pressing temperatures (200–230 °C) but far lower pressing times (1–2 min). This means that important enhancements have to be achieved in order to speed up the crosslinking kinetic of the tannin–

furfural resins (tailored catalysis), but on the other hand, the lower temperature applied may contribute to containing energy costs.

Conclusions

In this work, the efficacy of quebracho tannin–furfural adhesive for particleboards was studied by modifying pressing temperature (140, 160, 180, and 200 °C), pressing time (7, 9, 11, and minutes), and adhesive content (10, 15%). A preliminary chemical characterization of industrial quebracho extract highlighted high condensed tannin content and a limited sugar portion, confirming its suitability as a building block for adhesives. The tannin–furfural resins at 45% tannin content were tested, showing good processability and stability but also a longer gel time than typical UF synthetic resins. According to density profile analysis, the pressing time plays a major impact on the final mechanical board properties. Finally, the most effective pressing parameters for particleboards were identified: (i) Pressing temperature must be higher than 140 °C, (ii) a pressing time of 9 min at least, and (iii) 15% adhesive content. In particular, the particleboards produced at 160 °C for 9 and 11 min at 15% of tannin adhesive content registered, respectively, 0.32 MPa and 0.37 MPa of internal bond, satisfying the requirement for interior conditions according to EN 312 (2010). Ultimately, this work sheds new light on the totally renewable, sustainable, and formaldehyde–free wood adhesive for the manufacture of interior–grade particleboard.

References

1. De Carvalho Araújo, C.K.; Salvador, R.; Piekarski, C.M.; Sokulski, C.C.; de Francisco, A.C.; Camargo, S.K. de C.A. Circular economy practices on wood panels: A bibliographic analysis. *Sustainability* **2019**, *11*, 1057. https://doi.org/10.3390/su11041057.

2. FAOSTAT—Food and Agriculture Organization of the United Nations. 2017. Available online: http: //www.fao.org/faostat/en/#country (accessed on June 2022).

3. Pizzi, A. Recent developments in eco–efficient bio–based adhesives for wood bonding: Opportunities and issues. *J. Adhes. Sci. Technol.* **2006**, *20*, 829–846.

4. Frihart, C.R. Wood adhesives: Past, present, and future. *For. Prod. J.* **2015**, *65*, 4–8. https://doi.org/10.13073/65.1–2.4.

5. Carvalho, L.H.; Magalhães, F.D; Ferra, J.M. Formaldehyde emissions from wood–based panels—Testing methods and industrial perspectives. In *Formaldehyde: Chemistry, Applications and Role in Polymerization*; Nova Science Publishers, Inc.: Hauppauge, NY, USA, 2012.

6. Dunky, M. Adhesives in the wood industry. In *Handbook of Adhesive Technology*, 3rd ed.; Springer: Berlin/Heidelberg, Germany, 2003; pp. 223–262, ISBN 9781498736473.

7. Vnučec, D.; Kutnar, A.; Goršek, A. Soy–based adhesives for wood–bonding–a review. *J. Adhes. Sci. Technol.* **2017**, *31*, 910–931. https://doi.org/10.1080/01694243.2016.1237278.

8. Ferdosian, F.; Pan, Z.; Gao, G.; Zhao, B. Bio–based adhesives and evaluation for wood composites application. *Polymers* **2017**, *9*, 70. https://doi.org/10.3390/polym9020070.

9. Kim, K.H.; Jahan, S.A.; Lee, J.T. Exposure to formaldehyde and its potential human health Hazards. *J. Environ. Sci. Health Part C Environ. Carcinog. Ecotoxicol. Rev.* **2011**, *29*, 277–299. https://doi.org/10.1080/10590501.2011.629972.

10. Younesi–Kordkheili, H.; Pizzi, A. Ionic liquids as enhancers of urea–glyoxal panel adhesives as substitutes for urea– formaldehyde resins. *Eur. J. Wood Wood Prod.* **2017**, *75*, 481–483. https://doi.org/10.1007/s00107–016–1116–0.

11. Food and Agriculture Organization of the United Nations. *Forest Products Annual Market Review 2018–2019*; United Nations Publication: Herndon, VA, USA, 2019.

12. Ningsi, D.W.; Suhasman; Saad, S. Characteristic of Chitosan Adhesive from Shell Shrimp Litopenaeus vannamei and Their Application for Producing Particleboard. *IOP Conf. Ser. Mater. Sci. Eng.* **2019**, *593*, 012015. https://doi.org/10.1088/1757– 899X/593/1/012015.

13. Sulaiman, N.S.; Hashim, R.; Amini, M.H.M.; Sulaiman, O.; Hiziroglu, S. Evaluation of the properties of particleboard made using oil palm starch modified with epichlorohydrin. *BioResources* **2013**, *8*, 283–301. https://doi.org/10.15376/biores.8.1.283–301.

14. Bacigalupe, A.; Escobar, M.M. Soy Protein Adhesives for Particleboard Production—A Review. *J. Polym. Environ.* **2021**, *29*, 2033–2045. https://doi.org/10.1007/s10924–020–02036–8.

15. Liu, C.; Zhang, Y.; Li, X.; Luo, J.; Gao, Q.; Li, J. A high–performance bio–adhesive derived from soy protein isolate and condensed tannins. *RSC Adv.* **2017**, *7*, 21226–21233. https://doi.org/10.1039/C7RA01210A.

16. Lei, H.; Du, G.; Wu, Z.; Xi, X.; Dong, Z. Cross–linked soy–based wood adhesives for plywood. *Int. J. Adhes. Adhes.* **2014**, *50*, 199–203. https://doi.org/10.1016/j.ijadhadh.2014.01.026.

17. Prasittisopin, L.; Li, K. A new method of making particleboard with a formaldehyde–free soy–based adhesive. *Compos. Part A Appl. Sci. Manuf.* **2010**, *41*, 1447–1453. https://doi.org/10.1016/j.compositesa.2010.06.006.

18. Li, X.; Li, Y.; Zhong, Z.; Wang, D.; Ratto, J.A.; Sheng, K.; Sun, X.S. Mechanical and water soaking properties of medium density fiberboard with wood fiber and soybean protein adhesive. *Bioresour. Technol.* **2009**, *100*, 3556–3562. https://doi.org/10.1016/j.biortech.2009.02.048.

19. Gu, K.; Huang, J.; Li, K. Preparation and evaluation of particleboard bonded with a soy flour–based adhesive with a new curing agent. *J. Adhes. Sci. Technol.* **2013**, *27*, 2053–2064. https://doi.org/10.1080/01694243.2012.696950.

20. Gu, K.; Li, K. Preparation and evaluation of particleboard with a soy flour– polyethylenimine–maleic anhydride adhesive. *J. Am. Oil Chem. Soc.* **2011**, *88*, 673–679. https://doi.org/10.1007/s11746–010–1706–7.

21. Margarida Martins, M.; Carvalheiro, F.; Gírio, F. An overview of lignin pathways of valorization: From isolation to refining and conversion into value–added products. *Biomass Convers. Biorefinery* **2022**, 1–25. https://doi.org/10.1007/s13399–022–02701–z.

22. Gillet, S.; Aguedo, M.; Petitjean, L.; Morais, A.R.C.; Da Costa Lopes, A.M.; Łukasik, R.M.; Anastas, P.T. Lignin transformations for high value applications: Towards targeted modifications using green chemistry. *Green Chem.* **2017**, *19*, 4200–4233. https://doi.org/10.1039/c7gc01479a.

23. Chen, X.; Pizzi, A.; Zhang, B.; Zhou, X.; Fredon, E.; Gerardin, C.; Du, G. Particleboard bio–adhesive by glyoxalated lignin and oxidized dialdehyde starch crosslinked by urea. *Wood Sci. Technol.* **2022**, *56*, 63–85. https://doi.org/10.1007/s00226–021–01344–z.

24. El Mansouri, N.E.; Pizzi, A.; Salvadó, J. Lignin–based wood panel adhesives without formaldehyde. *Holz als Roh Werkst.* **2007**,*65*, 65–70. https://doi.org/10.1007/s00107–006–0130–z.

25. Paul, G.B.; Timar, M.C.; Zeleniuc, O.; Lunguleasa, A.; Coșereanu, C. Mechanical properties and formaldehyde release of particleboard made with lignin–based adhesives. *Appl. Sci.* **2021**, *11*, 8720. https://doi.org/10.3390/app11188720.

26. Aristri, M.A.; Lubis, M.A.R.; Yadav, S.M.; Antov, P.; Papadopoulos, A.N.; Pizzi, A.; Fatriasari, W.; Ismayati, M.; Iswanto, A.H. Recent developments in lignin– and tannin–based non–isocyanate polyurethane resins for wood adhesives—A review. *Appl. Sci.* **2021**, *11*, 4242. https://doi.org/10.3390/app11094242.

27. Glasser, W.G. About Making Lignin Great Again—Some Lessons From the Past. *Front. Chem.* **2019**, *7*, 565. https://doi.org/10.3389/fchem.2019.00565.

28. Ang, A.F.; Ashaari, Z.; Lee, S.H.; Md Tahir, P.; Halis, R. Lignin–based copolymer adhesives for composite wood panels—A review. *Int. J. Adhes. Adhes.* **2019**, *95*, 102408. https://doi.org/10.1016/j.ijadhadh.2019.102408.

29. Olivares, M.; Guzmán, J.A.; Natho, A.; Saavedra, A. Kraft lignin utilization in adhesives. *Wood Sci. Technol.* **1988**, *22*, 157–165. https://doi.org/10.1007/BF00355851.

30. Cheng, S.; Yuan, Z.; Leitch, M.; Anderson, M.; Xu, C.C. Highly efficient de–polymerization of organosolv lignin using a catalytic hydrothermal process and production of phenolic resins/adhesives with the depolymerized lignin as a substitute for phenol at a high substitution ratio. *Ind. Crops Prod.* **2013**, *44*, 315–322. https://doi.org/10.1016/j.indcrop.2012.10.033.

31. Hernes, P.J.; Hedges, J.I. Tannin signatures of barks, needles, leaves, cones, and wood at the molecular level. *Geochim. Cosmochim. Acta* **2004**, *68*, 1293–1307. https://doi.org/10.1016/j.gca.2003.09.015.

32. Shirmohammadli, Y.; Efhamisisi, D.; Pizzi, A. Tannins as a sustainable raw material for green chemistry: A review. *Ind. Crops Prod.* **2018**, *126*, 316–332. https://doi.org/10.1016/j.indcrop.2018.10.034.

33. Pizzi, A. Tannins: Prospectives and actual industrial applications. *Biomolecules* **2019**, *9*, 344. https://doi.org/10.3390/biom9080344.

34. Aristri, M.A.; Lubis, M.A.R.; Iswanto, A.H.; Fatriasari, W.; Sari, R.K.; Antov, P.; Gajtanska, M.; Papadopoulos, A.N.; Pizzi, A. Bio–based polyurethane resins derived from tannin: Source, synthesis, characterisation, and application. *Forests* **2021**, *12*, 516. https://doi.org/10.3390/f12111516.

35. Bisanda, E.T.N.; Ogola, W.O.; Tesha, J.V. Characterisation of tannin resin blends for particle board applications. *Cem. Concr. Compos.* **2003**, *25*, 593–598. https://doi.org/10.1016/S0958–9465(02)00072–0.

36. Cesprini, E.; Šket, P.; Causin, V.; Zanetti, M.; Tondi, G. Development of Quebracho (*Schinopsis balansae*) Tannin–Based Thermoset Resins. *Polymers* **2021**, *13*, 4412.

37. Tondi, G. Tannin–Based copolymer resins: Synthesis and characterization by solid state 13C NMR and FT–IR spectroscopy. *Polymers* **2017**, *9*, 223. https://doi.org/10.3390/polym9060223.

38. Pizzi, A. *Advanced Wood Adhesives Technology*; CRC Press: Boca Raton, FL, USA, 1994.

39. Engozogho Anris, S.P.; Bikoro Bi Athomo, A.; Safou–Tchiama, R.; Leroyer, L.; Vidal, M.; Charrier, B. Development of green adhesives for fiberboard manufacturing, using okoume bark tannins and hexamine–characterization by 1H NMR, TMA, TGA and DSC analysis. *J. Adhes. Sci. Technol.* **2021**, *35*, 436–449. https://doi.org/10.1080/01694243.2020.1808356.

40. Valenzuela, J.; Von Leyser, E.; Pizzi, A.; Westermeyer, C.; Gorrini, B. Industrial production of pine tannin–bonded particleboard and MDF. *Eur. J. Wood Wood Prod.* **2012**, *70*, 735–740. https://doi.org/10.1007/s00107–012–0610–2.

41. Ballerini, A.; Despres, A.; Pizzi, A. Non–toxic, zero emission tannin–glyoxal adhesives for wood panels. *Holz als Roh Werkst.* **2005**, *63*, 477–478. https://doi.org/10.1007/s00107–005–0048–x.

42. Luckeneder, P.; Gavino, J.; Kuchernig, R.; Petutschnigg, A.; Tondi, G. Sustainable phenolic fractions as basis for furfuryl alcohol– based co–polymers and their use as wood adhesives. *Polymers* **2016**, *8*, 396. https://doi.org/10.3390/polym8110396.

43. Jorda, J.; Cesprini, E.; Barbu, M.–C.; Tondi, G.; Zanetti, M.; Král, P. Quebracho Tannin Bio–Based Adhesives for Plywood. *Polymers* **2022**, *14*, 2257. https://doi.org/10.3390/polym14112257.

44. Kabbour, M.; Luque, R. *Furfural as a Platform Chemical: From Production to Applications*; Elsevier : Amsterdam, The Netherlands, 2019; ISBN 9780444643070.

45. Singleton, V.L.; Orthofer, R.; Lamuela–Raventos, R.M. Analysis of Total Phenols and Other Oxidation Substrates and Antioxidants by Means of Folin–Ciocalteu Reagent. *Methods Enzymol.* **1999**, *299*, 152–178. https://doi.org/10.1016/j.scienta.2016.11.004.

46. Seppepere, T.; Hernandez–Ramos, F.; Labidi, J.; Oostingh, G.J.; Bogner, B.; Petutschnigg, A.; Tondi, G. Purification of industrial tannin extract through simple solid–liquid extractions. *Ind. Crop. Prod*. **2019**, *139*, 111502.

47. De Iseppi, A.; Marangon, M.; Lomolino, G.; Crapisi, A.; Curioni, A. Red and white wine lees as a novel source of emulsifiers and foaming agents. *LWT* **2021**, *152*, 112273. https://doi.org/10.1016/j.lwt.2021.112273.

48. Hafiz, N.L.M.; Tahir, P.M.D.; Hua, L.S.; Abidin, Z.Z.; Sabaruddin, F.A.; Yunus, N.M.; Abdullah, U.H.; Abdul Khalil, H.P.S. Curing and thermal properties of co–polymerized tannin phenol–formaldehyde resin for bonding wood veneers. *J. Mater. Res. Technol.* **2020**, *9*, 6994–7001. https://doi.org/10.1016/j.jmrt.2020.05.029.

49. *SIST EN 323:1996*; Wood–Based Panels—Determination of Density. British Standards: London, UK, 1993.

50. *BS EN 319:1993*; Particleboards and Fiberboards—Determination of Tensile Strength Perpendicular to the Plane of Board. British Standards: London, UK, 1993.

51. *BS EN 310:1993*; Wood–based panels—Determination of Modulus of Elasticity in Bending and of Bending Strength. British Standards: London, UK, 1993; pp. 1–14.

52. *BS EN 317:1993*; Particleboards and Fiberboards—Determination of Swelling in Thickness after Immersion in Water. British Standards: London, UK, 1993.

53. RStudio. *Integrated Development Environment for R*; RStudio PBC: Boston, MA, USA, 2012.

54. Cesprini, E.; De Iseppi, A.; Giovando, S.; Tarabra, E.; Zanetti, M.; Primož, Š.; Matteo, M.; Tondi, G. Wood Science and Technology Chemical characterization of cherry (*Prunus avium*) tannins in comparison with commercial mimosa and chestnut tannin extracts. *Wood Sci. Technol.* **2022**, *56*, 1455–1473.

55. Watrelot, A.A.; Norton, E.L. Chemistry and reactivity of tannins in vitis spp.: A review. *Molecules* **2020**, *25*, 2110. https://doi.org/10.3390/molecules25092110.

56. Garro Galvez, J.M.; Riedl, B.; Conner, A.H. Analytical studies on tara tannins. *Holzforschung* **1997**, *51*, 235–243. https://doi.org/10.1515/hfsg.1997.51.3.235.

57. Bianchi, S.; Kroslakova, I.; Janzon, R.; Mayer, I.; Saake, B.; Pichelin, F. Characterization of condensed tannins and carbohydrates in hot water bark extracts of European softwood species. *Phytochemistry* **2015**, *120*, 53–61. https://doi.org/10.1016/j.phytochem.2015.10.006.

58. Navarrete, P.; Pizzi, A.; Tapin–Lingua, S.; Benjelloun–Mlayah, B.; Pasch, H.; Rode, K.; Delmotte, L.; Rigolet, S. Low formaldehyde emitting biobased wood adhesives manufactured from mixtures of tannin and glyoxylated lignin. *J. Adhes. Sci. Technol.* **2012**, *26*, 1667–1684. https://doi.org/10.1163/156856111X618489.

59. Hauptt, R.A.; Sellers, T. Characterizations of Phenol–Formaldehyde Resol Resins. *Ind. Eng. Chem. Res.* **1994**, *33*, 693–697. https://doi.org/10.1021/ie00027a030.

60. Wong, E.D.; Zhang, M.; Wang, Q.; Kawai, S. Formation of the density profile and its effects on the properties of particleboard.

Wood Sci. Technol. **1999**, *33*, 327–340. https://doi.org/10.1007/s002260050119.

61. *EN 312:2010*; Particleboards—Specifications. British Standards: London, UK, 2010.

62. de Palacios, P.; Fernández, F.G.; García–Iruela, A.; González–Rodrigo, B.; Esteban, L.G. Study of the influence of the physical properties of particleboard type P2 on the internal bond of panels using artificial neural networks. *Comput. Electron. Agric.* **2018**, *155*, 142–149. https://doi.org/10.1016/j.compag.2018.10.012.

63. Iswanto, A.H.; Febrianto, F.; Hadi, Y.S.; Ruhendi, S.; Hermawan, D. The Effect of Pressing Temperature and Time on the Quality of Particle Board Made from Jatropha Fruit Hulls Treated in Acidic Condition. *MAKARA J. Technol. Ser.* **2014**, *17*, 8. https://doi.org/10.7454/mst.v17i3.2930.

64. Ferrández–García, C.E.; Ferrández–García, A.; Ferrández–Villena, M.; Hidalgo–Cordero, J.F.; García–Ortuño, T.; Ferrández– García, M.T. Physical and mechanical properties of particleboard made from palm tree prunings. *Forests* **2018**, *9*, 755. https://doi.org/10.3390/f9120755.

65. Maloney, T. *Moder Particleboard and Dry–Process Fiberboard Manufacturing*; Miller Freeman: San Francisco, CA, USA, 1993.

66. Oktay, S.; Kızılcan, N.; Bengü, B. Development of bio–based cornstarch – Mimosa tannin – sugar adhesive for interior particleboard production. *Ind. Crops Prod.* **2021**, *170*, 113689. https://doi.org/10.1016/j.indcrop.2021.113689.

67. Alamsyah, E.M.; Sutrisno; Nuryawan, A.; Widyorini, R. Identifying best parameters of particleboard bonded with dextrin–based adhesives. *Open Agric.* **2020**, *5*, 345–351. https://doi.org/10.1515/opag–2020–0037.

68. Santos, J.; Antorrena, G.; Freire, M.S.; Pizzi, A.; González–Álvarez, J. Environmentally friendly wood adhesives based on chestnut (*Castanea sativa*) shell tannins. *Eur. J. Wood Wood Prod.* **2017**, *75*, 89–100. https://doi.org/10.1007/s00107–016–1054–x.
69. Zhao, Z.; Umemura, K. Investigation of a New Natural Particleboard Adhesive Composed of Tannin and Sucrose. 2. Effect of Pressing Temperature and Time on Board Properties, and Characterization of Adhesive. *BioResources* **2015**, *10*, 2444–2460.
70. Ghahri, S.; Pizzi, A. Improving soy–based adhesives for wood particleboard by tannins addition. *Wood Sci. Technol.* **2018**, *52*, 261–279. https://doi.org/10.1007/s00226–017–0957–y.
71. Mahieu, A.; Vivet, A.; Poilane, C.; Leblanc, N. Performance of particleboards based on annual plant byproducts bound with bio–adhesives. *Int. J. Adhes. Adhes.* **2021**, *107*, 102847. https://doi.org/10.1016/j.ijadhadh.2021.102847.
72. Iždinský, J.; Vidholdová, Z.; Reinprecht, L. Particleboards from recycled wood. *Forests* **2020**, *11*, 1166. https://doi.org/10.3390/f11111166.

4.2.3 Quebracho Tannin Bio–Based Adhesives for Plywood

Johannes Jorda, Emanuele Cesprini, Marius–Cătălin Barbu, Gianluca Tondi, Michela Zanetti and Pavel Král

Abstract

Wood–based products are traditionally bonded with synthetic adhesives. Resources avail– ability and ecological concerns have drawn attention to bio–based sources. The use of tannin–based adhesives for engineered wood products has been known for decades, however, these formulations were hardly used for the gluing of solid wood because their rigidity involved low performance. In this work, a completely bio–based formulation consisting of Quebracho (*Schinopsis balancae*) extract and furfural is characterized in terms of viscosity, gel time, and FT–IR spectroscopy. Further, the usability as an adhesive for beech (*Fagus sylvatica*) plywood with regard to press parameters (time and temperature) and its influence on physical (density and thickness) and mechanical properties (modulus of elasticity, modulus of rupture and tensile shear strength) were determined. These polyphenolic adhesives presented non–Newtonian behavior but still good spreading at room temperature as well as evident signs of crosslinking when exposed to 100 °C. Within the press temperature, a range of 125 °C to 140 °C gained suitable results with regard to mechanical properties. The modulus of elasticity of five layered 10 mm beech plywood ranged between 9600 $N \cdot mm^{-2}$ and 11,600 $N \cdot mm^{-2}$, respectively, with 66 $N \cdot mm^{-2}$ to 100 $N \cdot mm^{-2}$ for the modulus of rupture. The dry state tensile shear strength of ~2.2 $N \cdot mm^{-2}$ matched with other tannin–based formulations, but showed delamination after 24 h of water storage. The proposed quebracho tannin–furfural formulation can be a bio–based alternative adhesive for industrial applicability for special plywood products in a dry environment, and it offers new possibilities in terms of recyclability.

Introduction

Lignocellulosic are abundant bio–resources, nowadays perceived as a gamechanger in the scope of the climate crisis. Wood products contribute as carbon dioxide (CO_2) storage sinks due to increasing the time that CO_2 captured in forests is kept out of the atmosphere. Encouraging more forest growth, wood products enhance the efficiency of forest sinks by acting as carbon stores [1]. Indeed, numerous studies have emphasized the environmental benefits of wood–based materials compared to mineral–based compounds [2],[3], due to the low embodied emissions and the lower material intensity of wood [4]. Within wood– based products, wood panels cover a major assortment of applications in the construction, packaging, and furniture sectors [5]. In order to achieve well–distinct properties, wood panel manufacturing adapts the dimensions of engineered wood products (EWPs) through the intelligent (re)assembly of wooden parts. Assembly that is regularly done with the application of adhesive resins. The high market that EWPs are gaining have caused environmental concerns related to the emissions from formaldehyde and other volatile compound that underlie the main adhesives used [6]. Consequently, workable alternatives are required in accordance with environmental standards and safety and market demands to direct future development through a sustainable use of wood. For instance, the generation of adhesives from bio–resources enables both a reduction in the use of chemical reagents harmful to health and a further move away from petroleum derivatives, thus decreasing the carbon footprint of the final product [7]. Actually, recent market forecasts highlight the importance of the bio–adhesives field and a growth from between USD 3.7–6.0 billion in 2020 to USD 5.2–9.7 billion by 2025–2028 is expected [8],[9]. Different renewable substances have been proposed as a building block to manufacture bio–resins, from plant protein such as soy, starch based polysaccharides, and lignocellulosic molecules such as lignin and tannins [10],[11]. Additionally, to overcome issues related to toxic reagents such as the formaldehyde traditionally used to manufacture wood–based products [12], different bio–based formaldehyde free formulations have been developed. Oktay et al. (2021) used bio–based corn–starch Mimosa tannin sugar adhesives for panels to meet the EN 312:2010 particleboard (P2) standard requirements for interior fittings in a dry state [13]. Similar results are given by Paul et al. for particleboard bonded with lignin–based adhesives [14]. Plywood, for example, assembled with PVOH–lignin–hexamine showed a dry tensile shear strength of 0.95 $N \cdot mm^{-2}$ [15] or with a soybean meal–based adhesive, which displayed excellent water resistance with a tensile shear strength exceeding 1 $N \cdot mm^{-2}$ [16]. Ghahri et al. reported a wet state tensile shear strength of ~0.8 $N\cdot mm^{-2}$ for a Quebracho tannin and isolate soy protein adhesive without hardener [17]. According to the mentioned research, tannins are of particular interest due to their chemical structure and good reactivity [18],[19], which make these compounds great candidates. Tannins are classified into hydrolysable and condensed, the former class are mixtures of simple phenols, such as pyrogallol and ellagic acid, and esters of glucose, with gallic and digallic acids [20]. The latter, also known as proanthocyanins or flavanol, constitutes more than 90% of world production [20], which due to its reactivity is more suitable for industrial application. Condensed tannins are polyhydroxy–flavan–3–ol oligomers bonded together mostly by C–C bonds between the A rings of the flavanol units and the pyran rings of other flavanol units [19]. Particularly, the polyphenolic structure suggests the comparison and the possible replacement of phenol–formaldehyde (PF) synthetic resins used for gluing EWPs, whose production has seen a sharp increase in the last decade [21]. Moreover, during processing, PF resins have the highest environmental impact of all major synthetic resins [22], ranking tannins as a potential prime substitute.

Deep research has been carried out on the application of tannin adhesives [23–26]. However, it is useful to mention that a synthetic crosslinker is almost always required to form the three–dimensional polymeric structure. In the current study, an entirely renewable tannin–based adhesive is proposed, using furfural as hardener. Furfural, belonging to the furan compounds, is produced through the acid hydrolysis of biomass [27], and agricultural residues can be used, too [28]. The renewability and the abundance of lignocellulosic biomass make it a viable resource.

This study proposes a new Quebracho tannin–furfural adhesive formulation to be used for the production of plywood. The aim of our investigation is to characterize the Quebracho tannin–furfural adhesive, previously studied and compared with the main synthetic and non–synthetic hardeners [29], in terms of gel time, viscosity, and FT–IR spectroscopy as well as to determine the mechanical performance of five layered beech (*Fagus sylvatica*) plywood with regard to the press parameter of time and temperature, which consequently contribute to the production and the use of bio–based adhesives.

Materials and Methods

Materials

The tannin–based adhesives were prepared using Quebracho (*Schinopsis balancae*) tannin extract (Fintan 737B), kindly provided by the company Silvateam (S. Michele Mondovì).

The tannin–based adhesives were prepared using Quebracho (*Schinopsis balancae*) tannin extract (Fintan 737B), kindly provided by the company Silvateam (S. Michele Mondovì, Cuneo, Italy) and furfural (99%) obtained by International Furan Chemical IFC (Rotterdam, The Netherlands). Sodium hydroxide was purchased from Alfa Aesar (Thermo Fisher, Waltham, MA, USA) and it was applied to change the pH of the formulation.

Pre–conditioned (20 °C, 65% relative air humidity) rotary cut defect free beech (*Fagus sylvatica*) veneers, purchased from Europlac (Topolcany, Slovakia,), with a nominal thickness of 2.2 mm, an average density of 0.72 g·cm^{-3}, and an average moisture content of 12% were used to prepare the plywood for this study.

Methods

Adhesive Preparation

The tannin–furfural formulation was prepared by mixing under vigorous stirring the commercial extract with water to obtain a 65% homogeneous suspension. The starting pH of 6.7 was adjusted to 8 by adding a 33% sodium hydroxide solution and finally 10% of furfural calculated on solid tannin was added.

Adhesive Characterization

Gel time: 5 g of the formulation were inserted into a glass test tube which was immersed in an oil bath at 100 °C. The transition time to obtain a solid was recorded using a stopwatch. The tests were repeated three times.

Viscosity: A freshly prepared formulation was analyzed with Rheometer Kinexus Lab from Malvern Panalytical (Malvern, UK). The measurement was conducted at 25 °C using cone–shaped geometry spindles with a diameter of 4 cm and a gap between the plates of 0.15 mm. The rotational speed was set from 10 s^{-1} to 300 s^{-1}.

FT–IR: A Frontier ATR–FT–MIR from Perkin Elmer (Waltham, MA, USA) was used for scanning the industrial Quebracho powder, Quebracho furfural formulation dried at room temperature for 24 h and the same formulation cross–linked at 100 °C for 24 h. Every spectrum was acquired with the ATR diamond device with 32 scans from 4000 to 600 cm^{-1} and the fingerprint spectral region between 1800 and 600 cm^{-1} was considered after normalization and baseline correction.

Plywood Preparation

The plywood consisted of five layered 90° crosswise oriented 2.2 mm thick beech veneer plies. Adhesive application was carried out manually by weighing the required adhesive amount of 150 g/m^2 per glue line with a KERN ITB 35K1IP device (Balingen– Frommern, Germany). Pressing was conducted using a Höfler HLOP 280 (Taiskirchen, Austria). Pressure was set to 3 $N \cdot mm^{-2}$; press–time was 10 min, 15 min, respectively 20 min and press–temperature was 110 °C, 125 °C and 140 °C. A pretest to determine the time depended temperature behavior within the glue line during hot pressing as well as in order to check temperature difference between press and glue line was conducted using a Lutron electronic enterprise BTM 4208SD (Taipei City, Taiwan) datalogger with K–couple thermo–wired sensors. The sensors were placed on the outer plies surfaces and within the glue lines between the singular plies. The temperature at the press control unit was adjusted according to the pretest results. After pressing, the boards were stored until mass constancy under a climate of 20 °C and 65% relative humidity. Test specimen were cut from the plywood boards for the determination of density, bending strength (MOR), stiffness (MOE), and tensile shear strength (TSS).

Plywood Characterization

The density was determined according to EN 323:2005, and it was obtained from the bending test specimen [30]. The density profile was measured with a DENSE–LAB X (EWS, Hammeln, Germany) and the specimen dimensions 50 mm × 50 mm. The thickness was obtained from the bending test specimens. The "Degree of compression" (DoC) was calculated by the percentage based difference between the theoretical thickness of 11 mm of non–compressed veneer ply stack before pressing and the actual thickness of the bending test specimens according to Spulle et al. (2021) [31]. Dry state tensile shear strength (TSS) and 24 h water soaking TSS was determined according to EN 314:2005 with specimen dimensions 100 mm 25 mm [32]. Modulus of rupture (MOR) and modulus of elasticity (MOE) were determined by a three–point bending test according to EN 310:2005 with specimen dimensions 250 mm 50 mm [33]. All mechanical properties (SS, MOE, and MOR) were determined using a Zwick/Roell 250 8497.04.00 test device (Ulm, Germany) under constant climatic conditions (rel. humidity 65%, ambient temperature 20 °C). The set–up and the number of specimens of the conducted tests is given in Table 1.

Table 1. Number of test specimen for the physical and mechanical properties testing of Quebracho tannin–furfural bonded five layered beech plywood.

	Time [min]								
	10			15			200		
Temperature [°C]	110	125	140	110	125	140	110	125	140
	Number of test specimens N								
Density	5	5	5	5	5	5	5	5	5
Density profile	5	5	5	5	5	5	5	5	5
Thickness	5	5	5	5	5	5	5	5	5
MOE/MOR	5	5	5	5	5	5	5	5	5
TSS dry state & 24h	5	5	5	5	5	5	5	5	5

Data Analysis

For statistical evaluation IBM SPSS (Armonk, NY, USA) was used for descriptive data exploration and univariate and multivariate methods for the evaluation of the different Quebracho tannin–furfural bonded plywood test specimen. To determine differences between the press parameters, an ANOVA at a significance level of 95% was used. Multivariate ANOVA was used to determine the influence of "Temperature" and "Press–time" with the "Density" as covariant. The significance of correlations (Pearson) were evaluated using two–sided confidence intervals of 95%.

Results & Discussion

Adhesive Characterization

Tannin–furfural adhesives showed the most favorable hardening conditions at pH 8 [29]. Due to the limited viscosity of the adhesive at 50% solid content (s.c.), in this work tannin formulations with 65% s.c. were tested for their viscosity, gel time, and hardening. It was observed that concentrated tannin–furfural formulation presents a non–Newtonian pseudoplastic behavior (Figure 1), described as an increase of shear rate leading to a decrease of viscosity. In these conditions, the formulation easily resulted in being homogeneously spread on wood. The curing behavior of the formulation was measured through gel time at 100 °C, which was 238 (±10) seconds that is slightly slower than commercial urea–formaldehyde's (UF) as it hardens after 127 s [34] but rather faster than phenol–formaldehyde's (PF) with a gelation time ranging within 10 min [35].

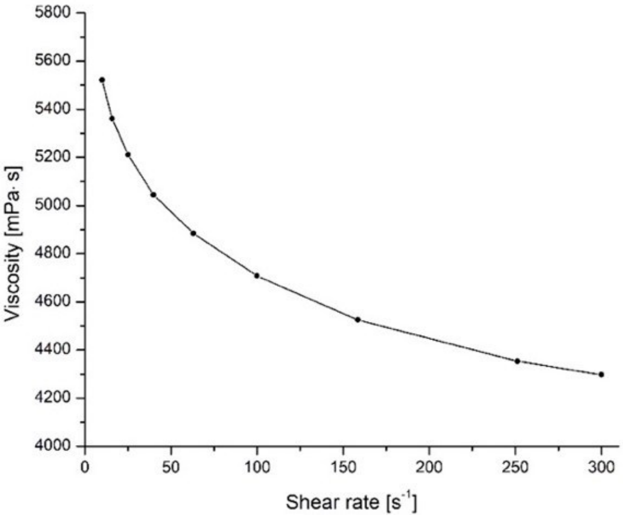

Figure 1. Viscosity of a 65% tannin furfural formulation.

From the chemical point of view, the curing process was observed comparing the spectra of the resin exposed 24 h at 25 and 100 °C. Figure 2 reports the spectra of the dry resin before and after curing. Comparing the two spectra, the most evident difference is that after curing the bands become broader suggesting the formation of polymeric structures, in particular the region at lower wavenumber become almost flat due to the steric hindrance for out of plane C–OH wagging and C–H bending vibrations [36,37]. Further major observations are the decreasing/disappearing of some signals such as those at 1670, 1392, 1018, 929, and 758 cm^{-1}, which are related to furfural compounds [38,39]. According to these observations, the crosslinking process could be similar to that observed for the polymer with Mimosa extract, involving the bridging through methylene–furanic units [40].

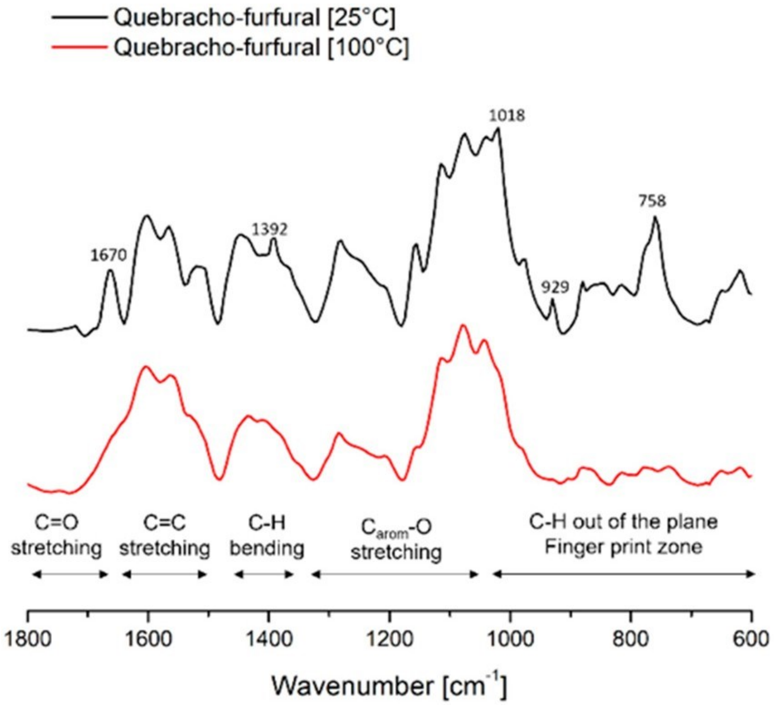

Figure 2. ATR–FTIR of Quebracho tannin furfural formulations at room temperature (black) and cured at 100 °C (red).

The main differences between Mimosa and Quebracho tannin is related to the nature of the B ring where the former bonds three hydroxyl groups (pyrogallic unit) [40]. Conversely, the B ring of Quebracho bonds principally two hydroxyl groups (catechol unit) decreasing the reactivity due to the chemistry of phenol [29]. Thus concluding, the reaction between Quebracho and furfural mainly involves the benzene ring A, as reported in Figure 3.

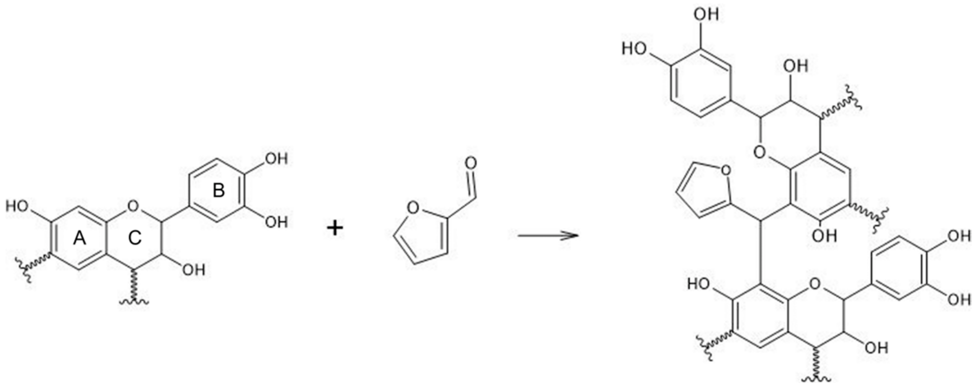

Figure 3. Possible product from Quebracho tannin and furfural reaction.

Plywood Characterization

Density

Density is one of the major physical parameters influencing the mechanical properties of plywood while enhancing MOE and tensile strength (TS) [41]. The mean density of the tested groups range between 0.768 g·cm^{-3} (press temperature 140 °C; press time 10 min) and 0.810 g·cm^{-3} (press temperature 125 °C; press time 20 min) (Figure 4a). The gained results are within the range compared to the values mentioned in the literature for identical five–layered beech plywood set–ups [42],[43]. Testing of the density specimen for 110 °C press temperature and 10 min press time was not possible due to delamination after pressing and conditioning.

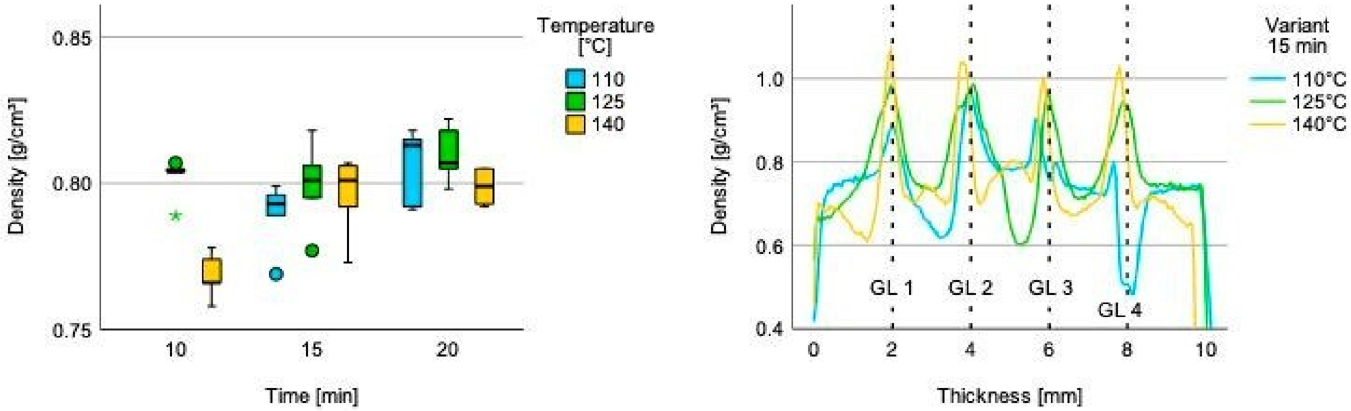

(a) (b)

Figure 4. (a) Density grouped by time and temperature. Dots and stars within the box plot indicate outliers and (b) density profile for the 5–layers plywood glued for 15 min with Quebracho tannin–furfural adhesives at different temperature.

The density profile, plotting density against thickness, displays a method to gain information of the bonding performance within the adhesive layer [44],[45]. The selected density profiles (Figure 4b) of specimen from the test set 15 min and three different temperatures, demonstrating differing bonding behavior. The specimen for the press temperature of 110 °C reveals delamination within the glue line (GL) 4 due to a significant sharp declined density gap and wider thickness. Further, a double peaking at glue line 3 indicates inappropriate bonding behavior. Test specimen for the press temperature of 125 °C illustrates a deeper adhesive penetration into the plies adjacent to the glue line due to wider and slightly lower density peaks than the selected specimen of the press temperature 140 °C. Compared to the previous described samples, the specimen for 140 °C has a sharper curvature of the density peaks indicating a reduced adhesive penetration into the adjacent wood layers, and a higher degree of compression is visible due to the lower thickness (<10 mm) compared to the other test specimen (>10 mm) with a lower temperature (Figure 5a).

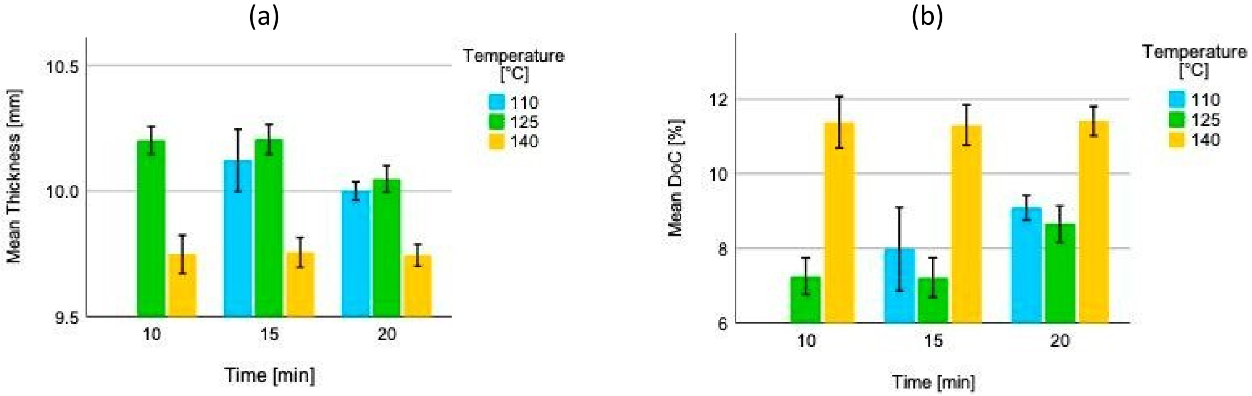

Figure 5. (a) Mean thickness and (b) mean degree of compression (DoC) of five layered Quebracho tannin furfural bonded plywood. The brackets within the figure indicate the interval ± 1 standard deviation (SD).

The thickness of the Quebracho tannin–furfural bonded five layered plywood ranges between 9.74 mm (press temperature 140 °C; press time 20 min) and 10.21 mm (press temperature 125 °C; press time 15 min) (Figure 5a), respectively, and between 11.45% and 7.18% for the degree of compression (DoC) (Figure 5b). This is according to Bekhta et al., stating a compression of ~10% for plywood manufacturing [46]. Thickness and therefore the degree of compression is influenced by the moisture content of veneers, press time and temperature. An elongated press time with a higher temperature influences the chemical wood structure due to a shift toward the glass transition of the singular chemical wood constituents while softening the natural polymeric cellular fiber composite character of wood [47].

Bending Properties

Modulus of elasticity (MOE) ranges between 448 (SD = 34) N·mm^{-2} (press–time 15 min/–temperature 110 °C) and 11,628 (SD = 592) N·mm^{-2} (press–time 10 min/–temperature 140 °C) (Figure 6a). Modulus of rupture (MOR) ranges between 18.73 (SD = 2.65) N·mm^{-2} (press–time 15 min/–temperature 110 °C) and 104.61 (SD = 20.67) N·mm^{-2} (press–time 15 min/–temperature 140 °C) (Figure 6b). Testing of specimen of test–group press time 10 min and press temperature 110 °C could not be carried out due to delamination after pressing and within conditioning. All tested specimen regardless of the test group failed within the adhesive layers, indicating low cohesive strength. Notable is the shift of the failure pattern from the pressure zone to the tension zone of the three–point bending test specimens, with increasing press–temperature and time. This fact reveals an improved adhesive performance with increasing press–time and temperature (Figure 7).

The modulus of elasticity is clearly affected by the combination of temperature and time. At a higher temperature, similar MOE are achieved independently of the pressing time.

Applying 20 min curing time, 110 °C is already sufficient to exceed 9000 N·mm^{-2}, while at 140 °C with 10 min already a modulus of elasticity exceeding 11,000 N·mm^{-2} is reached. Hence, an increase of the temperature above 15 min does not further influence the final MOE. Additionally, the modulus of rupture (MOR) is dependent on the combined effect between temperature and time, where temperature is still crucial (Figure 6b). It can be observed that, the overall preferable pressing conditions for the bending properties require higher temperature (140 °C) and a pressing time of 10 to 15 min.

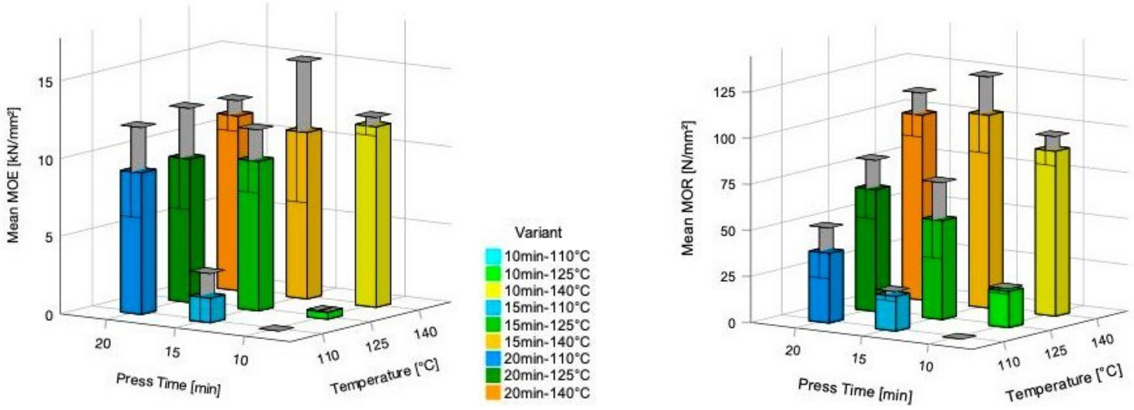

(a) (b)

Figure 6. Influence of press time and press temperature of five layered Quebracho Tannin furfural bonded beech plywood on (a) Modulus of elasticity (MOE) and (b) Modulus of rupture (MOR). The top of the column indicates the means and the bars within the figure represent the standard deviation (SD).

Comparing the presented MOE and MOR values to the literature, there is a general divergent picture. Niemz stated general values for MOE between 1500 and 7000 N·mm^{-2} for plywood without regard to adhesives [48]. Values for MOE according to DIN 68 705–5 range between 5900 and 9600 N·mm^{-2} [49]. Hrazsky and Kral (2005) stated a mean MOE of 12,493 N·mm^{-2} and a mean MOR of 77.50 N·mm^{-2} for seven layered foiled 10 mm thick beech plywood [50]. Biadala et al. obtained a mean MOE of 13,720 N·mm^{-2} for three layered phenol–formaldehyde bonded beech plywood with a nominal veneer thickness of 1.7 mm and a MOR of 158.4 N·mm–2 [51].

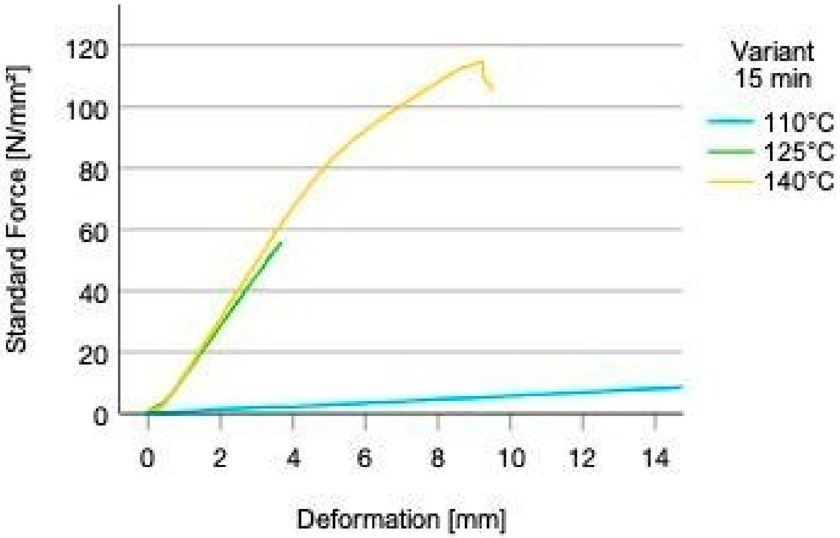

Figure 7. Stress–deformation behavior of selected samples for 15 min press time and three different temperatures.

Lower values are given by Dieste et al. for MOE with a mean of 9369 N·mm^{-2} of *Fagus sylvatica* five layered phenolic resin (150 g·m^{-2}) bonded plywood at 140 °C press temperature, 10 min of pressing and a pressure of 1 N·mm^{-2} [52]. This is 20% lower compared to the presented mean MOE of 11,628 N·mm^{-2} for 10 min and 140 °C of the current study. The variation within the numbers can be explained by the natural variation of native wood and its anisotropic behavior. Lohmann stated for the MOE of *Fagus sylvatica* a range between 10,000 to 18,000 N·mm^{-2} and for MOR 74 to 210 N·mm^{-2} [53]. Additionally, the mechanical performance of wood–based materials is influenced by the press parameters, according to Réh et al., as well as the specific lay–up of laminar wood–based products [54]. Further, the type of adhesive has a significant influence on MOE and MOR [55], concluding that the presented adhesive formulation can compete with synthetic phenolic resins in terms of MOE and MOR.

Tensile Shear Strength

Tensile shear strength had been tested in the dry state and after 24 h water storage. The results for the dry state tensile shear strength range between 0.00 N·mm^{-2} (press– time 10 min; press–temperature 110 °C), respectively, 1.74 (SD = 0.32) N·mm^{-2} (press–time 10 min; press–temperature 140 °C) and 2.29 (SD = 0.69) N·mm^{-2} (press–time 15 min; and press–temperature 125 °C) (Figure 8). It has to be noted that specimens of test group 110 °C/10 min failed subsequently before testing due to delamination and only two specimen per test group 125 °C/10 min and test group 110 °C/15 min due to delamination during specimen cutting could be tested. This indicates a poor bonding behavior within the glue line. Tensile shear strength testing at dry state revealed excellent results even at moderate curing temperature (125 °C) with limited influence of the press time.

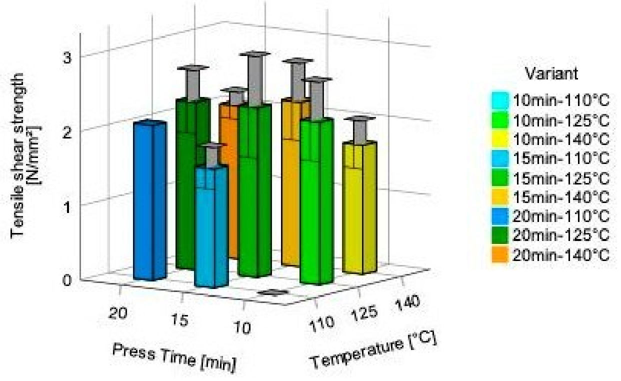

Figure 8. Dry state tensile shear strength for the 5–layered Quebracho tannin bonded plywood. The brackets within the columns of the figure indicate the standard deviation.

All tested specimens regardless of the test group failed within the glue line without displaying a wood fracture pattern according to EN 314 [56]. Testing of tensile shear strength for class 1 plywood applications according to EN 314 with 24 h water storage could not be carried out due to delamination failure of all test specimens within the 24 h of immersion into water [32].

Compared to the literature, Xi et al. (2020) gained values for tensile shear strength at a dry state between 0.98 and 1.99 N·mm^{-2} for three layered poplar (*Populus tremuloides*) plywood bonded with different Mimosa tannin glucose mixtures [57]. Similar results are stated by Hafiz et al. (2020) for tannin phenol–formaldehyde (TPF) co–polymer bonded rubber wood (*Hevea brasiliensis*) plywood in a range between 1.71 and 2.58 N·mm^{-2} and 3.41 N·mm^{-2} for the phenol–formaldehyde (PF) bonded reference [58]. Compared to industrial applicated adhesives, Jorda et al. (2021) stated for five layered beech (*Fagus sylvatica*) urea–formaldehyde (UF) bonded plywood a mean tensile shear strength in a dry state of 5.47 N·mm^{-2}, for melamine–urea formaldehyde (MUF) 6.29 N·mm^{-2} and polyurethane (PUR) of 6.74 N·mm^{-2} [42]. Biadala et al. (2020) obtained a tensile shear strength value for phenol formaldehyde resin bonded beech plywood after 24 h water soaking of 2.99 N·mm^{-2}, respectively 2.44 N·mm^{-2} after the boiling test [51]. Concluding that the presented Quebracho tannin–furfural adhesive formulation is capable of preserving with other mentioned tannin adhesives formulations for dry state tensile shear strength. Compared to industrial applicated adhesives, the dry–state performance is significantly lower and after 24 h water exposure incapable in terms of water resistance. This could be related to tensions induced by swelling of the singular veneer plies, especially beech (*Fagus sylvatica* L.) reacts sensitive to moisture induced swelling and shrinkage, resulting in low stress transfer capability within the glue line due to the brittle structure of the hardened Quebracho tannin–furfural adhesive. This is in line with several studies mentioning the brittle behavior of tannin–based adhesive formed glue lines [59–61].

Statistical Considerations

Significant correlations between thickness and MOE (R = –0.609; p–value 0.001), thickness and MOR (R = –0.823; p–value 0.001) and the correlation between MOE and MOR (R = 0.831; p–value 0.001) could be stated. The correlation of MOE versus density (R = 0.098; p–value 0.546) and MOR versus density (R = –0.025; p–value 0.876) is not detected. No correlation between tensile shear strength versus MOE (R = –0.147; p–value 0.456) and tensile shear strength versus MOR (R = –0.105; p–value 0.596) are detected.

The selected press parameters “time” and “temperature” have been accessed by uni and multivariate methods to determine the influence on density, thickness, modulus of elasticity, modulus of rupture, and tensile shear strength (Table 2).

Table 2. Results of statistical significance for one–way ANOVA.

Properties	Variable	Mean Square	F–Value	*p*–Value
Density	Temperature	0.001	4.671	0.016 *
	Time	0.001	6.021	0.005 *
Thickness	Temperature	0.654	90.577	<0.001 *
	Time	0.036	0.876	0.425
MOE	Temperature	130074609	7.985	0.001 *
	Time	489227828.8	2.360	0.108
MOR	Temperature	17277.397	47.926	<0.001 *
	Time	609.421	0.483	0.621
TSS	Temperature	0.360	1.850	0.178
	Time	0.206	0.994	0.384

The one–way ANOVA for the factor “temperature” reveals the influence on density (*p*–value = 0.016; η^2 0.202), thickness (*p*–value < 0.001; η^2 0.830), modulus of elasticity (*p*–value = 0.001; η^2 0.301) and modulus of rupture (*p*–value < 0.001; η^2 0.721). It does not influence tensile shear strength (*p*–value = 0.178; η^2 0.129). A significant influence can be stated for the factor “time” on density (*p*–value = 0.005; η^2 0.246) but not for thickness (*p*–value = 0.425; η^2 0.045), tensile shear strength (*p*–value = 0.384; η^2 0.074), modulus of elasticity (*p*–value = 0.108; η^2 0.113) and modulus of rupture (*p*–value = 0.621; η^2 0.025).

The multivariate test conducted for the factors “time” and “temperature” with the covariant “density” displays a similar picture for the factor “temperature” significantly influencing thickness (*p*–value < 0.001), modulus of elasticity (*p*–value < 0.001), modulus of rupture (*p*–value < 0.001) and tensile shear strength (*p*–value 0.048). The factor "time" does significantly influence the thickness (*p*–value < 0.001) but not tensile shear strength (*p*–value 0.127), modulus of elasticity (*p*–value 0.428) and modulus of rupture (*p*–value 0.271).

Comparing the trend of the estimated marginal means trends for temperature, increasing the temperature between 110 °C to 125 °C increases thickness. A further increase in temperature significantly decreases the thickness. This can be explained by the glass transition of the singular chemical constituents of wood resulting in a shape change of the cellular structure [45]. The factor press time displays a similar trend.

Interaction effects between the factors "time" and "temperature" are given for thick– ness and the mechanical properties of modulus of elasticity and modulus of rupture with a *p*–value < 0.001 but not for tensile shear strength with a *p*–value of 0.303.

For MOE, the "time" has a great influence at a low temperature; but, reaching a temperature between 125 and 140 °C, the increase of pressing time does not lead to improving properties. Similar behavior is found for MOR, but the temperature must reach 140 °C to achieve best features. Tensile shear strength is influenced by time only at 110 °C. With increasing temperature no similar trends are observed, as stated for MOE and MOR. Concluding the importance of the factor "temperature" on the performance of the mechanical properties led to suggest a temperature range between 125 °C and 140 °C in order to gain sufficient bonding quality. It can be explained by the phenolic character of tannin. The industrial applicated temperature for hot pressing of plywood with PF adhesives is ~ 130 °C [62].

Conclusions

The aim of the study was to determine the adhesive characteristics gel time and viscosity as well as the influence of the press parameters, time and temperature, on the selected physical and mechanical properties – density, thickness, modulus of elasticity, mod– ulus of rupture and tensile shear strength – of a totally bio–based sustainable Quebracho tannin–furfural bonded, five–layered beech plywood.

The presented adhesive formulation has shown good viscosity and curing behavior at a relatively low temperature (100 °C), producing polymers after curing. The non–reactivity at room temperature has to be highlighted as a clear advantage in terms of industrial application due to a prolonged open–time and storage duration. Their use as a fully bio–based sustainable adhesive for plywood displayed good bending (modulus of elasticity range ~9600 to ~11,600 N·mm^{-2}; modulus of rupture range 66 to 100 N·mm^{-2}) and acceptable tensile shear strength (~2.2 N·mm^{-2}) in a dry environment, especially for the test specimens in the temperature range 125–140 °C, concluding that the presented formulation is comparable to industrial applicated PF adhesives. Depending on the field of application, as a negative drawback, the low water–resistance due to the brittle character of the adhesive layer structure has to be mentioned as it limits the use of the proposed Quebracho tannin–furfural formulation. On the other hand, it can improve and contribute to recyclability for specific interior plywood applications, as a key element of the bio–based circular economy.

Further research should focus on improving the elastic character of the glue line and enhancing the water resistance of the adhesive, likewise by adding some proportion of isocyanate or epoxy resins in order to further improve the mechanical properties of the adhesive. Additionally, the usability of different wood species, due to the fact that beech (*Fagus sylvatica*) reacts sensitively to moisture induced swelling and shrinkage. Further investigation of press parameters such as pressure and adhesive amount per layer should be taken into consideration. This study used 3 N/mm^2 as press pressure whereas other studies about tannin–based adhesives range between 1.2 N/mm^2 [63] and 1.6 N·mm^{-2} [64] as well as ~1.4 N·mm^{-2} [51] for phenol formaldehyde plywood. For industrial application, the adhesive amount per layer could be further optimized.

References

1. Beyer, G.; Defays, M.; Fischer, M.; Fletcher, J.; de Munck, E.; de Jaeger, F.; Van Riet, C.; Vandeweghe, K.; Wijnendaele, K. *Tackle Clim. Change—Use Wood*; CEI–Bois: Brussels, Belgium, 2011; p. 84.
2. Oliver, C.D.; Nassar, N.T.; Lippke, B.R.; McCarter, J.B. Carbon, Fossil Fuel, and Biodiversity Mitigation with Wood and Forests. *J. Sustain. For.* **2014**, *33*, 248–275. https://doi.org/10.1080/10549811.2013.839386.
3. Moncaster, A.M.; Pomponi, F.; Symons, K.E.; Guthrie, P.M. Why Method Matters: Temporal, Spatial and Physical Variations in LCA and Their Impact on Choice of Structural System. *Energy Build.* **2018**, *173*, 389–398. https://doi.org/10.1016/j.enbuild.2018.05.039.
4. Churkina, G.; Organschi, A.; Reyer, C.P.O.; Ruff, A.; Vinke, K.; Liu, Z.; Reck, B.K.; Graedel, T.E.; Schellnhuber, H.J. Buildings as a Global Carbon Sink. *Nat. Sustain.* **2020**, *3*, 269–276. https://doi.org/10.1038/s41893–019–0462–4.
5. Irle, M.; Barbu, M.C. *Wood–Based Panels: An Introduction for Specialists*; Thoemen, M., Irle, M., Sernek, M., Eds.; Cost Action E49; Brunel University Press: London, UK, 2010; pp. 1–94.
6. Klaric´, S.; Obucˇina, M. New Trends in Engineering Wood Technologies. *Lect. Notes Netw. Syst.* **2020**, *76*, 712–727. https://doi.org/10.1007/978–3–030–18072–0_83.
7. Heinrich, L.A. Future Opportunities for Bio–Based Adhesives–Advantages beyond Renewability. *Green Chem.* **2019**, *21*, 1866–1888. https://doi.org/10.1039/c8gc03746a.
8. Alliedmarketresearch. Available online: https://www.alliedmarketresearch.com/bioadhesives–market–A11324 (accessed on 27 May 2022).
9. Marketsandmarkets. Available online: https://www.marketsandmarkets.com/Market–Reports/bioadhesive–market–16386893.html (accessed on 27 May 2022).
10. Hemmilä, V.; Adamopoulos, S.; Karlsson, O.; Kumar, A. Development of Sustainable Bio–Adhesives for Engineered Wood Panels–A Review. *RSC Adv.* **2017**, *7*, 38604–38630. Adhesives for Engineered Wood Panels–A Review. RSC Adv. 2017, 7, 38604–38630. https://doi.org/10.1039/c7ra06598a.
11. Ferdosian, F.; Pan, Z.; Gao, G.; Zhao, B. Bio–Based Adhesives and Evaluation for Wood Composites Application. *Polymers* **2017**, *9*, 70. https://doi.org/10.3390/polym9020070.
12. Kristak, L.; Antov, P.; Bekhta, P.; Lubis, M.A.R.; Iswanto, A.H.; Reh, R.; Sedliacik, J.; Savov, V.; Taghiyari, H.R.; Papadopoulos, A.N.; et al. Recent Progress in Ultra–Low Formaldehyde Emitting Adhesive Systems and Formaldehyde Scavengers in Wood–Based Panels: A Review. *Wood Mater. Sci. Eng.* **2022**. https://doi.org/10.1080/17480272.2022.2056080.
13. Oktay, S.; Kızılcan, N.; Bengü, B. Development of Bio–Based Cornstarch—Mimosa Tannin—Sugar Adhesive for Interior Particle– board Production. *Ind. Crops Prod.* **2021**, *170*, 113689. https://doi.org/10.1016/j.indcrop.2021.113689.

14. Paul, G.B.; Timar, M.C.; Zeleniuc, O.; Lunguleasa, A.; Cos, ereanu, C. Mechanical Properties and Formaldehyde Release of Particleboard Made with Lignin–Based Adhesives. *Appl. Sci.* **2021**, *11*, 8720. https://doi.org/10.3390/app11188720.
15. Lubis, M.A.R.; Labib, A.; Sudarmanto; Akbar, F.; Nuryawan, A.; Antov, P.; Kristak, L.; Papadopoulos, A.N.; Pizzi, A. Influence of Lignin Content and Pressing Time on Plywood Properties Bonded with Cold–Setting Adhesive Based on Poly (Vinyl Alcohol), Lignin, and Hexamine. *Polymers* **2022**, *14*, 2111. https://doi.org/10.3390/polym14102111.
16. Zhang, Y.; Shi, R.; Xu, Y.; Chen, M.; Zhang, J.; Gao, Q.; Li, J. Developing a Stable High–Performance Soybean Meal–Based Adhesive Using a Simple High–Pressure Homogenization Technology. *J. Clean. Prod.* **2020**, *256*, 120336. https://doi.org/10.1016/j.jclepro.2020.120336.
17. Ghahri, S.; Pizzi, A.; Hajihassani, R. A Study of Concept to Prepare Totally Biosourced Wood Adhesives from Only Soy Protein and Tannin. *Polymers* **2022**, *14*, 1150. https://doi.org/10.3390/polym14061150.
18. Pizzi, A. Recent Developments in Eco–Efficient Bio–Based Adhesives for Wood Bonding: Opportunities and Issues. *J. Adhes. Sci. Technol.* **2006**, *20*, 829–846. https://doi.org/10.1163/156856106777638635.
19. Shirmohammadli, Y.; Efhamisisi, D.; Pizzi, A. Tannins as a Sustainable Raw Material for Green Chemistry: A Review. *Ind. Crops Prod.* **2018**, *126*, 316–332. https://doi.org/10.1016/j.indcrop.2018.10.034.
20. Pizzi, A.; Mittal, K.L. *Handbook of Adhesive Technology*, 3rd ed.; CRC Press: Boca Raton, FL, USA, 2017; pp. 223–262. https://doi.org/10.1201/9781315120942.
21. Xu, Y.; Guo, L.; Zhang, H.; Zhai, H.; Ren, H. Research Status, Industrial Application Demand and Prospects of Phenolic Resin. *RSC Adv.* **2019**, *9*, 28924–28935. https://doi.org/10.1039/c9ra06487g.
22. Arias, A.; González–García, S.; Feijoo, G.; Moreira, M.T. Tannin–Based Bio–Adhesives for the Wood Panel Industry as Sustainable Alternatives to Petrochemical Resins. *J. Ind. Ecol.* **2021**, *26*, 627–642. https://doi.org/10.1111/jiec.13210.
23. Pizzi, A. The Chemistry and Development of Tannin/Urea–Formaldehyde Condensates for Exterior Wood Adhesives. *J. Appl. Polym. Sci.* **1979**, *23*, 2777–2792. https://doi.org/10.1002/app.1979.070230922.
24. Navarrete, P.; Pizzi, A.; Pasch, H.; Rode, K.; Delmotte, L. Characterization of Two Maritime Pine Tannins as Wood Adhesives. *J. Adhes. Sci. Technol.* **2013**, *27*, 2462–2479. https://doi.org/10.1080/01694243.2013.787515.
25. Engozogho Anris, S.P.; Bikoro Bi Athomo, A.; Safou–Tchiama, R.; Leroyer, L.; Vidal, M.; Charrier, B. Development of Green Adhesives for Fiberboard Manufacturing, Using Okoume Bark Tannins and Hexamine–Characterization by 1H NMR, TMA, TGA and DSC Analysis. *J. Adhes. Sci. Technol.* **2021**, *35*, 436–449. https://doi.org/10.1080/01694243.2020.1808356.

26. Ballerini, A.; Despres, A.; Pizzi, A. Non–Toxic, Zero Emission Tannin–Glyoxal Adhesives for Wood Panels. *Holz Roh–Werkst.* **2005**, *63*, 477–478. https://doi.org/10.1007/s00107–005–0048–x.

27. Kabbour, M.; Luque, R. Furfural as a Platform Chemical: From Production to Applications. In *Biomass, Biofuels, Biochemicals—Recent Advances in Development of Platform Chemicals*; Saravanamurugan, S., Pandey, A., Riisager, A., Eds.; Elsevier B.V.: Amsterdam, The Netherlands, 2020. https://doi.org/10.1016/B978–0–444–64307–0.00010–X.

28. Bozell, J.J.; Petersen, G.R. Technology Development for the Production of Biobased Products from Biorefinery Carbohydrates—The US Department of Energy's "Top 10" Revisited. *Green Chem.* **2010**, *12*, 539–555. https://doi.org/10.1039/b922014c.

29. Cesprini, E.; Šket, P.; Causin, V.; Zanetti, M. Development of Quebracho (*Schinopsis balansae*) Tannin–Based Thermoset Resins. *Polymers* **2021**, *13*, 4412.

30. *EN 323*; Wood–Based Panels—Determination of Density. European Committee for Standardization: Brussels, Belgium, 2005.

31. Spulle, U.; Meija, A.; Ku¯ linš, L.; Kopeika, E.; Liepa, K.H.; Šillers, H.; Zudrags, K. Influence of Hot Pressing Technological Parameters on Plywood Bending Properties. *BioResources* **2021**, *16*, 7550–7561.

32. *EN 314–1*; Plywood—Bonding Quality—Test Methods. European Committee for Standardization: Brussels, Belgium, 2005.

33. *EN 310*; Wood–Based Panels—Determination of Modulus of Elasticity in Bending and of Bending Strength. European Committee for Standardization: Brussels, Belgium, 2005.

34. Navarrete, P.; Pizzi, A.; Tapin–Lingua, S.; Benjelloun–Mlayah, B.; Pasch, H.; Rode, K.; Delmotte, L.; Rigolet, S. Low Formaldehyde Emitting Biobased Wood Adhesives Manufactured from Mixtures of Tannin and Glyoxylated Lignin. *J. Adhes. Sci. Technol.* **2012**, *26*, 1667–1684. https://doi.org/10.1163/156856111X618489.

35. Hauptt, R.A.; Sellers, T. Characterizations of Phenol–Formaldehyde Resol Resins. *Ind. Eng. Chem. Res.* **1994**, *33*, 693–697. https://doi.org/10.1021/ie00027a030.

36. Ricci, A.; Olejar, K.J.; Parpinello, G.P.; Kilmartin, P.A.; Versari, A. Application of Fourier Transform Infrared (FTIR) Spectroscopy in the Characterization of Tannins. *Appl. Spectrosc. Rev.* **2015**, *50*, 407–442. https://doi.org/10.1080/05704928.2014.1000461.

37. Tondi, G.; Petutschnigg, A. Middle Infrared (ATR FT–MIR) Characterization of Industrial Tannin Extracts. *Ind. Crops Prod.* **2015**, *65*, 422–428. https://doi.org/10.1016/j.indcrop.2014.11.005.

38. Mohamad, N.; Abd–Talib, N.; Kelly Yong, T.L. Furfural Production from Oil Palm Frond (OPF) under Subcritical Ethanol Conditions. *Mater. Today Proc.* **2020**, *31*, 116–121. https://doi.org/10.1016/j.matpr.2020.01.256.

39. Kane, S.N.; Mishra, A.; Dutta, A.K. Synthesis of Furfural from Water Hyacinth (*Eichornia croassipes*) This. *Mater. Sci. Eng.* **2017**, *172*, 012027. https://doi.org/10.1088/1742–6596/755/1/011001.

40. Tondi, G. Tannin–Based Copolymer Resins: Synthesis and Characterization by Solid State 13C NMR and FT–IR Spectroscopy. *Polymers* **2017**, *9*, 223. https://doi.org/10.3390/polym9060223.

41. Wagenführ, A.; Scholz, F. *Taschenbuch der Holztechnik*; Carl Hanser Verlag: München, Germany, 2008.

42. Jorda, J.; Kain, G.; Barbu, M.–C.; Petutschnigg, A.; Král, P. Influence of Adhesive Systems on the Mechanical and Physical Properties of Flax Fiber Reinforced Beech Plywood. *Polymers* **2021**, *13*, 3086. https://doi.org/10.3390/polym13183086.

43. Jorda, J.; Kain, G.; Barbu, M.–C.; Köll, B.; Petutschnigg, A.; Král, P. Mechanical Properties of Cellulose and Flax Fiber Unidirectional Reinforced Plywood. *Polymers* **2022**, *14*, 843. https://doi.org/10.3390/polym14040843.

44. Mansouri, H.R.; Pizzi, A.; Leban, J.M. Improved Water Resistance of UF Adhesives for Plywood by Small PMDI Additions. *Holz Roh–Werkst.* **2006**, *64*, 218–220. https://doi.org/10.1007/s00107–005–0046–z.

45. Luo, J.; Luo, J.; Gao, Q.; Li, J. Effects of Heat Treatment on Wet Shear Strength of Plywood Bonded with Soybean Meal–Based Adhesive. *Ind. Crops Prod.* **2015**, *63*, 281–286. https://doi.org/10.1016/j.indcrop.2014.09.054.

46. Bekhta, P.; Hiziroglu, S.; Shepelyuk, O. Properties of Plywood Manufactured from Compressed Veneer as Building Material. *Mater. Des.* **2009**, *30*, 947–953. https://doi.org/10.1016/j.matdes.2008.07.001.

47. Cabral, J.P.; Kafle, B.; Subhani, M.; Reiner, J.; Ashraf, M. Densification of Timber: A Review on the Process, Material Properties, and Application. *J. Wood Sci.* **2022**, *68*, 20. https://doi.org/10.1186/s10086–022–02028–3.

48. Niemz, P. *Physik des Holzes und der Holzwerkstoffe*; DRW Verlag Weinbrenner: Leinfelden–Echterdingen, Germany, 1993.

49. *DIN 68705–5*; Sperrholz Teil 5—Bau–Furniersperrholz aus Buche. Deutsches Institut für Normung: Berlin, Germany, 1980.

50. Hrázský, J.; Král, P. Assessing the Bending Strength and Modulus of Elasticity in Bending of Exterior Foiled Plywoods in Relation to Their Construction. *J. For. Sci.* **2005**, *51*, 77–94. https://doi.org/10.17221/4546–jfs.

51. Biadała, T.; Czarnecki, R.; Dukarska, D. Water Resistant Plywood of Increased Elasticity Produced from European Wood Species. *Wood Res.* **2020**, *65*, 111–124. https://doi.org/10.37763/wr.1336–4561/65.1.111124.

52. Dieste, A.; Krause, A.; Bollmus, S.; Militz, H. Physical and Mechanical Properties of Plywood Produced with 1.3–Dimethylol– 4.5–Dihydroxyethyleneurea (DMDHEU)–Modified Veneers of *Betula* sp. and *Fagus Sylvatica*. *Holz Roh–Werkst.* **2008**, *66*, 281–287. https://doi.org/10.1007/s00107–008–0247–3.

53. Lohmann, U. *Holz Handbuch*; DRW: Echterdingen–Leinenfelden, Germany, 2010; pp. 46–47.

54. Réh, R.; Krišťák, Ľ.; Sedliacˇik, J.; Bekhta, P.; Božiková, M.; Kunecová, D.; Vozárová, V.; Tudor, E.M.; Antov, P.; Savov, V. Utilization of Birch Bark as an Eco–Friendly Filler in Urea–Formaldehyde Adhesives for Plywood Manufacturing. *Polymers* **2021**, *13*, 511. https://doi.org/10.3390/polym13040511.

55. Bal, B.C.; Bektaþ, Ý. Some Mechanical Properties of Plywood Produced from Eucalyptus, Beech, and Poplar Veneer. *Maderas. Cienc. Tecnol.* **2014**, *16*, 99–108. https://doi.org/10.4067/S0718–221X2014005000009.

56. *EN 314–2*; Plywood—Bonding Quality—Part 2 Requierments. European Committee for Standardization: Brussels, Belgium, 2005.

57. Xi, X.; Pizzi, A.; Frihart, C.R.; Lorenz, L.; Gerardin, C. Tannin Plywood Bioadhesives with Non–Volatile Aldehydes Generation by Specific Oxidation of Mono– and Disaccharides. *Int. J. Adhes. Adhes.* **2020**, *98*, 102499. https://doi.org/10.1016/j.ijadhadh.2019.102499.

58. Hafiz, N.L.M.; Tahir, P.M.D.; Hua, L.S.; Abidin, Z.Z.; Sabaruddin, F.A.; Yunus, N.M.; Abdullah, U.H.; Abdul Khalil, H.P.S. Curing and Thermal Properties of Co–Polymerized Tannin Phenol–Formaldehyde Resin for Bonding Wood Veneers. *J. Mater. Res. Technol.* **2020**, *9*, 6994–7001. https://doi.org/10.1016/j.jmrt.2020.05.029.

59. Pizzi, A.; Scharfetter, H.O. The Chemistry and Development of Tannin–based Adhesives for Exterior Plywood. *J. Appl. Polym. Sci.* **1978**, *22*, 1745–1761. https://doi.org/10.1002/app.1978.070220623.

60. Ayla, C.; Parameswaran, N. Macro– and Microtechnological Studies on Beechwood Panels Bonded with *Pinus Brutia* Bark Tannin. *Holz Roh–Werkst.* **1980**, *38*, 449–459. https://doi.org/10.1007/BF02610428.

61. Ferreira, É.D.S.; Lelis, R.C.C.; Brito, E.D.O.; Iwakiri, S. Use of Tannin from *Pinus oocarpa* Bark for Manufacture of Plywood. In Proceedings of the LI International Convention of Society of Wood Science and Technology, Concepción, Chile, 10–12 November 2008; pp. 10–12.

62. Sedliacˇik, J.; Bekhta, P.; Potapova, O. Technology of Low–Temperature Production of Plywood Bonded with Modified Phenol– Formaldehyde Resin. *Wood Res.* **2010**, *55*, 123–130.

63. Moubarik, A.; Pizzi, A.; Allal, A.; Charrier, F.; Charrier, B. Cornstarch and Tannin in Phenol–Formaldehyde Resins for Plywood Production. *Ind. Crops Prod.* **2009**, *30*, 188–193. https://doi.org/10.1016/j.indcrop.2009.03.005.

64. Stefani, P.M.; Peña, C.; Ruseckaite, R.A.; Piter, J.C.; Mondragon, I. Processing Conditions Analysis of *Eucalyptus Globulus* Plywood Bonded with Resol–Tannin Adhesives. *Bioresour. Technol.* **2008**, *99*, 5977–5980. https://doi.org/10.1016/j.biortech.2007.10.013.

4.2.4 Bio–Based Tannin–Furanic–Silk Adhesives: Applications in Plywood and Chemical Cross–linking Mechanisms

Emanuele Cesprini, Johannes Jorda, Marco Paolantoni, Luca Valentini, Primož Šket, Valerio Causin, Diana E. Bedolla, Michela Zanetti, and Gianluca Tondi

Abstract

Wood polyphenolic extracts, commonly called tannins, are excellent candidates for the production of bioplastics due to their abundance in nature, their commercial availability, and their reactivity. In particular, they were tested as wood adhesives with several hardeners, but their low moisture resistance and their rigidity reduced their technological interest. In the present study, we combined regenerated silk (RS) with tannin–furanic formulations to improve their properties. Three–layer plywood glued with these several fully renewable tannin–silk–furanic adhesives were tested for their mechanical properties: the modulus of elasticity, the modulus of rupture, and both dry and wet shear strength were enhanced when 20 wt % of RS was added. Initially, the cross section of the prepared samples was investigated by scanning electron microscopy, indicating a good dispersion of RS within the tannin–furanic matrix. Afterward, thermomechanical analysis of the adhesive highlighted that RS slows down the polymerization rate, decreasing the cross–linking kinetics of polyfurfuryl alcohol. Chemical investigations through ATR–FTIR and 13C–NMR show the formation of covalent bonds between RS and the furanic matrix. In summary, the combination of bioresources from the vegetal and animal kingdom allows the manufacturing of fully bio–based adhesives with enhanced mechanical properties and water resistance. This represents an important breakthrough in the exploitation of polyphenols, opening perspectives for their application in material science.

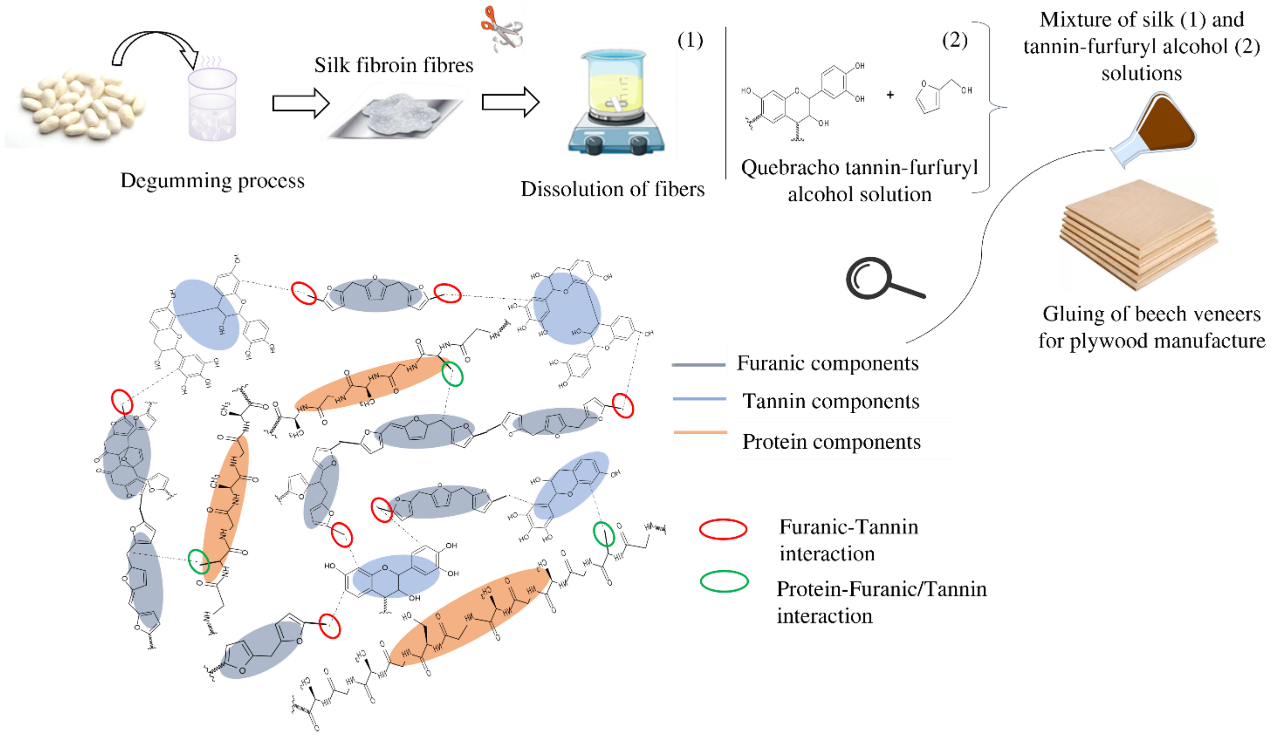

Introduction

Reducing the dependence on fossil derivatives has become a worldwide issue due to the necessity to restrain global warming and develop a sustainable economy.[1] For instance, the plastics field accounts for 5–7% of the consumption of oil derivatives, releasing more than 850 million tons of CO2 into the atmosphere.[2] Specifically, the higher GHG's emissions in the plastic manufacturing industry are related to the raw material extraction process (e.g. 61%) followed by the polymer production (e. g. 30%).[3] It has been estimated that replacing approximately 66% of conventional plastics with bio–based alternatives would avoid between 241 and 316 MtCO$_2$ equivalents per year[4]. Thus, explaining the need to seek sustainable alternatives to oil derivatives. Although the most common commercial plastics are still made from oil derivatives, the same materials may also be replaced by renewable resources. Monomers or also biopolymers can be obtained from nature with the goal of replacing synthetic plastic such as polyethylene (PE) or polypropylene (PP).[5] Tannins, which are wood extracts of polyphenolic nature, have been shown to be very attractive and perform for multiple purposes. These substances are produced by plants to protect the lignocellulosic body against biological and radiation attacks, due to their chemical structure and antioxidant capacity.[6] Furthermore, they have a 'green' extraction process through the use of water as a solvent under moderate pressure and temperature.[7] Tannins are extracted industrially and are therefore abundantly available because they were and are used as tanning agent in the leather tannery row because of their strong complexing power with proteins.[8] In addition to this, tannin extracts have been used for medical purposes as antioxidants and free radical scavengers.[9] In the last two decades, due to their appealing chemical features, tannins have been used to produce biobased plastics, with particular interest for insulation foams[10]–[12] wood preservatives[13],[14] and wood adhesives.[15],[16] The addition of mainly synthetic–based cross–linkers such as hexamine, formaldehyde or glyoxal, lead to stable three–dimensional thermosetting polymers.[17],[18] Despite the appealing features of the aforementioned tannin–based formulation, the concerns about health problems and the need for detachment from oil derivatives, lead the research to promote free–formaldehyde fully renewable formulations, as profitable source for greener products. In this direction, furfuryl alcohol is bio–derived material which is mainly obtained from the hydrogenation of furfural, itself a derivative of the dehydration of agricultural and forest waste from hemicelluloses.[19] The ability of furfuryl alcohol to self–cure under acidic conditions [20],[21] enables the design of different materials applicable in the field of engineered wood products, including impregnation [22] and modification [23] of woody material. Moreover, due to the resistance to acid, alkali, high temperature, fungal attack, corrosion [24]and because of its good interaction capacity with tannins[25], furfuryl alcohol can be involved as green crosslinker to produce fully renewable co–polymer.[26],[27]However, some critical drawbacks of furanic–tannin co–polymers like poor moisture resistance[28] and high rigidity[29] still limit the application. Hither, proteins have attracted great attention due to their renewability, effortless modification, biodegradability and abundance [30]. Although the use of protein–based adhesive resins alone does not allow for high performance [31], the combination of those with other resources, as tannins or furanic derivates, led to satisfactory results in the wood adhesive sector.[32],[33] Silk fibroin (hereinafter named regenerated silk, RS), is one of the most promising natural protein–based biomaterials due to its inspiring biodegradability, and superior mechanical performances.[34] Such biopolymer recovered from insect farming (i.e Bombyx mori (e. g. B. mori) silkworms) can be processed in solution to enable the fabrication of adhesives with tunable mechanical properties[35], opening up alternatives to the main plant proteins currently proposed [36],[37].

In this study, the effect of adding different amounts of RS into tannin–furfuryl alcohol formulations for plywood manufacturing was investigated. Further, the interaction between the components of the adhesive were observed during and after curing through thermomechanical analysis and solid state 13C–NMR FTIR spectroscopies.

Materials and methods

Materials

Quebracho (Schinopsis balancae) tannin extract (Fintan 737B) was kindly provided by the company Silvateam (S. Michele Mondovì, Cuneo, Italy) while furfuryl alcohol (99%) by International Furan Chemical IFC (Rotterdam, The Netherlands). Lowest grade Bombyx mori silk cocoons was provided by a local company (CREA–AA, Padova, Italy). Sodium hydrogen carbonate, calcium chloride, and formic acid were supplied by Alfa Aesar (Thermo Fisher, Waltham, MA, USA). Pre–conditioned (20°C, 65% relative air humidity) rotary cut defect–free beech (Fagus sylvatica) veneers, purchased from Europlac (Topolcany, Slovakia), with a nominal thickness of 2.2 mm, density of 0.72 $g \cdot cm^{-3}$ and 12% m.c., were used to prepare the three–layers plywood.

Synthesis of adhesive

The silk fibers dissolution method was carried out according to previous work.[38] Briefly, B. Mori silk cocoons (5g) were degummed in boiling water (300 mL) at 1.7% of NaHCO3 for 30 min and flushed with deionized water, the procedure was repeated twice. The degummed silk fibers were dried at room temperature under air flux, and thus dispersed into the formic acid/calcium chloride solution by magnetic stirring at room temperature for 5 min, until a homogeneous solution was obtained. The amount of calcium chloride was defined in function of silk content. Thus, the silk–calcium chloride weight ratio was set at 70:30, while a silk concentration of 0.11 $g \cdot ml^{-1}$ in formic acid was chosen. Meanwhile, a tannin–furfuryl alcohol solution was prepared at room temperature and under mechanical stirring, at the fixed weight ratio of 60:40. Afterwards, the two solutions were mixed and mechanically stirred at different RS concentrations calculated on fixed solid tannin content, obtaining different tannin–furfuryl alcohol formulations (TFS). The RS content was varied from 10wt% up to 30wt%. The composition of the formulations is reported in table1.

Table 1. Relative content of each component within the final formulations.

Samples	Tannin (wt%)	Furfuryl Alcohol (wt%)	RS (wt% on tannin)
TFS–0	60	40	/
TFS–10			10
TFS–15			15
TFS–20			20
TFS–30			30

Plywood manufacturing

The plywood lay–up consisted of three layered 90° crosswise oriented 2.2 mm thick beech veneers. Adhesive application was carried out manually by weighing 200 g/m^2 of adhesive per glue line. Pressing was conducted using a Höfler HLOP 280 (Taiskirchen, Austria) hot press. The pressing conditions were set as follows: pressure of 3 N·mm^{-2}, temperature 125°C and 15 minutes of pressing time. The as prepared boards were stored until constant weight in a climate chamber at 20°C and 65% of relative humidity. Test specimens were cut from the plywood boards for the determination of bending strength (MOR), stiffness (MOE), and dry and wet tensile shear strength (SS).

Mechanical characterization

Dry state SS and 24 h water soaking TSS were determined according to EN 314:2004[39] with specimen dimensions 100 mm x 25 mm. Modulus of rupture and MOE were determined by a three–point bending test according to EN 310:1993 with specimen dimensions 250 mm x 50 mm.[40]. All mechanical properties (SS, MOE, and MOR) were determined using a Zwick/Roell 250 8497.04.00 universal testing machine (Ulm, Germany).

SEM

The morphological characterization of the adhesives was performed by scanning electron analysis with FEI Quanta scanning electron microscopy (variable pressure environmental E/SEM). The instrument is also equipped with EDX (EDAX Element– C2B) for X–ray detection. The images were recorded at 20 kV.

Thermomechanical analysis (TMA)

Thermomechanical analysis was carried out with a TMA/SDTA840 Mettler Toledo (Mettler Toledo, Columbus, OH, USA) instrument equipped with a three–point bending probe. About 20 mg of tannin–based formulations (TSF–0, TFS–10, TFS–15, TFS–20, TFS–30) were applied between two beech wood plies (15 mm × 5 mm × 1.5 mm). Isothermal and non– isothermal methods were applied: the former was run at 25°C for 240 min, while the latter consisted of 10 °C·min^{-1} heating rate from 40°C to 200°C. For both methods a cycle of 0.1/0.5 N force was applied on the specimens, with each force cycle lasting 12 s (6 s/6 s).

In order to investigate the chemical bonding evolution, different spectroscopic investigations were performed on polyfurfuryl alcohol (PFA) crosslinked in formic acid, regenerated silk (RS) obtained by dissolution in formic acid, PFA–RS and PFA–RS–quebracho tannin (PFA–RS–T) were acquired and compared with the cured mixed formulation subject of this study.

13C–NMR solid state analysis

Solid–state 13C–NMR experiments were performed on a Bruker AVANCE NEO 400 MHz NMR spectrometer using a 4–mm CP–MAS probe. The sample spinning frequency was set to 15 kHz experiments consisted of excitation of protons with p/2 pulse of 3.0 s, CP block of 2 ms, and signal acquisition with high–power proton decoupling. A total of ca. 2,000 to 14,000 scans were accumulated with the repetition delay of 5 s.

ATR–FTIR analysis

Fourier transform infrared (FTIR) spectra measurements were done in Attenuated Total Reflection (ATR) mode using an Alpha (Bruker Optics) spectrometer equipped with a Platinum ATR module. The spectra were registered in the range between 400 and 4000 cm^{-1}, averaging over 30 scans with a resolution of 2 cm^{-1}. The spectra were then baseline corrected, normalized and smoothed with the RStudio Team (2021) software.

FTIR

FTIR hyperspectral images were acquired by using a bidimensional 64x64 pixels focal plane array (FPA) coupled to a VIS–IR microscope Hyperion 3000 (Bruker Optics, Billerica, US) and with a VERTEX 70v in–vacuum interferometer (Bruker Optics, Billerica, US) through a 15x Cassegrain objective–condenser pair in transmission mode. Slices of 10 um of PFA–tannin and PFA–tannin–silk were prepared with a rotary microtome (Leica RM2245; Leica Biosystems, Nussloch, Germany),so that the samples could be measured in transmission mode. For each tile 4096 spectra were acquired with 256 scans at a spectral resolution of 4cm^{-1}. Data were corrected for water vapor using Opus 8.5 SP1

(Bruker Optics, Billerica, US) and then analyzed using Quasar (https:\\quasar.codes). [41],[42] All spectra were vector normalized, cut in the region 1850–850 cm^{-1} and baseline corrected with the rubber band correction. Integration was calculated on the average spectra of the whole tile (4096 scans) of each sample with the height of the band around 1715 and the band around 1520. Finally, its ratio was estimated and compared.

Statistical analysis

Analysis of variance was used to assess significant differences between the investigated formulations through one–way ANOVA and Kruskal test, depending on whether the data are normally or non–normally distributed, respectively. Any groups that showed a significant difference were discriminated according to the Tukey multi–range test for ANOVA or to Dunn test for Kruskal, and a 95% confidence level was selected. Statistical analysis was performed using RStudio Team (2021). Kruskal–Wallis multiple comparison p–values was carried out to analyze the correlation between MOR of the fabricated adhesives, because of non–normal data distribution.

Result and discussion

The mechanical properties of the three–layer plywood are depicted in figures 1 A and 1 B. In the production of multilayer panels, one of the key parameters refers to the glue line property, which shall guarantee sufficient adhesion for the final stability of the panel. The most significant physical indicator is the shear strength in both wet and dry conditions (Figure 1A). One–way ANOVA reported high correlation between the silk concentration and SS dry (p–value = $6.29 \cdot 10^{-5}$). Specifically, a significant difference (p–value<0.05) between the reference panels (TFS–0) and TFS–15/20/30 is highlighted by Tukey test, confirming the higher adhesive property of the TFS–20 sample (e. g. 3.2 MPa). In contrast, any substantial difference between TFS–0 and TFS–10 (p–value = 0.052) was not observed.

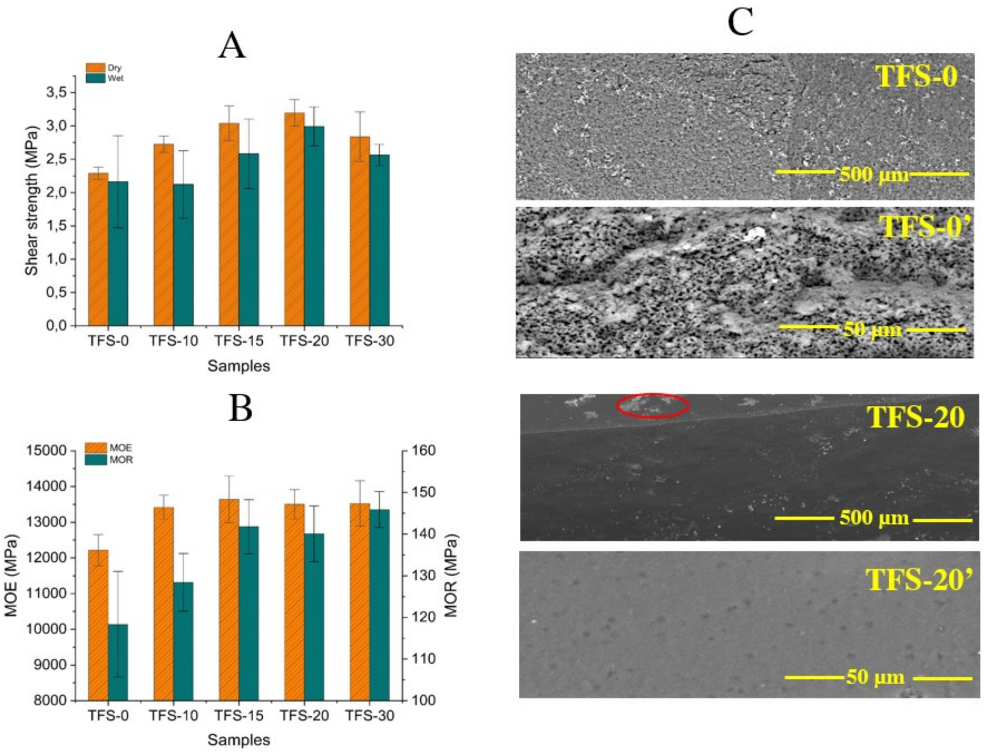

Figure 1. A: Dry and 24h wet shear strength of reference panels (TSF–0) and TFS samples synthesized at different wt% of RS. B: Modulus of elasticity (MOE) and modulus of rupture (MOR) of reference panels (TFS–0) and TFS samples synthesized at different wt% of RS. C: Scanning electron microscopy images of TFS–0, TSF–20 and of TFS–0', TSF–20' samples, at different magnifications (e. g. x100 and x 1000, respectively).

After 24 h of water storage at room temperature, the shear stress was evaluated and the tendency is reported by the red curve in Figure 1A. The addition of RS to tannin–furfuryl alcohol matrix led to an increase in panel stability (p–value = 0.0261), reaching its highest value (eg 2.8 MPa) for the TFS–20 formulation. A proportional increase in tensile shear strength is achieved up to 20% of RS, followed by a decrease when the RS concentration reaches 30%. Although the stability of the adhesive reaches its best properties at 20wt% of RS, the results obtained are all compliant for dry condition purposes according to the European standards that set the wet shear strength above 1 MPa[39]. The effect of RS addition on both MOE and MOR was investigated and reported in Figure 1B. The addition of RS increases the values of both the MOE and MOR. Specifically, the RS addition affects the MOE (p–value = 0.0144), showing a significant change between the reference panels (TSF–0) and those where RS was added (p–value < 0.05). Otherwise, no differences in MOE were highlighted by increasing the RS content (p–value>0.05). Finally, the silk addition positively affects the mechanical properties, registering a p–value of 0.0043 for MOR. Similarly, when silk was added, an increase of the MOR from 128 MPa to 146 MPa was recorded, respectively.

Focusing on the critical tensile shear strength parameter, the comparison of the current formulations with literature studies highlighted the competitiveness of this adhesive resin.

In particular, the use of fully renewable tannin–furfural adhesives showed poor moisture resistance.[29] Indeed, although a dry shear stress strength between 1.7 MPa and 2.3 MPa is registered, the formulation denoted no resistance to moisture due to the panels delamination during the 24h water soaking for plywood EN 314 class 1 application.[29] The grafting of counterparts to the tannic base skeleton is therefore necessary to achieve competitive properties. In this way, the inclusion of oxidized glucose to mimosa tannin allowed dry SS between 1.4 MPa – 2.0 MPa, increasing the moisture resistance until 0.3–0.5 MPa after 24 hour water soaking.[43] Chen et al. report a wet tensile shear strength of 1.1 MPa for soybean meal flour, larch tannin and triglycidylamine adhesive formulation.[44] Similar results are reported by Zhou et al.,[45] who have achieved a dry and wet shear strengths of 2.1MPa and 1.6 MPa, respectively, building a complex structure of layered double hydroxide (LDH), anchored chicken feather fiber (CFF), tannic acid (TA) and soybean meal (SM). The combination of polyfurfuryl alcohol with gluten proteins showed good bonding properties, achieving a shear strength after 24 in cold water of about 0.9 MPa [32]. Good strength is also reported for 3 hours in boiling water[32].

Another interesting natural resource of polyphenolic character is lignin, which is also used in combination with different kind proteins to produce plywood boards. On this wise, Pang et al.[46] and Liu et al.[47] reported a lower values of both SS dry and SS wet than the results reached by the proposed tannin silk formulation, which displayed to be competitive with PF bonded plywood too.[48]

Moreover, in terms of MOE and MOR the current formulation has shown properties comparable with the main synthetic adhesives. Indeed, Jorda et al. reported for epoxy, urea–formaldehyde, melamine–urea–formaldehyde, phenol–formaldehyde and polyurethane resins bonded five layer beech (Fagus sylvatica) plywood an MOE between 9,500 and 11,700 MPa, while for MOR the values fall between 95 and 115 MPa[49]. Additionally, Biadala et al.[50] reported a mean MOE of 13,720 MPa for three layered PF bonded beech plywood and a MOR of 158.4 MPa . Thus, with an MOE over 13,000 MPa and MOR beyond 140 MPa, the co–polymers of furfuryl alcohol–tannin–fibroin exhibit mechanical properties at least comparable to the main synthetic resins.

The morphology of the reference (TFS–0) and TSF–20 samples was investigated by SEM analysis as reported in Figure 1C. The TFS–0 and TFS' show jagged morphology due to the fast evaporation of formic acid during the crosslinking. On the contrary, the addition of RS (TFS–20 and TSF–20') results in a more compact material. Salts crystals, e.g. $CaCl_2$, are visible, along with the appearance of RS agglomerates (red cycle in Figure 1C, TFS–20' sample, and Figure S1 in SI section).

In order to understand and correlate the different formulations and their reactivity, a comparison between the reference and the silk–added samples were monitored through non–isothermal and isothermal TMA. In Figure 2, the thermomechanical behavior of formulations described in table 1 is reported. Focalizing on the non–isothermal method, heat affects the sample behaviors simultaneously in two different ways, namely by physical and chemical effects.[51] For the former an increase of temperature leads to the softening and decrease the stiffness of the polymers, which happens to all samples before 80°C. By raising the temperature, the chemical effect of cross–linking overcomes the physical one, and an increase in stiffness was registered between 80 and 180°C, due to the starting of the polymerization process.

Although all samples showed a maximum MOE peak around 180°C, the addition of RS shifts the starting of curing of about 10°C. This suggests (see below) that the addition of fibroin delays the co–polymerization of tannin and furfuryl alcohol. Once the curing process starts, the presence of fibroin accelerates the hardening and this can be seen by the slope of the thermograms which are particularly visible for the formulation containing at least 15wt% of RS. However, at the end of the polymerization process, the presence of silk increased the properties of the co–polymer. This result supports the observations already considered in the mechanical tests: in this case as well the TFS–20 registered the highest MOE compared to the other formulations.

The isothermal curves for the TFS–20 and TFS–0 (black and pink) are shown in Figure 2. After 240 min of reaction at room temperature, the reference (TFS–0, black curve) reached a higher MOE value than the TFS–20, indicating faster reaction kinetics. The acidity resulting from the presence of formic acid allows as for a fast self–polymerization [52] of furfuryl alcohol as well as a co–polymerization with tannin.[53]

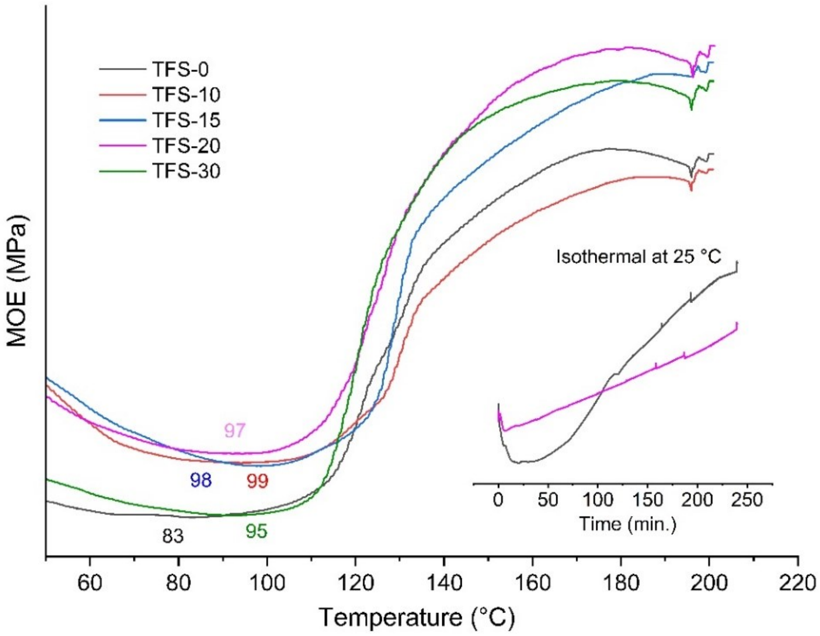

Figure 2. Non–isothermal and isothermal (see the inset) mechanical analysis of TSF–0 and TFS samples synthesized at different wt% of RS.

13C–NMR and ATR–FTIR analysis were performed to understand the chemical interactions occurring between silk and the tannin–furanic matrix.

Many studies involved the characterization of the polyfurfuryl alcohol (PFA) since the last century,[21],[54],[55] but the debate is still open due to its utilization as renewable and abundant material, with more molecular rearrangements that have been proposed over the years.[25],[56],[57] In short there are two reactions occurring: i) the linear polymerization summarized in the Scheme 1A and the ii) Diels–Alder crosslinking of the ring–opened structures reported in Scheme 1B.

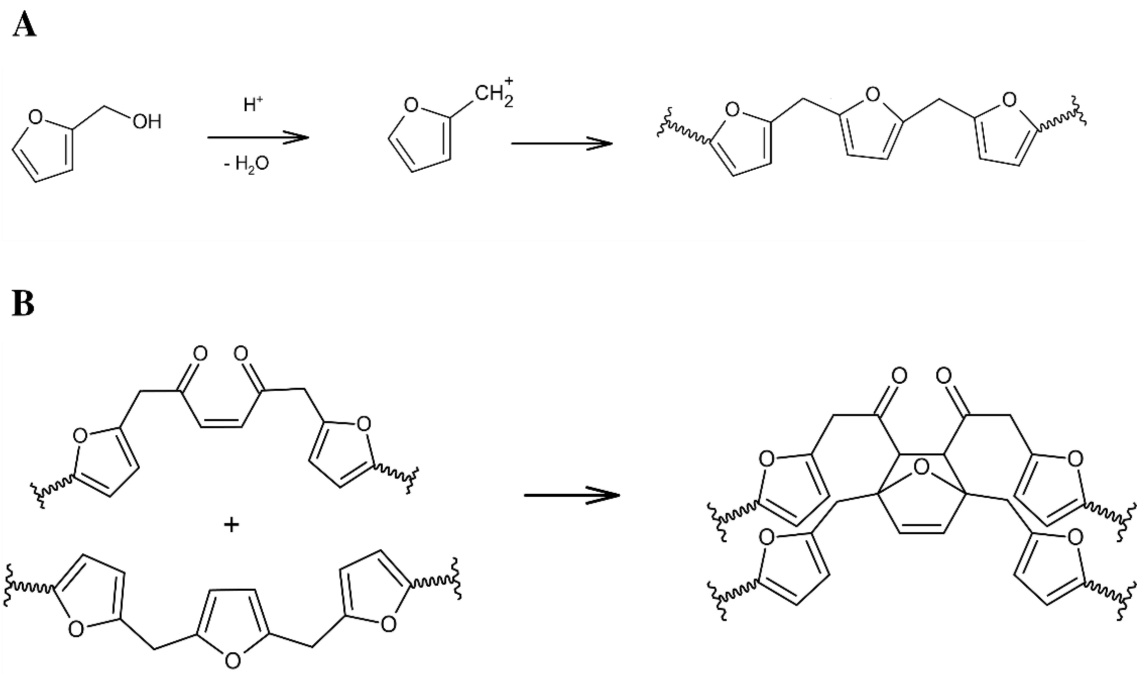

Scheme 1. A: Principal mechanism of reaction of furfuryl alcohol polymerization. B: Diels Alder reaction mechanism involved in the polymerization of furfuryl alcohol.

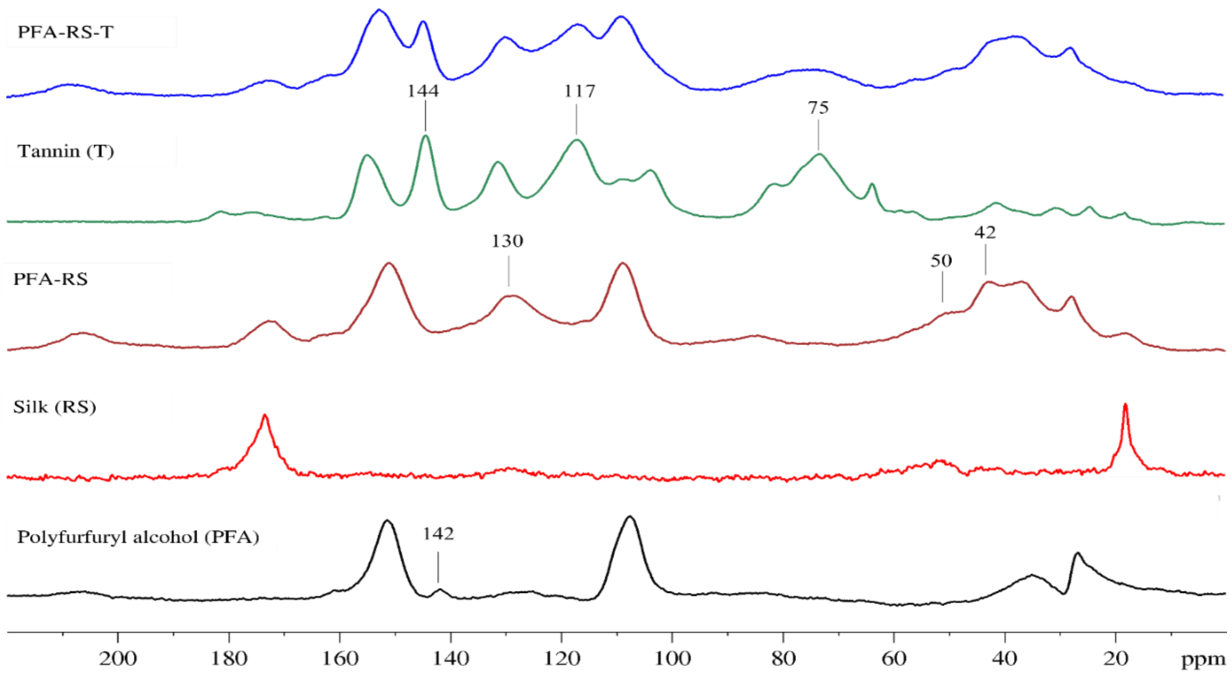

Figure 3. 13C–NMR spectra of: furfuryl alcohol (PFA, black curve), regenerated silk (RS, red curve), polyfurfuryl alcohol– regenerated silk (PFA–RS, brown), quebracho tannin (T, green curve) and quebracho polyfurfuryl alcohol–regenerated silk–quebracho tannin (PFA–RS–T, blue curve).

In Figure 3 the 13C–NMR spectra of polyfurfuryl alcohol (PFA), regenerated silk (RS), PFA–RS, quebracho tannin(T) and PFA–RS–T are reported. Comparing the spectra PFA and PFA–RS, it can be seen that despite many signals are obtained by superposition of each component, new or highly enhanced peaks were observed. Indeed, when silk is added (PFA–RS, brown curve), the band at 142 ppm disappears/strongly reduces its intensity, while the peak at around 130 ppm is severely enhanced, and the signal at 50 ppm as well the shoulder at around 40 ppm appear. The signal at 142 ppm related to –C=C– in Diels–Alder bicycle[56] disappears, suggesting a decrease of the cycloaddition crosslinking mechanism, while the enhancement of the signal at 130 ppm can be attributed to the C=C of dienophile reagent (Scheme 1B), which is not involved anymore in Diels Alder reaction. On the other hand, between 40 and 50 ppm a signal is detected in the PFA–RS spectrum, which is probably related to more substituted carbons (e.g. ternary carbon).[21],[25] Indeed, the acidity of the solution may lead to the formation of carbocation –CH2+ in the primary alcohol of sericin (Scheme 2A). The silk carbocation may interact with nucleophilic centers as PFA linear conjugated system, whose presence is already confirmed by several authors [25],[57],[58], leading to final three dimensional network represented in Scheme 2B. The coupling between those two species could justify the resonance between 50 and 40 ppm which produces secondary and ternary carbons. Furthermore, in support of what has just been hypothesized, Chen et al. have recently confirmed the formation of covalent bonds between PFA and reactive functional groups of gluten protein.[32]

The addition of tannin increases the complexity of the system and the overlapping of signals does not facilitate the recognition of any interactions. Definitely, the peaks visible at 144 ppm, 117ppm and around 75 ppm are related to –C–O of B ring, –C–C– of A ring, and C aliphatic involved in the polyphenolic structure.[18],[53] On the other hand, the interaction of the silk carbocation with the nucleophilic centers of the aromatic rings cannot be excluded (Scheme 2B). However, a stable network between tannin and RS is also guaranteed by strong hydrogen and hydrophobic interaction of those components[59]. Thus, the presence of the silk within network allow to more flexible and elastic system (black circle, Scheme 2B), which is not guaranteed without the protein due to the more branched final structure (red circle, Scheme 2B).

The samples were also investigated by ATR–FTIR spectroscopy. The spectra are reported in Figure 4.

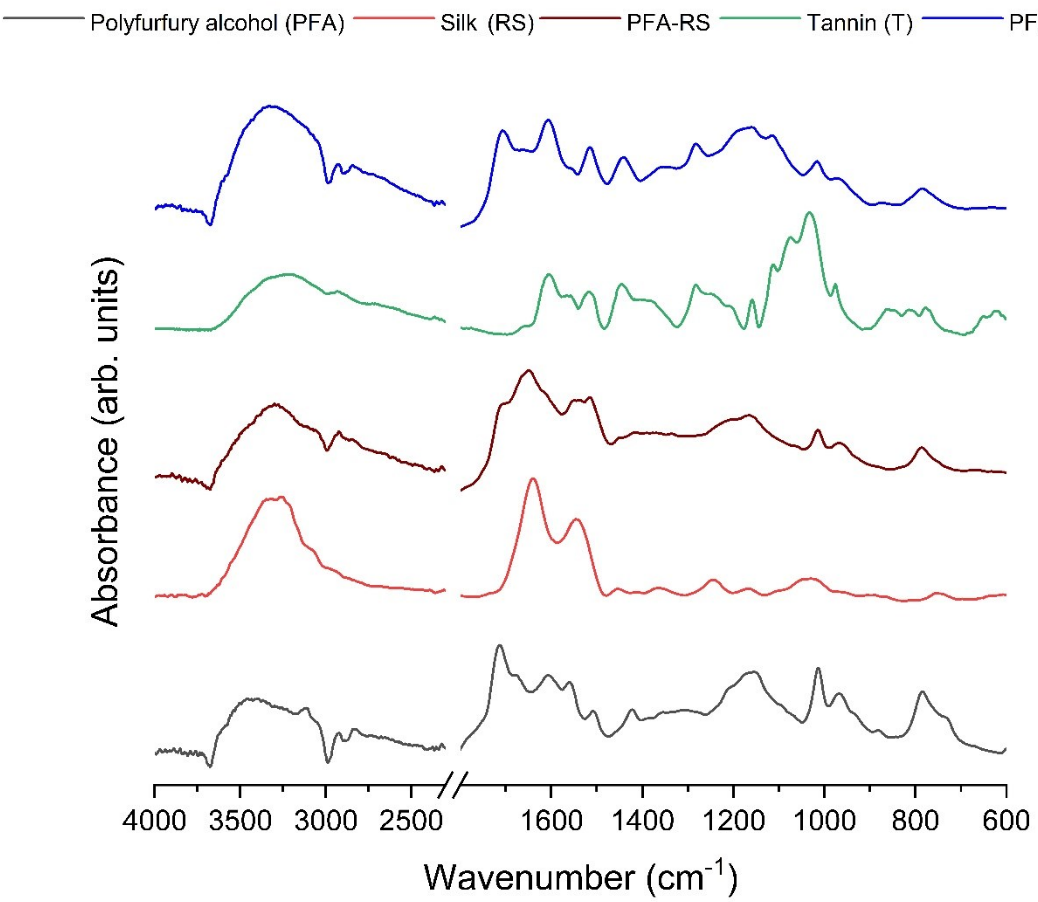

Figure 4. ATR–FT–IR spectra of: furfuryl alcohol (PFA, black curve), regenerated silk (RS, red curve), polyfurfuryl alcohol–regenerated silk (PFA–RS, brown), quebracho tannin (T, green curve) and quebracho polyfurfuryl alcohol–regenerated silk–quebracho tannin (PFA–RS–T, blue curve).

The spectrum of PFA obtained in the present investigation shows several diagnostic signals already observed in a previous work, when PFA was prepared using a similar procedure.[56] The peaks at ca. 1520 cm^{-1}, 1420 cm^{-1}, 1013 cm^{-1} and 785 cm^{-1} can be ascribed to the linear PFA structure, while the bands at 1715 cm^{-1}, 1660 cm^{-1} and 965 cm^{-1} suggest the presence of the Diels–Alder product within the polymer matrix. [56] The spectrum of PFA–RS still evidences the signals related to the linear PFA structures at ca. 1520 cm^{-1}, 1013 cm^{-1} and 785 cm^{-1}, the contribution at ca. 1715 cm^{-1} due to the Diels–Alder product and the broad band at 965 cm^{-1} related to ring–opened and/or Diels–Alder structures. Interestingly, it has been proposed that the presence of a contribution at ca. 735 cm^{-1} might be used in conjunctions to the peak at 785 cm^{-1} to estimate the relative amount of single–linked and double–linked furan rings within the PFA matrix. [57] In this respect, the spectra indicate that the relative intensity of the contribution at ca. 735 cm^{-1} decreases going from PFA to PFA–RS, suggesting that the presence of silk reduces the relative fraction of single–linked furan rings. This is consistent with a silk–induced modulation of the cycloaddition crosslinking.

The spectrum of the PFA–RS–T sample is dominated by the tannin contribution; in any case the signals at 1013 cm^{-1} (linear PFA), 965 cm^{-1} (ring–opened and/or Diels–Alder PFA) and 785 cm^{-1} (linear PFA) can be still recognized. Similarly to the case of the binary PFA–RS sample, a contribution at ca. 735 cm^{-1} was not observed, in line with the idea that the silk mainly affects the polymerization process even in the ternary system.

To notice that a carbonyl resonance is still present in the spectrum (1715 cm^{-1}) of the PFA–RS–T sample (blue spectra, Figure 4). This might be attributed to the C=O stretching of both the formylated tannin (Figure S2 in SI section) and the Diels–Alder product. In order to obtain more information two samples crosslinked in formic acid (PFA–T and PFA–RS–T) were analyzed and the absorbance spectra obtained from FTIR imaging were compared. The relative analysis were compared, as reported in figure 5.

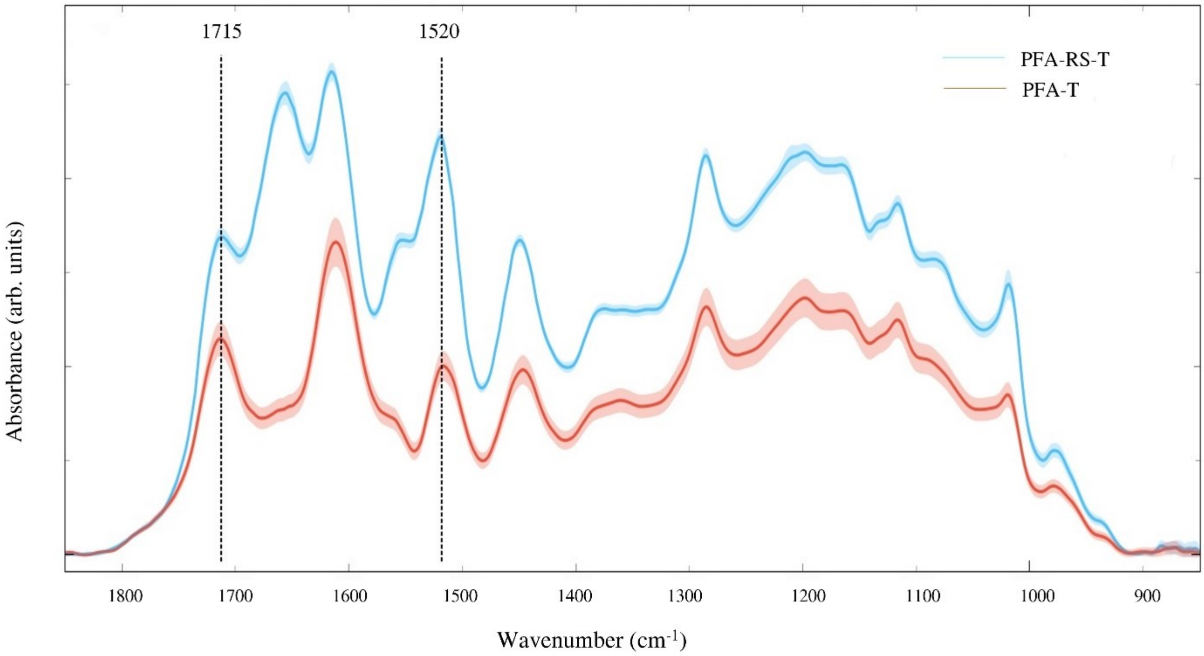

Figure 5. Average FTIR spectra of surface samples of polyfurfuryl alcohol–quebracho tannin (PFA–T, red curve) and polyfurfuryl alcohol–regenerated silk–quebracho tannin (PFA–RS–T, light blue curve).

The integration ratio between the peak at 1715 cm^{-1} (C=O) and at 1520 cm^{-1} (C=C asymmetric stretching of tannin), is found to be 1.3 and 0.6 for PFA–T and PFA–RS–T, respectively. Thus, resulting in a decrease of more than 50% percent when RS is added to the PFA–tannin polymer.

This confirms that the addition of silk inhibits the Diels–Alder reaction, as reported in Scheme 2B . The protein chains fit into the polymer matrix by establishing secondary interactions, limiting the crosslinking to proceed. Due to the strong acidic environment, the formation of the covalent bonds between silk and furfuryl alcohol (proposed after 13C–NMR observation) cannot be excluded, the vibration of the CH2–CH proposed would be overlapped (Stretching at around 3,000 and bending at below 1000 cm^{-1}) .

In relation to the intrinsic acidity of our formulation, it has to be noticed that despite no specific standards limits the pH range of an adhesives60, often too acid glues involve wood delamination.[61],[62] The formic acid applied for solubilizing the silk is involved also as activator for the formylation of tannin and as catalyst for furfuryl alcohol activation. Therefore it is expected that free HCOOH is limited and it can easily evaporate during the pressing stage. However, this aspect will be considered for future gluing durability study.

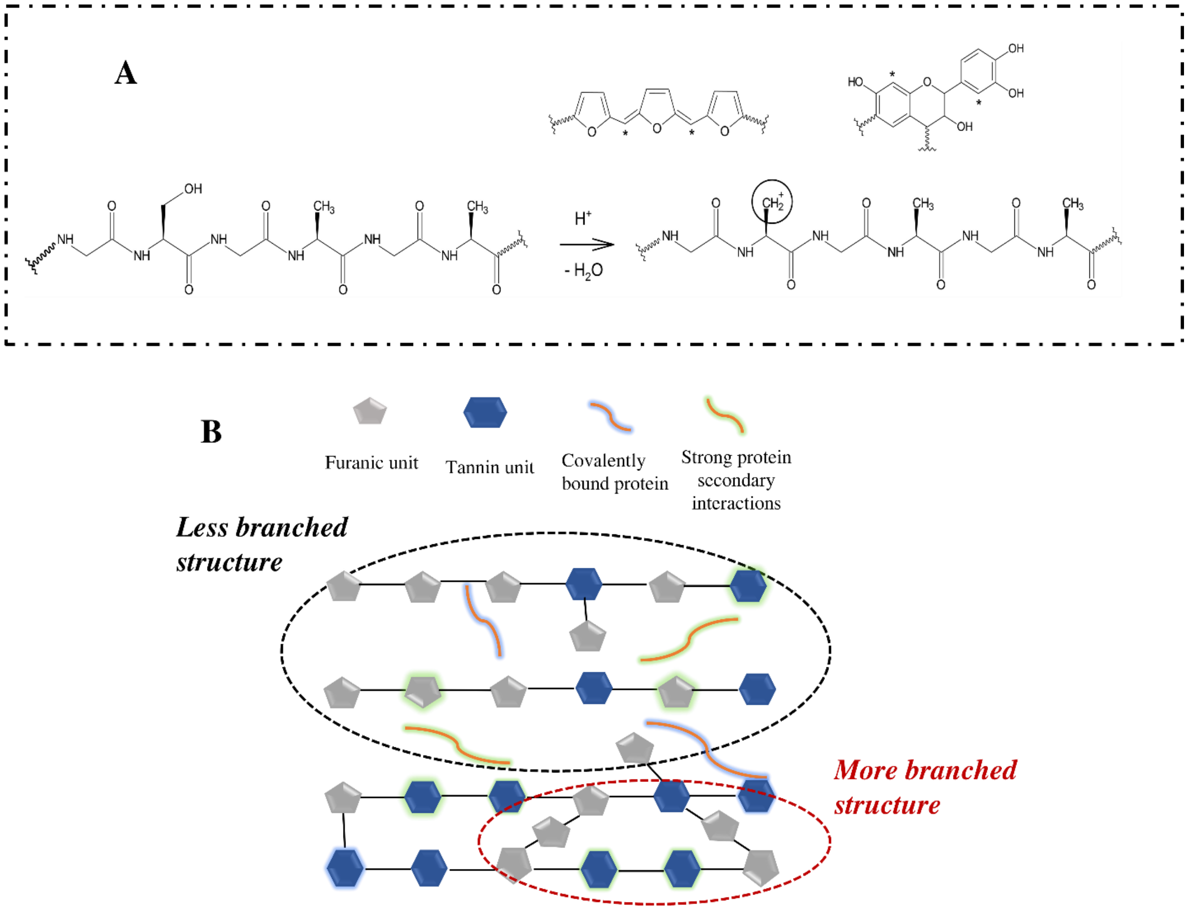

Scheme 2. A: possible carbocation formation in a primary alcohol of the silk protein structure and interaction with nucleophilic centers*. B: schematic representation and possible interaction of a tannin–alcohol furfuryl co–polymer and silk

Conclusions

In this study RS was successfully added to tannin–furanic formulation to produce bio–based adhesives with enhanced mechanical properties. Significant enhancement of about 20–30% were observed in plywood gluing when 15–20 wt% of RS was added to the reference formulation in both dry and wet conditions.

These findings were rationalized considering that the presence of the RS limits the crosslinking of the furanic polymer resulting in a homogeneous network in which the presence of chemical bonding between the silk and the furanic adduct are proposed.

This strategy provides an approach to developing formaldehyde–free bio–based wood adhesive with rapid preparation, excellent performance, and sustainability. It was shown that the combination between vegetal and animal bioresources can cooperate synergically for the production of performing wood adhesives. The interaction between silk, tannin and furanics can be considered also for other applications in the field of material science with particularly interesting perspectives in bio–plastic, construction composites and automotive but also in medical and biological devices.

References

1. Söderholm, P. The Green Economy Transition: The Challenges of Technological Change for Sustainability. Sustain. Earth **2020**, 3 (1), 6. https://doi.org/10.1186/s42055–020–00029–y.

2. CIEL. Plastic & Climate: The Hidden Costs of a Plastic Planet; 2019.

3. Zheng, J.; Suh, S. Strategies to Reduce the Global Carbon Footprint of Plastics. Nat. Clim. Chang. 2019, 9 (5), 374–378. https://doi.org/10.1038/s41558–019–0459–z.

4. Spierling, S.; Knüpffer, E.; Behnsen, H.; Mudersbach, M.; Krieg, H.; Springer, S.; Albrecht, S.; Herrmann, C.; Endres, H. J. Bio–Based Plastics – A Review of Environmental, Social and Economic Impact Assessments. J. Clean. Prod. **2018**, 185, 476–491. https://doi.org/10.1016/j.jclepro.2018.03.014.

5. Rosenboom, J. G.; Langer, R.; Traverso, G. The Hidden Costs of a Plastic Planet. Nat. Rev. Mater. 2022, 7 (2), 117–137. https://doi.org/10.1038/s41578–021–00407–8.

6. Cesprini, E.; De Iseppi, A.; Giovando, S.; Tarabra, E.; Zanetti, M.; Šket, P.; Marangon, M.; Tondi, G. Chemical Characterization of Cherry (Prunus Avium) Extract in Comparison with Commercial Mimosa and Chestnut Tannins. Wood Sci. Technol. **2022**, 56, 1455–1473. https://doi.org/10.1007/s00226–022–01401–1.

7. Shirmohammadli, Y.; Efhamisisi, D.; Pizzi, A. Tannins as a Sustainable Raw Material for Green Chemistry: A Review. Ind. Crops Prod. **2018**, 126 (June), 316–332. https://doi.org/10.1016/j.indcrop.2018.10.034.

8. Falcão, L.; Araújo, M. E. M. Vegetable Tannins Used in the Manufacture of Historic Leathers. Molecules 2018, 23, 8–10. https://doi.org/10.3390/molecules23051081.

9. Cook, N. C.; Samman, S. Flavonoids – Chemistry, Metabolism, Cardioprotective Effects, and Dietary Sources. J. Nutr. Biochem. **1996**, 7 (2), 66–76. https://doi.org/10.1016/0955–2863(95)00168–9.

10. Eckardt, J.; Neubauer, J.; Sepperer, T.; Donato, S.; Zanetti, M.; Cefarin, N.; Vaccari, L.; Lippert, M.; Wind, M.; Schnabel, T.; Petutschnigg, A.; Tondi, G. Synthesis and Characterization of High–Performing Sulfur–Free Tannin Foams. Polymers (Basel). **2020**, 12 (3). https://doi.org/10.3390/polym12030564.

11. Tondi, G.; Pizzi, A. Tannin–Based Rigid Foams: Characterization and Modification. Ind. Crops Prod. 2009, 29 (2–3), 356–363. https://doi.org/10.1016/j.indcrop.2008.07.003.

12. Arbenz, A.; Avérous, L. Chemical Modification of Tannins to Elaborate Aromatic Biobased Macromolecular Architectures. Green Chem. **2015**, 17 (5), 2626–2646. https://doi.org/10.1039/c5gc00282f.

13. Sommerauer, L.; Thevenon, M. F.; Petutschnigg, A.; Tondi, G. Effect of Hardening Parameters of Wood Preservatives Based on Tannin Copolymers. Holzforschung **2019**, 73 (5), 457–467. https://doi.org/10.1515/hf–2018–0130.

14. Cesprini, E.; Baccini, R.; Urso, T.; Zanetti, M.; Tondi, G. Quebracho–Based Wood Preservatives : Effect of Concentration and Hardener on Timber Properties. coatings **2022**, 12, 568. https://doi.org/https:// doi.org/10.3390/coatings12050568.

15. Pizzi, A. Recent Developments in Eco–Efficient Bio–Based Adhesives for Wood Bonding : Opportunities and Issues. J. Adhes. Sci. Technol. **2012**, No. December, 37–41.

16. Hemmilä, V.; Adamopoulos, S.; Karlsson, O.; Kumar, A. Development of Sustainable Bio–Adhesives for Engineered Wood Panels–A Review. RSC Adv. **2017**, 7 (61), 38604–38630. https://doi.org/10.1039/c7ra06598a.

17. Pizzi, A. Tannins: Prospectives and Actual Industrial Applications. Biomolecules **2019**, 9 (8). https://doi.org/10.3390/biom9080344.

18. Tondi, G. Tannin–Based Copolymer Resins: Synthesis and Characterization by Solid State 13C NMR and FT–IR Spectroscopy. Polymers (Basel). **2017**, 9 (6). https://doi.org/10.3390/polym9060223.

19. Gandini, A. Polymers from Renewable Resources: A Challenge for the Future of Macromolecular Materials. Macromolecules **2008**, 41 (24), 9491–9504. https://doi.org/10.1021/ma801735u.

20. Choura, M.; Belgacem, N. M.; Gandini, A. The Acid–Catalyzed Polycondensation of Furfuryl Alcohol: Old Puzzles Unravelled. Macromol. Symp. **1997**, 122, 263–268. https://doi.org/10.1002/masy.19971220141.

21. Choura, M.; Belgacem, N. M.; Gandini, A. Acid–Catalyzed Polycondensation of Furfuryl Alcohol: Mechanisms of Chromophore Formation and Cross–Linking. Macromolecules **1996**, 29 (11), 3839–3850. https://doi.org/10.1021/ma951522f.

22. Pfriem, A.; Dietrich, T.; Buchelt, B. Furfuryl Alcohol Impregnation for Improved Plasticization and Fixation during the Densification of Wood. Holzforschung **2012**, 66 (2), 215–218. https://doi.org/10.1515/HF.2011.134.

23. Kong, L.; Guan, H.; Wang, X. In Situ Polymerization of Furfuryl Alcohol with Ammonium Dihydrogen Phosphate in Poplar Wood for Improved Dimensional Stability and Flame Retardancy. ACS Sustain. Chem. Eng. **2018**, 6 (3), 3349–3357. https://doi.org/10.1021/acssuschemeng.7b03518.

24. Yao, M.; Yang, Y.; Song, J.; Yu, Y.; Jin, Y. Lignin–Based Catalysts for Chinese Fir Furfurylation to Improve Dimensional Stability and Mechanical Properties. Ind. Crops Prod. **2017**, 107 (May), 38–44. https://doi.org/10.1016/j.indcrop.2017.05.038.

25. Falco, G.; Guigo, N.; Vincent, L.; Sbirrazzuoli, N. Opening Furan for Tailoring Properties of Bio–Based Poly(Furfuryl Alcohol) Thermoset. ChemSusChem **2018**, 11 (11), 1805–1812. https://doi.org/10.1002/cssc.201800620.

26. Luckeneder, P.; Gavino, J.; Kuchernig, R.; Petutschnigg, A.; Tondi, G. Sustainable Phenolic Fractions as Basis for Furfuryl Alcohol–Based Co–Polymers and Their Use as Wood Adhesives. Polymers (Basel). **2016**, 8 (11). https://doi.org/10.3390/polym8110396.

27. Szczurek, A.; Fierro, V.; Thébault, M.; Pizzi, A.; Celzard, A. Structure and Properties of Poly(Furfuryl Alcohol)–Tannin PolyHIPEs. Eur. Polym. J. **2016**, 78, 195–212. https://doi.org/10.1016/j.eurpolymj.2016.03.037.

28. Cesprini, E.; Causin, V.; Iseppi, A. De; Zanetti, M.; Marangon, M.; Barbu, M. C.; Tondi, G. Renewable Tannin–Based Adhesive from Quebracho Extract and Furfural for Particleboards. **2022**, 13, 1781.

29. Jorda, J.; Cesprini, E.; Barbu, M.–C.; Tondi, G.; Zanetti, M.; Král, P. Quebracho Tannin Bio–Based Adhesives for Plywood. Polymers (Basel). **2022**, 14 (11), 2257. https://doi.org/10.3390/polym14112257.

30. Zhang, J.; Long, C.; Zhang, X.; Liu, Z.; Zhang, X.; Liu, T.; Li, J.; Gao, Q. An Easy–Coating, Versatile, and Strong Soy Flour Adhesive via a Biomineralized Structure Combined with a Biomimetic Brush–like Polymer. Chem. Eng. J. **2022**, 450 (P4), 138387. https://doi.org/10.1016/j.cej.2022.138387.

31. Xu, Y.; Han, Y.; Li, J.; Luo, J.; Shi, S. Q.; Li, J.; Gao, Q.; Mao, A. Research Progress of Soybean Protein Adhesive: A Review. J. Renew. Mater. **2022**, 10 (10), 2519–2541. https://doi.org/10.32604/jrm.2022.020750.

32. Chen, X.; Yang, Z.; Yang, F.; Pizzi, A.; Essawy, H.; Du, G.; Zhou, X. Development of Easy–Handling, Formaldehyde–Free, High–Bonding Performance Bio–Sourced Wood Adhesives by Co–Reaction of Furfuryl Alcohol and Wheat Gluten Protein. Chem. Eng. J. **2022**, 462, 142161. https://doi.org/10.2139/ssrn.4281052.

33. Zhao, X.; Liu, T.; Ou, R.; Hao, X.; Fan, Q.; Guo, C.; Sun, L.; Liu, Z.; Wang, Q. Fully Biobased Soy Protein Adhesives with Integrated High–Strength, Waterproof, Mildew–Resistant, and Flame–Retardant Properties. ACS Sustain. Chem. Eng. **2022**, 10 (20), 6675–6686.

34. Cao, Z.; Chen, X.; Yao, J.; Huang, L.; Shao, Z. The Preparation of Regenerated Silk Fibroin Microspheres. Soft Matter **2007**, 3 (7), 910–915. https://doi.org/10.1039/b703139d.

35. Ceccarini, M. R.; Palazzi, V.; Salvati, R.; Chiesa, I.; Maria, C. De; Bonafoni, S.; Mezzanotte, P.; Codini, M.; Pacini, L.; Errante, F.; Rovero, P.; Morabito, A.; Beccari, T.; Roselli, L.; Valentini, L. Biomaterial Inks from Peptide–Functionalized Silk Fibers for 3D Printing of Futuristic Wound–Healing and Sensing Materials. **2023**, 24, 947.

36. Santoni, I.; Pizzo, B. Evaluation of Alternative Vegetable Proteins as Wood Adhesives. Ind. Crops Prod. **2013**, 45, 148–154. https://doi.org/10.1016/j.indcrop.2012.12.016.

37. Raydan, N. D. V.; Leroyer, L.; Charrier, B.; Robles, E. Recent Advances on the Development of Protein–Based Adhesives for Wood Composite Materials—a Review. Molecules **2021**, 26 (24). https://doi.org/10.3390/molecules26247617.

38. Valentini, L.; Ceccarini, M. R.; Verdejo, R.; Tondi, G.; Beccari, T. Stretchable, Bio–Compatible, Antioxidant and Self–Powering Adhesives from Soluble Silk Fibroin and Vegetal Polyphenols Exfoliated Graphite. Nanomaterials **2021**, 11 (9). https://doi.org/10.3390/nano11092352.

39. British Standards, E. B. Plywood — Bonding Quality — EN 314–1:2004. 2004, 3.

40. British Standards, E. B. Wood–Based Panels — Determination of Modulus of Elasticity in Bending and of Bending Strength– EN 310:1993. 1993, 1–14.

41. Toplak, M.; Read, S. T.; Sandt, C.; Borondics, F. Quasar: Easy Machine Learning for Biospectroscopy. Cells **2021**, 10 (9), 1–10. https://doi.org/10.3390/cells10092300.

42. Toplak, M.; Birarda, G.; Read, S.; Sandt, C.; Rosendahl, S. M.; Vaccari, L.; Demšar, J.; Borondics, F. Infrared Orange: Connecting Hyperspectral Data with Machine Learning. Synchrotron Radiat. News **2017**, 30 (4), 40–45. https://doi.org/10.1080/08940886.2017.1338424.

43. Xi, X.; Pizzi, A.; Frihart, C. R.; Lorenz, L.; Gerardin, C. Tannin Plywood Bioadhesives with Non–Volatile Aldehydes Generation by Specific Oxidation of Mono– and Disaccharides. Int. J. Adhes. Adhes. **2020**, 98. https://doi.org/10.1016/j.ijadhadh.2019.102499.

44. Liu, Z.; Chen, M.; Xu, Y.; Zhang, J.; Huang, X.; Luo, J.; Li, J.; Shi, S. Q.; Gao, Q. Preparation of a Strong and Multiple–Function Soybean Flour Adhesive via the Construction of Tannin Microspheres with a Core–Shell Structure. Compos. Part B Eng. **2022**, 242 (February), 110114. https://doi.org/10.1016/j.compositesb.2022.110114.

45. Zhou, Y.; Zeng, G.; Zhang, F.; Tang, Z.; Luo, J.; Li, K.; Li, X.; Li, J.; Shi, S. Q. Preparation of Functional Fiber Hybrid Enhanced High Strength and Multifunctional Protein Based Adhesive. Mater. Des. **2022**, 224, 111289. https://doi.org/10.1016/j.matdes.2022.111289.

46. Pang, H.; Zhao, S.; Mo, L.; Wang, Z.; Zhang, W.; Huang, A.; Zhang, S.; Li, J. Mussel–Inspired Bio–Based Water–Resistant Soy Adhesives with Low–Cost Dopamine Analogue–Modified Silkworm Silk Fiber. J. Appl. Polym. Sci. **2020**, 137 (23), 1–10. https://doi.org/10.1002/app.48785.

47. Liu, Z.; Liu, T.; Jiang, H.; Zhang, X.; Li, J.; Shi, S. Q.; Gao, Q. Biomimetic Lignin–Protein Adhesive with Dynamic Covalent/Hydrogen Hybrid Networks Enables High Bonding Performance and Wood–Based Panel Recycling. Int. J. Biol. Macromol. **2022**, 214 (April), 230–240. https://doi.org/10.1016/j.ijbiomac.2022.06.042.

48. Hafiz, N. L. M.; Tahir, P. M. D.; Hua, L. S.; Abidin, Z. Z.; Sabaruddin, F. A.; Yunus, N. M.; Abdullah, U. H.; Abdul Khalil, H. P. S. Curing and Thermal Properties of Co–Polymerized Tannin Phenol–Formaldehyde Resin for Bonding Wood Veneers. J. Mater. Res. Technol. **2020**, 9 (4), 6994–7001. https://doi.org/10.1016/j.jmrt.2020.05.029.

49. Jorda, J.; Kain, G.; Barbu, M. C.; Petutschnigg, A.; Král, P. Influence of Adhesive Systems on the Mechanical and Physical Properties of Flax Fiber Reinforced Beech Plywood. Polymers (Basel). **2021**, 13 (18), 1–15. https://doi.org/10.3390/polym13183086.

50. Biadała, T.; Czarnecki, R.; Dukarska, D. Water Resistant Plywood of Increased Elasticity Produced from European Wood Species. Wood Res. **2020**, 65 (1), 111–123. https://doi.org/10.37763/wr.1336–4561/65.1.111124.

51. Lei, H.; Frazier, C. E. Curing Behavior of Melamine–Urea–Formaldehyde (MUF) Resin Adhesive. Int. J. Adhes. Adhes. **2015**, 62, 40–44. https://doi.org/10.1016/j.ijadhadh.2015.06.013.

52. Cefarin, N.; Bedolla, D. E.; Surowka, A.; Donato, S.; Sepperer, T.; Tondi, G.; Dreossi, D.; Sodini, N.; Birarda, G.; Vaccari, L. Study of the Spatio–Chemical Heterogeneity of Tannin–Furanic Foams: From

1D FTIR Spectroscopy to 3D FTIR Micro–Computed Tomography. Int. J. Mol. Sci. **2021**, 22 (23). https://doi.org/10.3390/ijms222312869.

53. Cesprini, E.; Šket, P.; Causin, V.; Zanetti, M.; Tondi, G. Development of Quebracho (Schinopsis Balansae) Tannin–Based Thermoset Resins. **2021**, 13, 4412.

54. Conley, R. .; Metil, I. An Investigation of the Structure of Furfuryl Alcohol Polycondensates with Infrared Spectroscopy; Reinhold Publishing Corporation, New York, 1963. https://doi.org/10.1002/app.1963.070070104.

55. Myers, G. E. 13C NMR Study of Curing in Furfuryl Alcohol Resins. Macromolecules **1984**, 17, 1087–1090.

56. Tondi, G.; Cefarin, N.; Sepperer, T.; D'Amico, F.; Berger, R. J. F.; Musso, M.; Birarda, G.; Reyer, A.; Schnabel, T.; Vaccari, L. Understanding the Polymerization of Polyfurfuryl Alcohol: Ring Opening and Diels–Alder Reactions. Polymers (Basel). **2019**, 11 (12), 1–15. https://doi.org/10.3390/polym11122126.

57. D'Amico, F.; Musso, M. E.; Berger, R. J. F.; Cefarin, N.; Birarda, G.; Tondi, G.; Bertoldo Menezes, D.; Reyer, A.; Scarabattoli, L.; Sepperer, T.; Schnabel, T.; Vaccari, L. Chemical Constitution of Polyfurfuryl Alcohol Investigated by FTIR and Resonant Raman Spectroscopy. Spectrochim. Acta – Part A Mol. Biomol. Spectrosc. **2021**, 262 (June), 120090. https://doi.org/10.1016/j.saa.2021.120090.

58. Buchwalter, S. L. Polymerization of Furfuryl Acetate in Acetonitrole. J. Polym. Sci. A1. **1985**, 23 (12), 2897–2911. https://doi.org/10.1002/pol.1985.170231202.

59. Ma, M.; Dong, S.; Hussain, M.; Zhou, W. Effects of Addition of Condensed Tannin on the Structure and Properties of Silk Fibroin Film. Polym. Int. **2017**, 66 (1), 151–159. https://doi.org/10.1002/pi.5272.

4.3 Life cycle assessment of silk protein used in the tannin–based adhesive formulation

4.3.1 Assessing the Environmental Impact of Silk Protein Production for Bio–Based Materials: A Life Cycle Assessment Study

Abstract

Substituting petroleum–based materials with renewable alternatives is a crucial step toward decarbonization. One promising avenue involves harnessing natural resources, such as proteins, to create biobased materials that are applicable in various fields. Silk cocoons, in particular, have emerged as a valuable raw material for developing protein bioplastics. Although the chemical and physical properties of silk cocoons remain indisputable, some studies in the literature have classified this fibre as a high impact environmental product. It is worth noting that these studies often refer to intensive practices, which differ from those currently employed in European contexts, notably in Italy. To comprehensively assess the environmental footprint of silk cocoon production, we conducted a life cycle assessment (LCA) study, utilizing both primary and secondary data. Primary data were collected from Italian farmers that covered every phase of the silk cocoon supply chain, from mulberry harvesting to worm rearing. Secondary data from Ecoinvent 3.9 database were also included in the model, to provide emission factors. Environmental impacts were quantified using the CML 2001 baseline method, with a focus on impact categories related to air, soil, and water pollution. The findings from the model underscore the significant reduction in environmental impact across all categories when employing sustainable agricultural practice when compared with scientific literature. Specifically, in impact categories like Global Warming Potential, Eutrophication, Freshwater Ecotoxicity, and Terrestrial Ecotoxicity, reported values of 10.7 kg CO_2 eq., 0.031 kg PO_4 eq., 9.3 kg 1.4 DB eq., and 0.069 kg 1.4–DB eq., respectively. Therefore, the aim of this study was to contextualize silk production within a European context, with the goal of expanding the potential applications of this material, particularly as an additive for wood adhesives.

Life cycle assessment of protein counterpart involved in the tannin–based adhesive formulation.

Introduction

Today, in the urgent pursuit of combating climate change and implementing robust decarbonization strategies, the application of environmental impact assessment methods, such as Life Cycle Assessment (LCA), is of paramount importance. LCA emerges as a valuable environmental methodology to monitor the environmental impacts related to a product, process, or activity throughout their entire life cycle. This analytical tool proves to be instrumental in showcasing the environmental advantages of green products and innovative technologies in contrast to their petroleum–based counterparts [1],[2]. Within the realm of LCA methodology, each stage of the supply chain is meticulously quantified to analyze its environmental impact, establishing potential areas for reduction commonly known as "hotspots." These hotspots serve as focal points, helping stakeholders identify the most environmentally taxing processes within their value chain. To guide this assessment, the International Organization for Standardization (ISO) has introduced a comprehensive framework [3]. ISO 14040 [4] delineates the principles and overarching framework for LCA, while ISO 14044 [5] outlines specific requirements and provides guidelines for conducting a Life Cycle Assessment.

A critical aspect of this ecological transition involves steering away from the reliance on fossil resources and instead embracing materials of natural origin. In fact, harnessing natural resources for biomaterial production is a central challenge in the global industrial landscape. However, the label "renewable" does not always automatically equate to "sustainable." For example, among both natural and synthetic fibers, silk is recognized as the highest impact fiber [6],[7]. Sericulture revolves around the cultivation of mulberry silkworms (Bombyx mori) and comprises three primary activities: cultivation of mulberry trees, rearing of silkworms, and silk harvesting. Mulberry, a fast–growing tree adaptable to various soils and climates, has a lifespan of 70 to 90 years but can survive up to 250 years [8]. Resilient and versatile, it thrives in diverse environments and is used for land reclamation. As a rapid growth specie, mulberry trees show potential for reducing greenhouse gas emissions, as seen in a study in Haining, China, where negative carbon emissions from mulberry plantations over two years, with additional gains possible through reduced nitrogen fertilizer use, is reported [9].

Although the historical application of fibroin fibers has always been alongside to the fashion market, the peculiar characteristics of this material have shifted attentions into different kinds of applications, creating high–performance bio materials for applications in several fields [10],[11]. The silk fiber itself consists of two fibroin proteins, bound together by a distinct protein called sericin. Sericin stands out as a result of its increased hydrophilicity compared to fibroin. It serves a dual role as an adhesive that bonds the filaments and as a structural reinforcement for the cocoon [12]. Interestingly, both proteins possess distinct and valuable properties in various industrial applications, which makes this material of significant industrial interest [13]. As previously mentioned, despite the renewability and exceptional physicochemical attributes of its components, prominent studies in the literature consistently underscore the significant environmental footprint associated with this material [14][15]. In particular, it was highlighted that the cultivation of mulberry leaves, used as feed, is the main source of environmental impact for silkworm supply chain [6]. In fact, although the intrinsic characteristics of this species lay the foundations for a sustainable development of these plantations, the high productivity of silkworms requires a high production of mulberry leaves to feed the animals.

In fact, according to the main studies present in literature mulberry tree management is based on unsustainable agricultural practices, characterized by excessive water use, heavy fertilizer and pesticide application, sustain a high intensity production model [6],[14].

However, it is important to note that the silk production chain should not consider cocoons as the sole industrial product. Instead, with effective organization, the industry could harness various by–products, currently classified as waste materials, such as sericin, pupae, wood and bio waste [16]. In this way, Altman and Alman and Farell [7] recently examined an intriguing perspective on the importance of this supply chain, as shown on the left side of the Figure 1. The authors concluded by highlighting how sericulture, which functions as a holistic agricultural production system, epitomizes an environmentally friendly endeavor that might be ideal for climate resilience, sustainability, and equitable trade practices. It presents a cost–effective approach that yields high productivity while reaping benefits at each stage, from mulberry cultivation and fruit harvesting to the use of insect resources such as pupae and both silk proteins [8]. In the same direction, the authors of a recent review highlighted several critical factors that impede the progress of the silk industry. These include challenges related to the availability of high–quality eggs, farm efficiency, health management, inadequate government support, unsustainable production practices, and competition from imported products. These issues collectively pose obstacles to the overall development of both upstream and downstream aspects of the industry. [13]. Boosting sericulture profitability requires legislative support, investments, and the adoption of advanced procedures and methods.

In this study, we examine an innovative example: a small silk cocoon supply chain in northeast Italy, specifically in the Veneto region. A life cycle assessment has been performed to identify key hotspots in the chain and propose potential solutions, considering the entire process, with a view to the application of the main protein component, fibroin, as an additive in the field of bio–adhesives for wood products.

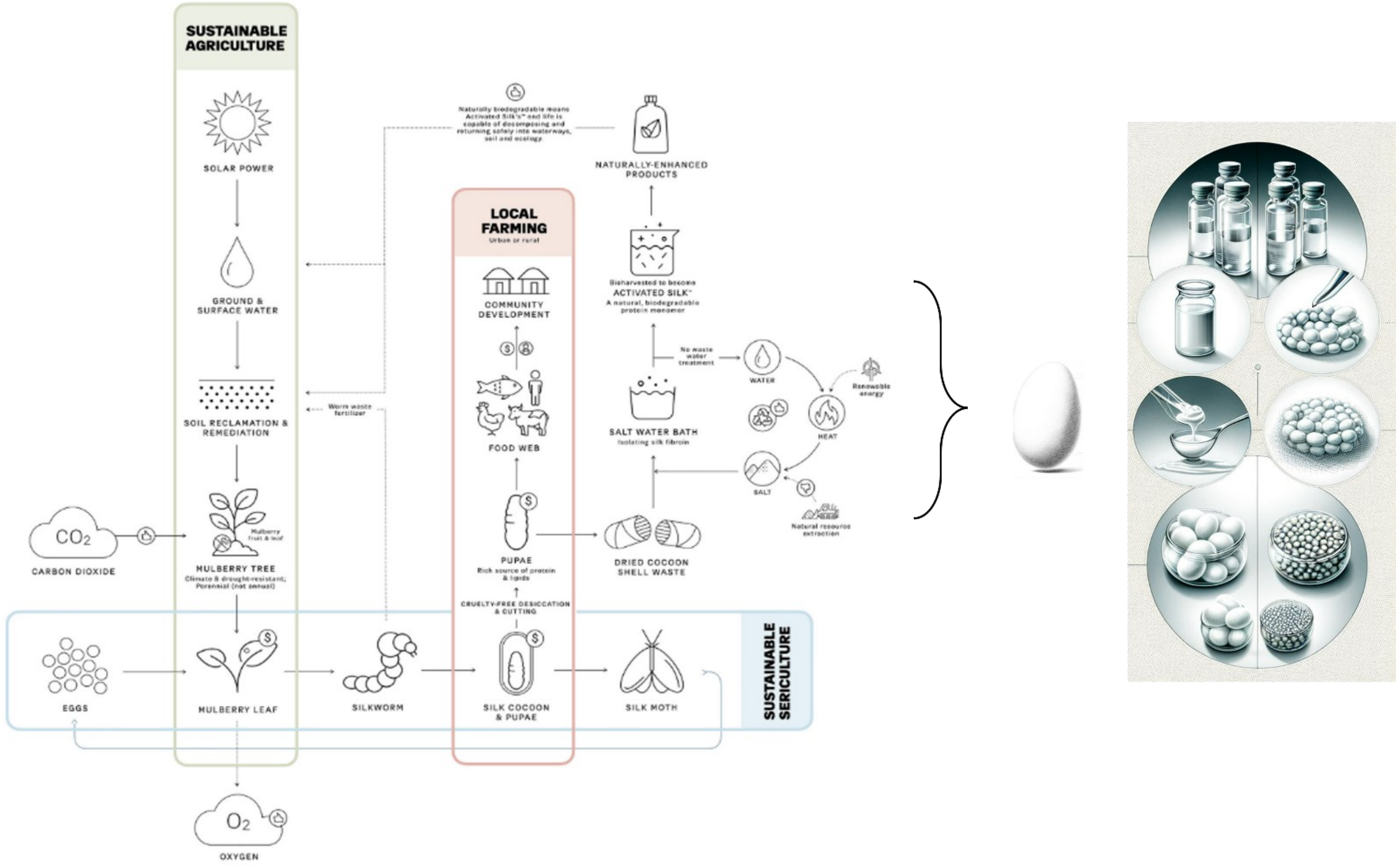

Figure 1. Overview of silk environmental friendly silk supply chain [7] and the alternative uses of silk proteins.

Methodology

Definition of goals and scope

The current study examines the 'cradle–to–gate' environmental impact by the raw silk production of Italian research center, known as CREA, and several famers involved within the supply chain. To conduct a thorough evaluation of the environmental impact, the research presents the life cycle impact assessment (LCIA) embodied in the CML–IA baseline method, including Abiotic depletion (kg Sb eq), Abiotic depletion, Fossil Fuels (MJ), Global warming potential (kg CO_2 eq), Ozone layer depletion (kg CFC–11 eq), Human toxicity (kg 1,4–DB eq), Fresh water aquatic ecotoxicity (kg 1,4–DB eq), Marine aquatic ecotoxicity (kg 1,4–DB eq), Terrestrial ecotoxicity (kg 1,4–DB eq), Photochemical oxidation (kg C_2H_4 eq), Acidification (kg SO_2 eq), Eutrophication (kg PO_4 eq). The system was modelled with SimaPro (version 9.5; Prè Consultants, 2015) [17]. The functional unit is 1 kg of dried cocoons, including both the shell and pupae, for a possible alternative application in the field of adhesive for wood and biobased material [18]. The model was set according to the energy and material consumption for a production cycle within the Italian Veneto region.

Therefore, the objectives of the study are as follows:

- Perform a cradle–to–gate life–cycle assessment of cocoon production and by–products.
- Compare the practices performed in the current study with the main research found in bibliography by analyzing differences and equalities.
- Analize the alternative application of silk proteins within the field of biomaterial with a focus on wood adhesives.

System boundaries

The study adopts a cradle–to– gate approach, from the refrigeration of the eggs of previous year to the dry process of the silk cocoons, strategically examining both the overarching processes, encompassing the background intricacies associated with Mulberry cultivation practices, and the foreground processes, with a detailed analysis of the sequential steps entailed in the silk cocoon rearing process. The data are collected for the production season of 2021–2022. Except for the dry equipment, infrastructure processes such as facilities, equipment necessary for production activities, both for mulberry and cocoon production were included within the system boundaries, thus their impacts were accounted for. As mentioned above, for the applications in the field of biomaterials, specifically for wood adhesives, one of the two proteins contained within the silk cocoon, fibroin, is to be used. Due to the lack of industrial data, the separation process of fibroin and sericin was not included in the model, and therefore its impact on the final product.

Allocation procedures

As allocation method, for the upstream and foreground processes the cut–off classification and market process have been selected [19], thus all impacts were attributed to the process that generated it, not penalizing other entries. In the baseline scenario, the entire impact was attributed to 1 kg of silk cocoons, including both cocoon and pupae. As alternative scenarios, the incorporation of wood waste biomass for wood chips production is offered, and economic allocation was employed to distribute the impacts between silk cocoons and wood chips. This economic allocation was determined considering the average prices of three distinct silkworm quality classes, as provided by the CREA center, and utilizing the 2022 market value of Italian wood chips in 2022 [20].

Assumption and limitations

As the majority processes lacked information tailored to Italian conditions in the LCI (Ecoinvent v.3.9) database, there exists uncertainty within the presented system. The reference used may not accurately reflect the local reality, introducing a level of uncertainty in the analysis. In addition, the production chain involves the weaning center (CREA, Padova, Italy) and local farmers located across the Veneto region, specifically in north–east Italy, who reared 16 boxes in 2022. In this analysis, the breeding of silkworms from external sources, even though supplied by the CREA center, has not been incorporated. This exclusion is attributed to the scarcity of dependable data concerning the productivity and practices related to these external sources. In addressing the impacts linked to mulberry orchards, a reference has been drawn from the practices of Azienda Agricola Dametto Roberto, situated in Altivole, Italy. It is noteworthy that the cultivation methods adopted by this farmer serve as a representative model for all farmers in the region. Finally, adjustments have been made to all secondary processes in accordance with the following criteria:

1. Whenever possible, we prioritized the use of Italian (IT) databases. In cases where Italian data were not available, Switzerland (CH) data has been used. This choice was influenced by similar energy practices and policies observed in both countries. In the absence of specific processes for IT and CH, Europe (RER) and Rest of the World (ROW) were used in this order.

2. For all secondary processes that involved energy consumption, they have been updated to reflect the specific energy mix of Italy (IT) in order to make the model more consistent with the Italian reality.

Life Cycle Inventory

The detailed flow chart of the model is reported in Figure 2. Numeric values refer to a production of 31 kg of leaves, which are necessary to feed 1667 eggs, which in turn lead to 1 kg of dry cocoons.

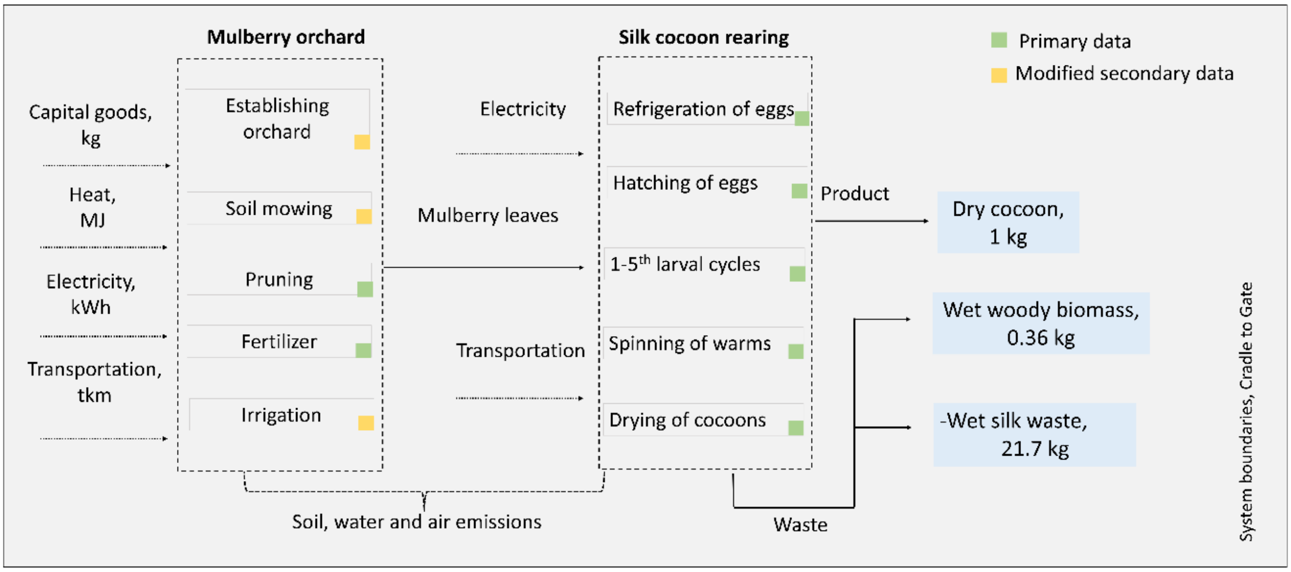

Figure 2. Detailed schematic representation of the silk cocoon rearing divided into the two main subprocess: background (Mulberry orchard) and foreground (Silk cocoon rearing). The numerical values of the inputs are related to 1 kg of dry silk cocoons production.

Mulberry orchard

The mulberry orchard model was developed in collaboration with Dametto Ss, an agricultural company located in Altivole, Veneto, Italy. This partnership involved obtaining primary data on planting and maintenance procedures. For modeling the practices associated with the management and cultivation of mulberry orchards (Mulberry leaves IN, mulberry production| Cut–off, U), the Ecoinvent 3.9 database process from the SimaPro 9.5 software [17] was utilized and adapted to align with Italian production standards. Figure 2 illustrates the key processes and practices involved, while Table 1 details the inputs required for the production of 1 kg of mulberry leaves.

Table1. Cultivation practices data for one hectare of mulberry orchard.

Indicator	Veneto supply chain (Italy)
Pesticide (kg/ha/year)*	20
Compost (q/year)	300
Mulberry leaf (ton/ha)	10 (least)
Irrigation requirements (m3/ha/year)	691
Annual pruning (electric scissor, kWh/ha year)	3.6
Soil tillage (kWh/ ha year)	0.0036
Feed requirement (kg leaf/ kg cocoons)	10–16

Cocoon yield (kg/ha)	(600–1000)

**Used to combat bacterial blight in 2021 (used 2 times with the doses specified by the manufacturer–see attached).*

Silk cocoon rearing

The rearing process, depicted in Figure 2, involves a series of sequential steps outlined below. The cycle initiates with the refrigeration of eggs in three chambers, each one equipped with a power of 1.82 kW and a total maximum theoretical capacity of 5000 boxes. Subsequently, the process advances to a ventilated and temperature-controlled chamber with a power of 2.25 kW and a theoretical capacity of 120 boxes, where hatching takes place over a 10 to 12-day period. Then, the eggs are distributed across boxes (considering 16 boxes in this study), each containing 20,000 eggs, and allocated to farmers responsible for overseeing the five larval cycles. Farmers categorize these cycles based on the silkworm's developmental stages, with the last two cycles, leading up to cocoon formation, being particularly demanding. During this phase, the silkworm consumes around 90% of the mulberry leaves, necessitating multiple daily feedings with substantial amounts of food. After completing the fifth stage, the silkworms transition to plastic trays to commence cocoon spinning. The cultivation process concludes with the drying phase, conducted at the Bernardo farm in Massanzago, Veneto, Italy. The wet cocoons are transported to a dryer, where the drying process takes approximately 10–12 hours, contingent on climate conditions, and involves maintaining wet cocoons at temperatures ranging from 60–65°C. The main consumptions related to the silkworm growth process are summarized in Table 2 The values were scaled from the 2022 production for the Veneto chain of 180.5 kg to 1 kg final product.

Table 2. Consumption related to the worm growth process for the production of one dry kg of silk cocoons.

Material	Reference process	Value
NaClO	Hatching of eggs (disinfection)	0.006 kg
H_2O_2	1–3th larval cycle (disinfection)	0.06 kg
Water consumption	Chemical solution	0.13 L
Paper, Newsprint	1–3th larval cycle (worm bed)	0.07 kg
Plastic ray	Spinning of cocoons	0.23 kg

Mulberry leaves	Feed of cocoons	31 kg
Transportation	Movement of cocoons	5.3 kg
Building hall	Rearing of cocoons	0.005 m^2
Electricity	Processes for cocoons rearing	0.71 kWh
Electricity	Utilities	7.8 kWh

Veneto supply chain

Figure 3 illustrates the cocoon production supply chain in the Veneto region, Italy. The various agricultural operations within the chain are distinctly marked by colored labels, each signifying the specific tasks assigned to the respective farms. The CREA research center, identified by the green label, specializes in intricate processes such as refrigeration, egg incubation, and crossbreeding among different breeds. Following the hatching phase, the resulting animals seamlessly transition, typically after a few days, to the Il Brolo farm, located 8.2 km from the CREA research center and denoted by the red label in Figure 3. At Il Brolo, the initial three larval cycles are meticulously executed. Subsequently, animals designated for the fourth and fifth larval cycles undergo systematic distribution among other farms within the network. The use of a grey label designates the Bernardo farm, which is 41.3 km from Il Brolo. In addition to its role in silkworm breeding, the Bernardo farm plays a crucial role by providing a reference drying facility that serves the entire agricultural chain. Regarding logistical movements, the noticeable displacements encompass the following trajectories, resulting in calculated distances for both outward and return journeys: CREA to Brolo (16.4 km), Brolo to various participating farms (468.4 km), farmers to the Bernardo farm (255.6 km), and, finally, the Bernardo farm back to CREA (60 km). This results in a total path within the supply chain of around 964 km. Each farmer is responsible for collecting and managing the animals, making the process 'Transport, passenger car, Euro 4 (RER), Cut–off, U' the chosen reference in the model. This decision is grounded in the fact that each farmer transports limited quantities of animals and can use their own vehicle for transportation. This intricate network underscores a comprehensive and interconnected approach to the multifaceted processes involved in egg incubation, larval development, and silkworm breeding, with each farm playing a specialized role in the overarching agricultural chain.

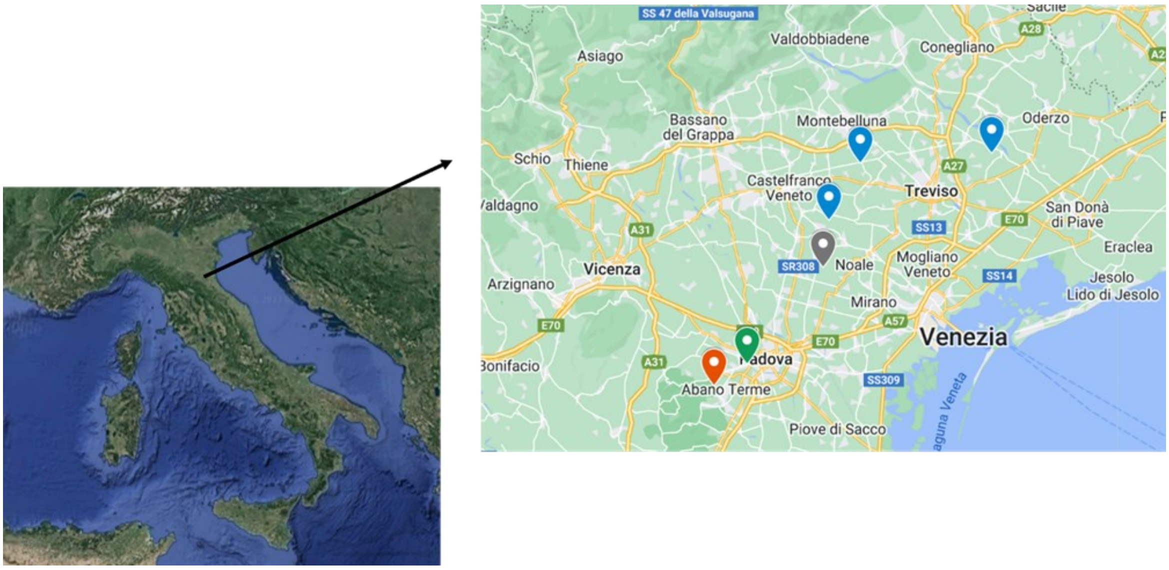

Figure 3. Veneto Supply chain of silk cocoons.(green label: CREA research center, red label: il Brolo farm, grey label: Bernardo farm, blue label: Dametto, Trevisan and Massimo Miolo farms).

Results

Base scenario

The contribution analysis for the production of 1 kg of dry cocoons is visually presented in Figure 4. It is worth highlighting that the farmers participating in this supply chain adhere to environmentally friendly agricultural practices, abstaining, when possible, from the use of fertilizers and pesticides. However, for the year 2021 and 2022 to combat bacterial blight an certain amount of pesticide was used, and the moderate impact of its use is then shown in Figure 4, which does not overcame 3% across all the impact categories. As mentioned before, the Dametto farm serves as a model for managing a mulberry orchard established five years ago, replacing a kiwi crop. The two to three–year establishment phase employed compost exclusively, omitting fertilizers and pesticides. The Ecoinvent process, "Establishment of Orchard (CH)|Cut–off, U", was adapted to Italian dimensions, ensuring scientific accuracy. The deliberate use of compost aligns with sustainable practices, promoting soil health. This tailored model contributes to the impact categories within a range of 5 and 10%. As for the annual management of the mulberry orchard this simply involves mowing grass twice a year, and tree pruning is done with electric scissors. The two impacts have been grouped together and their impact along the different categories is limited and less than an average of 3–4%. Finally, the “Irrigation (CH)|irrigation, drip| Cut–off, U” Ecoinvent process was used and modified with the water consumption recorded for the year under consideration, and no other process modifications were made. Although water consumption is relatively low, the impacts from the use of raw materials for the construction of the water system leads to a relatively large impact on the final model. However, the environmental impact associated with the mulberry crop remains limited, particularly when compared to existing literature findings [6],[14]. For instance, Barcelos et al. observed significant impacts associated with mulberry practices, particularly noting a 100% impact in categories such as freshwater and terrestrial ecotoxicity, as well as freshwater eutrophication, while the impact for GWP was approximately 50% on the total processes impact [6]. In contrast, the implementation of low–intensity practices and sustainable orchard management significantly influenced these categories. Specifically, the percentage recorded values were 15% for GWP, 59% for eutrophication, and 28% and 37 % for freshwater and terrestrial ecotoxicity, respectively.

Given the relatively low impact associated with mulberry practices, the current classification is predominantly influenced by energy consumption, contributing 30% to Global Warming Potential (GPW), 33% to abiotic depletion (fossil fuels), 32% to human toxicity, and up to 35% to ozone layer depletion of the total environmental impact. The entire process, from rearing to hatching the eggs, takes place at the CREA research centre. As this production chain is still in its early stages, striving to establish a presence in a local economy it has been absent from for decades, it lacks the efficiencies of an established supply chain. Primarily focused on research activities, the centre distributes only a minimal portion of eggs to farmers for sale, limiting productivity. Consequently, the electricity consumption per kilogram of silk cocoons is notably high, depicted by the light blue segment in Figure 4. Notably, only 8% of the total consumption is related to the energy required for machinery directly linked to silkworm cultivation, while the remaining energy consumption is attributed to utilities.

The optimal growth of silkworms demands particular attention, particularly during the final two larval cycles – the fourth and fifth stages. In these critical phases, the silkworm exhibits heightened requirements, necessitating approximately 90% of its dietary intake in the form of mulberry leaves. Furthermore, the silkworm's need for expansive spaces becomes pronounced, with an estimated space requirement of around 20 m^2 per every box during the growth period. This emphasizes the significance of providing both an ample leaf supply and spacious environments to facilitate the flourishing development of silkworms, ensuring the successful culmination of their growth. The spatial requirements for animal growth yield a relatively modest overall impact. Specifically, when considering all impact categories, the associated impact attributable to the building hall averages around 17%. Notably, the impacts rises to 28% for abiotic depletion and 23% for photochemical oxidation, underscoring the nuanced nature of environmental considerations associated with the designated space for animal development.

Despite the relatively short distances between farmers and the animal collection centre, as illustrated in Figure 3, the restricted production capacity emerges as a contributing factor to heightened impacts, particularly in the realm of transportation. Notably, farmers participating in this chain primarily view silkworm cultivation as a secondary business, with their primary activities spanning diverse sectors such as nurseries, wine production, or vegetable cultivation. This dual involvement accentuates the multifaceted nature of their agricultural pursuits, introducing a layer of complexity to the overall supply chain dynamics. Ultimately, the consumption linked to materials like plastic beams, newsprint, and chemical agents is characterized by judicious dosing, resulting in limited impacts across all considered categories.

In addition, silkworm production yields significant by-products. Specifically, based on gathered data, every dried kilogram of raw cocoons results in approximately 15 kg of fresh wood waste from mulberry cultivation practices and nearly 22 kg of biowaste from the rearing of cocoons, including undigested leaves and worm excrements. The disposal of these wastes has a substantial impact in the whole process, showing, for example, a 19% impact on the total GWP. Moreover, impact categories like acidification and eutrophication are most affected by the treatment of wood waste and biowaste, reaching percentage values of 26% and 67%, respectively. Due to the nascent stage of the supply chain, there is currently an absence of a standardized waste management framework, with each participant following individual practices.

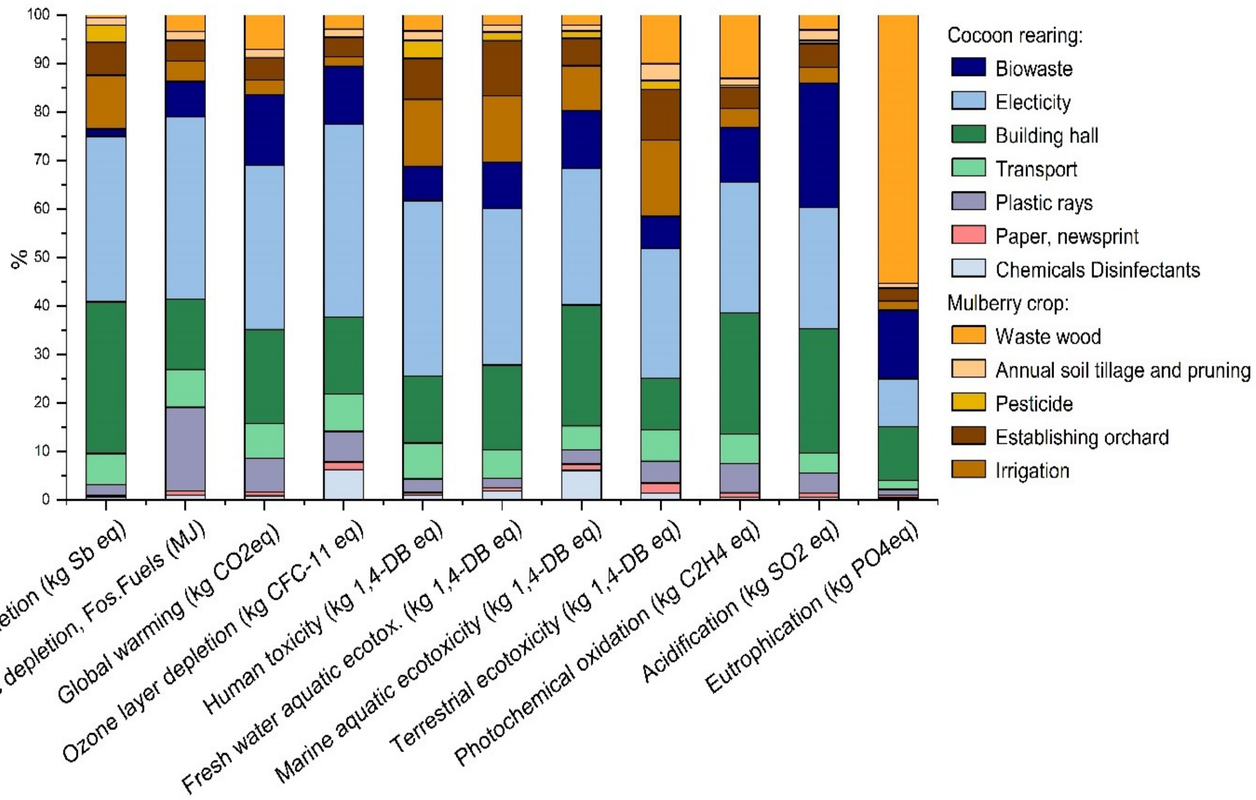

Figure 4. Environmental impacts contribution analysis of silk cocoon production based on the Italian supply chain. Impacts were divided according to two macro–processes: foreground (cocoon rearing) and background (mulberry crop).

To enhance clarity for each impact category, Table 3 presents the primary chemical compounds expressed in equivalent contributions. By analysing the data in the table 3, it can be inferred which substances contribute the most for each process considered. Moreover, the percentage values of each impact substance have been presented in Table 1 within Annex 2 of the appendix.

Table 3. Inventory analysis of the main substances contributing to the impacts for the production of 1 kg of silk cocoons for the main processes involved. The rows in the table in reference to "remaining substances" refer to the application of a 5% Cut–off.

Substance	**Compartment**	**Total**	**Mulberry leaves**	**Paper, newsprint**	**Plastic rays**	**Chemical disinfectants**	**Transport**	**Building**	**Electricity**	**Biowaste**
Abiotic depletation (kg Sb eq)										
Total of all compartments		1.21E–04	2.57E–05	3.18E–07	2.43E–06	7.05E–07	1.85E–05	3.42E–05	3.73E–05	1.71E–06
Remaining substances		8.34E–06	2.57E–06	2.97E–08	2.34E–07	7.61E–08	1.02E–06	9.94E–07	3.23E–06	1.99E–07
Copper	Raw	1.15E–05	3.68E–06	3.14E–08	2.66E–07	7.50E–08	9.36E–07	1.18E–06	5.12E–06	2.13E–07
Gold	Raw	1.45E–05	1.24E–06	4.91E–08	5.81E–07	1.72E–07	8.21E–06	1.52E–06	2.51E–06	1.94E–07
Lead	Raw	1.87E–05	1.04E–06	3.71E–08	6.84E–08	1.93E–08	1.38E–06	1.49E–05	1.22E–06	7.76E–08
Silver	Raw	1.46E–05	1.40E–06	2.96E–08	1.44E–07	4.21E–08	2.94E–06	6.68E–06	3.20E–06	1.27E–07
Tellurium	Raw	4.59E–05	1.54E–05	1.27E–07	1.11E–06	3.14E–07	3.46E–06	3.10E–06	2.15E–05	8.74E–07
Zinc	Raw	7.30E–06	3.99E–07	1.45E–08	2.65E–08	7.47E–09	5.11E–07	5.86E–06	4.48E–07	2.94E–08
Abiotic depletation, Fossil fuels (MJ)										
Total of all compartments		128.72	15.65	0.94	19.69	1.08	23.63	16.60	42.87	8.26
Remaining substances		2.14	0.24	0.13	0.07	0.06	0.30	0.56	0.71	0.07
Coal, hard	Raw	18.52	1.77	0.16	0.76	0.16	2.65	5.41	7.03	0.57
Gas, natural/m^3	Raw	51.09	3.04	0.40	7.81	0.57	2.57	4.26	31.05	1.40
Oil, crude	Raw	56.97	10.61	0.24	11.05	0.28	18.10	6.38	4.08	6.21
Global worming potential (kg CO2 eq)										
Total of all compartments		1.07E+01	1.58E+00	7.93E–02	6.66E–01	7.68E–02	1.84E+00	1.85E+00	3.24E+00	1.40E+00
Remaining substances		3.73E–01	3.28E–02	2.14E–03	4.23E–03	7.32E–04	1.77E–02	2.12E–02	6.50E–02	2.29E–01
Carbon dioxide, fossil	Air	8.44E+00	1.02E+00	7.09E–02	5.49E–01	6.68E–02	1.66E+00	1.69E+00	2.78E+00	5.95E–01
Methane, biogenic	Air	9.69E–01	4.17E–01	5.21E–04	2.67E–03	1.86E–03	9.27E–04	4.79E–03	3.88E–02	5.03E–01
Methane, fossil	Air	9.49E–01	1.06E–01	5.70E–03	1.11E–01	7.38E–03	1.53E–01	1.37E–01	3.54E–01	7.47E–02
Ozone depletion layer (kg CFC–11 eq)										
Total of all compartments		1.88E–07	1.75E–08	2.58E–09	1.04E–08	1.04E–08	3.44E–08	2.63E–08	6.63E–08	1.99E–08
Remaining substances		1.48E–08	7.36E–10	7.11E–11	2.83E–09	7.71E–11	4.01E–09	9.90E–10	5.81E–09	2.75E–10
Methane, bromochlorodifluoro–, Halon 1211	Air	2.07E–08	5.29E–10	2.45E–10	1.65E–09	2.98E–10	2.36E–10	1.13E–09	1.61E–08	4.41E–10
Methane, bromotrifluoro–, Halon 1301	Air	8.80E–08	1.24E–08	9.03E–10	4.08E–09	8.93E–10	2.15E–08	8.91E–09	3.05E–08	8.80E–09
Methane, chlorodifluoro–, HCFC–22	Air	1.89E–08	2.26E–09	6.00E–11	2.54E–10	5.62E–11	2.74E–09	1.02E–08	2.23E–09	1.07E–09
Methane, tetrachloro–, CFC–10	Air	4.55E–08	1.55E–09	1.31E–09	1.63E–09	9.03E–09	6.00E–09	5.04E–09	1.15E–08	9.36E–09
Human toxicity (kg 1,4–DB eq)										
Total of all compartments		1.13E+01	3.14E+00	5.64E–02	2.83E–01	9.31E–02	1.98E+00	1.39E+00	3.65E+00	7.19E–01
Remaining substances		4.12E+00	7.96E–01	2.81E–02	8.05E–02	3.88E–02	1.25E+00	5.89E–01	8.74E–01	4.63E–01
Arsenic, ion	Air	2.02E+00	6.37E–01	7.31E–03	4.83E–02	1.42E–02	1.59E–01	1.69E–01	8.95E–01	8.54E–02
Chromium (VI)	Air	7.29E–01	3.30E–01	7.25E–03	5.20E–02	1.16E–02	1.22E–01	4.76E–02	1.27E–01	3.09E–02
Thallium (I)	Water	3.82E+00	1.21E+00	1.13E–02	9.19E–02	2.61E–02	3.58E–01	3.43E–01	1.70E+00	7.52E–02
Vanadium (V)	Water	6.31E–01	1.67E–01	2.40E–03	1.02E–02	2.32E–03	9.19E–02	2.38E–01	5.43E–02	6.45E–02
Fresh water ecotoxicity (kg 1,4–DB eq)										
Total of all compartments		9.34E+00	2.59E+00	5.38E–02	1.63E–01	1.55E–01	1.34E+00	1.49E+00	2.75E+00	8.10E–01
Remaining substances		8.81E–01	1.90E–01	7.43E–03	1.86E–02	6.37E–03	1.08E–01	1.24E–01	2.40E–01	1.87E–01
Beryllium (II)	Water	7.65E–01	1.30E–01	1.72E–02	2.82E–02	1.10E–01	7.14E–02	1.69E–01	2.04E–01	3.46E–02

Life cycle assessment of protein counterpart involved in the tannin–based adhesive formulation.

Substance	**Compartment**	**Total**	**Mulberry leaves**	**Paper, newsprint**	**Plastic rays**	**Chemical disinfectants**	**Transport**	**Building**	**Electricity**	**Biowaste**
Copper, ion	Water	4.96E+00	1.64E+00	9.53E–03	6.24E–02	2.15E–02	7.66E–01	3.19E–01	1.92E+00	2.26E–01
Nickel (II)	Water	9.45E–01	1.56E–01	1.28E–02	2.45E–02	1.01E–02	1.32E–01	2.02E–01	2.30E–01	1.79E–01
Vanadium (V)	Water	1.79E+00	4.75E–01	6.82E–03	2.89E–02	6.58E–03	2.61E–01	6.77E–01	1.54E–01	1.83E–01
Marine acquatic ecotoxicity (kg 1,4–DB eq)										
Total of all compartments		1.27E+04	2.32E+03	1.58E+02	3.45E+02	7.05E+02	1.53E+03	2.93E+03	3.29E+03	1.41E+03
Remaining substances		1.98E+03	4.35E+02	1.45E+01	4.46E+01	1.45E+01	2.81E+02	2.51E+02	5.98E+02	3.44E+02
Beryllium (II)	Water	4.52E+03	7.68E+02	1.01E+02	1.67E+02	6.52E+02	4.21E+02	9.99E+02	1.21E+03	2.04E+02
Copper, ion	Water	9.97E+02	3.29E+02	1.92E+00	1.26E+01	4.33E+00	1.54E+02	6.41E+01	3.86E+02	4.53E+01
Hydrogen fluoride	Air	2.82E+03	2.23E+02	2.49E+01	7.68E+01	2.15E+01	3.34E+02	8.33E+02	7.94E+02	5.16E+02
Nickel (II)	Water	6.57E+02	1.08E+02	8.92E+00	1.70E+01	7.06E+00	9.18E+01	1.40E+02	1.60E+02	1.24E+02
Vanadium (V)	Water	1.71E+03	4.55E+02	6.52E+00	2.76E+01	6.29E+00	2.49E+02	6.47E+02	1.47E+02	1.75E+02
Terrestrial ecotoxicity (kg 1,4–DB eq)										
Total of all compartments		6.91E–02	2.59E–02	1.32E–03	2.80E–03	8.27E–04	1.08E–02	6.64E–03	1.67E–02	4.18E–03
Remaining substances		1.20E–02	5.52E–03	5.63E–04	2.17E–04	6.32E–05	2.03E–03	1.08E–03	2.12E–03	4.21E–04
Arsenic, ion	Air	9.33E–03	2.95E–03	3.38E–05	2.24E–04	6.56E–05	7.38E–04	7.81E–04	4.14E–03	3.95E–04
Chromium (III)	Air	2.93E–02	1.29E–02	2.30E–04	1.89E–03	4.03E–04	4.78E–03	2.21E–03	5.42E–03	1.44E–03
Chromium (III)	Soil	5.51E–03	9.86E–04	3.58E–04	1.74E–04	1.76E–04	1.01E–03	7.43E–04	1.65E–03	4.07E–04
Mercury (II)	Air	6.84E–03	2.40E–03	5.73E–05	1.29E–04	8.02E–05	6.79E–04	1.21E–03	1.31E–03	9.75E–04
Vanadium (V)	Air	6.13E–03	1.15E–03	7.82E–05	1.65E–04	3.90E–05	1.53E–03	6.05E–04	2.02E–03	5.38E–04
Photochemical oxidation (kg C_2H_4 eq)										
Total of all compartments		2.70E–03	5.68E–04	2.14E–05	1.48E–04	1.39E–05	3.95E–04	6.12E–04	6.61E–04	2.79E–04
Remaining substances		5.26E–04	1.57E–04	3.77E–06	4.23E–05	2.03E–06	1.20E–04	6.54E–05	9.88E–05	3.63E–05
Carbon monoxide, biogenic	Air	1.41E–04	9.14E–05	4.55E–07	8.17E–07	1.81E–07	9.16E–07	6.07E–06	1.03E–05	3.13E–05
Carbon monoxide, fossil	Air	5.49E–04	7.95E–05	4.42E–06	2.34E–05	1.78E–06	9.18E–05	2.01E–04	1.02E–04	4.57E–05
Methane, biogenic	Air	2.08E–04	8.93E–05	1.12E–07	5.72E–07	3.99E–07	1.99E–07	1.03E–06	8.32E–06	1.08E–04
Methane, fossil	Air	2.03E–04	2.27E–05	1.22E–06	2.37E–05	1.58E–06	3.28E–05	2.94E–05	7.59E–05	1.60E–05
Pentane	Air	2.15E–04	1.02E–05	6.27E–07	2.18E–06	3.72E–07	2.44E–05	1.51E–04	1.73E–05	8.77E–06
Sulfur dioxide	Air	8.55E–04	1.18E–04	1.08E–05	5.53E–05	7.59E–06	1.25E–04	1.58E–04	3.49E–04	3.29E–05
Acidification (kg SO_2 eq)										
Total of all compartments		4.93E–02	6.47E–03	3.79E–04	1.90E–03	2.55E–04	5.03E–03	1.18E–02	1.16E–02	1.18E–02
Remaining substances		3.94E–06	9.60E–07	5.69E–08	2.45E–07	8.36E–08	4.12E–07	1.19E–06	6.20E–07	3.79E–07
Ammonia	Air	1.45E–02	8.93E–05	6.18E–06	2.69E–05	4.01E–06	8.10E–05	5.15E–03	3.59E–04	8.77E–03
Nitrogen oxides	Air	1.34E–02	3.44E–03	1.04E–04	4.88E–04	6.08E–05	1.84E–03	2.72E–03	2.50E–03	2.25E–03
Sulfur dioxide	Air	2.14E–02	2.94E–03	2.69E–04	1.38E–03	1.90E–04	3.12E–03	3.95E–03	8.71E–03	8.23E–04
Eutrophication (kg PO_4 eq)										
Total of all compartments		3.14E–02	1.86E–02	1.91E–04	3.46E–04	1.18E–04	1.50E–03	3.37E–03	3.02E–03	4.31E–03
Remaining substances		1.88E–03	1.04E–03	2.02E–05	1.58E–05	7.08E–06	7.68E–05	9.90E–05	1.40E–04	4.79E–04
Ammonia	Air	3.17E–03	1.95E–05	1.35E–06	5.88E–06	8.77E–07	1.77E–05	1.13E–03	7.85E–05	1.92E–03
COD (Chemical Oxygen Demand)	Water	1.64E–02	1.57E–02	9.32E–06	1.99E–05	1.15E–05	1.89E–04	1.13E–04	4.46E–05	2.66E–04
Nitrogen oxides	Air	3.49E–03	8.95E–04	2.70E–05	1.27E–04	1.58E–05	4.77E–04	7.08E–04	6.51E–04	5.85E–04
Phosphate	Water	6.55E–03	9.23E–04	1.33E–04	1.78E–04	8.23E–05	7.42E–04	1.32E–03	2.11E–03	1.07E–03

Alternative scenario

To explore potential avenues for cohesive development, two alternative scenarios are presented below. Two distinct scenarios have analyzed and compared with the base one, and the results are summarized in Table 4. Notably, Alternative Scenario 1, which entails the production and complete sale of wood chips, leads to reduced environmental impacts. A noteworthy 10% reduction in GWP is evident, attributed to the economic allocation of wood chips. Furthermore, the sale of the chips results in a significant 56% decrease in the eutrophication impact category, marking a substantial improvement compared to the base case. On the other hand, the use of a woodchip boiler to power the dryer does not seem to lead to environmental benefits; in fact, alternative scenario 2 shows no particular advantages over scenario 1. Indeed, the energy demand for the dehydration of silk cocoons is low, quantified at 0.104 kWh for kg of cocoons. This quantity pales in comparison to the overall energy potential inherent in the wood waste generated throughout the process. Consequently, establishing a furnace for the sole purpose of generating such a limited amount of energy is deemed non–advantageous.

Table 4. LCA results for the Base Case and Alternative Scenarios. Scenario 1 includes chipping of wood waste and sale of wood chips in the Italian market; Scenario 2 includes using wood chips to dry the cocoons and sale of the leftover wood chips.

%	**Base scenario**	**Alternative scenario 1**	**Alternative scenario 2**
Abiotic depletion (kg Sb eq)	1.208E–4	1.148 E–4 (↓5.0)	1.1490 E–4 (↓4.9)
Abiotic depletion, Fossil Fuels (MJ)	128.7	119.9(↓6.8)	120.3(↓6.5)
Global warming (kg CO_2eq)	10.7	9.7 (↓10)	9.7 (↓9.7)
Ozone layer depletion (kg CFC–11 eq)	1.8E–07	1.7–07 (↓7.1)	1.8–07(↓6.1)
Human toxicity (kg 1,4–DB eq)	11.3	10.5 (↓7.4)	10.5(↓7.1)
Fresh water aquatic ecotoxicity (kg 1,4–DB eq)	9.3	8.7(↓7.1)	8.8 (↓6.0)
Marine aquatic ecotoxicity (kg 1,4–DB eq)	12694.2	11328.9(↓10.8)	11948.4 (↓5.9)
Terrestrial ecotoxicity (kg 1,4–DB eq)	0.0691	0.0599(↓13.4)	0.0604 (↓12.7)

Photochemical oxidation (kg C_2H_4 eq)	0.00270	0.00229(↓15.4)	0.00230 (↓15.1)
Acidification (kg SO_2 eq)	0.0493	0.0459 (↓6.8)	0.0460 (↓6.7)
Eutrophication (kg PO_4eq)	0.0314	0.0139(↓55.7)	0.0140 (↓55.5)

Moreover, in a recent research conducted by CREA the potential of utilizing undigested mulberry leaves as a renewable source for bioethanol production has been underscored. Remarkably, research has revealed an impressive yield of approximately 50% from mulberry leaves for biofuel production, exhibiting superior characteristics when compared to other plant species such as panicum, poplar, or thistle [21]. In alignment with sustainable practices, the utilization of biowaste for bioethanol production presents a prospective avenue to mitigate the environmental impacts associated with waste disposal. However, the absence of suitable models in SimaPro 9.5 and the unavailability of primary production data poses a significant challenge, further complicating the development of a comprehensive model to understand the actual environmental benefits. Nevertheless, it is imperative to underscore the theoretical viability of this prospect, particularly noting that the wet biowaste generated per dry kilogram of cocoons is estimated to be approximately 22 kilograms. Further research and data acquisition are warranted to substantiate the potential environmental advantages inherent in this proposed bioethanol production approach.

Discussion

As previously discussed, silk fiber has been categorized as having a notable environmental impact, surpassing even prominent synthetic and natural fibers [14],[15]. For centuries, silk fibers have been celebrated for their traditional uses. However, in recent times, the spotlight has shifted towards the extraordinary chemical and physical properties inherent in its primary protein, fibroin. This versatile substance is now emerging as a key player in diverse fields, with a notable impact in the realm of biomedical applications [10]. Numerous research efforts have paved the way for the creation of innovative fibroin–based materials, showcasing their intelligence and adaptability across various domains [22],[23]. This newfound recognition is steering the trajectory of silk from a historical luxury to a cutting–edge material with promising implications for the future. Hence, a reassessment of the predominant benefits associated with this material is warranted, along with a comprehensive review of the entire supply chain. The adoption of animal–derived alternative proteins, such as fibroin, has emerged as a strategy to explore bioresource alternatives within the biomaterials domain, specifically in comparison to soy protein which is often proposes as building block for biomaterials. While the environmental impact of one kilogram of both proteins favors soy protein [24],[25], it is important to acknowledge the presence of various assumptions in this comparison. Firstly, comparing LCA studies can be challenging and may not always be fully representative. For instance, Dalgaard et al. note that the production impact of one kilogram of soy protein is equivalent to 0.3 kg of CO_2 eq in terms of global warming potential [24]. Differently, Zhang et al. reported a value ten times higher for the production of 1 kg of soybeans, highlighting a value of 3.33 kg of CO_2 eq. [25]. These differences can be explained by several factors that characterize LCA studies such as the choice of model, system boundaries, assumptions, limitations and finally the type of study, such as attributional or consequential. However, although these values differ from each other by a factor of 10 for the GPW impact category, both are lower than what was highlighted in the present study, where a value of 10.7 kg of CO_2. Nevertheless, it is imperative to take into account supplementary factors. With the global population steadily increasing and heightened apprehensions regarding the scarcity of primary resources, there is a growing skepticism towards the predominant utilization of materials, particularly within the agrifood industry. In addition, environmental impact studies concerning silk often overlook the allocation of by–products within the supply chain, notably pupae and sericin – the secondary protein within cocoons. Pupae, rich in nutritional value, could find application in agribusiness feeds [26],[27], while sericin already boasts various uses, such as in cosmetics [8]. Proper allocation of these by–products has the potential to mitigate the overall environmental impact associated with silk production. Furthermore, the expanding utilization of these materials beyond the high fashion industry opens up the possibility of enhancing silkworm productivity. This is because the fibers, being dissolved in a solution, alleviate the necessity for high cocoon quality, thereby reducing production waste.

Obtaining an objective comparison between different bioresources, such as soy and silk proteins, is currently challenging. This complexity arises also from the varied treatments that their raw materials undergo before being employed in the formulation of biomaterials. Delving deeper into the primary focus of this doctoral thesis, compelling evidence was presented showcasing the efficacy of fibroin as a supplementary component in wood adhesives. In particular, in our previous study, silk fibroin solution was applied as an additive within tannin–based adhesives for wood products so as to enhance their properties. It has been studied how low amounts of the protein are able to greatly increase the properties of the woody joint, especially in a humid environment. Indeed, the introduction of approximately 5 % by weight of silk to the overall tannin solid content of the formulation proves highly effective in significantly enhancing the adhesive's properties.

In this context, Arias et al. [28] have highlighted the attractive attributes of tannin–based adhesives in comparison to both other bioresources and synthetic resins. The authors assert that tannin–based resin not only shows a comparable or even lower overall environmental impact (as indicated by the final single score) than well–known synthetic resins such as UF, PF, and MUF, aligning with findings by Yang M. and Rosentrater as well [29], but also exhibits significantly lower values compared to adhesives based on lignin. While similar impacts were pointed out between tannin and soy protein–based adhesives [28]. Therefore, it is noteworthy that the incorporation of low quantities of fibroin has led to a significant enhancement in the properties of the resin, and might open to the new utilization of this bioresource in a wise way.

Conclusion

LCA methodology, has uncovered intriguing insights into the potential of this hypothetical industry. The notion of revitalizing the cocoon industry stems from the remarkable properties that can be harnessed from their protein components, extending beyond their current primary application in the fashion sector. The concerted efforts undertaken by CREA and various farmers are aimed at resurrecting a market that has been abandoned for decades. It is important to note that the results presented here pertain to a small–scale operation, characterized by limited production, and a lack of exclusive dedication to the business market. Consequently, when interpreting the environmental impact analysis of such a scenario, one must exercise caution due to the reliance on several assumptions. While it remains challenging to comprehensively quantify the environmental impact of the protein, considering all by–products and waste within the intricate supply chain, the potential of this material in the realm of wood bio–based adhesives remains affirmatively promising. Particularly noteworthy is its advantageous application in tannin–based resins, which have demonstrated environmental benefits compared to both other bioresources, like several kind lignin, and synthetic resins. Through the implementation of sustainable agriculture and non–intensive practices, the relative environmental impact of silk cocoons is notably lower, even within a supply chain that is still in its early stages of development. However, while providing specific numerical values proves challenging due to variations in model specifications across various LCA studies, this model distinctly showcases a substantial reduction across all impact categories compared to the existing literature. The study also illustrated that utilizing simple woody biomass in wood chip production can lead to a reduction across all impact categories, particularly notable for GWP, photochemical oxidation, and eutrophication. Additionally, significant preliminary findings underscore the potential utilization of the produced biowaste as a valuable resource for bioethanol production. However, future studies remain imperative to achieve a reliable final results.

References

1. Cherubini, F.; Strømman, A. H. Bioresource Technology Life Cycle Assessment of Bioenergy Systems : State of the Art and Future Challenges. Bioresour. Technol. **2011**, 102 (2), 437–451. https://doi.org/10.1016/j.biortech.2010.08.010.

2. Rajagopalan, N.; Bilec, M. M.; Landis, A. E. Life Cycle Assessment Evaluation of Green Product Labeling Systems for Residential Construction. **2012**, 753–763. https://doi.org/10.1007/s11367–012–0416–9.

3. Glassner, D. A.; Gruber, P. R.; Vink, E. T. H.; Ra, K. R. Applications of Life Cycle Assessment to NatureWorks TM Polylactide (PLA) Production. **2003**, 80, 403–419. https://doi.org/10.1016/S0141–3910(02)00372–5.

4. British Standards. BSI Standards Publication Environmental Management — Life Cycle Assessment — Principles and Framework BS EN ISO 14040:2006+A1:2020. Br. Stand. 2006.

5. British Standards. BSI Standards Publication Environmental Management — Life Cycle Assessment — Principles and Framework BS EN ISO 14044:2006+A2:2020. Br. Stand. 2006.

6. Barcelos, S. M. B. D.; Salvador, R.; da Graça Guedes, M.; de Francisco, A. C. Opportunities for Improving the Environmental Profile of Silk Cocoon Production under Brazilian Conditions. Sustain. **2020**, 12 (8). https://doi.org/10.3390/SU12083214.

7. Astudillo, M. F.; Thalwitz, G.; Vollrath, F. Life Cycle Assessment of Silk Production–a Case Study from India; Elsevier Ltd, 2015. https://doi.org/10.1016/B978–0–08–100169–1.00011–3.

8. Altman, G. H.; Farrell, B. D. Sericulture as a Sustainable Agroindustry. Clean. Circ. Bioeconomy 2022, 2, 100011. https://doi.org/10.1016/j.clcb.2022.100011.

9. Madhana, K.; Kanubothula, S.; Reddy, S. Amelioration of Drought–Induced Negative Responses by Elevated - CO 2 in Field Grown Short Rotation Coppice Mulberry (Morus Spp .), a Potential Bio–Energy Tree Crop. Photosynth. Res. **2017**, 132 (2), 151–164. https://doi.org/10.1007/s11120–017–0351–5.

10. Nguyen, T. P.; Nguyen, Q. V.; Nguyen, V.; Le, T.; Le, Q. Van. Silk Fibroin–Based Biomaterials for Biomedical. *Polymers (Basel).* **2019**, *11*, 1–25. https://doi.org/doi:10.3390/polym11121933

11. Koh, L.; Cheng, Y.; Teng, C.; Khin, Y.; Loh, X.; Tee, S.; Low, M.; Ye, E.; Yu, H.; Zhang, Y.; Han, M. Structures, Mechanical Properties and Applications of Silk Fibroin Materials. Prog. Polym. Sci. **2015**, 46, 86–110. https://doi.org/10.1016/j.progpolymsci.2015.02.001.

12. Valentini, L.; Ceccarini, M. R.; Verdejo, R.; Tondi, G.; Beccari, T. Stretchable, Bio–Compatible, Antioxidant and Self–Powering Adhesives from Soluble Silk Fibroin and Vegetal Polyphenols Exfoliated Graphite. Nanomaterials **2021**, 11 (9). https://doi.org/10.3390/nano11092352.

13. Hăbeanu, M.; Gheorghe, A.; Mihalcea, T. Silkworm Bombyx Mori—Sustainability and Economic Opportunity, Particularly for Romania. Agriculture **2023**, 13 (6), 1209. https://doi.org/10.3390/agriculture13061209.

14. Astudillo, M. F.; Thalwitz, G.; Vollrath, F. Life Cycle Assessment of Indian Silk. J. Clean. Prod. **2014**, 81, 158–167. https://doi.org/10.1016/j.jclepro.2014.06.007.

15. Gonzalez, V.; Lou, X.; Chi, T. Evaluating Environmental Impact of Natural and Synthetic Fibers: A Life Cycle Assessment Approach. Sustain. **2023**, 15 (9). https://doi.org/10.3390/su15097670.

16. Barcelos, S. M. B. D.; Salvador, R.; Barros, M. V.; de Francisco, A. C.; Guedes, G. Circularity of Brazilian Silk: Promoting a Circular Bioeconomy in the Production of Silk Cocoons. J. Environ. Manage. **2021**, 296 (April), 113373. https://doi.org/10.1016/j.jenvman.2021.113373.

17. PRé Consultants (2015) SimaPro 9.5 [Computer Software]. PRé Consultants, The Netherlands.

18. Mano, F. Biomimetic Approaches for Biomaterials Development; Wiley-VCH Verlag GmbH & Co. KGaA, Ed.; 2012.

19. Ecoinvent. Allocation Cut–Off by Classification. 2019. Available online: http://www.ecoinvent.org/database/ system–models–in–ecoinvent–3/cut–off–system–model/allocation–cut–off–by–classification.html (accessed on 24 November 2023).

20. AIEL. https://www.aielenergia.it/pubblicazioni–agriforenergy (accessed on November 2023)

21. CREA. Relazione Finale Progetto Biosegen – Unità Di Ricerca Di Apicoltura e Bachicoltura.

22. Ciabattini, S.; Raggi, V.; Valentini, L.; Morabito, A. Silk Fibroin Hybrids for Biological Scaffolds with Adhesive Surface and Adaptability to the Target Tissue Change. Eurobiotech J. **2023**, 7 (1), 75–86. https://doi.org/10.2478/ebtj–2023–0005.

23. Ceccarini, M. R.; Palazzi, V.; Salvati, R.; Chiesa, I.; Maria, C. De; Bonafoni, S.; Mezzanotte, P.; Codini, M.; Pacini, L.; Errante, F.; Rovero, P.; Morabito, A.; Beccari, T.; Roselli, L.; Valentini, L. Biomaterial Inks from Peptide–Functionalized Silk Fibers for 3D Printing of Futuristic Wound–Healing and Sensing Materials. **2023**, 24, 947.

24. Dalgaard, R.; Schmidt, J.; Halberg, N.; Christensen, P.; Thrane, M.; Pengue, W. a. LCA for Food Products: Case Study LCA of Soybean Meal. LCA Food Prod. **2008**, 10 (7), 240–254.

25. Zhang, Q.; Hong, J.; Zhang, T.; Tian, X.; Geng, Y.; Chen, W.; Zhai, Y.; Liu, W.; Shen, X.; Bai, Y. Environmental Footprints of Soybean Production in China. Environ. Dev. Sustain. **2023**, 25 (9), 9047–9065. https://doi.org/10.1007/s10668–022–02424–1.

26. Sadat, A.; Biswas, T.; Cardoso, M. H.; Mondal, R.; Ghosh, A.; Dam, P.; Nesa, J.; Chakraborty, J.; Bhattacharjya, D.; Franco, O. L.; Gangopadhyay, D.; Mandal, A. K. Silkworm Pupae as a Future Food with Nutritional and Medicinal Benefits. Curr. Opin. Food Sci. **2022**, 44. https://doi.org/10.1016/j.cofs.2022.100818.

27. Karnjanapratum, S.; Kaewthong, P.; Indriani, S.; Petsong, K.; Takeungwongtrakul, S. Characteristics and Nutritional Value of Silkworm (Bombyx Mori) Pupae–Fortified Chicken Bread Spread. Sci. Rep. **2022**, 12 (1), 1–12. https://doi.org/10.1038/s41598–022–05462–x.

28. Arias, A.; González–García, S.; González–Rodríguez, S.; Feijoo, G.; Moreira, M. T. Cradle–to–Gate Life Cycle Assessment of Bio–Adhesives for the Wood Panel Industry. A Comparison with Petrochemical Alternatives. Sci. Total Environ. **2020**, 738, 140357. https://doi.org/10.1016/j.scitotenv.2020.140357.

29. Yang, M.; Rosentrater, K. A. Life Cycle Assessment of Urea–Formaldehyde Adhesive and Phenol–Formaldehyde Adhesives. Environ. Process. **2020**, 7 (2), 553–561. https://doi.org/10.1007/s40710–020–00432–9.

4.4 Chemical investigation of polyphenolic wood extractive.

4.1.1 Chemical characterization of cherry (*Prunus avium*) extract in comparison with commercial mimosa and chestnut tannins

Emanuele Cesprini, Alberto De Iseppi, Samuele Giovando, Elisa Tarabra, Michela Zanetti, Primož Šket, Matteo Marangon, Gianluca Tondi.

The work has published as:

Cesprini E., De Iseppi A., Giovando S., Tarabra E., Šket P., Zanetti M., Marangon M., Tondi G. Chemical characterization of cherry (Prunus Avium) extract in comparison with commercial mimosa and chestnut tannins. Wood Science and Technology (2022), 56, 1455–1473, https://doi.org/10.1007/s00226–022–01401–1

Abstract

In a growing context of green and circular economy, gaining knowledge of the com– position of every crop is crucial, as this will allow for their full exploitation. Cherry (*Prunus avium* L.) is a widespread tree of particular interest for its fruits and its valuable timber. Its wood is rich in extractives and its characterization will allow to consider other applications for this feedstock. In this study, chipped cherry wood was extracted and chemically analyzed to determine its total phenolic content, total condensed tannin, antioxidant capacity, and polysaccharide content through wet chemistry analysis. These investigations were coupled with 13C–NMR and FTIR spectrometry, with HPLC as well as elemental analysis to conduct a comprehensive chemical characterization. Thermogravimetric measurements were also taken to understand the behaviour of the extract when exposed to high temperature. The registered findings were benchmarked against commercial mimosa (*Acacia mearnsii* De Wild.) and chestnut (*Castanea sativa* Mill.) tannins which were selected as template for condensed and hydrolysable tannins, respectively. Cherry extract was found to be the poorest in phenolics which are mainly constituted of pyrogallic flavonoids strongly interconnected with significant amounts of polysaccharides.

Introduction

Tannins are natural polyphenolic substances produced by plants to protect from UV, free–radicals and biological decay agents such as animals, insects, fungi and bacteria [1]. These compounds can be easily extracted from wood and commercially exploited for different purposes [2],[3]. Historically, the first application of these extracts is leather tanning [4]. Nowadays, the tannin extract is industrially extracted and it is mostly used to obtain vegetable–tanned leather [5]. The high affinity of the polyphenolic structure of tannins with collagen, the skin's main protein, allows an irreversible change in structure resulting in an excellent leather's stability. Soon, the critical protective abilities offered by tannins were also exploited in the medical field, thus benefiting from their antioxidant and free radical scavenger capabilities, inhibiting low–density lipoprotein oxidation [6]. In addition, the complexing properties of tannins can also be exploited in water remediation by trapping heavy metals [7]. Another widespread application is in food industry. In particular, tannins are key constituents in popular beverages as tea and coffee, of fruit juices, and of alcoholic beverages as beer and wine [8],[9]. Tannins are also present in significant quantities in distillates aged in wooden barrels such as brandy, whiskey, grappa and cognac [10]. In the case of wine, tannins are extracted from grapes and play a major role in wine quality as they contribute to color, mouthfeel, stability, and longevity. Given their importance, especially for red wines, winemakers adopt processing techniques suitable to enrich the wine in tannins, for example by extending the skin maceration step, by adding tannin extracts to the wines [11], or by ageing the wines in barrels made with different wood types. The most common wood used to produce barrels for wine ageing is oak, even if wood species as chestnut and cherry, the subject of this study, are also used. In winemaking, different wood types contribute differently to the ageing kinetic, to the type and amount of tannins released into the wines, and to the wine flavor [12], so that wood contact is used also as a tool to modify the sensorial properties of the wines. A similar approach is adopted in the production of Italian balsamic vinegar, where the aging in cherry barrels is part of the traditional production method [13]. In these contexts, cherry wood exhibits high potentiality as it confers a distinctive flavor to the product [14],[15]. Considering the increasing sensibility for producing sustainable and renewable materials, tannins are increasingly attracting the interest of other engineering sectors. While their use as adhesives for wood is known since the middle of the last century [16],[17] their application as wood preservative is more recent[18],[19] and both are suggestive alternative to synthetic plastics and coatings [20]. In the last decade, other engineered materials were produced from tannins: Insulating foams have attracted the interest of green building construction[21],[22], furanic bio–based plastics were successfully produced [23] and also ultralight aerogels were synthesized [24],[25].

Tannins are mainly divided into condensed and hydrolysable, these having different chemical structures and consequently, different properties. The former consists of flavonoid oligomers/polymers with a variable degree of polymerization [26]. The units are usually linked C4 to C6 or C4 to C8 to form various length chains depending on the type of tannin [27]. Hydrolysable tannins are esters of phenolic acids such as gallic, ellagic or more complex tryaril acids with easy sugars such as glucose and xylose [28]–[30].

Therefore, these families have different physical and chemical properties and are used industrially according to the characteristics required for the specific use, it is of fundamental importance to clarify the class to which a tannin extract belongs to direct its possible employment.

In this study, the cherry (Prunus avium L.) tannin extract is compared with two commercial tannin extracts. That of mimosa bark (Acacia mearnsii De Wild.) is taken as reference for condensed tannins [31] while the extract of chestnut wood (Castanea sativa Mill.) as the reference for the hydrolysable ones [32]. Wet analytical chemical experiments, spectroscopic (13C–NMR and ATR FT–IR), elemental and thermal analyses (TGA) were applied to characterize the three extracts.

Experimental

Materials

Debarked cherry (*Prunus avium* L.) wood chips at 10% moisture content were provided by Silva Team (San Michele Mondovì, Italy). Industrial tannin powders of chestnut (*Castanea sativa* Mill.) and mimosa (*Acacia mearnsii* De Wild.) were supplied by Saviolife (Viadana, MN, Italy) and Silva Team (S. Michele Mondovì, CN, Italy) respectively, and were used as benchmark respectively for hydrolysable and condensed tannin in the investigation of the cherry extract. High purity (≥99%) ethanol, sodium carbonate, sulphuric acid, sodium acetate trihydrate, acetic acid, 2,4,5–tripyridyl–s–triazine, HCl, ferric chloride, ammonium formate, pectin, and dextran were purchased from Sigma–Aldrich (St. Louis, MO, USA). Folin–Ciocalteu's phenol reagent and vanillin were purchased by Merck (Darmstadt, Germany).

Equipment

The following equipment was used to perform extraction and characterization of the extracts: Spectroscopic investigation were carried out with a Varian Cary 50 Bio UV–Visible spectrophotometer; the solid state NMR was performed with a Bruker AVANCE NEO 400 MHz NMR tool equipped with 4 mm CP–MAS probe while the FT–IR analysis were done on a Nicolet, NEXUS, B70, FT–IR instrument set up with ATR unit. The chromatography analysis were performed in Agilent 1260 series II quaternary pump LC (Agilent Technologies) equipped with G7162A refractive index detector (RID) and G117C diode array detector (DAD). The separation was carried out using a gel permeation HPLC column (PL–Aquagel–OH, Agilent). Thermo Fischer Scientific FLASH 2000 element analyzer equipped with MAS 200 R autosampler thermal conductivity detector (TCD), and two analytical chromatographic columns was used for elemental investigation. The thermal behavior of the extracts was investigated with an SDT 2960 Simultaneous DSC–TGA TA instrument (Waters – TA instruments, New Castle, DE, USA)

Methods

Extraction of cherry tannin powder

The cherry extract was obtained by a double extraction of the wood chips with boiling water maintained in temperature with an external heather. Firstly, 250 g of chips were extracted with 1,500 g of deionized water for 1 h. The suspension was filtered and then the wet chips were further extracted using additional 1000 g of boiling water for 1 h. This second suspension was also filtered and the two brown solutions obtained were then evaporated until dry in a rotavapor at 70 °C and the remaining dry brown powder was collected and characterized.

Purification of the tannin extracts

The three tannin powders were submitted to a preliminary extraction to remove impurities. The process involved the dissolution of 100 mg of the three tannin powders in 5 mL of EtOH / H_2O (80/20 v/v), followed by mechanical stirring for 30 minutes at 25°C. The samples were then centrifuged for 15 minutes at 4°C and 10,000 rpm, and the supernatants analyzed to assess their antioxidant capacity, as well as their content in total polyphenols, condensed tannins, and polysaccharides. This procedure was similar to that presented by [33].

Total polyphenol content

Determination of total phenolic content (TPC) was performed using the Folin–Ciocalteu assay [34]. In brief, 1 ml of diluted tannin extract, 1 ml of Folin reagent (Sigma–Aldrich) (diluted 1:10 with deionized water), and 0.8 ml of sodium carbonate solution (7.5 %) were added. The mixture was left in the dark at 40 °C. After 30 minutes the absorbance was read at 765 nm. Each measurement was repeated three times. The calibration curve was created with a serial dilution of gallic acid.

Total condensed tannin

The transformation of condensed tannin into anthocyanidols under the presence of sulphuric acid and vanillin allows to calculate the concentration of total condensed tannins (TCT) [35]. In brief, 50 µl of the ethanol tannin solution (1 $mg \cdot ml^{-1}$) were added to 2 ml of 4% methanol vanillin solution and 450 µl concentrated sulphuric acid. After 15 min, the absorbance was read at 527 nm and the results were expressed as relative ratio of equivalent catechin ($\mu gC \cdot mg^{-1}$).

Antioxidant capacity

FRAP assay was performed for determination of the extracts' antioxidant capacity [36]. FRAP reagent was prepared by mixing 25 ml of 0.3 M sodium acetate buffer (pH 3.6), 2.5 mL of 10 mM 2,4,5–tripyridyl–s–triazine HCl solution, and 2.5 ml of 20 mM ferric chloride. In brief, 100 µl of EtOH/H2O tannin extract were added to 990 µl FRAP reagent. After incubation (37°C, 30 min), the absorbance was measured spectrophotometrically at 593 nm. The FRAP values were expressed in µg of ascorbic acid equivalents (AAE)$\cdot mg^{-1}$ tannins.

13C–NMR solid state

Solid–state 13C–NMR experiments of the three tannin extracts were performed on a Bruker AVANCE NEO 400 MHz NMR spectrometer using a 4 mm CP–MAS probe. The sample spinning frequency was 15 kHz. The 13C CP–MAS NMR experiments consisted of excitation of protons with p/2 pulse of 3.0 s, CP block of 2 ms, and signal acquisition with high–power proton decoupling. A total of ca. 2,000 to 14,000 scans were accumulated with the repetition delay of 5 s. The chemical shifts were referenced externally using adamantine. This analysis was lead applying methodology [37].

FT–IR ATR spectroscopy

The FT–IR ATR spectra of the tannin powders were acquired with 32 scans from 4,500 to 600 cm^{-1}, focusing the investigation between 1,800 and 600 cm^{-1}. This analysis was conducted according to [38] The spectra were normalized, and baseline corrected with the software OriginPro 8.5.0 SR1.

Determination of polysaccharides by High–resolution size–exclusion chromatography (HRSEC)

The polysaccharides' quantity and molecular distribution were measured by analyzing the tannin powders' extracts by HRSEC [39],[40]. Briefly, 1 mg of sample was dissolved in 1 mL of running buffer (50 $mmol \cdot l^{-1}$) aqueous solution ammonium formiate), and sterile filtered (0.22 µm acetate cellulose filters, Millipore) directly into HPLC glass vials. Then, 10 µl were injected into the chromatographic system. Samples were held at 4°C prior to injection in a temperature controlled auto–sampler. The separation was carried out at 20°C using a gel permeation HPLC. The mobile phase was applied at a constant flow of 0.6 ml/min for 35 min, and the temperature of the RID cell was kept at 35°C. The molecular weight distribution of the extracts' polysaccharides was identified using a qualitative calibration curve made with 10 pullulan standards (Merk) at MW ranging between 342 and 805,000 Da, while pectin and dextran were used in the range between 0 and 2 g/l to create the calibration curve for polysaccharide quantification.

Thermogravimetry (TGA)

The thermal behavior of tannin samples was investigated during heating through a temperature ramp of 10 °C/min up to 800°C. The percentage weight loss of the samples as a function of temperature was then recorded. The tests were carried out in an inert environment with a flow of nitrogen. The first derivative (DTGA) of the thermograms was calculated to highlight the degradation peaks. Experiment and elaboration were done according to the method of [41].

Organic Elemental Analyzer "OEA"

The atomic composition of Carbon, Hydrogen, Nitrogen, Sulphur of the tannin powders was investigated. The Eager Xperience software was used for data analysis. Experiment and elaboration were done according recent work. [42]

Statistical analysis

Statistical analyses were performed using OriginPro 8.5.0 SR1 software (OriginLab Corp., Northampton, MA, USA). One–way Analyses of Variance (ANOVA) followed by post–hoc Tukey test ($p \leq 0.05$) were used to ascertain significant difference within mean values.

Results and Discussion

Chemical analysis

The cherry extract obtained from the extraction process presented a yield of 3% of dry extract on dry raw material. The quantification of the total phenolic content (TPC), total condensed tannins (TCT), antioxidant capacity (FRAP), and polysaccharide content (PS) of the three tannin extracts is shown in Table 1.

Table 1. Total phenolic content, total condensed tannins, antioxidant capacity and polysaccharide fraction of the three extracts.

Parameters	Cherry	Mimosa	Chestnut
TPC (µg GAE·mg^{-1})	342^{a}	630^{b}	608^{b}
TCT (µg CE·mg^{-1})	208^{a}	260^{b}	27^{c}
FRAP (µgAAE·mg^{-1})	490^{a}	940^{b}	1950^{c}
PS (mg·l^{-1})	899^{a}	477^{b}	411^{b}
PS/TPC ratio	2.62	0.76	0.67

Note: Different letters indicate significant differences at $p \leq 0.05$ by analysis of variance (ANOVA) and Tukey's test

Mimosa and chestnut extracts contained comparable amounts of total polyphenols, with values that are in line with those reported in previous studies [35],[43]. Unsurprisingly, mimosa extract contained about 10 times more condensed tannins than chestnut, a finding in agreement with the literature as chestnut extracts mostly contain hydrolysable tannins [31],[32]. The cherry extract contained a significantly lower amount of phenolic compounds than mimosa and chestnut (<45%), but with a condensed tannin amount closer to that of mimosa, thus suggesting a strong flavonoid nature of its tannins. The antioxidant activity of the cherry extract is around half of that of mimosa, an occurrence attributable to its lower phenolic content. Indeed, different studies report a linear correlation between antioxidant capacity and TPC [44],[45], and this is in agreement with our findings. The chestnut extract shows the highest antioxidant capacity confirming the findings of a recent study where it was compared with quebracho using Trolox as reference [46]. The fact that mimosa and chestnut extracts have similar total phenolic content but very different antioxidant activities suggest that hydrolysable tannins have significantly more antioxidant activity than the condensed ones [47]. The lower amount of phenolics of condensed class, explain the limited antioxidant activity of the cherry extract. The HRSEC analysis of the three extracts allowed to determine their total polysaccharides' content. The cherry extract exhibited the largest concentration in polysaccharides containing 88.5% more polysaccharides than Mimosa, and 118.6% more polysaccharides than the chestnut extract. The chemical profile of the cherry extract was very different than the other two. Indeed, the ratio PS/TPC for cherry was almost 4 times higher than mimosa and chestnut, a value that contributes to justify the lower antioxidant capacity measured for cherry extract.

Elemental analysis

The elemental analysis of the three tannin powders is presented in table 2.

Table 2. Elemental analysis of cherry, mimosa and chestnut extracts

Elements (%)	Cherry	Mimosa	Chestnut
C	47.24	51.19	45.99
H	5.62	5.27	4.45
N	0.34	0.38	0.16

Condensed tannins are generally richer in carbons than the hydrolysable ones [48], but the significative carbohydrate fraction in the cherry extract contributes to decrease the carbon fraction almost at the level of chestnut. Small amounts of nitrogen were detected, probably due to fixed proteins, while no sulphur was registered confirming that the industrial extracts were obtained by simple water extraction.

Solid state 13C NMR spectroscopy

The 13C NMR spectra of the three tannin extracts is reported in Fig.1. These spectra can be analysed dividing the spectral field into four main regions, based on the chemical shift of the different bondings:

- 190 – 135 ppm: signals due to Carom directly linked to oxygen;
- 135 – 90 ppm: signals due to Carom not directly bound to oxygen;
- 90 – 50 ppm: signals due to Caliph directly bound to oxygen;
- 50 – 10 ppm: signals due to Caliph not directly bound to oxygen.

Comparing the NMR spectra of cherry with the other two, there are two observations that shine: i) The region between δ 90 and 60 ppm is very prominent and ii) the region between δ 190 and 135 ppm is very similar to that of mimosa. These two findings are in line with the results of the wet chemistry tests: cherry extract results richer in polysaccharides and the polyphenolics principally belong to the condensed tannin family. Focusing on the low field chemical shifts, the differences between the classes of condensed (mimosa) and hydrolysable (chestnut) tannins are already visible. At δ 168 ppm, chestnut shows the peak due to the carbonyl group of gallic acid. 13C NMR spectra of mimosa and cherry in the range between δ 170 to 180 ppm show lower absorption rates. This spectral area can be divided into two sub–areas: δ 180–177 ppm, typical of the presence of quinone structure, due to phenolic hydroxyl oxidation and between δ 170–176 ppm, where the carbonyls of catechin/epicatechin gallate resonate[49].

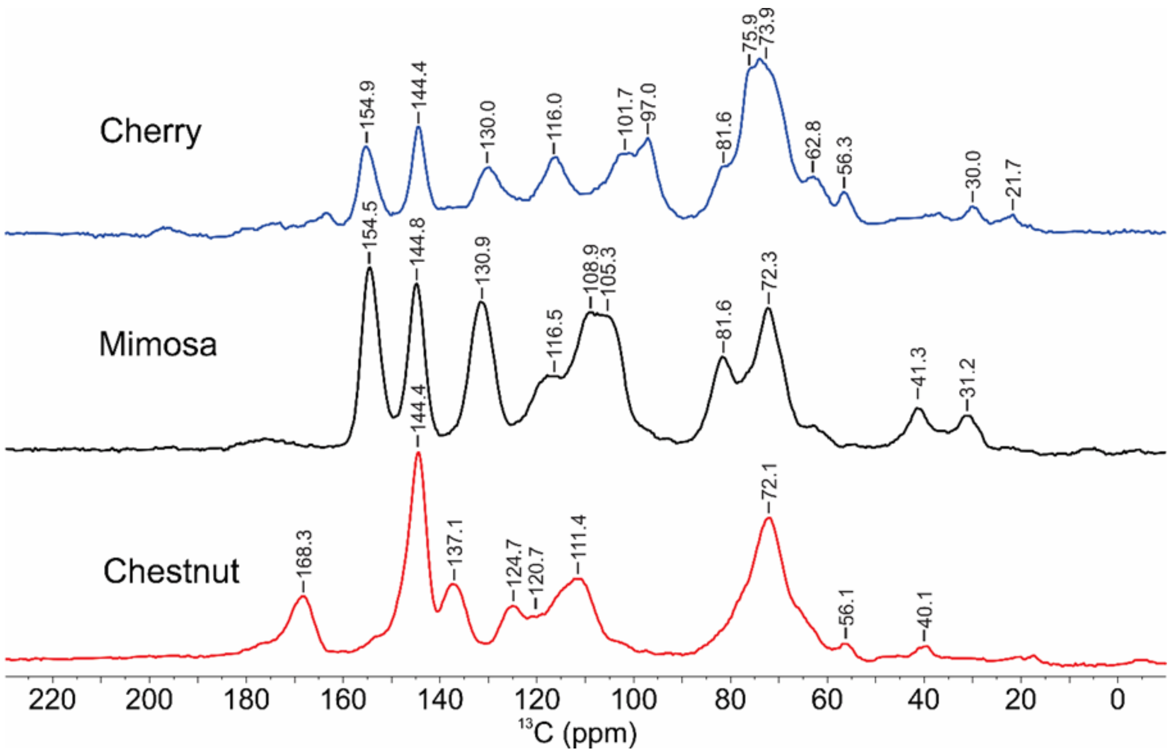

Figure 1. 13C NMR spectra of cherry, mimosa and chestnut extracts.

In the area between 200 and 190 ppm typical for aldehydes, weak signals are observable for cherry. We attribute this signal to: i) small amount of galloylated catechin, ii) possible oxidized or open forms of sugar portion. Between δ 160 and 140 ppm signals characteristic of the Carom–O bond occurs. The 13C NMR spectra of mimosa and cherry show two signals at δ 154 and δ 144 ppm attributed to the C–OH of the two rings (A– and B– ring of the flavonoid [50],[51]. The intensity of these two peaks is inverse between the two tannins. From the relative area integration, assigning the value 1 for both spectra to the signal at δ 154 ppm, the integral of the signal at δ 144 ppm is 1.195 for the cherry whereas 0.841 was obtained for the mimosa. This can be explained by the different classes of anthocyanin that constitutes the two extracts. Mimosa tannin typically consists of cyanidins with a greater number of phenolic groups on the A ring, such as catechin, epicatechin or epiafzelechin, while cherry has flavonoids with a greater number of Carom–O bonds on the B ring, such as epicatechin gallate, epigallocatechin, mesquitol or robinetidin. Conversely, chestnut spectrum presents signals at 144 and 137 ppm attributed to Carom–O of the gallic moieties (C3/C5 and C4, respectively).

In the area of the spectrum between δ 135 and 90 ppm other interesting features could be highlighted. C1' and C5' of the B–ring of flavonoids resonate at δ 130 and 116 ppm respectively [52], and visible for cherry and mimosa. Moving towards lower chemical shift, signals of cherry tannin appears to be shifted to higher fields than from mimosa. These shifts could be due to a less cross–linked structure [53]. In particular, mimosa shows two peaks which falls between 105 and 95 ppm while for cherry the absorption is among δ 100 and 90 ppm. The two signals occurring at higher frequencies are due to the interflavonoid bonds C4–C8 and C4–C6, while the ones at lower frequencies can be assigned to unreacted C6, C8, C10 [51],[54]. Cherry tannin shows the signal relative to unreacted carbons with higher intensity. Conversely, Mimosa's signals between δ 90 and 50 ppm can be assigned to the C2 and C3 of the A–ring of the flavonoids [55], but this region is also dominated by carbohydrate absorptions. In this case, the relative signal intensity for cherry tannin is much higher than for the other two samples. This is due to a higher presence of carbohydrates whose carbons resonate in this spectral area [51]. Another identifying marker for the sugar portion of cherry tannin is the signal at around δ 56 ppm [49], which is also present for chestnut, which has a glycosidic units in its structure [51],[56].

ATR FT–IR spectroscopy

The ATR FT–IR spectroscopy was also applied as it is an effective technique to investigate tannin extracts. The region of greatest interest for investigating these compounds is from 1800 to 600 cm^{-1}. Figure 2 shows the three spectra of tannin powders.

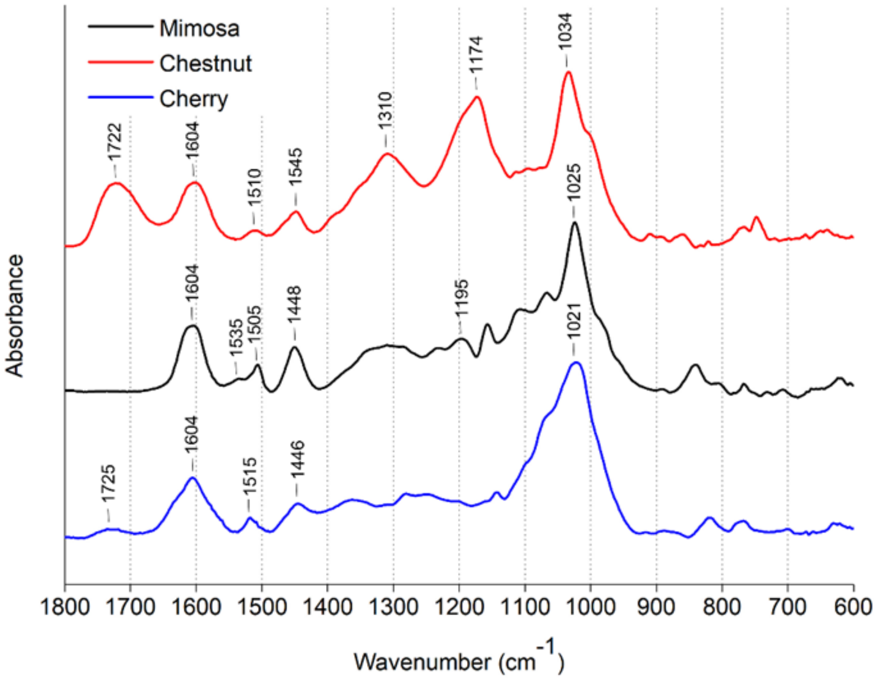

Figure 2. ATR FT–IR spectra of cherry, mimosa and chestnut extracts.

At a first glance it is possible to notice that the profile of cherry's spectrum is similar to that of mimosa. In particular the C=C aromatic stretching region at around 1600 cm^{-1} so as the major band around 1000 cm^{-1}. This immediately allows to confirm the main observations obtained from the 13C–NMR analysis.

Considering the profiles into details, the region between 1730 and 1700 cm^{-1} is related to the C=O stretching of carbonyl group which is due to gallic and ellagic acid, typical moieties of hydrolysable tannins [28],[57] Cherry's spectrum presents a very weak peak in this region, suggesting the presence of small amount of carbonyl groups due to the presence galloylated catechins related to condensate tannins [58], or to possible oxided or open forms of small carbohydrates [49] as we already assumed for the low chemical shield signal in 13C–NMR.

C=C aromatic stretching vibrations absorb between 1620 and 1500 cm^{-1} and all the extracts present relatively similar signals at 1604 cm^{-1} (symmetric stretching) and around 1510 cm^{-1} (asymmetric) [59]. Only the small shoulder at 1535 cm^{-1} of mimosa could provide some structural information. Model compounds suggest that this type of signal is more frequent in species containing aromatic rings with two hydroxyl groups. Flavonoids such as profisetinidin or procyanidin with a majority of di–hydroxy–aromatic rings should be responsible for the presence of the signal [60].

The region between 1500 and 1100 cm^{-1} is generally dominated by C–H bending and C–O stretching vibrations, often overlapping and hence hard to attribute uniquely. However, it is possible to observe that at 1310 and 1174 cm^{-1} the two dominant signals are attributed to C–O stretching of gallic acid and its ester, (typical for hydrolysable tannins) [49],[61] do not occur in cherry.

The area between 1100 to 600 cm^{-1} is characterised by the overlap of several bands, the assignment of which is very difficult. This region is strongly dominated by the broad band at around 1030 cm–1 which can be attributed to the C–O stretching of the methoxy groups with C–C, C–OH, C–H of the sugar fractions [62]. This band is prominent for cherry which confirms the presence of important fractions of sugars.

Summarizing, also the FT–IR confirms results of the wet chemistry test of Table 1 as well as that of 13C–NMR, indicating that cherry extract is constituted by higher amount of carbohydrates, and that its polyphenols mostly belongs to the condensed family.

Polysaccharides

The chromatography study of tannin extracts allowed to investigate their polysaccharide's content and nature, as well as the interaction that might occur between polyphenols and carbohydrate moieties. Figure 3 shows that the three extracts contained carbohydrates. The chromatographic profile of the extracts was similar, while the concentration of carbohydrates clearly differed, with cherry being the richest in polysaccharides while chestnut the poorest (see Table 1). Interestingly, when looking at the molecular weight distribution of the carbohydrate material, it is visible that most of it is comprised between 1 and 20 kDa, that is the interval in which the two main peaks are eluted for all extracts. In particular, the highest peak is entirely eluted in the oligosaccharide region between 18 and 20 minutes (1 – 7.5 kDa). Considering the ratio between the two main peaks (9kDa/3kDa), cherry showed an intermediate value (2.5), mimosa the highest (3.8) and chestnut the lowest (1.3), suggesting that their carbohydrates' composition also presents differences. Additionally, cherry was the only extract which has a small fraction coming out of the column earlier (10 minutes) meaning that the extract also contains polysaccharide moieties of high molecular mass (> 1,500 kDa).

In order to study whether polysaccharide material could be covalently associated with phenolic material in the extracts, the high–resolution size exclusion chromatography (HRSEC) analyses also included the recording of the 210 nm Absorbance (Figure 4).

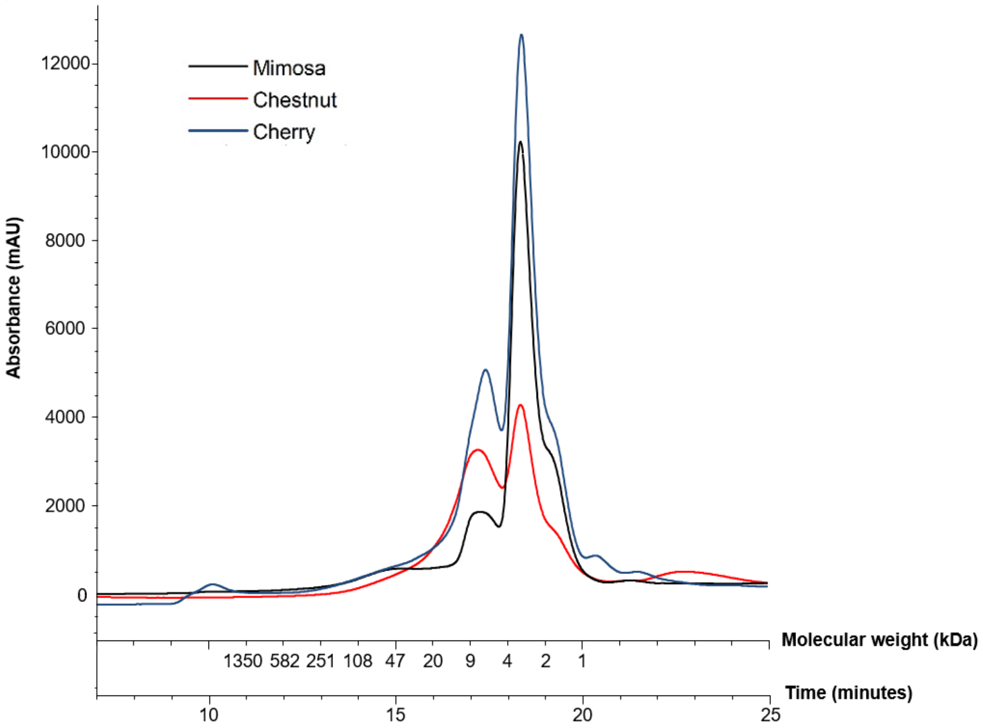

Figure 3. Polysaccharides' profiles by HRSEC–RID of cherry, mimosa, and chestnut extracts.

Comparing the chromatograms obtained with the detector sensitive for polysaccharides (RID) with those obtained from the detector sensitive for aromatics (DAD, 210nm) it is visible that all the peaks found with the RID are also found with the DAD, while some of the peaks visible in DAD cannot be seen with the RID (Figure 4). This is an indication of the likely interaction occurring between carbohydrate and phenolic material in the extracts. Indeed, the chromatograms suggest that polysaccharides are always eluted together with phenolic compounds, so an association between these two classes of molecules can be hypothesized. Despite there are no experiments that can undoubtedly prove the nature of the interaction between phenolic and carbohydrate moieties, all the experiments done in this study and in previous [31],[35],[38], seems to highlight that the interaction these bonds are covalent because it is almost impossible to selectively separate the two families of compounds. However, it is also clear that part of the tannins, especially those with lower molecular weight, are present in free form.

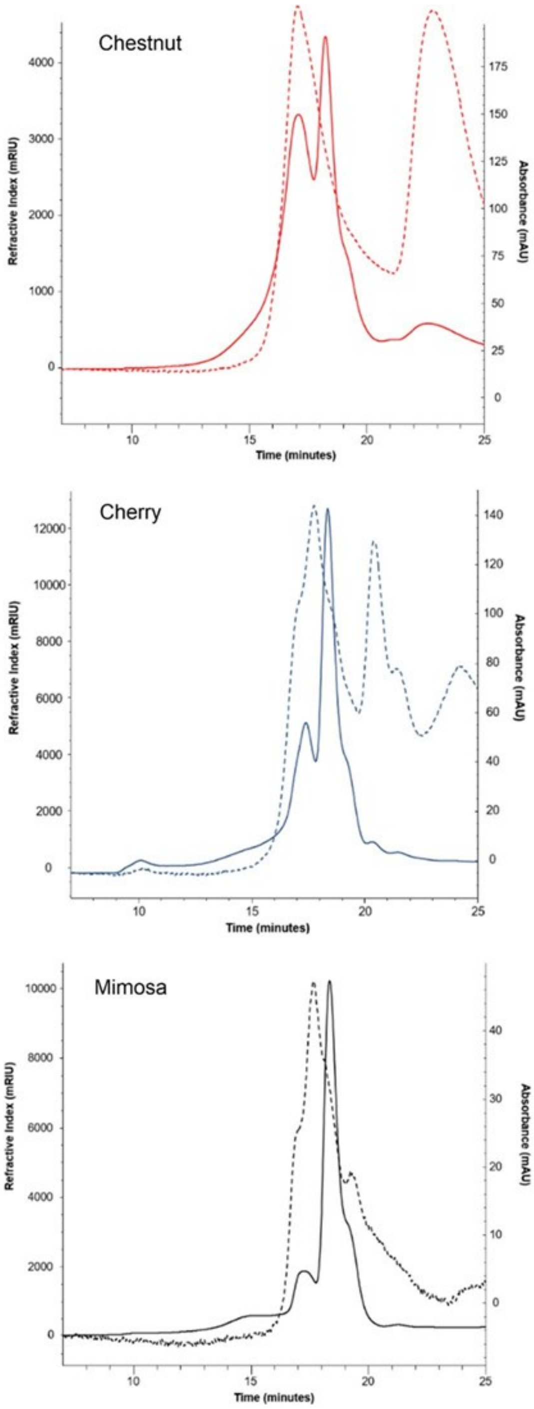

Figure 4. Chromatograms of cherry extract registered with RID (continuous line) and DAD (dashed line) detectors.

Results are in line with previous data on extracts composition. Indeed, the ratios RID/DAD in both peaks are the highest for mimosa and the lowest for chestnut. This observation further highlights that cherry extract is more similar to mimosa and that the main fractions are richer in carbohydrates. In summary, the above reported data indicate that total phenolic content is similar between chestnut and mimosa, this means that the chestnut extract is made of polyphenols (covalently) combined with small moieties of carbohydrates, while mimosa is made by a mixture of macromolecules with heavy saccharide chains and sugar–free shorter chains. A schematic representation of these structures is reported in Figure 5.

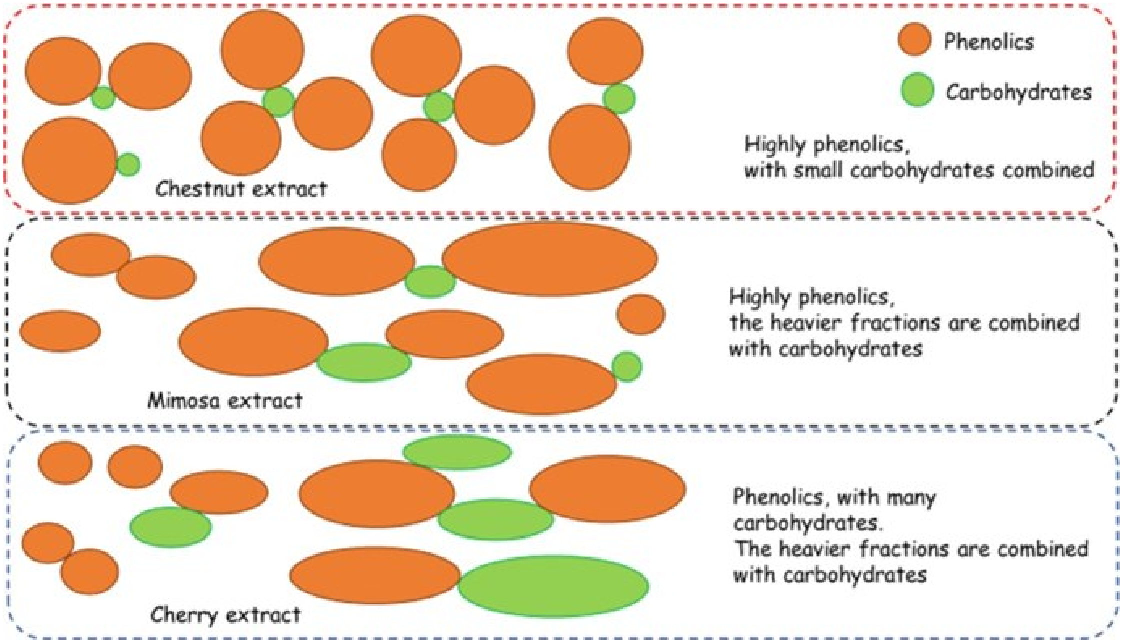

Figure 5. Schematic representation of the interaction phenolic–saccharides in chestnut, mimosa and cherry extracts

Thermogravimetric analysis (TGA)

The weight loss (TGA) and the first derivate weight loss (D–TGA) are reported in function of the temperature in figure 6. The three thermograms have similar trend of a relatively constant degradation. Cherry degrades slightly faster and reaches 36% of its original weight at 800°C. Mimosa and chestnut are more stable until 500°C, then chestnut degrades reaching similar weight loss than cherry, while mimosa results slightly more stable registering a remaining weight of 41% at the end of the experiment. The presence of a peak at 260°C is major for all three extracts. This signal is probably due to the decarboxylation of the RCOOH groups with the release of carbon dioxide [63]. Chestnut differs from the mimosa in the presence of a second peak close to this one, at around 298 °C. It is likely that the high presence of gallic acid derivatives requires higher temperatures to complete decarboxylation. The behaviour of cherry tannin seems to be intermediate. Degradation starts substantially earlier and between 150 and 200°C several degradation peaks can be seen from the first derivative curve. The presence of these confirms the high content of sugars highlighted in previous analyses.

Figure 6. Thermograms and their derivatives of mimosa, chestnut, and cherry extracts

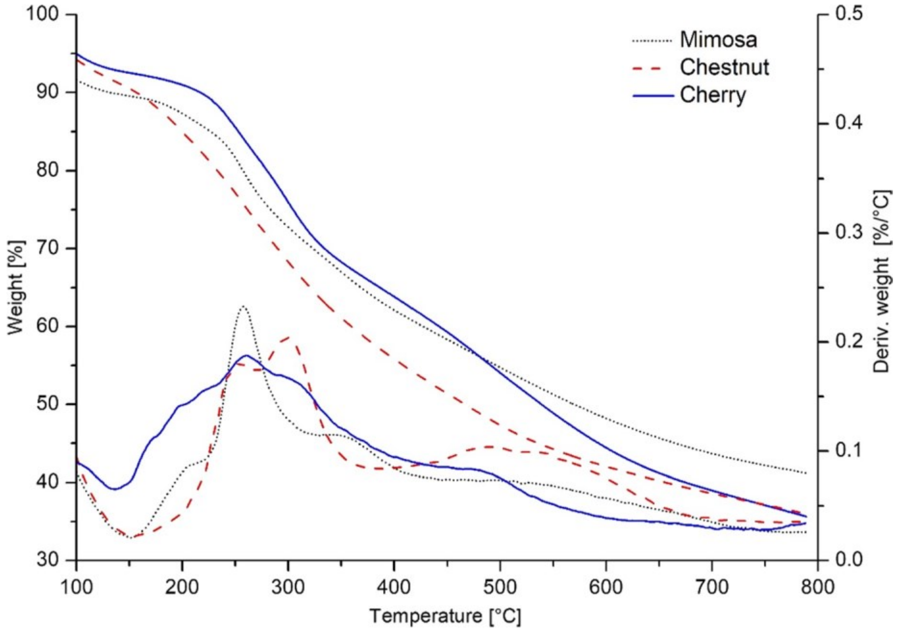

In particular, the polysaccharide fraction takes the degradation at lower temperature than the polyphenolic compounds [64]. The late degradation starts from 400°C and occurs similarly for the three powders. Here the weight loss is related to the oxidation of the residual carbon [65]; the major resistance of the mimosa is due to the easier arrangement in carbon networks because of the more compacted three–dimensional arrangement the condensed tannin, which present already aggregates of rings [66].

Conclusion

In this study a cherry (Prunus avium L.) extract was obtained and compared with two commercial wood extracts, namely one mostly composed of condensed tannin (Acacia mimosa De Wild.), and one typically constituted of hydrolysable tannins (Castanea sativa Mill.). The cherry extract resulted rich of condensed tannins with an important amount of carbohydrates strongly linked to the flavonoids. HRSEC analysis of the extract suggested the presence of probably covalent interactions between the phenolic and the saccharide moieties. The flavonoids of the cherry extracts are richer on hydroxy groups in the B–ring, hence with higher proportion of pyrogallic units and also of lower crosslinking degree, possibly due to the higher proportion of carbohydrates. This abundant presence of carbohydrates was deemed responsible for the lower antioxidant capacity and thermal resistance of this extract. These findings shed new light on the cherry extract that could be applied as milder antioxidant or as building block for bio–composites.

References

1. Tondi, G.; Thevenon, M. F.; Mies, B.; Standfest, G.; Petutschnigg, A.; Wieland, S. Impregnation of Scots Pine and Beech with Tannin Solutions: Effect of Viscosity and Wood Anatomy in Wood Infiltration. Wood Sci. Technol**. 2013**, 47, 615–626. https://doi.org/10.1007/s00226–012–0524–5.

2. Pizzi, A. Tannins: Prospectives and Actual Industrial Applications. Biomolecules **2019**, 9 (8). https://doi.org/10.3390/biom9080344.

3. Shirmohammadli, Y.; Efhamisisi, D.; Pizzi, A. Tannins as a Sustainable Raw Material for Green Chemistry: A Review. Ind. Crops Prod. **2018,** 126, 316–332. https://doi.org/10.1016/j.indcrop.2018.10.034.

4. Falcão, L.; Araújo, M. E. M. Vegetable Tannins Used in the Manufacture of Historic Leathers. Molecules 2018, 23, 8–10. https://doi.org/10.3390/molecules23051081.

5. Auad, P.; Spier, F.; Gutterres, M. Vegetable Tannin Composition and Its Association with the Leather Tanning Effect. Chem. Eng. Commun. **2020**, 207 (5), 722–732. https://doi.org/10.1080/00986445.2019.1618843.

6. Cook, N. C.; Samman, S. Flavonoids – Chemistry, Metabolism, Cardioprotective Effects, and Dietary Sources. J. Nutr. Biochem. **1996**, 7 (2), 66–76. https://doi.org/10.1016/0955–2863(95)00168–9.

7. Yu, B.; Zhang, Y.; Shukla, A.; Shukla, S. S.; Dorris, K. L. The Removal of Heavy Metals from Aqueous Solutions by Sawdust Adsorption – Removal of Lead and Comparison of Its Adsorption with Copper. J. Hazard. Mater. **2001**, 84 (1), 83–94. https://doi.org/10.1016/S0304–3894(01)00198–4.

8. Li, L.; Li, Z.; Wei, Z.; Yu, W.; Cui, Y. Effect of Tannin Addition on Chromatic Characteristics, Sensory Qualities and Antioxidant Activities of Red Wines. RSC Adv. **2020**, 10 (12), 7108–7117. https://doi.org/10.1039/c9ra09846a.

9. Giacosa, S.; Parpinello, G. P.; Río Segade, S.; Ricci, A.; Paissoni, M. A.; Curioni, A.; Marangon, M.; Mattivi, F.; Arapitsas, P.; Moio, L.; Piombino, P.; Ugliano, M.; Slaghenaufi, D.; Gerbi, V.; Rolle, L.; Versari, A. Diversity of Italian Red Wines: A Study by Enological Parameters, Color, and Phenolic Indices. Food Res. Int. **2021**, 143 , 110277. https://doi.org/10.1016/j.foodres.2021.110277.

10. De Rosso, M.; Marangon, M.; Flamini, R. Characterization of Ellagitannins and Oak Lactone Precursors in Oak Wood–Aged Grappa by High–Resolution Mass Spectrometry. J. Mass Spectrom. **2020**, 55 (7), 4472. https://doi.org/10.1002/jms.4472.

11. Harbertson, J. F.; Parpinello, G. P.; Heymann, H.; Downey, M. O. Impact of Exogenous Tannin Additions on Wine Chemistry and Wine Sensory Character. Food Chem. **2012**, 131 (3), 999–1008. https://doi.org/10.1016/j.foodchem.2011.09.101.

12. Rosso, M. De; Panighel, A.; Vedova, A. D.; Stella, L.; Flamini, R. Changes in Chemical Composition of a Red Wine Aged in Acacia, Cherry, Chestnut, Mulberry, and Oak Wood Barrels. J. Agric. Food Chem. **2009**, 57 (5), 1915–1920. https://doi.org/10.1021/jf803161r.

13. Guerrero, E. D.; Chinnici, F.; Natali, N.; Marín, R. N.; Riponi, C. Solid–Phase Extraction Method for Determination of Volatile Compounds in Traditional Balsamic Vinegar. J. Sep. Sci. **2008**, 31 (16–17), 3030–3036. https://doi.org/10.1002/jssc.200800307.

14. Versari, A.; Du Toit, W.; Parpinello, G. P. Oenological Tannins: A Review. Aust. J. Grape Wine Res. **2013,** 19 (1), 1–10. https://doi.org/10.1111/ajgw.12002.

15. Rinaldi, A.; Moio, L. Effect of Enological Tannin Addition on Astringency Subqualities and Phenolic Content of Red Wines. J. Sens. Stud. **2018**, 33 (3), 1–11. https://doi.org/10.1111/joss.12325.

16. Pizzi, A. Tannin–Based Adhesives. J. Macromol. Sci. Part C **1980,** C18 (2), 247–315.

17. Cesprini, E.; Šket, P.; Causin, V.; Zanetti, M.; Tondi, G. Development of Quebracho (Schinopsis Balansae) Tannin–Based Thermoset Resins. **2021**, 13, 4412.

18. Tondi, G.; Wieland, S.; Wimmer, T.; Thevenon, M. F.; Pizzi, A.; Petutschnigg, A. Tannin–Boron Preservatives for Wood Buildings: Mechanical and Fire Properties. Eur. J. Wood Wood Prod. **2012**, 70 (5), 689–696. https://doi.org/10.1007/s00107–012–0603–1.

19. Sommerauer, L.; Thevenon, M. F.; Petutschnigg, A.; Tondi, G. Effect of Hardening Parameters of Wood Preservatives Based on Tannin Copolymers. Holzforschung **2019**, 73 (5), 457–467. https://doi.org/10.1515/hf–2018–0130.

20. Cesprini, E.; Baccini, R.; Urso, T.; Zanetti, M.; Tondi, G. Quebracho–Based Wood Preservatives : Effect of Concentration and Hardener on Timber Properties. coatings **2022**, 12, 568. https://doi.org/https:// doi.org/10.3390/coatings12050568.

21. Tondi, G.; Pizzi, A.; Olives, R. Natural Tannin–Based Rigid Foams as Insulation for Doors and Wall Panels. Maderas Cienc. y Tecnol. **2008**, 10 (3), 219–228. https://doi.org/10.4067/S0718–221X2008000300005.

22. Tondi, G.; Link, M.; Kolbitsch, C.; Lesacher, R.; Petutschnigg, A. Pilot Plant Up–Scaling of Tannin Foams. Ind. Crops Prod. 2016, 79, 211–218. https://doi.org/10.1016/j.indcrop.2015.11.013.

23. Li, X.; Nicollin, A.; Pizzi, A.; Zhou, X.; Sauget, A.; Delmotte, L. Natural Tannin–Furanic Thermosetting Moulding Plastics. RSC Adv. **2013**, 3 (39), 17732–17740. https://doi.org/10.1039/c3ra43095b.

24. Amaral–Labat, G.; Szczurek, A.; Fierro, V.; Pizzi, A.; Celzard, A. Systematic Studies of Tannin–Formaldehyde Aerogels: Preparation and Properties. Sci. Technol. Adv. Mater. **2013**, 14 (1), 015001. https://doi.org/10.1088/1468–6996/14/1/015001.

25. Koopmann, A. K.; Malfait, W. J.; Sepperer, T.; Huesing, N. A Systematic Study on Bio–Based Hybrid Aerogels Made of Tannin and Silica. Materials (Basel). **2021**, 14 (18). https://doi.org/10.3390/ma14185231.

26. Drewes, S.; Roux, D. Condensed Tannins. 15. Interrelationships of Flavonoid Components in Wattle–Bark Extract. Biochem. J. **1963**, 87 (1), 167–172. https://doi.org/10.1042/bj0870167.

27. Pizzi, A. Advanced Wood Adhesives Technology, 1st Editio.; CRC Press, 1994.

28. Michel, J.; Jourdes, M.; Silva, M. A.; Giordanengo, T.; Mourey, N.; Teissedre, P. L. Impact of Concentration of Ellagitannins in Oak Wood on Their Levels and Organoleptic Influence in Red Wine. J. Agric. Food Chem. **2011**, 59 (10), 5677–5683. https://doi.org/10.1021/jf200275w.

29. Arbenz, A.; Avérous, L. Chemical Modification of Tannins to Elaborate Aromatic Biobased Macromolecular Architectures. Green Chemistry. Royal Society of Chemistry, **2015**, 2626–2646. https://doi.org/10.1039/c5gc00282f.

30. Muller–Harvey, I. Analysis of Hydrolizable Tannins. Anim. Feed Sci. Technol. **2001**, 91, 3–20.

31. Missio, A.; Tischer, B.; Dos Santos, P. Analytical Characterization of Purified Mimosa (Acacia Mearnsii) Industrial Tannin Extract: Single and Sequential Fractionation | Elsevier Enhanced Reader. Sep. Purif. Technol. **2017**, No. 186, 218–225.

32. Campo, M.; Pinelli, P.; Romani, A. Hydrolyzable Tannins from Sweet Chestnut Fractions Obtained by a Sustainable and Eco–Friendly Industrial Process. Nat. Prod. Commun. **2016**, 11 (3), 409–415. https://doi.org/10.1177/1934578x1601100323.

33. Katalinić, V.; Možina, S. S.; Skroza, D.; Generalić, I.; Abramovič, H.; Miloš, M.; Ljubenkov, I.; Piskernik, S.; Pezo, I.; Terpinc, P.; Boban, M. Polyphenolic Profile, Antioxidant Properties and Antimicrobial Activity of Grape Skin Extracts of 14 Vitis Vinifera Varieties Grown in Dalmatia (Croatia). Food Chem**. 2010**, 119, 715–723. https://doi.org/10.1016/j.foodchem.2009.07.019.

34. Singleton, V. L.; Orthofer, R.; Lamuela–Raventos, R. M. Analysis of Total Phenols and Other Oxidation Substrates and Antioxidants by Means of Folin–Ciocalteu Reagent. Methods Enzymol. **1999**, 299, 152–178. https://doi.org/10.1016/j.scienta.2016.11.004.

35. Sepperer, T.; Hernandez–Ramos, F.; Labidi, J.; Oostingh, G. J.; Bogner, B.; Petutschnigg, A.; Tondi, G. Purification of Industrial Tannin Extract through Simple Solid–Liquid Extractions. Ind. Crops Prod. **2019**, 139, 111502. https://doi.org/10.1016/j.indcrop.2019.111502.

36. Galiñanes, C.; Freire, M. S.; González–Álvarez, J. Antioxidant Activity of Phenolic Extracts from Chestnut Fruit and Forest Industries Residues. Eur. J. Wood Wood Prod. **2015**, 73 (5), 651–659. https://doi.org/10.1007/s00107–015–0936–7.

37. Kotar, A.; Kotar, M.; Sket, P.; Plavec, J. Potential of Solid–State NMR and SEM in Characterization of Tablets of Ibuprofen. Curr. Pharm. Anal. **2014**, 11, 124–130. https://doi.org/10.2174/1573412910666141111231325.

38. Sepperer, T.; Neubauer, J.; Eckardt, J.; Schnabel, T.; Petutschnigg, A.; Tondi, G. Pollutant Absorption as a Possible End–of–Life Solution for Polyphenolic Polymers. Polymers (Basel). **2019**, 11, 911. https://doi.org/10.3390/polym11050911.

39. Ayestarán, B.; Guadalupe, Z.; León, D. Quantification of Major Grape Polysaccharides (Tempranillo v.) Released by Maceration Enzymes during the Fermentation Process. Anal. Chim. Acta **2004**, 513 (1), 29–39. https://doi.org/10.1016/j.aca.2003.12.012.

40. De Iseppi, A.; Marangon, M.; Vincenzi, S.; Lomolino, G.; Curioni, A.; Divol, B. A Novel Approach for the Valorization of Wine Lees as a Source of Compounds Able to Modify Wine Properties. Lwt **2021**, 136 (P1), 110274. https://doi.org/10.1016/j.lwt.2020.110274.

41. Zanetti, M.; Causin, V.; Saini, R.; Cardin, A.; Cavalli, R. Effect of Tannin on Increasing UF Adhesive Performance at High Temperature Investigated by TMA and TGA Analysis. Eur. J. Wood Wood Prod. **2014**, 72, 385–392. https://doi.org/10.1007/s00107–014–0795–7.

42. Kapen, P. T.; Tenkeu, M. N.; Yadjie, E.; Tchuen, G. Production and Characterization of Environmentally Friendly Charcoal Briquettes Obtained from Agriculture Waste: Case of Cameroon. Int. J. Environ. Sci. Technol. **2021**. https://doi.org/10.1007/s13762–021–03497–7.

43. Panzella, L.; Moccia, F.; Toscanesi, M.; Trifuoggi, M.; Giovando, S.; Napolitano, A. Exhausted Woods from Tannin Extraction as an Unexplored Waste Biomass: Evaluation of the Antioxidant and Pollutant Adsorption Properties and Activating e Ects of Hydrolytic Treatments. Antioxidants **2019**, 8 (4), 10–14. https://doi.org/10.3390/antiox8040084.

44. Vázquez, G.; Fontenla, E.; Santos, J.; Freire, M. S.; González–Álvarez, J.; Antorrena, G. Antioxidant Activity and Phenolic Content of Chestnut (Castanea Sativa) Shell and Eucalyptus (Eucalyptus Globulus) Bark Extracts. Ind. Crops Prod. **2008**, 28 (3), 279–285. https://doi.org/10.1016/j.indcrop.2008.03.003.

45. Maksimovíc, Z.; Maleňcíc, D.; Kovăcevíc, N. Polyphenol Contents and Antioxidant Activity of Maydis Stigma Extracts. Bioresour. Technol. **2005**, 96 (8), 873–877. https://doi.org/10.1016/j.biortech.2004.09.006.

46. Molino, S.; Fernández–Miyakawa, M.; Giovando, S.; Rufián–Henares, J. Á. Study of Antioxidant Capacity and Metabolization of Quebracho and Chestnut Tannins through in Vitro Gastrointestinal Digestion–Fermentation. J. Funct. Foods **2018**, 49, 188–195. https://doi.org/10.1016/j.jff.2018.07.056.

47. Vignault, A.; González–Centeno, M. R.; Pascual, O.; Gombau, J.; Jourdes, M.; Moine, V.; Iturmendi, N.; Canals, J. M.; Zamora, F.; Teissedre, P. L. Chemical Characterization, Antioxidant Properties and Oxygen Consumption Rate of 36 Commercial Oenological Tannins in a Model Wine Solution. Food Chem. **2018**, 268, 210–219. https://doi.org/10.1016/j.foodchem.2018.06.031.

48. Zanetti, M.; Cesprini, E.; Marangon, M.; Szczurek, A.; Tondi, G. Thermal Valorization and Elemental Composition of Industrial Tannin Extracts. Fuel 2021, 289 (August 2020), 119907. https://doi.org/10.1016/j.fuel.2020.119907.

49. Konai, N.; Raidandi, D.; Pizzi, A.; Meva'a, L. Characterization of Ficus Sycomorus Tannin Using ATR–FT MIR, MALDI–TOF MS and 13C NMR Methods. Eur. J. Wood Wood Prod. **2017**, 75 (5), 807–815. https://doi.org/10.1007/s00107–017–1177–8.

50. Vázquez, G.; Pizzi, A.; Freire, M. S.; Santos, J.; Antorrena, G.; González–Álvarez, J. MALDI–TOF, HPLC–ESI–TOF and 13C–NMR Characterization of Chestnut (Castanea Sativa) Shell Tannins for Wood Adhesives. Wood Sci. Technol. **2013**, 47 (3), 523–535. https://doi.org/10.1007/s00226–012–0513–8.

51. Navarrete, P.; Pizzi, A.; Pasch, H.; Rode, K.; Delmotte, L. MALDI–TOF and 13C NMR Characterization of Maritime Pine Industrial Tannin Extract. Ind. Crops Prod. **2010**, 32 (2), 105–110. https://doi.org/10.1016/j.indcrop.2010.03.010.

52. Davis, A. L.; Cai, Y.; Davies, A. P.; Lewis, J. R. 1H and 13C NMR Assignments of Some Green Tea Polyphenols. Magn. Reson. Chem. **1996**, 34 (11), 887–890. https://doi.org/10.1002/(SICI)1097–458X(199611)34:11<887::AID–OMR995>3.0.CO;2–U.

53. Tondi, G. Tannin–Based Copolymer Resins: Synthesis and Characterization by Solid State 13C NMR and FT–IR Spectroscopy. Polymers (Basel). **2017**, 9 (6). https://doi.org/10.3390/polym9060223.

54. Wawer, I.; Wolniak, M.; Paradowska, K. Solid State NMR Study of Dietary Fiber Powders from Aronia, Bilberry, Black Currant and Apple. Solid State Nucl. Magn. Reson. **2006**, 30 (2), 106–113. https://doi.org/10.1016/j.ssnmr.2006.05.001.

55. Zhang, L. L.; Lin, Y. M.; Zhou, H. C.; Wei, S. D.; Chen, J. H. Condensed Tannins from Mangrove Species Kandelia Candel and Rhizophora Mangle and Their Antioxidant Activity. Molecules **2010**, 15 (1), 420–431. https://doi.org/10.3390/molecules15010420.

56. Santos, J.; Antorrena, G.; Freire, M. S.; Pizzi, A.; González–Álvarez, J. Environmentally Friendly Wood Adhesives Based on Chestnut (Castanea Sativa) Shell Tannins. Eur. J. Wood Wood Prod. **2017**, 75 (1), 89–100. https://doi.org/10.1007/s00107–016–1054–x.

57. Falcão, L.; Araújo, M. E. M. Application of ATR–FTIR Spectroscopy to the Analysis of Tannins in Historic Leathers: The Case Study of the Upholstery from the 19th Century Portuguese Royal Train. Vib. Spectrosc**. 2014**, 74, 98–103. https://doi.org/10.1016/j.vibspec.2014.08.001.

58. Hagerman, A. E.; Zhao, Y.; Johnson, S. Methods for Determination of Condensed and Hydrolyzable Tannins; 1997; Vol. 662. https://doi.org/10.1021/bk–1997–0662.ch012.

59. Tondi, G.; Petutschnigg, A. Middle Infrared (ATR FT–MIR) Characterization of Industrial Tannin Extracts. Ind. Crops Prod. **2015**, 65, 422–428. https://doi.org/10.1016/j.indcrop.2014.11.005.

60. Haslam, E. Practical Polyphenolics: From Structure to Molecular Recognition and Physiological Action, 1°.; Cambridge University Press, 1998.

61. Ricci, A.; Olejar, K. J.; Parpinello, G. P.; Kilmartin, P. A.; Versari, A. Application of Fourier Transform Infrared (FTIR) Spectroscopy in the Characterization of Tannins. Appl. Spectrosc. Rev. **2015**, 50 (5), 407–442. https://doi.org/10.1080/05704928.2014.1000461.

62. Schwanninger, M.; Rodrigues, J. C.; Pereira, H.; Hinterstoisser, B. Effects of Short–Time Vibratory Ball Milling on the Shape of FT–IR Spectra of Wood and Cellulose. Vib. Spectrosc. **2004**, 36 (1), 23–40. https://doi.org/10.1016/j.vibspec.2004.02.003.

63. Garro Galvez, J. M.; Riedl, B.; Conner, A. H. Analytical Studies on Tara Tannins; **1997;** Vol. 51.

64. Gaugler, M.; Grigsby, W. J. Thermal Degradation of Condensed Tannins from Radiata Pine Bark. J. Wood Chem. Technol. **2009**, 29 (4), 305–321. https://doi.org/10.1080/02773810903165671.

65. Tondi, G.; Pizzi, A.; Pasch, H.; Celzard, A. Structure Degradation, Conservation and Rearrangement in the Carbonisation of Polyflavonoid Tannin/Furanic Rigid Foams – A MALDI–TOF Investigation. Polym. Degrad. Stab. **2008**, 93, 968–975. https://doi.org/10.1016/j.polymdegradstab.2008.01.024.

66. Konai, N.; Raidandi, D.; Pizzi, A.; Girods, P.; Lagel, M. C.; Kple, M. Thermogravimetric Analysis of Anningre Tannin Resin. Maderas Cienc. y Tecnol. **2016**, 18 (2), 245–252. https://doi.org/10.4067/S0718–221X2016005000022

5. Conclusions

The central objective of this research was to develop bio-based resins suitable for the efficient production of EWPs. Therefore, the aim was to ensure that the resulting materials demonstrate physico–mechanical properties comparable with those achieved by synthetic adhesives, thereby trying to meet the international standards. The ongoing research project was specifically dedicated to the exploration of a distinct wood extractive named Fintan 737B, with the primary aim of harnessing its potential for the synthesis of biobased polymers. Our investigation into Fintan 737B provides valuable insights that can be meaningfully compared with previous researches with other condensed tannins. The research, was mainly divided into four topics, each of them referring to different aspects of the research and discussed within the Chapter 4.

Subchapter 4.1 delves into the exploration of employing quebracho tannin extract as a polymer matrix. The study proposed six distinct hardeners, namely formaldehyde, hexamine, glyoxal, furfural, furfuryl alcohol, and maleic anhydride. Through the study of leaching resistance, which gives an idea of the ration of the polymerization, the effectiveness of the hardeners in forming a stable three–dimensional polymer network was evaluated. The leaching resistance for the formulation proposed reached values of around 80%, suggesting that part of the extract does not take part in the curing process and can be removed easily. Specifically, the leached part of the compound can be attributed to the non–phenolic component of the extract, such as carbohydrates, which do not take part in cross–linking. The evidence of structure tightening can be seen in both spectroscopies, FT–IR and 13C–NMR, showing that quebracho polymers are connected principally through the A–ring with every hardener, and the crosslinking products are similar to those occurring with the mimosa extract. The proposal of alternative hardeners holds substantial industrial importance, particularly as viable substitutes for formaldehyde, a widely recognized carcinogenic compound. Thus, the formulations developed in this study present an attractive alternative to thermosetting polymers, offering a viable substitute for phenolic resins in applications such as adhesives, coatings, and, more broadly, as versatile bio plastic.

Following the exclusion of formaldehyde-based adhesives, the focus shifted to various alternative and most promising crosslinkers into the production of EWPs, with a comprehensive discussion presented in subchapter 4.2.Primarily recognized as a hardening agent, hexamine exhibited notable affinity with the employed tannin, resulting in the formation of stable polymers, even at concentrations below 5%. Consequently, a decision was made to scrutinize its efficacy as a potential preservative for various wood species, through an impregnation process of wood samples. Moreover, two other specific hardeners were chosen for further applications, due to several key factors: (i) they are derivative of the dehydration of agricultural and forest waste from hemicelluloses, making all the formulation entire renewable, and finally (ii) due to the limited existing literature. (iii) they demonstrated promising preliminary results. Both of those compounds fall within the furanic class of molecules, namely furfural and furfuryl alcohol.

Therefore, starting with the use of tannin–hexamine solutions, the impregnation of several wood species, such as: spruce (*Picea abies*), pine (*Pinus spp.*), poplar (*Populus alba*) and beech (*Fagus sylvatica*). The initial phase of the investigation systematically examined impregnating solution concentrations customized for two distinct tree species—one representing deciduous trees and the other, coniferous trees. The wet retention of spruce, belonging to the latter category, is influenced by the concentrations of impregnating solutions. In contrast, beech, representing hardwood, is more permeable due to differences in wood anatomy between soft and hard wood. Generally, the presence of quebracho tannin networked with hexamine embedded in the structure contributes to enhance the mechanical properties of timber especially the modulus of rupture and the surface hardness of the samples with lower density. For the enhancement of mechanical properties and resistance to leach, formulations with 10% quebracho tannin and 2.5% hexamine (w./w. tannin) are already effective. Although hexamine has long been known as a viable alternative to formaldehyde, scientific evidence of efficacy at rates of less than 5% had not been highlighted.

Differently, there is a conspicuous gap in the existing literature regarding the use of tannin and furfural resins as wood adhesives. Consequently, the subsequent two research initiatives redirected their focus towards incorporating this hardener in adhesive production. The primary objective was centred on utilizing these adhesives initially in the fabrication of particleboard and subsequently in the manufacturing of 5–layer plywood. Specifically, the efficacy of quebracho tannin–furfural adhesive for particleboards was studied by modifying pressing temperature, pressing time, and the adhesive content. Initially, examinations were conducted on tannin–furfural resins containing 45% tannin, revealing commendable processability and stability. Thus, optimal pressing parameters for particleboards were identified: (i) a pressing temperature exceeding 140 °C, (ii) a minimum pressing time of 9 minutes, and (iii) an adhesive content of 15%. Under these reaction conditions, the outcomes align with the criteria specified for interior conditions according to the EN 312 standard.

Simultaneously, the adhesive resin was used to produce 5–layer plywood by adjusting the tannin starting solution's concentration in water, ranging from 45% to 65%. The adhesive formulation has shown good viscosity and curing behaviour at a relatively low temperature of 100 °C, producing polymers after curing. Firstly, the non–reactivity at room temperature and at high tannin concentrations has to be highlighted as a clear advantage in terms of industrial application due to a prolonged open–time and storage duration. Their use as a fully bio–based sustainable adhesive for plywood displayed good bending (modulus of elasticity range ~9600 to ~11,600 N·mm^{-2}; modulus of rupture range 66 to 100 N·mm^{-2}) and acceptable tensile shear strength (~2.2 N·mm^{-2}) in a dry environment, especially for the test specimens in the temperature range 125–140 °C, concluding that the presented formulation is comparable to industrial applied PF adhesives. However, as negative drawback, the low water–resistance due to the brittle character of the adhesive layer structure has to be mentioned as it limits the use of the proposed quebracho tannin–furfural formulation for both particleboard and plywood. This deficiency significantly constrains their potential applications and hinders their viable integration into the market.

In order to move beyond this issue, a counterpart within furanic-tannin formulation was investigated to enhance the final properties of the resin. This time, furfuryl alcohol, a product obtained through the hydrogenation of furfural, was selected as the hardener. Silk fibroin stands out as a highly promising natural protein–based biomaterial, owing to its remarkable biodegradability and superior mechanical properties. Derived from insect farming, specifically Bombyx mori silkworms, this biopolymer can be processed in solution, facilitating the production of adhesives with adjustable mechanical characteristics. Within this study, the impact of incorporating varying proportions of fibroin into tannin–furfuryl alcohol formulations (TFS) for plywood manufacturing was systematically explored. Thus, successful integration of RS into the matrix resulted in the creation of bio–based adhesives showcasing improved mechanical attributes. Notably, a substantial enhancement of approximately 20–30% was observed in plywood bonding when 15–20 wt% of RS solution was introduced into the reference formulation, under both dry and wet conditions. This network is characterized by the establishment of novel chemical bonds between silk and the furanic adduct. Such a strategy not only introduces a novel formaldehyde–free bio–based wood adhesive with rapid preparation but also offer superior performance respect classical tannin–based adhesive formulations.

Examining available literature, silk stands out as a fibre with significant environmental impact, surpassing values associated with synthetic and primary natural fibers. Collaborating with the CREA rearing centre, our study delves into the environmental impact of silk supply, contextualizing the Italian reality within the global silk production landscape (Chapter 4.3). Utilizing LCA methodology, the study unveils insights into the potential of revitalizing the cocoon industry beyond its traditional fashion application. It is essential to note that our findings are based on a small–scale operation with limited production and a lack of exclusive commitment to the business market. Furthermore, caution is needed in interpreting the environmental impact analysis, given its reliance on several assumptions. However, environmental benefits are evident when comparing intensive production scenarios with our illustrative case. Indeed, the environmentally conscious management of the mulberry orchard significantly mitigates impacts, leading to lower impacts along all impact categories investigated. In conclusion, the results highlighted the challenges and potential of revitalizing the silk industry. While silk's environmental impact is notable, sustainable practices and innovative applications, such as incorporating silk fibroin into adhesives, showcase promising avenues for balancing environmental concerns with material properties. In conclusion, the research has highlighted the potential of specific industrial tannin extract as key components for wood adhesives. Various hardeners, particularly furanic molecules, have successfully induced polymerization in thermosetting resins, showcasing renewability. Notably, the addition of silk protein to the quebracho–furfuryl alcohol formulation exhibited enhanced properties, even in humid conditions. Yet, further tests are essential to explore potential industrial applications of this resin. In essence, the findings of this PhD thesis underscore the importance of merging environmental considerations with the physicochemical characteristics of a new materials, urging the widespread adoption of sustainable practices to enhance the properties of the final product.

Acknowledgements

I wish to extend my heartfelt gratitude to the people who have played pivotal roles in supporting and guiding me throughout this journey of both professional and personal development. Foremost, I express my deep appreciation to my advisor, Prof. Michela Zanetti and co–advisor Prof. Gianluca Tondi, whose contagious enthusiasm and dedication to research and the realm of wood have inspired me. Special recognition is also to Professor Valerio Causin, my former master thesis advisor, for his unwavering support over the course of these three years, consistently offering valuable guidance. I also express my sincere gratitude to Silva Company for their generous contribution in providing polyphenolic extracts of tannin for. Furthermore, I extend my profound gratitude to the professors, Thomas Schnabel and Indroneil Ganguly, who provided me with invaluable opportunities during my experiences abroad. Professor Schnabel supervised my time at the University of Salzburg, Austria, while Professor Ganguly guided me during my stay at the University of Washington, Seattle, USA. Additionally, my sincere thanks go to my family, whose enduring investment in my education and unwavering belief in my choices have been a constant source of motivation. Finally, I am grateful to my friends, especially my fellow PhD colleagues, whose closeness and lightness have added joy to this three–year journey.

Supplementary informations

Annex 1

In relation to chapter 5, subsection 5.4:

Bio–based Tannin–Furanic–Silk Adhesives: Applications in Plywood and Chemical Crosslinking Mechanisms

In order to understand the nature of the agglomerated highlighted in figure 3C, similar sample areas were analysed before and after a further solubilisation in formic acid/$CaCl_2$, and the experiment is reported in figure SF1. The sample treated with the acid solution clearly shows a porous structure with visible cavities from the silk lump, confirming what was previously assumed. Compositional analysis further confirms the silk inhomogeneity within the system. A C/O ratio of 1.00 was calculated in the vicinity of the silk agglomeration, while following solubilisation at the same point the ratio rises to a value of 2 units. Confirming that the high C/O ratio is due to an increased presence of silk in the specific area. According to these findings it could be necessary to modify the processing in order to further homogenise the dispersion, eventually by increasing stirring time and speed so as the mixing temperature.

In order to justify the formylation reaction between tannin and formic acid, a ATR FT–IR analysis is reported. A leached sample of formylated tannin, reacted at 100°C for one hour, and powder of quebracho tannin are reported and compared if figure SF2. As clearly visible new carbonyl peak appears at 1705 cm^{-1}, (red spectra, formylated tannin) due to the occurrence of formylation.

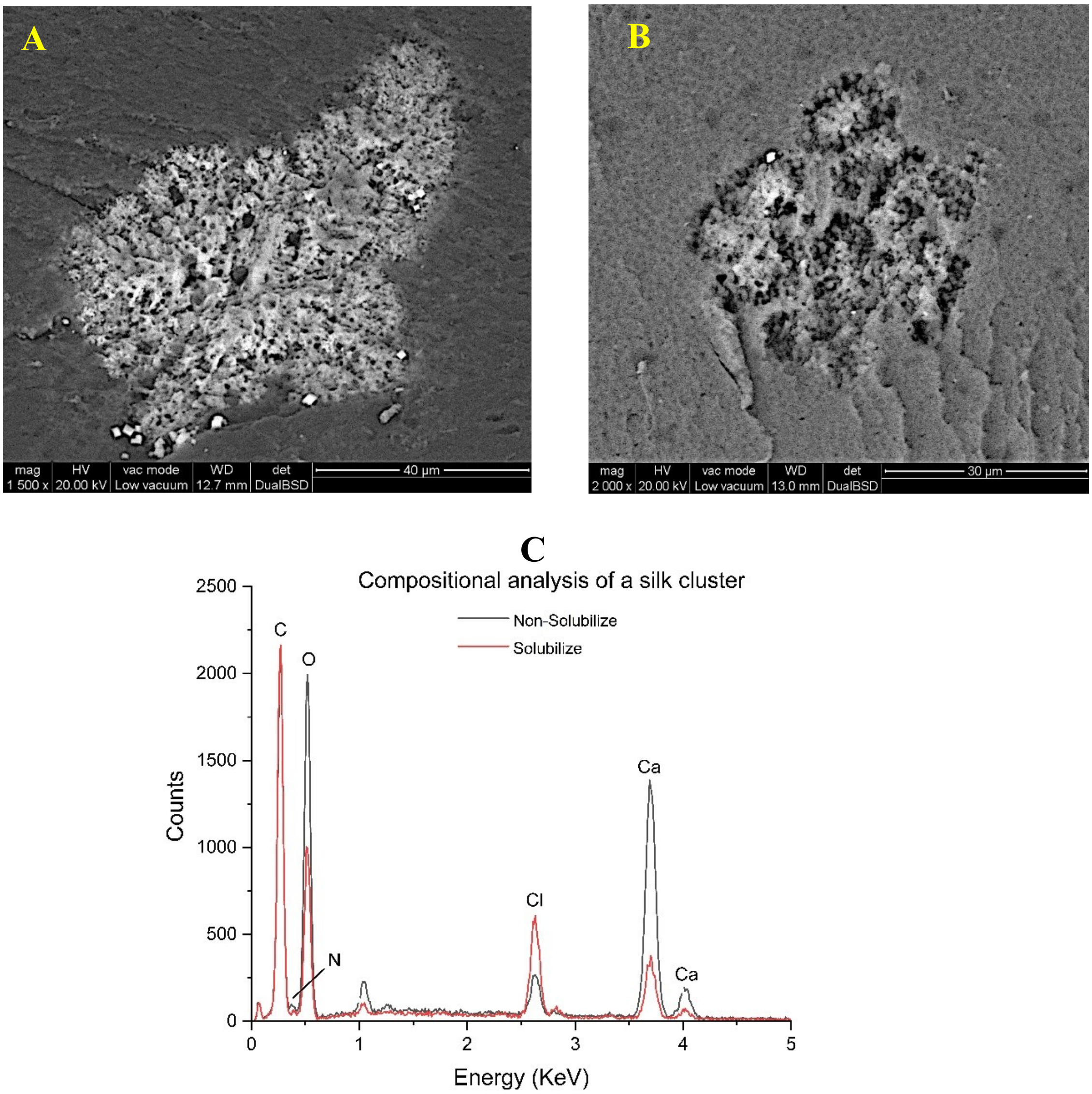

Figure SF1. Scanning electron microscopy images of TSF–20 before (A) and after (B) solubilization into acid formic–$CaCl_2$ solution and relative chemical analysis (C)

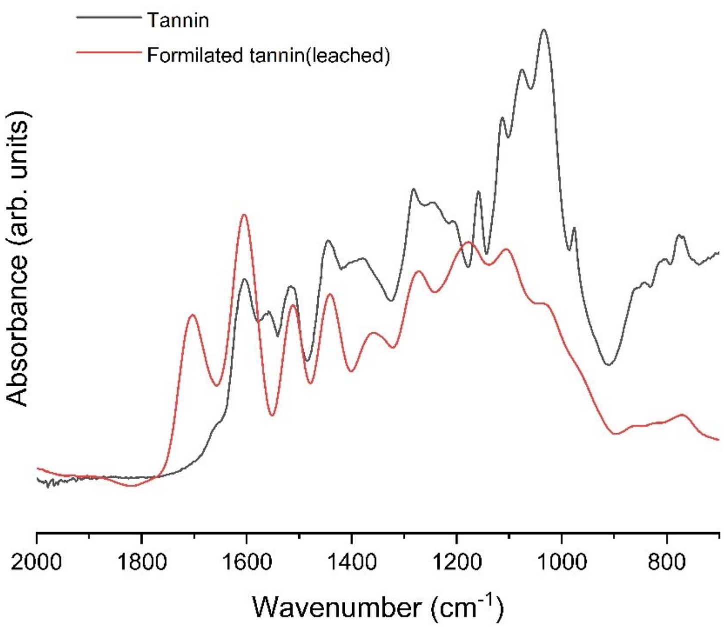

Figure SF2. ATR–FT–IR spectra of quebracho tannin powder (black curve) and leached quebracho tannin after reaction with formic acid at 100°C for one hour.

Annex 2

In relation to chapter 6, subsection 6.1:

Assessing the Environmental Impact of Silk Protein Production for Bio–Based Materials: A Life Cycle Assessment Study

Table1. Inventory analysis of the main substances contributing to the impacts for the production of 1 kg of silk cocoons for the main processes involved, expressed in relative percentage values. The rows in the table in reference to "remaining substances" refer to the application of a 5% Cut–off.

Substance %	**Compartment**	**Total**	**Mulberry leaves**	**Paper, newsprint**	**Plastic rays**	**Chemical disinfectants**	**Transport**	**Building**	**Electricity**	**Biowaste**
Abiotic depletion (kg Sb eq)										
Remaining substances		6.9	10.0	9.3	9.6	10.8	5.5	2.9	8.7	11.6
Copper	Raw	9.5	14.3	9.9	11.0	10.6	5.1	3.4	13.8	12.5
Gold	Raw	12.0	4.8	15.4	24.0	24.3	44.5	4.5	6.7	11.3
Lead	Raw	15.5	4.0	11.7	2.8	2.7	7.5	43.5	3.3	4.5
Silver	Raw	12.1	5.4	9.3	5.9	6.0	15.9	19.5	8.6	7.4
Tellurium	Raw	38.0	59.8	39.9	45.6	44.5	18.8	9.1	57.8	51.0
Zinc	Raw	6.0	1.6	4.6	1.1	1.1	2.8	17.1	1.2	1.7
Abiotic depletion, Fossil fuels (MJ)										
Remaining substances		1.7	1.5	14.0	0.4	5.8	1.3	3.4	1.6	0.9
Coal, hard	Raw	14.4	11.3	17.5	3.8	15.1	11.2	32.6	16.4	7.0
Gas, natural/m^3	Raw	39.7	19.4	43.1	39.7	52.9	10.9	25.6	72.4	17.0
Oil, crude	Raw	44.3	67.8	25.5	56.1	26.2	76.6	38.4	9.5	75.2
Global worming potential (kg CO2 eq)										
Remaining substances		3.5	2.1	2.7	0.6	1.0	1.0	1.1	2.0	16.4
Carbon dioxide, fossil	Air	78.6	64.7	89.5	82.3	87.0	90.7	91.2	85.9	42.4
Methane, biogenic	Air	9.0	26.4	0.7	0.4	2.4	0.1	0.3	1.2	35.9
Methane, fossil	Air	8.8	6.7	7.2	16.6	9.6	8.3	7.4	10.9	5.3
Ozone depletion layer (kg CFC–11 eq)										
Remaining substances		7.9	4.2	2.8	27.1	0.7	11.6	3.8	8.8	1.4
Methane, bromochlorodifluoro–, Halon 1211	Air	11.0	3.0	9.5	15.8	2.9	0.7	4.3	24.4	2.2
Methane, bromotrifluoro–, Halon 1301	Air	46.9	71.0	34.9	39.1	8.6	62.3	33.9	46.1	44.1
Methane, chlorodifluoro–, HCFC–22	Air	10.0	12.9	2.3	2.4	0.5	8.0	38.8	3.4	5.4
Methane, tetrachloro–, CFC–10	Air	24.2	8.8	50.5	15.6	87.2	17.4	19.2	17.4	46.9
Human toxicity (kg 1,4–DB eq)										
Remaining substances		36.4	25.3	49.9	28.5	41.7	63.0	42.5	23.9	64.4
Arsenic, ion	Air	17.8	20.3	13.0	17.1	15.2	8.1	12.2	24.5	11.9
Chromium (VI)	Air	6.4	10.5	12.9	18.4	12.5	6.2	3.4	3.5	4.3
Thallium (I)	Water	33.7	38.5	20.0	32.5	28.1	18.1	24.7	46.6	10.5
Vanadium (V)	Water	5.6	5.3	4.3	3.6	2.5	4.6	17.2	1.5	9.0
Fresh water ecotoxicity (kg 1,4–DB eq)										
Remaining substances		9.4	7.3	13.8	11.5	4.1	8.1	8.3	8.7	23.1

Supplementary informations

Substance %	Compartment	Total	Mulberry leaves	Paper, newsprint	Plastic rays	Chemical disinfectants	Transport	Building	Electricity	Biowaste
Beryllium (II)	Water	8.2	5.0	31.9	17.4	71.2	5.3	11.3	7.4	4.3
Copper, ion	Water	53.1	63.3	17.7	38.4	13.9	57.3	21.4	69.9	27.9
Nickel (II)	Water	10.1	6.0	23.9	15.1	6.5	9.8	13.5	8.4	22.1
Vanadium (V)	Water	19.2	18.4	12.7	17.8	4.2	19.5	45.4	5.6	22.6
Marine acquatic ecotoxicity (kg 1,4–DB eq)										
Remaining substances		15.6	18.8	9.1	12.9	2.1	18.3	8.6	18.2	24.4
Beryllium (II)	Water	35.6	33.1	64.1	48.3	92.4	27.5	34.0	36.7	14.5
Copper, ion	Water	7.9	14.2	1.2	3.6	0.6	10.1	2.2	11.7	3.2
Hydrogen fluoride	Air	22.3	9.6	15.8	22.2	3.1	21.8	28.4	24.1	36.6
Nickel (II)	Water	5.2	4.7	5.6	4.9	1.0	6.0	4.8	4.9	8.8
Vanadium (V)	Water	13.5	19.6	4.1	8.0	0.9	16.3	22.1	4.5	12.4
Terrestrial ecotoxicity (kg 1,4–DB eq)										
Remaining substances		17.4	21.3	42.7	7.7	7.6	18.9	16.3	12.7	10.1
Arsenic, ion	Air	13.5	11.4	2.6	8.0	7.9	6.8	11.8	24.9	9.5
Chromium (III)	Air	42.4	49.8	17.4	67.6	48.7	44.4	33.3	32.5	34.5
Chromium (III)	Soil	8.0	3.8	27.1	6.2	21.3	9.4	11.2	9.9	9.7
Mercury (II)	Air	9.9	9.2	4.3	4.6	9.7	6.3	18.3	7.9	23.3
Vanadium (V)	Air	8.9	4.4	5.9	5.9	4.7	14.2	9.1	12.1	12.9
Photochemical oxidation (kg C_2H_4 eq)										
Remaining substances		19.5	27.7	17.7	28.5	14.6	30.4	10.7	15.0	13.0
Carbon monoxide, biogenic	Air	5.2	16.1	2.1	0.6	1.3	0.2	1.0	1.6	11.2
Carbon monoxide, fossil	Air	20.4	14.0	20.7	15.8	12.7	23.3	32.9	15.4	16.4
Methane, biogenic	Air	7.7	15.7	0.5	0.4	2.9	0.1	0.2	1.3	38.7
Methane, fossil	Air	7.5	4.0	5.7	16.0	11.4	8.3	4.8	11.5	5.7
Pentane	Air	8.0	1.8	2.9	1.5	2.7	6.2	24.7	2.6	3.1
Sulfur dioxide	Air	31.7	20.7	50.4	37.3	54.5	31.6	25.8	52.7	11.8
Acidification (kg SO_2 eq)										
Remaining substances		0.0	0.0	0.0	0.0	0.0	0.0	0.0	0.0	0.0
Ammonia	Air	29.4	1.4	1.6	1.4	1.6	1.6	43.6	3.1	74.0
Nitrogen oxides	Air	27.2	53.2	27.4	25.7	23.9	36.5	23.0	21.6	19.0
Sulfur dioxide	Air	43.4	45.4	71.0	72.8	74.5	61.9	33.4	75.3	7.0
Eutrophication (kg PO_4 eq)										
Remaining substances		6.0	5.6	10.6	4.6	6.0	5.1	2.9	4.6	11.1
Ammonia	Air	10.1	0.1	0.7	1.7	0.7	1.2	33.4	2.6	44.5
COD (Chemical Oxygen Demand)	Water	52.0	84.5	4.9	5.7	9.8	12.5	3.4	1.5	6.2
Nitrogen oxides	Air	11.1	4.8	14.2	36.6	13.4	31.8	21.0	21.5	13.6
Phosphate	Water	20.8	5.0	69.7	51.3	70.0	49.4	39.3	69.7	24.7

References

AIEL. https://www.aielenergia.it/pubblicazioni–agriforenergy. (accessed on November 2023)

Akhtar, T.; Lutfullah, G.; Ullah, Z. Lignonsulfonate–Phenolformaldehyrde Adhesive: A Potential Binder for Wood Panel Industries. J. Chem. Soc. Pakistan **2011**, 33(4), 535–538.

Alamsyah, E.M.; Sutrisno; Nuryawan, A.; Widyorini, R. Identifying best parameters of particleboard bonded with dextrin–based adhesives. Open Agric. **2020**, 5, 345–351. https://doi.org/10.1515/opag–2020–0037.

Alliedmarketresearch. Available online: https://www.alliedmarketresearch.com/bioadhesives–market–A11324 (accessed on 27 May 2022).

Alonso, M. V; Rodrı, J. J.; Oliet, M.; Rodrı, F. Characterization and Structural Modification of Ammonic Lignosulfonate by Methylolation. **2001**, 2661–2668. https://doi.org/10.1002/app.2119.

Altman, G. H.; Farrell, B. D. Sericulture as a Sustainable Agroindustry. Clean. Circ. Bioeconomy **2022**, 2, 100011. https://doi.org/10.1016/j.clcb.2022.100011.

Amaral–Labat, G.; Szczurek, A.; Fierro, V.; Pizzi, A.; Celzard, A. Systematic Studies of Tannin–Formaldehyde Aerogels: Preparation and Properties. Sci. Technol. Adv. Mater. **2013**, 14 (1), 015001. https://doi.org/10.1088/1468–6996/14/1/015001.

Amico, S. D.; Hrabalova, M.; Müller, U.; Berghofer, E. Bonding of Spruce Wood with Wheat Flour Glue — Effect of Press Temperature on the Adhesive Bond Strength. **2010**, 31, 255–260. https://doi.org/10.1016/j.indcrop.2009.11.001.

Ang, A.F.; Ashaari, Z.; Lee, S.H.; Md Tahir, P.; Halis, R. Lignin–based copolymer adhesives for composite wood panels—A review. Int. J. Adhes. Adhes. **2019,** 95, 102408. https://doi.org/10.1016/j.ijadhadh.2019.102408.

Ansell, M. P. Wood Composites. In Handbook of Wood Chemistry and Wood Composites; 2005; pp 281–301. https://doi.org/10.1016/C2014–0–02700–1.

Araújo, C. K. de C.; Salvador, R.; Piekarski, C. M.; Sokulski, C. C.; de Francisco, A. C.; Camargo, S. K. de C. A. Circular Economy Practices on Wood Panels: A Bibliographic Analysis. Sustain. **2019**, 11 (4), 1–21. https://doi.org/10.3390/su11041057.

Arbenz, A.; Avérous, L. Chemical Modification of Tannins to Elaborate Aromatic Biobased Macromolecular Architectures. Green Chem. **2015**, 17 (5), 2626–2646. https://doi.org/10.1039/c5gc00282f.

Arbenz, A.; Avérous, L. Chemical Modification of Tannins to Elaborate Aromatic Biobased Macromolecular Architectures. Green Chemistry. Royal Society of Chemistry May 1, **2015**, pp 2626–2646. https://doi.org/10.1039/c5gc00282f.

Arias, A.; González–García, S.; Feijoo, G.; Moreira, M. T. Environmental Benefits of Soy–Based Bio–Adhesives as an Alternative to Formaldehyde–Based Options. Environ. Sci. Pollut. Res. **2021**, 29781–29794. https://doi.org/10.1007/s11356–021–12766–4.

References

Arias, A.; González–García, S.; Feijoo, G.; Moreira, M.T. Tannin–Based Bio–Adhesives for the Wood Panel Industry as Sustainable Alternatives to Petrochemical Resins. J. Ind. Ecol. **2021**, 26, 627–642. https://doi.org/10.1111/jiec.13210.

Arias, A.; González–García, S.; González–Rodríguez, S.; Feijoo, G.; Moreira, M. T. Cradle–to–Gate Life Cycle Assessment of Bio–Adhesives for the Wood Panel Industry. A Comparison with Petrochemical Alternatives. Sci. Total Environ. **2020**, 738, 140357. https://doi.org/10.1016/j.scitotenv.2020.140357.

Aristri, M.A.; Lubis, M.A.R.; Iswanto, A.H.; Fatriasari, W.; Sari, R.K.; Antov, P.; Gajtanska, M.; Papadopoulos, A.N.; Pizzi, A. Bio–based polyurethane resins derived from tannin: Source, synthesis, characterisation, and application. Forests **2021**, 12, 516. https://doi.org/10.3390/f12111516.

Aristri, M.A.; Lubis, M.A.R.; Yadav, S.M.; Antov, P.; Papadopoulos, A.N.; Pizzi, A.; Fatriasari, W.; Ismayati, M.; Iswanto, A.H. Recent developments in lignin– and tannin–based non–isocyanate polyurethane resins for wood adhesives—A review. Appl. Sci. **2021**, 11, 4242. https://doi.org/10.3390/app11094242.

Aspé, E.; Fernández, K. The Effect of Different Extraction Techniques on Extraction Yield, Total Phenolic, and Anti–Radical Capacity of Extracts from Pinus Radiata Bark. Ind. Crops Prod. **2011**, 34 (1), 838–844. https://doi.org/10.1016/j.indcrop.2011.02.002.

Astudillo, M. F.; Thalwitz, G.; Vollrath, F. Life Cycle Assessment of Indian Silk. J. Clean. Prod. **2014**, 81, 158–167. https://doi.org/10.1016/j.jclepro.2014.06.007.

Astudillo, M. F.; Thalwitz, G.; Vollrath, F. Life Cycle Assessment of Silk Production–a Case Study from India; Elsevier Ltd, **2015**. https://doi.org/10.1016/B978–0–08–100169–1.00011–3.

Auad, P.; Spier, F.; Gutterres, M. Vegetable Tannin Composition and Its Association with the Leather Tanning Effect. Chem. Eng. Commun. **2020**, 207 (5), 722–732. https://doi.org/10.1080/00986445.2019.1618843.

Auad, P.; Spier, F.; Gutterres, M. Vegetable tannin composition and its association with the leather tanning effect. Chem. Eng. Commun. **2020**, 207, 722–732.

Ayestarán, B.; Guadalupe, Z.; León, D. Quantification of Major Grape Polysaccharides (Tempranillo v.) Released by Maceration Enzymes during the Fermentation Process. Anal. Chim. Acta 2004, 513 (1), 29–39. https://doi.org/10.1016/j.aca.**2003**.12.012.

Ayla, C.; Parameswaran, N. Macro– and Microtechnological Studies on Beechwood Panels Bonded with Pinus Brutia Bark Tannin. Holz Roh–Werkst. **1980**, 38, 449–459. https://doi.org/10.1007/BF02610428.

Bacelo, H.; Vieira, B.R.C.; Santos, S.C.R.; Boaventura, R.A.R.; Botelho, C.M.S. Recovery and valorization of tannins from a forest waste as an adsorbent for antimony uptake. J. Clean. Prod. **2018,** 198, 1324–1335.

Bacigalupe, A.; Escobar, M.M. Soy Protein Adhesives for Particleboard Production—A Review. J. Polym. Environ. **2021**, 29, 2033–2045. https://doi.org/10.1007/s10924–020–02036–8.

Bal, B.C.; Bektaþ, Ý. Some Mechanical Properties of Plywood Produced from Eucalyptus, Beech, and Poplar Veneer. Maderas. Cienc. Tecnol. **2014**, 16, 99–108. https://doi.org/10.4067/S0718–221X2014005000009.

Ballerin, A.; Depres, A.; Pizzi, A. Non–Toxic, Zero Emission Tannin–Glyoxal Adhesives for Wood Panels. Holz Roh. Werkst. **2005**, 63, 477–478.

Ballerini, A.; Despres, A.; Pizzi, A. Non–Toxic, Zero Emission Tannin–Glyoxal Adhesives for Wood Panels. Holz als Roh – und Werkst. **2005**, 63 (6), 477–478. https://doi.org/https://doi.org/10.1007/s00107–005–0048–x.

Ballerini, A.; Despres, A.; Pizzi, A. Non–toxic, zero emission tannin–glyoxal adhesives for wood panels. Holz als Roh Werkst. **2005**, 63, 477–478. https://doi.org/10.1007/s00107–005–0048–x.

Barbero–López, A.; Akkanen, J.; Lappalainen, R.; Peräniemi, S.; Haapala, A. Bio–based wood preservatives: Their efficiency, leaching and ecotoxicity compared to a commercial wood preservative. Sci. Total Environ. **2021**, 753, 142013.

Barcelos, S. M. B. D.; Salvador, R.; Barros, M. V.; de Francisco, A. C.; Guedes, G. Circularity of Brazilian Silk: Promoting a Circular Bioeconomy in the Production of Silk Cocoons. J. Environ. Manage. **2021**, 296 (April), 113373. https://doi.org/10.1016/j.jenvman.2021.113373.

Barcelos, S. M. B. D.; Salvador, R.; da Graça Guedes, M.; de Francisco, A. C. Opportunities for Improving the Environmental Profile of Silk Cocoon Production under Brazilian Conditions. Sustain. **2020**, 12 (8). https://doi.org/10.3390/SU12083214.

Bauman, H.; Tillman, A. The Hitch Hiker´s Guide to LCA – An Orientation in LCA Methodology and Application. Int. J. Life Cycle Assess. **2004**, 11 (2), 142–142. https://doi.org/10.1065/lca2006.02.008.

Bekhta, P.; Hiziroglu, S.; Shepelyuk, O. Properties of Plywood Manufactured from Compressed Veneer as Building Material. Mater. Des. **2009**, 30, 947–953. https://doi.org/10.1016/j.matdes.2008.07.001.

Bekhta, P.; Sedliačik, J.; Jones, D. Effect of Short–Term Thermomechanical Densification of Wood Veneers on the Properties of Birch Plywood. Eur. J. Wood Wood Prod. **2018**, 76 (2), 549–562. https://doi.org/10.1007/s00107–017–1233–4.

Benar, P.; Gonçalves, A. R.; Mandelli, D.; Schuchardt, U. Eucalyptus Organosolv Lignins: Study of the Hydroxymethylation and Use in Resols. Bioresour. Technol. **1999**, 68 (1), 11–16. https://doi.org/10.1016/S0960–8524(98)00076–5.

Bernard, J. K. Feed Concentrates : Oilseed and Oilseed Meals. In Reference Module in Food Science; **2016**; pp 349–355. https://doi.org/10.1016/B978–0–08–100596–5.00756–3.

Beyer, G.; Defays, M.; Fischer, M.; Fletcher, J.; de Munck, E.; de Jaeger, F.; Van Riet, C.; Vandeweghe, K.; Wijnendaele, K. Tackle Climate Change—Use Wood; CEI–Bois: Brussels, Belgium, **2011**; p. 84.

Biadała, T.; Czarnecki, R.; Dukarska, D. Water Resistant Plywood of Increased Elasticity Produced from European Wood Species. Wood Res. **2020**, 65 (1), 111–123. https://doi.org/10.37763/wr.1336–4561/65.1.111124.

Biadała, T.; Czarnecki, R.; Dukarska, D. Water Resistant Plywood of Increased Elasticity Produced from European Wood Species. Wood Res. **2020**, 65, 111–124. https://doi.org/10.37763/wr.1336–4561/65.1.111124.

Bianchi, S.; Kroslakova, I.; Janzon, R.; Mayer, I.; Saake, B.; Pichelin, F. Characterization of condensed tannins and carbohydrates in hot water bark extracts of European softwood species. Phytochemistry **2015**, 120, 53–61. https://doi.org/10.1016/j.phytochem.2015.10.006.

Bisanda, E. T. N.; Ogola, W. O.; Tesha, J. V. Characterisation of Tannin Resin Blends for Particle Board Applications. Cem. Concr. Compos. **2003**, 25 (6), 593–598. https://doi.org/10.1016/S0958–9465(02)00072–0.

Bozell, J.J.; Petersen, G.R. Technology Development for the Production of Biobased Products from Biorefinery Carbohydrates—The US Department of Energy's "Top 10" Revisited. Green Chem. **2010,** 12, 539–555. https://doi.org/10.1039/b922014c.

British Standards, BSI Standards Publication Environmental Management — Life Cycle Assessment — Principles and Framework BS EN ISO 14044:2006+A2:2020. Br. Stand. 2006.

British Standards, BSI Standards Publication Environmental Management — Life Cycle Assessment — Principles and Framework BS EN ISO 14040:2006+A1:2020. Br. Stand. 2006.

British Standards, E. B. — Wood–Based Panels—Determination of Density. EN 323. Br. Stand. 2005

British Standards, E. B. Plywood — Bonding Quality — EN 314–1:2004. Br. Stand. 2004.

British Standards, E. B. Wood–Based Panels — Determination of Modulus of Elasticity in Bending and of Bending Strength — EN 310:1993. Br. Stand. 1993.

British Standards, E.B. — Particleboards and Fiberboards — Determination of Tensile Strength Perpendicular to the Plane of Board. BS EN 319:1993. Br. Stand. 1993.

British standards, E.B. — Particleboards and Fiberboards—Determination of Swelling in Thickness after Immersion in Water. BS EN 317:1993; Br. Stand. 1993.

British Standards, E.B. — Particleboards—Specifications. EN 312:2010 . Br. Stand. 2010.

British Standards, E.B. — Plywood—Bonding Quality—Test Methods. EN 314–1: 2005. Br. Stand. 2005.

British Standards, E.B. — Wood Flooring — Determination of Resistance to Indentation–Test Method; EN 1534 : 2010. Br. Stand. 2010.

British Standards, E.B. — Wood–Based Panels—Determination of Modulus of Elasticity in Bending and of Bending Strength. EN 310: 2005. Br. Stand. 2005.

British Standards, E.B. —Plywood—Bonding Quality—Part 2 Requierments. EN 314–2: 2005 Br. Stand. 2005.

Buchwalter, S. L. Polymerization of Furfuryl Acetate in Acetonitrole. J. Polym. Sci. A1. **1985**, 23 (12), 2897–2911. https://doi.org/10.1002/pol.1985.170231202.

Budzinski, M.; Bezama, A.; Thrän, D. Estimating the potentials for reducing the impacts on climate change by increasing the cascade use and extending the lifetime of wood products in Germany. Resour. Conserv. Recycl. X **2020**, 6, 100034.

Butarbutar, T.; Köhl, M.; Neupane, P. R. Harvested Wood Products and REDD+: Looking beyond the Forest Border. Carbon Balance Manag. **2016**, 11 (1). https://doi.org/10.1186/s13021–016–0046–9.

Cabiyo, B.; Fried, J. S.; Collins, B. M.; Stewart, W.; Wong, J.; Sanchez, D. L. Innovative Wood Use Can Enable Carbon–Beneficial Forest Management in California. Proc. Natl. Acad. Sci. U. S. A. **2021**, 118 (49), e2019073118. https://doi.org/10.1073/pnas.2019073118.

Cabral, J.P.; Kafle, B.; Subhani, M.; Reiner, J.; Ashraf, M. Densification of Timber: A Review on the Process, Material Properties, and Application. J. Wood Sci. **2022**, 68, 20. https://doi.org/10.1186/s10086–022–02028–3.

Campo, M.; Pinelli, P.; Romani, A. Hydrolyzable Tannins from Sweet Chestnut Fractions Obtained by a Sustainable and Eco–Friendly Industrial Process. Nat. Prod. Commun. **2016**, 11 (3), 409–415. https://doi.org/10.1177/1934578x1601100323.

Cao, Z.; Chen, X.; Yao, J.; Huang, L.; Shao, Z. The Preparation of Regenerated Silk Fibroin Microspheres. Soft Matter **2007**, 3 (7), 910–915. https://doi.org/10.1039/b703139d.

Carvalho, A. G.; Mori, F. A.; Mendes, R. F.; Zanuncio, A. J. V.; Silva, M. G. da; Mendes, L. M.; De Oliveira Mori, C. L. . Use of Tannin Adhesive from Stryphnodendron Adstringens (Mart.) Coville in the Production of OSB Panels. Eur. J. Wood Prod. **2014**, 72, 425–432.

Carvalho, L.H.; Magalhães, F.D; Ferra, J.M. Formaldehyde emissions from wood–based panels—Testing methods and industrial perspectives. In Formaldehyde: Chemistry, Applications and Role in Polymerization; Nova Science Publishers, Inc.: Hauppauge, NY, USA, 2012.

Ceccarini, M. R.; Palazzi, V.; Salvati, R.; Chiesa, I.; Maria, C. De; Bonafoni, S.; Mezzanotte, P.; Codini, M.; Pacini, L.; Errante, F.; Rovero, P.; Morabito, A.; Beccari, T.; Roselli, L.; Valentini, L. Biomaterial Inks from Peptide–Functionalized Silk Fibers for 3D Printing of Futuristic Wound–Healing and Sensing Materials. **2023**, 24, 947.

Cefarin, N.; Bedolla, D. E.; Surowka, A.; Donato, S.; Sepperer, T.; Tondi, G.; Dreossi, D.; Sodini, N.; Birarda, G.; Vaccari, L. Study of the Spatio–Chemical Heterogeneity of Tannin–Furanic Foams: From 1D FTIR Spectroscopy to 3D FTIR Micro–Computed Tomography. Int. J. Mol. Sci. **2021**, 22 (23). https://doi.org/10.3390/ijms222312869.

Cesprini, E.; Baccini, R.; Urso, T.; Zanetti, M.; Tondi, G. Quebracho–Based Wood Preservatives : Effect of Concentration and Hardener on Timber Properties. coatings **2022**, 12, 568. https://doi.org/https:// doi.org/10.3390/coatings12050568.

Cesprini, E.; Causin, V.; Iseppi, A. De; Zanetti, M.; Marangon, M.; Barbu, M. C.; Tondi, G. Renewable Tannin–Based Adhesive from Quebracho Extract and Furfural for Particleboards. **2022**, 13, 1781.

Cesprini, E.; De Iseppi, A.; Giovando, S.; Tarabra, E.; Zanetti, M.; Primož, Š.; Matteo, M.; Tondi, G. Wood Science and Technology Chemical characterization of cherry (Prunus avium) tannins in comparison with commercial mimosa and chestnut tannin extracts. Wood Sci. Technol. **2022**, 56, 1455–1473. https://doi.org/10.1007/s00226-022-01401-1.

Cesprini, E.; Resente, G.; Causin, V.; Urso, T.; Cavalli, R.; Zanetti, M. Energy Recovery of Glued Wood Waste – A Review. Fuel **2020**, 262, 116520. https://doi.org/10.1016/j.fuel.2019.116520.

Cesprini, E.; Šket, P.; Causin, V.; Zanetti, M. Development of Quebracho (Schinopsis balansae) Tannin–Based Thermoset Resins. Polymers **2021**, 13, 4412. https://doi.org/10.3390/polym13244412.

Cetin, N. S.; Ozmen, N. Use of Organosolv Lignin in Phenol – Formaldehyde Resins for Particleboard Production I . Organosolv Lignin Modified Resins. **2002**, 22, 477–480.

Chatterjee, A.; Rakshit, A.; Singh, N. N. Strategies for the Determination of Bioactive Phenols in Plants, Fruit and Vegetables. J. Chromatogr. A **2003**, 1000, 657–691. https://doi.org/10.1007/978–3–642–33965–3_2.

Chen, C. X.; Pierobon, F.; Ganguly, I. Life Cycle Assessment (LCA) of Cross–Laminated Timber (CLT) Produced in Western Washington: The Role of Logistics and Wood Species Mix. Sustain. **2019**, 11 (5). https://doi.org/10.3390/su11051278.

Chen, J.; Ter–Mikaelian, M. T.; Yang, H.; Colombo, S. J. Assessing the Greenhouse Gas Effects of Harvested Wood Products Manufactured from Managed Forests in Canada. Forestry **2018**, 91 (2), 193–205. https://doi.org/10.1093/forestry/cpx056.

Chen, X.; Pizzi, A.; Zhang, B.; Zhou, X.; Fredon, E.; Gerardin, C.; Du, G. Particleboard bio–adhesive by glyoxalated lignin and oxidized dialdehyde starch crosslinked by urea. Wood Sci. Technol. **2022**, 56, 63–85. https://doi.org/10.1007/s00226–021–01344–z.

Chen, X.; Yang, Z.; Yang, F.; Pizzi, A.; Essawy, H.; Du, G.; Zhou, X. Development of Easy–Handling, Formaldehyde–Free, High–Bonding Performance Bio–Sourced Wood Adhesives by Co–Reaction of Furfuryl Alcohol and Wheat Gluten Protein. Chem. Eng. J. **2022**, 462, 142161. https://doi.org/10.2139/ssrn.4281052.

Cheng, H. N.; Ford, C.; Dowd, M. K.; He, Z. Use of Additives to Enhance the Properties of Cottonseed Protein as Wood Adhesives. Int. J. Adhes. Adhes. **2016**, 68, 156–160. https://doi.org/10.1016/j.ijadhadh.2016.02.012.

Cheng, S.; Yuan, Z.; Leitch, M.; Anderson, M.; Xu, C.C. Highly efficient de–polymerization of organosolv lignin using a catalytic hydrothermal process and production of phenolic resins/adhesives with the depolymerized lignin as a substitute for phenol at a high substitution ratio. Ind. Crops Prod. **2013**, 44, 315–322. https://doi.org/10.1016/j.indcrop.2012.10.033.

Cherubini, F.; Strømman, A. H. Bioresource Technology Life Cycle Assessment of Bioenergy Systems : State of the Art and Future Challenges. Bioresour. Technol. **2011**, 102 (2), 437–451. https://doi.org/10.1016/j.biortech.2010.08.010.

Choura, M.; Belgacem, N. M.; Gandini, A. Acid–Catalyzed Polycondensation of Furfuryl Alcohol: Mechanisms of Chromophore Formation and Cross–Linking. Macromolecules **1996**, 29 (11), 3839–3850. https://doi.org/10.1021/ma951522f.

Choura, M.; Belgacem, N. M.; Gandini, A. The Acid–Catalyzed Polycondensation of Furfuryl Alcohol: Old Puzzles Unravelled. Macromol. Symp. **1997**, 122, 263–268. https://doi.org/10.1002/masy.19971220141.

Churkina, G.; Organschi, A.; Reyer, C.P.O.; Ruff, A.; Vinke, K.; Liu, Z.; Reck, B.K.; Graedel, T.E.; Schellnhuber, H.J. Buildings as a Global Carbon Sink. Nat. Sustain. **2020**, 3, 269–276. https://doi.org/10.1038/s41893–019–0462–4.

Ciabattini, S.; Raggi, V.; Valentini, L.; Morabito, A. Silk Fibroin Hybrids for Biological Scaffolds with Adhesive Surface and Adaptability to the Target Tissue Change. Eurobiotech J. **2023**, 7 (1), 75–86. https://doi.org/10.2478/ebtj–2023–0005.

CIEL. Plastic & Climate: The Hidden Costs of a Plastic Planet; 2019.

Climate Action Tracker, 'Global Update: Governments Still Showing Little Sign of Acting on Climate Crisis https://climateactiontracker.org/publications/governments–still–not–acting–on–climate–crisis/ (accessed 2023 –10 –09).

Confente, I.; Scarpi, D.; Russo, I. Marketing a new generation of bio–plastics products for a circular economy: The role of green self–identity, self–congruity, and perceived value. J. Bus. Res. **2020**, 112, 431–439.

Conley, R. .; Metil, I. An Investigation of the Structure of Furfuryl Alcohol Polycondensates with Infrared Spectroscopy; Reinhold Publishing Corporation, New York, **1963**. https://doi.org/10.1002/app.1963.070070104.

Cook, N. C.; Samman, S. Flavonoids – Chemistry, Metabolism, Cardioprotective Effects, and Dietary Sources. J. Nutr. Biochem. **1996**, 7 (2), 66–76. https://doi.org/10.1016/0955–2863(95)00168–9.

Corradini, G.; Pierobon, F.; Zanetti, M. Product Environmental Footprint of a Cross–Laminated Timber System: A Case Study in Italy. **2019**, 24 (5), 975–988. https://doi.org/10.1007/s11367–018–1541–x.

CREA. Relazione Finale Progetto Biosegen – Unità Di Ricerca Di Apicoltura e Bachicoltura.

D'Amico, B.; Pomponi, F.; Hart, J. Global Potential for Material Substitution in Building Construction: The Case of Cross Laminated Timber. J. Clean. Prod. **2021**, 279, 123487. https://doi.org/10.1016/j.jclepro.2020.123487.

D'Amico, F.; Musso, M. E.; Berger, R. J. F.; Cefarin, N.; Birarda, G.; Tondi, G.; Bertoldo Menezes, D.; Reyer, A.; Scarabattoli, L.; Sepperer, T.; Schnabel, T.; Vaccari, L. Chemical Constitution of Polyfurfuryl Alcohol Investigated by FTIR and Resonant Raman Spectroscopy. Spectrochim. Acta – Part A Mol. Biomol. Spectrosc. **2021**, 262 (June), 120090. https://doi.org/10.1016/j.saa.2021.120090.

Daigneault, A.; Baker, J. S.; Guo, J.; Lauri, P.; Favero, A.; Forsell, N.; Johnston, C.; Ohrel, S. B.; Sohngen, B. How the Future of the Global Forest Sink Depends on Timber Demand, Forest Management, and Carbon Policies. Glob. Environ. Chang. **2022**, 76, 102582. https://doi.org/10.1016/j.gloenvcha.2022.102582.

Dalgaard, R.; Schmidt, J.; Halberg, N.; Christensen, P.; Thrane, M.; Pengue, W. a. LCA for Food Products: Case Study LCA of Soybean Meal. LCA Food Prod. **2008**, 10 (7), 240–254.

Danielson, B.; Simonson, R. Journal of Adhesion Science and Kraft Lignin in Phenol Formaldehyde Resin . Part 1 . Partial Replacement of Phenol by Kraft Lignin in Phenol Formaldehyde Adhesives for Plywood. J. Adhes. Sci. Technol. **1998**, 12 (9), 923–939. https://doi.org/10.1163/156856198X00542.

Davis, A. L.; Cai, Y.; Davies, A. P.; Lewis, J. R. 1H and 13C NMR Assignments of Some Green Tea Polyphenols. Magn. Reson. Chem. **1996**, 34 (11), 887–890. https://doi.org/10.1002/(SICI)1097–458X(199611)34:11<887::AID–OMR995>3.0.CO;2–U.

De Carvalho Araújo, C.K.; Salvador, R.; Piekarski, C.M.; Sokulski, C.C.; de Francisco, A.C.; Camargo, S.K. de C.A. Circular economy practices on wood panels: A bibliographic analysis. Sustainability **2019**, 11, 1057. https://doi.org/10.3390/su11041057.

De Iseppi, A.; Marangon, M.; Lomolino, G.; Crapisi, A.; Curioni, A. Red and white wine lees as a novel source of emulsifiers and foaming agents. LWT **2021**, 152, 112273. https://doi.org/10.1016/j.lwt.2021.112273.

De Iseppi, A.; Marangon, M.; Vincenzi, S.; Lomolino, G.; Curioni, A.; Divol, B. A Novel Approach for the Valorization of Wine Lees as a Source of Compounds Able to Modify Wine Properties. Lwt **2021**, 136 (P1), 110274. https://doi.org/10.1016/j.lwt.2020.110274.

De Palacios, P.; Fernández, F.G.; García–Iruela, A.; González–Rodrigo, B.; Esteban, L.G. Study of the influence of the physical properties of particleboard type P2 on the internal bond of panels using artificial neural networks. Comput. Electron. Agric. **2018**, 155, 142–149. https://doi.org/10.1016/j.compag.2018.10.012.

De Rosso, M.; Marangon, M.; Flamini, R. Characterization of Ellagitannins and Oak Lactone Precursors in Oak Wood–Aged Grappa by High–Resolution Mass Spectrometry. J. Mass Spectrom. **2020**, 55 (7), 4472. https://doi.org/10.1002/jms.4472.

Dhawale, P. V.; Vineeth, S. K.; Gadhave, R. V.; Fatima M. J., J.; Supekar, M. V.; Thakur, V. K.; Raghavan, P. Tannin as a Renewable Raw Material for Adhesive Applications: A Review. Mater. Adv. **2022**. https://doi.org/10.1039/d1ma00841b.

Dieste, A.; Krause, A.; Bollmus, S.; Militz, H. Physical and Mechanical Properties of Plywood Produced with 1.3–Dimethylol– 4.5–Dihydroxyethyleneurea (DMDHEU)–Modified Veneers of Betula sp. and Fagus Sylvatica. Holz Roh–Werkst. **2008**, 66, 281–287. https://doi.org/10.1007/s00107–008–0247–3.

DIN 68705–5; Sperrholz Teil 5—Bau–Furniersperrholz aus Buche. Deutsches Institut für Normung: Berlin, Germany, 1980.

Domenech, T.; Bahn–walkowiak, B. Transition towards a Resource Efficient Circular Economy in Europe: Policy Lesson from the EU and the Members States. Ecol. Econ. **2017**, 155, 7–19. https://doi.org/10.1016/j.ecolecon.2017.11.001.

Domke, G. M.; Oswalt, S. N.; Walters, B. F.; Morin, R. S. Tree Planting Has the Potential to Increase Carbon Sequestration Capacity of Forests in the United States. Proc. Natl. Acad. Sci. U. S. A. **2020**, 117 (40), 24649–24651. https://doi.org/10.1073/pnas.2010840117.

Dong, Y.; Yan, Y.; Wang, K.; Li, J.; Zhang, S.; Xia, C.; Cai, L. Improvement of water resistance, dimensional stability, and mechanical properties of poplar wood by rosin impregnation. Eur. J. Wood Wood Prod. **2016**, 74, 177–184.

Drewes, S.; Roux, D. Condensed Tannins. 15. Interrelationships of Flavonoid Components in Wattle–Bark Extract. Biochem. J. **1963**, 87 (1), 167–172. https://doi.org/10.1042/bj0870167.

Dunky, M. Adhesives in the wood industry. In Handbook of Adhesive Technology, 3rd ed.; Springer: Berlin/Heidelberg, Germany, 2003; pp. 223–262, ISBN 9781498736473.

Dunky, M. Adhesives in the Wood Industry. In Handbook of Adhesive Technology, Third Edition; 2003; pp 223–262. https://doi.org/10.1201/9781315120942.

Dunky, M. Wood Adhesives Based on Natural Resources: A Critical Review: Part III. Tannin– and Lignin–Based Adhesives. Prog. Adhes. Adhes. Vol. 6 **2021**, 6, 383–530. https://doi.org/10.1002/9781119846703.ch10.

Eckardt, J.; Neubauer, J.; Sepperer, T.; Donato, S.; Zanetti, M.; Cefarin, N.; Vaccari, L.; Lippert, M.; Wind, M.; Schnabel, T.; Petutschnigg, A.; Tondi, G. Synthesis and Characterization of High–Performing Sulfur–Free Tannin Foams. Polymers (Basel). **2020**, 12 (3). https://doi.org/10.3390/polym12030564.

Ecoinvent. Allocation Cut–Off by Classification. 2019. Available online: http://www.ecoinvent.org/database/ system–models–in–ecoinvent–3/cut–off–system–model/allocation–cut–off–by–classification.html (accessed on 24 November 2023).

El Mansouri, N.E.; Pizzi, A.; Salvadó, J. Lignin–based wood panel adhesives without formaldehyde. Holz als Roh Werkst. **2007**,65, 65–70. https://doi.org/10.1007/s00107–006–0130–z.

El–Sayed, E. S.; El–Sakhawy, M.; Kamel, S.; El–Gendy, A.; Abou–Zeid, R. E. Eco–Friendly Mimosa Tannin Adhesive System for Bagasse Particleboard Fabrication. Egypt.J.Chem **2019**, 65 (5), 1–12. https://doi.org/10.21608/ejchem.2018.5413.1479.

Engozogho Anris, S.P.; Bikoro Bi Athomo, A.; Safou–Tchiama, R.; Leroyer, L.; Vidal, M.; Charrier, B. Development of Green Adhesives for Fiberboard Manufacturing, Using Okoume Bark Tannins and Hexamine–Characterization by 1H NMR, TMA, TGA and DSC Analysis. J. Adhes. Sci. Technol. **2021**, 35, 436–449. https://doi.org/10.1080/01694243.2020.1808356.

Esteves, B.; Nunes, L.; Domingos, I.; Pereira, H. Improvement of termite resistance, dimensional stability and mechanical properties of pine wood by paraffin impregnation. Eur. J. Wood Wood Prod. **2014**, 72, 609–615.

European Commission–Joint Research Center. COMMISSION RECOMMENDATION (EU) 2021/2279 of 15 December 2021 on the Use of the Environmental Footprint Methods to Measure and Communicate the Life Cycle Environmental Performance of Products and Organisations. Off. J. Eur. Union L 471/1 2021

European Environment Agency. Trends and Projections in Europe 2018. Tracking Progress towards Europe's Climate and Energy Targets; **2018**. https://doi.org/10.2800/931891.

Falcão, L.; Araújo, M. E. M. Application of ATR–FTIR Spectroscopy to the Analysis of Tannins in Historic Leathers: The Case Study of the Upholstery from the 19th Century Portuguese Royal Train. Vib. Spectrosc. **2014**, 74, 98–103. https://doi.org/10.1016/j.vibspec.2014.08.001.

Falcão, L.; Araújo, M. E. M. Vegetable Tannins Used in the Manufacture of Historic Leathers. Molecules **2018**, 23, 8–10. https://doi.org/10.3390/molecules23051081.

Falco, G.; Guigo, N.; Vincent, L.; Sbirrazzuoli, N. Opening Furan for Tailoring Properties of Bio–Based Poly(Furfuryl Alcohol) Thermoset. ChemSusChem **2018**, 11 (11), 1805–1812. https://doi.org/10.1002/cssc.201800620.

FAOSTAT—Food Food and Agriculture Organization of the United Nations. 2017. Available online: http: //www.fao.org/faostat/en/#country (accessed on June 2022).

Ferdosian, F.; Pan, Z.; Gao, G.; Zhao, B. Bio–Based Adhesives and Evaluation for Wood Composites Application. Polymers (Basel). **2017**, 9 (2). https://doi.org/10.3390/polym9020070.

Ferrández–García, C.E.; Ferrández–García, A.; Ferrández–Villena, M.; Hidalgo–Cordero, J.F.; García–Ortuño, T.; Ferrández– García, M.T. Physical and mechanical properties of particleboard made from palm tree prunings. Forests **2018**, 9, 755. https://doi.org/10.3390/f9120755.

Ferreira, É.D.S.; Lelis, R.C.C.; Brito, E.D.O.; Iwakiri, S. Use of Tannin from Pinus oocarpa Bark for Manufacture of Plywood. In Proceedings of the LI International Convention of Society of Wood Science and Technology, Concepción, Chile, 10–12 November **2008**; pp. 10–12.

Food and Agriculture Organization of the United Nations. Forest Products Annual Market Review 2018–2019; United Nations Publication: Herndon, VA, USA, **2019**.

Forster, E. J.; Healey, J. R.; Dymond, C.; Styles, D. Commercial Afforestation Can Deliver Effective Climate Change Mitigation under Multiple Decarbonisation Pathways. Nat. Commun. **2021**, 12 (1), 1–12. https://doi.org/10.1038/s41467–021–24084–x.

Frihart, C.R. Wood adhesives: Past, present, and future. For. Prod. J. **2015**, 65, 4–8. https://doi.org/10.13073/65.1–2.4.

Galiñanes, C.; Freire, M. S.; González–Álvarez, J. Antioxidant Activity of Phenolic Extracts from Chestnut Fruit and Forest Industries Residues. Eur. J. Wood Wood Prod. **2015**, 73 (5), 651–659. https://doi.org/10.1007/s00107–015–0936–7.

Gandini, A. Polymers from Renewable Resources: A Challenge for the Future of Macromolecular Materials. Macromolecules **2008**, 41 (24), 9491–9504. https://doi.org/10.1021/ma801735u.

Garro Galvez, J.M.; Riedl, B.; Conner, A.H. Analytical studies on tara tannins. Holzforschung **1997**, 51, 235–243. https://doi.org/10.1515/hfsg.1997.51.3.235.

Gaugler, M.; Grigsby, W. J. Thermal Degradation of Condensed Tannins from Radiata Pine Bark. J. Wood Chem. Technol. **2009**, 29 (4), 305–321. https://doi.org/10.1080/02773810903165671.

Ghaffar, S. H.; Fan, M. Lignin in Straw and Its Applications as an Adhesive. Int. J. Adhes. Adhes. **2014**, 48, 92–101. https://doi.org/10.1016/j.ijadhadh.2013.09.001.

Ghahri, S.; Pizzi, A. Improving soy–based adhesives for wood particleboard by tannins addition. Wood Sci. Technol. **2018**, 52, 261–279. https://doi.org/10.1007/s00226–017–0957–y.

Ghahri, S.; Pizzi, A.; Hajihassani, R. A Study of Concept to Prepare Totally Biosourced Wood Adhesives from Only Soy Protein and Tannin. Polymers **2022**, 14, 1150. https://doi.org/10.3390/polym14061150.

Giacosa, S.; Parpinello, G. P.; Río Segade, S.; Ricci, A.; Paissoni, M. A.; Curioni, A.; Marangon, M.; Mattivi, F.; Arapitsas, P.; Moio, L.; Piombino, P.; Ugliano, M.; Slaghenaufi, D.; Gerbi, V.; Rolle, L.; Versari, A. Diversity of Italian Red Wines: A Study by Enological Parameters, Color, and Phenolic Indices. Food Res. Int. **2021**, 143 , 110277. https://doi.org/10.1016/j.foodres.2021.110277.

Gillet, S.; Aguedo, M.; Petitjean, L.; Morais, A.R.C.; Da Costa Lopes, A.M.; Łukasik, R.M.; Anastas, P.T. Lignin transformations for high value applications: Towards targeted modifications using green chemistry. Green Chem. **2017**, 19, 4200–4233. https://doi.org/10.1039/c7gc01479a.

Gindl, W.; Müller, U.; Teischinger, A. Transverse compression strength and fracture of spruce wood modified by melamine– formaldehyde impregnation of cell walls. Wood Fiber Sci. **2003**, 35, 239–246.

Glasser, W. G. About Making Lignin Great Again—Some Lessons From the Past. Front. Chem. **2019**, 7, 1–17. https://doi.org/10.3389/fchem.2019.00565.

Glassner, D. A.; Gruber, P. R.; Vink, E. T. H.; Ra, K. R. Applications of Life Cycle Assessment to NatureWorks TM Polylactide (PLA) Production. **2003**, 80, 403–419. https://doi.org/10.1016/S0141–3910(02)00372–5.

Gonultas, O. Properties of Pine Bark Tannin–Based Adhesive Produced with Various Hardeners. BioResources **2018**, 13 (4), 9066–9078. https://doi.org/10.15376/BIORES.13.4.9066–9078.

Gonzalez, V.; Lou, X.; Chi, T. Evaluating Environmental Impact of Natural and Synthetic Fibers: A Life Cycle Assessment Approach. Sustain. **2023**, 15 (9). https://doi.org/10.3390/su15097670.

Gu, K.; Huang, J.; Li, K. Preparation and evaluation of particleboard bonded with a soy flour–based adhesive with a new curing agent. J. Adhes. Sci. Technol. **2013**, 27, 2053–2064. https://doi.org/10.1080/01694243.2012.696950.

Gu, K.; Li, K. Preparation and evaluation of particleboard with a soy flour– polyethylenimine–maleic anhydride adhesive. J. Am. Oil Chem. Soc. **2011**, 88, 673–679. https://doi.org/10.1007/s11746–010–1706–7.

Guerrero, E. D.; Chinnici, F.; Natali, N.; Marín, R. N.; Riponi, C. Solid–Phase Extraction Method for Determination of Volatile Compounds in Traditional Balsamic Vinegar. J. Sep. Sci. **2008,** 31 (16–17), 3030–3036. https://doi.org/10.1002/jssc.200800307.

Hăbeanu, M.; Gheorghe, A.; Mihalcea, T. Silkworm Bombyx Mori—Sustainability and Economic Opportunity, Particularly for Romania. Agriculture **2023**, 13 (6), 1209. https://doi.org/10.3390/agriculture13061209.

Hafiz, N. L. M.; Tahir, P. M. D.; Hua, L. S.; Abidin, Z. Z.; Sabaruddin, F. A.; Yunus, N. M.; Abdullah, U. H.; Abdul Khalil, H. P. S. Curing and Thermal Properties of Co–Polymerized Tannin Phenol–

Formaldehyde Resin for Bonding Wood Veneers. J. Mater. Res. Technol. **2020**, 9 (4), 6994–7001. https://doi.org/10.1016/j.jmrt.2020.05.029.

Hagerman, A. E.; Zhao, Y.; Johnson, S. Methods for Determination of Condensed and Hydrolyzable Tannins; **1997**; Vol. 662. https://doi.org/10.1021/bk–1997–0662.ch012.

Hani, U.; Abdullah, B. Tannin–Furfuryl Alcohol Wood Panel Adhesives without Formaldehyde. **2013**, 71, 131–132 https://doi.org/10.1007/s00107–012–0629–4.

Harbertson, J. F.; Parpinello, G. P.; Heymann, H.; Downey, M. O. Impact of Exogenous Tannin Additions on Wine Chemistry and Wine Sensory Character. Food Chem. **2012**, 131 (3), 999–1008. https://doi.org/10.1016/j.foodchem.2011.09.101.

Haslam, E. Practical Polyphenolics: From Structure to Molecular Recognition and Physiological Action. Cambridge University Press, **1998**.

Hauptt, R.A.; Sellers, T. Characterizations of Phenol–Formaldehyde Resol Resins. Ind. Eng. Chem. Res. **1994,** 33, 693–697. https://doi.org/10.1021/ie00027a030.

Heinrich, L.A. Future Opportunities for Bio–Based Adhesives–Advantages beyond Renewability. Green Chem. **2019**, 21, 1866–1888. https://doi.org/10.1039/c8gc03746a.

Hemmilä, V.; Adamopoulos, S.; Karlsson, O.; Kumar, A. Development of Sustainable Bio–Adhesives for Engineered Wood Panels–A Review. RSC Adv. **2017**, 7 (61), 38604–38630. https://doi.org/10.1039/c7ra06598a.

Heredia, J.B.; Martín, J.S. Removing heavy metals from polluted surface water with a tannin–based flocculant agent. J. Hazard. Mater. **2009**, 165, 1215–1218.

Hernes, P.J.; Hedges, J.I. Tannin signatures of barks, needles, leaves, cones, and wood at the molecular level. Geochim. Cosmochim. Acta **2004**, 68, 1293–1307. https://doi.org/10.1016/j.gca.2003.09.015.

Hildebrandt, J.; Hagemann, N.; Thrän, D. The contribution of wood–based construction materials for leveraging a low carbon building sector in Europe. Sustain. Cities Soc. **2017**, 34, 405–418.

Hill, C.; Hughes, M.; Gudsell, D. Environmental impact of wood modification. Coatings. **2021**, 11, 366.

Hoong, Y. B.; Paridah, M. T.; Luqman, C. A.; Koh, M. P.; Loh, Y. F. Fortification of Sulfited Tannin from the Bark of Acacia Mangium with Phenol – Formaldehyde for Use as Plywood Adhesive. **2009**, 30, 416–421. https://doi.org/10.1016/j.indcrop.2009.07.012.

Hrázský, J.; Král, P. Assessing the Bending Strength and Modulus of Elasticity in Bending of Exterior Foiled Plywoods in Relation to Their Construction. J. For. Sci. **2005**, 51, 77–94. https://doi.org/10.17221/4546–jfs.

Hu, J.; Thevenon, M.F.; Palanti, S.; Tondi, G. Tannin–caprolactam and Tannin–PEG formulations as outdoor wood preservatives: Biological properties. Ann. For. Sci. **2017**, 74, 1–9.

Hudiburg, T. W.; Law, B. E.; Moomaw, W. R.; Harmon, M. E.; Stenzel, J. E. Meeting GHG Reduction Targets Requires Accounting for All Forest Sector Emissions. Environ. Res. Lett. **2019**, 14 (9). https://doi.org/10.1088/1748–9326/ab28bb.

Hussein, A. S.; Ibrahim, K. I.; Abdulla, K. . Tannin–Phenol Formaldehyde Resins as Binders for Cellulosic Fibers: Mechanical Properties. Nat. Resour. **2011**, 2, 98–101.

Imam, S. H.; Mao, L.; Diego, S.; Chen, L.; Greene, R. V. Wood Adhesive from Crosslinked Poly (Vinyl Alcohol) and Partially Gelatinized Starch : Preparation and Properties. Starch/Stärke **1999**, 51 (6), 225–229.

International Organization for Standardization. Physical and Mechanical Properties of Wood—Test Methods for Small Clear Wood Specimens—Part 2: Determination of Density for Physical and Mechanical Tests; ISO 13061–2:2014; International Organization for Standardization: Geneva, Switzerland, 2014.

Iordan, C. M.; Hu, X.; Arvesen, A.; Kauppi, P.; Cherubini, F. Contribution of Forest Wood Products to Negative Emissions: Historical Comparative Analysis from 1960 to 2015 in Norway, Sweden and Finland. Carbon Balance Manag. **2018**, 13 (1). https://doi.org/10.1186/s13021–018–0101–9.

Irbe, I.; Sable, I.; Noldi, G.; Grinfelds, U.; Jansons, A.; Treimanis, A.; Koch, G. Wood and tracheid properties of Norway Spruce (Picea abies (L.) Karst) clones Grown on former agricultural land in Latvia. Balt. For. **2015**, 21, 114–123.

Irle, M.; Barbu, M.C. Wood–Based Panels: An Introduction for Specialists. Thoemen, M., Irle, M., Sernek, M., Eds.; Cost Action E49; Brunel University Press: London, UK, 2010; pp. 1–94.

Irman, N.; Abd Latif, N. H.; Brosse, N.; Gambier, F.; Syamani, F. A.; Hussin, M. H. Preparation and Characterization of Formaldehyde–Free Wood Adhesive from Mangrove Bark Tannin. Int. J. Adhes. Adhes**. 2022**, 114, 103094. https://doi.org/10.1016/j.ijadhadh.2022.103094.

Iswanto, A.H.; Febrianto, F.; Hadi, Y.S.; Ruhendi, S.; Hermawan, D. The Effect of Pressing Temperature and Time on the Quality of Particle Board Made from Jatropha Fruit Hulls Treated in Acidic Condition. MAKARA J. Technol. Ser. **2014**, 17, 8. https://doi.org/10.7454/mst.v17i3.2930.

Iždinský, J.; Vidholdová, Z.; Reinprecht, L. Particleboards from recycled wood. Forests **2020**, 11, 1166. https://doi.org/10.3390/f11111166.

Jaski, A. C.; Schmitz, F.; Horta, R. P.; Cadorin, L.; Silva, B.; Andreaus, J.; Paes, M. C.; Riegel–Vidotti, I.; Zimmermann, L. Zein – a Plant–Based Material of Growing Importance: New Perspectives for Innovative Uses. Ind. Crops Prod. **2022**, 186, 115250. https://doi.org/10.1016/j.indcrop.2022.115250.

Jones–Moore, H.R.; Jelley, R.E.; Marangon, M.; Fedrizzi, B. The interactions of wine polysaccharides with aroma compounds, tannins, and proteins, and their importance to winemaking. Food Hydrocoll. **2021**, 123, 107150.

Jorda, J.; Cesprini, E.; Barbu, M.–C.; Tondi, G.; Zanetti, M.; Král, P. Quebracho Tannin Bio–Based Adhesives for Plywood. Polymers **2022**, 14, 2257. https://doi.org/10.3390/polym14112257.

Jorda, J.; Kain, G.; Barbu, M. C.; Petutschnigg, A.; Král, P. Influence of Adhesive Systems on the Mechanical and Physical Properties of Flax Fiber Reinforced Beech Plywood. Polymers (Basel). **2021**, 13 (18), 1–15. https://doi.org/10.3390/polym13183086.

Jorda, J.; Kain, G.; Barbu, M.–C.; Köll, B.; Petutschnigg, A.; Král, P. Mechanical Properties of Cellulose and Flax Fiber Unidirectional Reinforced Plywood. Polymers **2022**, 14, 843. https://doi.org/10.3390/polym14040843.

Jorda, J.; Kain, G.; Barbu, M.–C.; Petutschnigg, A.; Král, P. Influence of Adhesive Systems on the Mechanical and Physical Properties of Flax Fiber Reinforced Beech Plywood. Polymers **2021**, 13, 3086. https://doi.org/10.3390/polym13183086.

Kabbour, M.; Luque, R. Furfural as a Platform Chemical: From Production to Applications. In Biomass, Biofuels, Biochemicals—Recent Advances in Development of Platform Chemicals; Saravanamurugan, S., Pandey, A., Riisager, A., Eds.; Elsevier B.V.: Amsterdam, The Netherlands, **2020**. https://doi.org/10.1016/B978–0–444–64307–0.00010–X.

Kain, G.; Güttler, V.; Lienbacher, B.; Barbu, M.C.; Petutschnigg, A.; Richter, K.; Tondi, G. Effects of different flavonoid extracts in optimizing tannin–glued bark insulation boards. Wood Fiber Sci. **2015,** 47, 258–269.

Kane, S.N.; Mishra, A.; Dutta, A.K. Synthesis of Furfural from Water Hyacinth (Eichornia croassipes) This. Mater. Sci. Eng. **2017**, 172, 012027. https://doi.org/10.1088/1742–6596/755/1/011001.

Kapen, P. T.; Tenkeu, M. N.; Yadjie, E.; Tchuen, G. Production and Characterization of Environmentally Friendly Charcoal Briquettes Obtained from Agriculture Waste: Case of Cameroon. Int. J. Environ. Sci. Technol. 2021. https://doi.org/10.1007/s13762–021–03497–7.

Karnjanapratum, S.; Kaewthong, P.; Indriani, S.; Petsong, K.; Takeungwongtrakul, S. Characteristics and Nutritional Value of Silkworm (Bombyx Mori) Pupae–Fortified Chicken Bread Spread. Sci. Rep. **2022**, 12 (1), 1–12. https://doi.org/10.1038/s41598–022–05462–x.

Kashiwada, Y.; Nonaka, G.I.; Nishioka, I.; Chang, J.J.; Lee, K.H. Antitumors agents, 1290 . Tannins and related compounds as selective cytotoxic agents. J. Nat. Prod. **1992**, 55, 1033–1043.

Katalinić, V.; Možina, S. S.; Skroza, D.; Generalić, I.; Abramovič, H.; Miloš, M.; Ljubenkov, I.; Piskernik, S.; Pezo, I.; Terpinc, P.; Boban, M. Polyphenolic Profile, Antioxidant Properties and Antimicrobial Activity of Grape Skin Extracts of 14 Vitis Vinifera Varieties Grown in Dalmatia (Croatia). Food Chem. **2010**, 119, 715–723. https://doi.org/10.1016/j.foodchem.2009.07.019.

Kim, K.H.; Jahan, S.A.; Lee, J.T. Exposure to formaldehyde and its potential human health Hazards. J. Environ. Sci. Health Part C Environ. Carcinog. Ecotoxicol. Rev. **2011**, 29, 277–299. https://doi.org/10.1080/10590501.2011.629972.

Kirby, K.S.; White, T. Minor constituents of Quebracho tannin extract. Biochem. J. **1995**, 60, 582.

Klaric´, S.; Obucˇina, M. New Trends in Engineering Wood Technologies. Lect. Notes Netw. Syst. **2020**, 76, 712–727. https://doi.org/10.1007/978–3–030–18072–0_83.

Koh, L.; Cheng, Y.; Teng, C.; Khin, Y.; Loh, X.; Tee, S.; Low, M.; Ye, E.; Yu, H.; Zhang, Y.; Han, M. Structures, Mechanical Properties and Applications of Silk Fibroin Materials. Prog. Polym. Sci. **2015**, 46, 86–110. https://doi.org/10.1016/j.progpolymsci.2015.02.001.

Konai, N.; Raidandi, D.; Pizzi, A.; Girods, P.; Lagel, M.C.; Kple, M. Thermogravimetric analysis of anningre tannin resin. Madera. Cienc. Tecnol. **2016**, 18, 245–252.

Konai, N.; Raidandi, D.; Pizzi, A.; Meva'a, L. Characterization of Ficus Sycomorus Tannin Using ATR–FT MIR, MALDI–TOF MS and 13C NMR Methods. Eur. J. Wood Wood Prod. **2017**, 75 (5), 807–815. https://doi.org/10.1007/s00107–017–1177–8.

Kong, L.; Guan, H.; Wang, X. In Situ Polymerization of Furfuryl Alcohol with Ammonium Dihydrogen Phosphate in Poplar Wood for Improved Dimensional Stability and Flame Retardancy. ACS Sustain. Chem. Eng. **2018**, 6 (3), 3349–3357. https://doi.org/10.1021/acssuschemeng.7b03518.

Koopmann, A. K.; Malfait, W. J.; Sepperer, T.; Huesing, N. A Systematic Study on Bio–Based Hybrid Aerogels Made of Tannin and Silica. Materials (Basel). **2021**, 14 (18). https://doi.org/10.3390/ma14185231.

Kotar, A.; Kotar, M.; Sket, P.; Plavec, J. Potential of Solid–State NMR and SEM in Characterization of Tablets of Ibuprofen. Curr. Pharm. Anal. **2014**, 11, 124–130. https://doi.org/10.2174/1573412910666141111231325.

Kretschmann, D. Mechanical properties of wood. In Wood Handbook: Wood as an Engineering Material; Centennial Edition; General Technical Report FPL; GTR–190; Department of Agriculture, Forest Service, Forest Products Laboratory: Madison, WI, USA, **2010**; Chapter 5; pp. 5.1–5.46.

Kristak, L.; Antov, P.; Bekhta, P.; Lubis, M.A.R.; Iswanto, A.H.; Reh, R.; Sedliacik, J.; Savov, V.; Taghiyari, H.R.; Papadopoulos, A.N.; et al. Recent Progress in Ultra–Low Formaldehyde Emitting Adhesive Systems and Formaldehyde Scavengers in Wood–Based Panels: A Review. Wood Mater. Sci. Eng. **2022**. https://doi.org/10.1080/17480272.2022.2056080.

Kryn, J.M. Quebracho, Quebracho Colorado, Quebracho Macho: Schinopsis Lorentzii Engl. and Schinopsis balansae Engl., Family Anacardiaceae; U.S. Department of Agriculture: Washington, DC, USA, **1954**.

Laks, P.E.; McKaig, P.A.; Hemingway, R.W. Flavonoid biocides: Wood preservatives based on condensed tannins. Holzforschung, **1988**, 42, 299–306.

Lauri, P.; Forsell, N.; Korosuo, A.; Havlík, P.; Obersteiner, M.; Nordin, A. Impact of the 2 °C Target on Global Woody Biomass Use. For. Policy Econ. **2017**, 83, 121–130. https://doi.org/10.1016/j.forpol.2017.07.005.

Law, B. E.; Hudiburg, T. W.; Berner, L. T.; Kent, J. J.; Buotte, P. C.; Harmon, M. E. Land Use Strategies to Mitigate Climate Change in Carbon Dense Temperate Forests. Proc. Natl. Acad. Sci. U. S. A. **2018**, 115 (14), 3663–3668. https://doi.org/10.1073/pnas.1720064115.

Lei, H.; Du, G.; Wu, Z.; Xi, X.; Dong, Z. Cross–linked soy–based wood adhesives for plywood. Int. J. Adhes. Adhes. **2014**, 50, 199–203. https://doi.org/10.1016/j.ijadhadh.2014.01.026.

Lei, H.; Frazier, C. E. Curing Behavior of Melamine–Urea–Formaldehyde (MUF) Resin Adhesive. Int. J. Adhes. Adhes. **2015**, 62, 40–44. https://doi.org/10.1016/j.ijadhadh.2015.06.013.

Lei, H.; Pizzi, A.; Navarrete, P.; Rigolet, S.; Redl, A.; Wagner, A. Gluten Protein Adhesives for Wood Panels. **2010**, 24, 1583–1596. https://doi.org/10.1163/016942410X500963.

Lewandowski, I.; Bahrs, E.; Dahmen, N.; Hirth, T.; Rausch, T.; Weidtmann, A. Biobased value chains for a growing bioeconomy.GCB Bioenergy **2019**, 11, 4–8.

Lewis, S. L.; Wheeler, C. E.; Mitchard, E. T. A.; Koch, A. Restoring Natural Forests Is the Best Way to Remove Atmospheric Carbon. Nature **2019**, 568 (7750), 25–28. https://doi.org/10.1038/d41586–019–01026–8.

Li, L.; Li, Z.; Wei, Z.; Yu, W.; Cui, Y. Effect of Tannin Addition on Chromatic Characteristics, Sensory Qualities and Antioxidant Activities of Red Wines. RSC Adv. **2020**, 10 (12), 7108–7117. https://doi.org/10.1039/c9ra09846a.

Li, X.; Li, Y.; Zhong, Z.; Wang, D.; Ratto, J.A.; Sheng, K.; Sun, X.S. Mechanical and water soaking properties of medium density fiberboard with wood fiber and soybean protein adhesive. Bioresour. Technol. **2009**, 100, 3556–3562. https://doi.org/10.1016/j.biortech.2009.02.048.

Li, X.; Nicollin, A.; Pizzi, A.; Zhou, X.; Sauget, A.; Delmotte, L. Natural Tannin–Furanic Thermosetting Moulding Plastics. RSC Adv. **2013**, 3 (39), 17732–17740. https://doi.org/10.1039/c3ra43095b.

Liu, C.; Zhang, Y.; Li, X.; Luo, J.; Gao, Q.; Li, J. A high–performance bio–adhesive derived from soy protein isolate and condensed tannins. RSC Adv. **2017**, 7, 21226–21233. https://doi.org/10.1039/C7RA01210A.

Liu, Z.; Chen, M.; Xu, Y.; Zhang, J.; Huang, X.; Luo, J.; Li, J.; Shi, S. Q.; Gao, Q. Preparation of a Strong and Multiple–Function Soybean Flour Adhesive via the Construction of Tannin Microspheres with a Core–Shell Structure. Compos. Part B Eng. **2022**, 242 (February), 110114. https://doi.org/10.1016/j.compositesb.2022.110114.

Liu, Z.; Liu, T.; Jiang, H.; Zhang, X.; Li, J.; Shi, S. Q.; Gao, Q. Biomimetic Lignin–Protein Adhesive with Dynamic Covalent/Hydrogen Hybrid Networks Enables High Bonding Performance and Wood–Based Panel Recycling. Int. J. Biol. Macromol. **2022**, 214 (April), 230–240. https://doi.org/10.1016/j.ijbiomac.2022.06.042.

Lohmann, U. Holz Handbuch; DRW: Echterdingen–Leinenfelden, Germany, **2010**; pp. 46–47.

Lora, J. H.; Glasser, W. G. Recent Industrial Applications of Lignin : A Sustainable Alternative to Nonrenewable Materials. **2002**, 10 (April).

Lorenz, L.; Conner, A.; Christiansen, A. The Effect of Soy Protein Additions on the Reactivity and Formaldehyde Emission of UF Adhesive Resins. **1999**, 49 (3), 73–78.

Lu, Y.; Shi, Q. Larch Tannin Adhesive for Particleboard. Holz Roh. Werkst. **1995**, 53, 17–19.

Lubis, M.A.R.; Labib, A.; Sudarmanto; Akbar, F.; Nuryawan, A.; Antov, P.; Kristak, L.; Papadopoulos, A.N.; Pizzi, A. Influence of Lignin Content and Pressing Time on Plywood Properties Bonded with Cold–Setting Adhesive Based on Poly (Vinyl Alcohol), Lignin, and Hexamine. Polymers **2022**, 14, 2111. https://doi.org/10.3390/polym14102111.

Luckeneder, P.; Gavino, J.; Kuchernig, R.; Petutschnigg, A.; Tondi, G. Sustainable phenolic fractions as basis for furfuryl alcohol– based co–polymers and their use as wood adhesives. Polymers **2016**, 8, 396. https://doi.org/10.3390/polym8110396.

Luckeneder, P.; Gavino, J.; Kuchernig, R.; Petutschnigg, A.; Tondi, G. Sustainable Phenolic Fractions as Basis for Furfuryl Alcohol–Based Co–Polymers and Their Use as Wood Adhesives. Polymers (Basel). **2016**, 8 (11), 396. https://doi.org/10.3390/polym8110396.

Luo, J.; Luo, J.; Gao, Q.; Li, J. Effects of Heat Treatment on Wet Shear Strength of Plywood Bonded with Soybean Meal–Based Adhesive. Ind. Crops Prod. **2015**, 63, 281–286. https://doi.org/10.1016/j.indcrop.2014.09.054.

Ma, M.; Dong, S.; Hussain, M.; Zhou, W. Effects of Addition of Condensed Tannin on the Structure and Properties of Silk Fibroin Film. Polym. Int. **2017**, 66 (1), 151–159. https://doi.org/10.1002/pi.5272.

Ma, R.; Xu, Y.; Zhang, X. Catalytic Oxidation of Biorefinery Lignin to Value–Added Chemicals to Support Sustainable Biofuel Production. **2014**, 1–29. https://doi.org/10.1002/cssc.201402503.

Madhana, K.; Kanubothula, S.; Reddy, S. Amelioration of Drought–Induced Negative Responses by Elevated - CO 2 in Field Grown Short Rotation Coppice Mulberry (Morus Spp .), a Potential Bio–Energy Tree Crop. Photosynth. Res. **2017**, 132 (2), 151–164. https://doi.org/10.1007/s11120–017–0351–5.

Mahieu, A.; Vivet, A.; Poilane, C.; Leblanc, N. Performance of particleboards based on annual plant byproducts bound with bio–adhesives. Int. J. Adhes. Adhes. **2021**, 107, 102847. https://doi.org/10.1016/j.ijadhadh.2021.102847.

Maksimovíc, Z.; Maleňcíc, D.; Kovăcevíc, N. Polyphenol Contents and Antioxidant Activity of Maydis Stigma Extracts. Bioresour. Technol. **2005**, 96 (8), 873–877. https://doi.org/10.1016/j.biortech.2004.09.006.

Maloney, T. Moder Particleboard and Dry–Process Fiberboard Manufacturing; Miller Freeman: San Francisco, CA, USA, **1993**.

Mano, F. Biomimetic Approaches for Biomaterials Development; Wiley-VCH Verlag GmbH & Co. KGaA, Ed.; **2012**.

Mansouri, H.R.; Pizzi, A.; Leban, J.M. Improved Water Resistance of UF Adhesives for Plywood by Small PMDI Additions. Holz Roh–Werkst. **2006**, 64, 218–220. https://doi.org/10.1007/s00107–005–0046–z.

Mansouri, N. El; Salvad, J. Structural Characterization of Technical Lignins for the Production of Adhesives : Application to Lignosulfonate , Kraft , Soda–Anthraquinone , Organosolv and Ethanol Process Lignins. **2006**, 24, 8–16. https://doi.org/10.1016/j.indcrop.2005.10.002.

Margarida Martins, M.; Carvalheiro, F.; Gírio, F. An overview of lignin pathways of valorization: From isolation to refining and conversion into value–added products. Biomass Convers. Biorefinery **2022**, 1–25. https://doi.org/10.1007/s13399–022–02701–z.

Marketsandmarkets. Available online: https://www.marketsandmarkets.com/Market–Reports/bioadhesive–market–16386893.html (accessed on 27 May 2022).

Martinez de Yuso, A.; Lagel, M.C.; Pizzi, A.; Fierro, V.; Celzard, A. Structure and properties of rigid foams derived from quebracho tannin. Mater. Des. **2014**, 63, 208–212.

Martinez, S. Inhibitory Mechanism of Mimosa Tannin Using Molecular Modeling and Substitutional Adsorption Isotherms. Mater. Chem. Phys**.** **2003**, 77 (1), 97–102. https://doi.org/10.1016/S0254–0584(01)00569–7.

Masina, N.; Choonara, Y. E.; Kumar, P.; Toit, L. C.; Govender, M.; Indermun, S.; Pillay, V. A Review of the Chemical Modification Techniques of Starch. Carbohydr. Polym. **2016.** https://doi.org/10.1016/j.carbpol.2016.09.094.

McDevitt, J. E.; Grigsby, W. J. Life Cycle Assessment of Bio– and Petro–Chemical Adhesives Used in Fiberboard Production. J. Polym. Environ. **2014**, 22 (4), 537–544. https://doi.org/10.1007/s10924–014–0677–4.

McKillip,W.J. Chemistry of furan polymers. Adhes. Renew. Resour. **1989**, 408–423.

Michel, J.; Jourdes, M.; Silva, M. A.; Giordanengo, T.; Mourey, N.; Teissedre, P. L. Impact of Concentration of Ellagitannins in Oak Wood on Their Levels and Organoleptic Influence in Red Wine. J. Agric. Food Chem. **2011**, 59 (10), 5677–5683. https://doi.org/10.1021/jf200275w.

Missio, A.; Tischer, B.; Dos Santos, P. Analytical Characterization of Purified Mimosa (Acacia Mearnsii) Industrial Tannin Extract: Single and Sequential Fractionation | Elsevier Enhanced Reader. Sep. Purif. Technol. **2017**, No. 186, 218–225.

Mohamad, N.; Abd–Talib, N.; Kelly Yong, T.L. Furfural Production from Oil Palm Frond (OPF) under Subcritical Ethanol Conditions. Mater. Today Proc. **2020**, 31, 116–121. https://doi.org/10.1016/j.matpr.2020.01.256.

Molino, S.; Fernández–Miyakawa, M.; Giovando, S.; Rufián–Henares, J. Á. Study of Antioxidant Capacity and Metabolization of Quebracho and Chestnut Tannins through in Vitro Gastrointestinal Digestion–Fermentation. J. Funct. Foods **2018**, 49 (July), 188–195. https://doi.org/10.1016/j.jff.2018.07.056.

Moncaster, A.M.; Pomponi, F.; Symons, K.E.; Guthrie, P.M. Why Method Matters: Temporal, Spatial and Physical Variations in LCA and Their Impact on Choice of Structural System. Energy Build. **2018**, 173, 389–398. https://doi.org/10.1016/j.enbuild.2018.05.039.

Moubarik, A.; Allal, A.; Pizzi, A. P. Characterization of a Formaldehyde–Free Cornstarch–Tannin Wood Adhesive for Interior Plywood Journal: Eur. J. Wood Wood Prod. **2010**, 68 (4), 427–433. https://doi.org/10.1007/s00107–009–0379–0.

Moubarik, A.; Causse, N.; Poumadere, T.; Allal, A. Shear Refinement of Formaldehyde–Free Corn Starch and Mimosa Tannin (Acacia Mearnsii) Wood Adhesives. J. Adhes. Sci. Technol. **2011**, 2, 1–13. https://doi.org/10.1163/016942411X576176.

Moubarik, A.; Charrier, B.; Alla0l, A.; Charrier, F.; Pizzi, A. Development and optimization of a new formaldehyde–free cornstarch and tannin wood adhesive. Eur. J. Wood Wood Prod. **2009**, 68, 167–177.

Moubarik, A.; Pizzi, A.; Allal, A.; Charrier, F.; Charrier, B. Cornstarch and Tannin in Phenol–Formaldehyde Resins for Plywood Production. Ind. Crops Prod. **2009**, 30 (2), 188–193. https://doi.org/10.1016/j.indcrop.2009.03.005.

Moubarik, A.; Pizzi, A.; Allal, A.; Charrier, F.; Charrier, B. Cornstarch and tannin in phenol–formaldehyde resins for plywood production. Ind. Crops Prod. **2009**, 30, 188–193.

Muller–Harvey, I. Analysis of Hydrolizable Tannins. Anim. Feed Sci. Technol. **2001**, 91, 3–20.

Myers, G. E. 13C NMR Study of Curing in Furfuryl Alcohol Resins. Macromolecules **1984**, 17, 1087–1090.

Nabuurs, G.; Delacote, P.; Ellison, D.; Hanewinkel, M.; Hetemäki, L.; Lindner, M. By 2050 the Mitigation Effects of EU Forests Could Nearly Double through Climate Smart Forestry. Forests **2017**, 8 (12), 484. https://doi.org/https://doi.org/10.3390/f8120484.

Nabuurs, G.; Delacote, P.; Ellison, D.; Hanewinkel, M.; Lindner, M.; Nesbit, M.; Ollikainen, M.; Savaresi, A. A New Role for Forests and the Forest Sector in the EU Post–2020 Climate Targets. From Science to Policy 2.; **2015**. https://doi.org/https://doi.org/10.36333/fs02.

Naudts, K.; Chen, Y.; McGrath, M. J.; Ryder, J.; Valade, A.; Otto, J.; Luyssaert, S. Europe's Forest Management Did Not Mitigate Climate Warming. Science. **2016**, 351 (6273), 597–601.

Navarrete, P.; Pizzi, A.; Pasch, H.; Rode, K.; Delmotte, L. Characterization of Two Maritime Pine Tannins as Wood Adhesives. J. Adhes. Sci. Technol. **2013**, 27 (22), 2462–2479. https://doi.org/10.1080/01694243.2013.787515.

Navarrete, P.; Pizzi, A.; Pasch, H.; Rode, K.; Delmotte, L. Characterization of Two Maritime Pine Tannins as Wood Adhesives. J. Adhes. Sci. Technol. **2013**, 27, 2462–2479. https://doi.org/10.1080/01694243.2013.787515.

Navarrete, P.; Pizzi, A.; Pasch, H.; Rode, K.; Delmotte, L. MALDI–TOF and 13C NMR Characterization of Maritime Pine Industrial Tannin Extract. Ind. Crops Prod. **2010**, 32 (2), 105–110. https://doi.org/10.1016/j.indcrop.2010.03.010.

Navarrete, P.; Pizzi, A.; Tapin–Lingua, S.; Benjelloun–Mlayah, B.; Pasch, H.; Rode, K.; Delmotte, L.; Rigolet, S. Low Formaldehyde Emitting Biobased Wood Adhesives Manufactured from Mixtures of Tannin and Glyoxylated Lignin. J. Adhes. Sci. Technol. **2012,** 26, 1667–1684. https://doi.org/10.1163/156856111X618489.

Nguyen, T. P.; Nguyen, Q. V.; Nguyen, V.; Le, T.; Le, Q. Van. Silk Fibroin–Based Biomaterials for Biomedical. Polymers (Basel). **2019**, 11, 1–25. https://doi.org/doi:10.3390/polym11121933.

Nicollin, A.; Kueny, R.; Toniazzo, L.; Pizzi, A. High density biocomposite from natural fibers and tannin resin. J. Adhes. Sci. Technol. **2012**, 26, 1537–1545.

Nie, Y. of different duration of acid hydrolisi on the properties starch based wood adhesive. pdfna.; Tian, X.; Liu, Y.; Wu, K.; Wang, J. Research on Starch– g –Polyvinyl Acetate and Epoxy Resin–Modified Corn Starch Adhesive. Polym. Compos. **2013**, 87. https://doi.org/10.1002/pc.

Niemz, P. Physik des Holzes und der Holzwerkstoffe; DRW Verlag Weinbrenner: Leinfelden–Echterdingen, Germany, **1993**.

Ningsi, D.W.; Suhasman; Saad, S. Characteristic of Chitosan Adhesive from Shell Shrimp Litopenaeus vannamei and Their Application for Producing Particleboard. IOP Conf. Ser. Mater. Sci. Eng. **2019**, 593, 012015. https://doi.org/10.1088/1757– 899X/593/1/012015.

Noël, M.; Mougel, E.; Fredon, E.; Masson, D.; Masson, E. Lactic acid/wood–based composite material. Part 2: Physical and mechanical performance. Bioresour. Technol. **2009,** 100, 4717–4722.

Noll, M.; Buettner, C.; Lasota, S. Copper containing wood preservatives shifted bacterial and fungal community compositions in pine sapwood in two field sites. Int. Biodeterior. Biodegrad. **2019**, 142, 26–35.

Nordqvist, P.; Khabbaz, F.; Malmstr, E. Comparing Bond Strength and Water Resistance of Alkali–Modified Soy Protein Isolate and Wheat Gluten Adhesives. **2010**, 30, 72–79. https://doi.org/10.1016/j.ijadhadh.2009.09.002.

Nordqvist, P.; Nordgren, N.; Khabbaz, F.; Malmström, E. Plant Proteins as Wood Adhesives : Bonding Performance at the Macro– and Nanoscale. Ind. Crop. Prod. **2013**, 44, 246–252. https://doi.org/10.1016/j.indcrop.2012.11.021.

Oktay, S.; Kızılcan, N.; Bengü, B. Development of Bio–Based Cornstarch—Mimosa Tannin—Sugar Adhesive for Interior Particle– board Production. Ind. Crops Prod. **2021**, 170, 113689. https://doi.org/10.1016/j.indcrop.2021.113689.

Olivares, M.; Guzmán, J.A.; Natho, A.; Saavedra, A. Kraft lignin utilization in adhesives. Wood Sci. Technol. **1988**, 22, 157–165. https://doi.org/10.1007/BF00355851.

Oliver, C. D.; Nassar, N. T.; Lippke, B. R.; McCarter, J. B. Carbon, Fossil Fuel, and Biodiversity Mitigation With Wood and Forests. J. Sustain. For. **2014**, 33 (3), 248–275. https://doi.org/10.1080/10549811.2013.839386.

Osuri, A. M.; Gopal, A.; Raman, T. R. S.; Defries, R.; Cook–Patton, S. C.; Naeem, S. Greater Stability of Carbon Capture in Species–Rich Natural Forests Compared to Species–Poor Plantations. Environ. Res. Lett. **2020**, 15, 034011. https://doi.org/10.1088/1748–9326/ab5f75.

Ou, X.; Xue, B.; Lao, Y.; Wutthinitikornkit, Y.; Tian, R.; Zou, A.; Yang, L.; Wang, W.; Cao, Y.; Li, J. Structure and Sequence Features of Mussel Adhesive Protein Lead to Its Salt–Tolerant Adhesion Ability. **2020**, 6, 1–12.

Özacar, M.; Soykan, C.; Şengil, I. A. Studies on Synthesis, Characterization, and Metal Adsorption of Mimosa and Valonia Tannin Resins. J. Appl. Polym. Sci. **2006**, 102 (1), 786–797. https://doi.org/10.1002/app.23944.

Paiva, N. T.; Henriques, A.; Cruz, P.; Ferra, J.; Carvalho, L. Production of Melamine Fortified Urea–Formaldehyde Resins with Low Formaldehyde Emission. J. Appl. Polym. Sci. **2012**, 124, 2311–2317.

Pang, H.; Zhao, S.; Mo, L.; Wang, Z.; Zhang, W.; Huang, A.; Zhang, S.; Li, J. Mussel–Inspired Bio–Based Water–Resistant Soy Adhesives with Low–Cost Dopamine Analogue–Modified Silkworm Silk Fiber. J. Appl. Polym. Sci**. 2020**, 137 (23), 1–10. https://doi.org/10.1002/app.48785.

Panzella, L.; Moccia, F.; Toscanesi, M.; Trifuoggi, M.; Giovando, S.; Napolitano, A. Exhausted Woods from Tannin Extraction as an Unexplored Waste Biomass: Evaluation of the Antioxidant and Pollutant Adsorption Properties and Activating e Ects of Hydrolytic Treatments. Antioxidants **2019**, 8 (4), 10–14. https://doi.org/10.3390/antiox8040084.

Parker, M.; Smith, P.A.; Birse, M.; Francis, I.L.; Kwiatkowski, M.J.; Lattey, K.A.; Liebich, B.; Herderich, M.J.B. The effect of post–ferment additions of grape derived tannin on Shiraz wine sensory properties and phenolic composition. Aust. J. Grape Wine Res. **2007**, 13, 30–37.

Patel, A. R.; Velikov, K. P. Zein as a Source of Functional Colloidal Nano– and Microstructures. Curr. Opin. Colloid Interface Sci. **2014**, 19 (5), 450–458. https://doi.org/10.1016/j.cocis.2014.08.001.

Patel, D. S.; Toliwal, S. D.; Patel, J. V. Eco–Friendly Adhesives Based on Tannin and N,N–Bis(2–Hydroxy–Ethyl) Fatty Amides (HEFAs) from Non–Traditional Oils for Wood Bonding. J. Adhes. Sci. Technol. **2012**, 26 (18–19), 2217–2227. https://doi.org/10.1163/156856111X610144.

Paul, G.B.; Timar, M.C.; Zeleniuc, O.; Lunguleasa, A.; Coșereanu, C. Mechanical properties and formaldehyde release of particleboard made with lignin–based adhesives. Appl. Sci. **2021**, 11, 8720. https://doi.org/10.3390/app11188720.

Pei, S.; van de Lindt, J. W.; Popovski, M.; Berman, J. W.; Dolan, J. D.; Ricles, J.; Sause, R.; Blomgren, H.; Rammer, D. R. Cross–Laminated Timber for Seismic Regions: Progress and Challenges for Research and Implementation. J. Struct. Eng. **2016**, 142 (4), 1–11. https://doi.org/10.1061/(asce)st.1943–541x.0001192.

Peng, Y.; Wang, Y.; Zhang, R.; Wang, W.; Cao, J. Improvement of wood against UV weathering and decay by using plant origin substances: Tannin acid and tung oil. Ind. Crops Prod. **2021**, 168, 113606.

Petinarakis, J. H.; Kavvouras, P. K. Technological Factors Affecting the Emission of Formaldehyde from Particleboards. Wood Res. **2006,** 51 (1), 31–40.

Pfriem, A.; Dietrich, T.; Buchelt, B. Furfuryl Alcohol Impregnation for Improved Plasticization and Fixation during the Densification of Wood. Holzforschung **2012**, 66 (2), 215–218. https://doi.org/10.1515/HF.2011.134.

Philp, J.C.; Ritchie, R.J.; Guy, K. Biobased plastics in a bioeconomy. Trends Biotechnol. **2013**, 31, 65–67.

Pichelin, F.; Kamoun, C.; Pizzi, A. Hexamine hardener behaviour: Effects on wood glueing, tannin and other wood adhesives. Holz Als Roh–Und Werkst. **1999**, 57, 305–317.

Pichelin, F.; Nakatani, M.; Pizzi, A.; Wieland, S.; Despres, A.; Rigolet, S. Structural Beams from Thick Wood Panels Bonded Industrially with Formaldehyde–Free Tannin Adhesives. For. Prod. J. **2006**, 56 (5), 31–36.

Pierobon, F.; Huang, M.; Simonen, K.; Ganguly, I. Environmental Benefits of Using Hybrid CLT Structure in Midrise Non–Residential Construction: An LCA Based Comparative Case Study in the U.S. Pacific Northwest. *J. Build. Eng.* **2019**, *26*, 100862. https://doi.org/10.1016/j.jobe.2019.100862.

Pierobon, F.; Zanetti, M.; Grigolato, S.; Sgarbossa, A.; Anfodillo, T.; Cavalli, R. Life Cycle Environmental Impact of Firewood Production – A Case Study in Italy. *Appl. Energy* **2015**, *150*, 185–195. https://doi.org/10.1016/j.apenergy.2015.04.033.

Ping, L.; Pizzi, A.; Guo, Z. D.; Brosse, N. Condensed Tannins from Grape Pomace: Characterization by FTIR and MALDI TOF and Production of Environment Friendly Wood Adhesive. Ind. Crop. Prod. **2012**, 40, 13–20. https://doi.org/https://doi.org/10.1016/j.indcrop.2012.02.039.

Pizzi, A. Advanced Wood Adhesives Technology, 1st ed.; CRC Press: New York, NY, USA, 1994; p. 289.

Pizzi, A. Condensed tannins for adhesives. Ind. Eng. Chem. Prod. Res. Dev. 1982, 21, 359–369.

Pizzi, A. Hardening Mechanism of Tannin Adhesives with Hexamine. Eur. J. Wood Ind. **1994**, 52, 229–229. https://doi.org/10.1007/BF02619098.

Pizzi, A. Natural Phenolic Adhesives I: Tannin. In Handbook of adhesive technology 2; Marcel Dekker Madison, Ed.; 2003; pp 573–589.

Pizzi, A. P. Industrial Application of Wattle Tannin/Urea–Formaldehyde Fortified Starch Adhesives for Damp–Proof Corrugated Cardboard. Holzforsch. und Holzverwertung. **1979**, 6, 131–133.

Pizzi, A. Polyflavonoid Tannins Self– Condensation Adhesives For. **2009**, 85 (2–3), 57–68. https://doi.org/10.1080/00218460902781917.

Pizzi, A. Recent Developments in Eco–Efficient Bio–Based Adhesives for Wood Bonding : Opportunities and Issues. J. Adhes. Sci. Technol. **2012**, No. December, 37–41.

Pizzi, A. Recent Developments in Eco–Efficient Bio–Based Adhesives for Wood Bonding: Opportunities and Issues. J. Adhes. Sci. Technol. **2006**, 20, 829–846. https://doi.org/10.1163/156856106777638635.

Pizzi, A. Tannin–based adhesives. J. Macromol. Sci. Rev. Macromol. Chem. **1980**, 18, 247–315.

Pizzi, A. Tannins: Prospectives and Actual Industrial Applications. Biomolecules **2019**, 9 (8) 344. https://doi.org/10.3390/biom9080344.

Pizzi, A. The Chemistry and Development of Tannin/Urea–Formaldehyde Condensates for Exterior Wood Adhesives. J. Appl. Polym. Sci. **1979**, 23, 2777–2792. https://doi.org/10.1002/app.1979.070230922.

Pizzi, A. Wood Products and Green Chemistry. Ann. For. Sci. **2016**, 73 (1), 185–203. https://doi.org/10.1007/s13595–014–0448–3.

Pizzi, A.; Inrae, E. A.; Aiguillettes, B. Little Secrets for the Successful Industrial Use of Tannin Adhesives : A Review**. 2023**. https://doi.org/10.32604/jrm.2023.030930.

Pizzi, A.; Mittal, K.L. Handbook of Adhesive Technology, 3rd ed.; CRC Press: Boca Raton, FL, USA, **2017**; pp. 223–262. https://doi.org/10.1201/9781315120942.

Pizzi, A.; Papadopoulos, A. N.; Policardi, F. Wood Composites and Their Polymer Binders. Polymers (Basel). **2020**, 12 (5). https://doi.org/10.3390/POLYM12051115.

Pizzi, A.; Roux, D. G. The Chemistry and Development of Tannin–Based Weather–Proof and Boil–Proof Cold–Setting and Fast–Setting Adhesives for Wood. J. Appl. Polym. Sci. **1978**, 22 (7), 1945–1954.

Pizzi, A.; Scharfetter, H.O. The Chemistry and Development of Tannin–based Adhesives for Exterior Plywood. J. Appl. Polym. Sci. **1978**, 22, 1745–1761. https://doi.org/10.1002/app.1978.070220623.

Pizzi, A.; Simon, C.; George, B.; Perrin, D.; Triboulot, M.C. Tannin antioxidant characteristics in leather versus leather light stability: Models. J. Appl. Polym. Sci. **2004**, 91, 1030–1040.

Pizzi, A.; Stephanou, A. Fast vs. Slow–Reacting Non–Modified Tannin Extracts for Exterior Particleboard Adhesives. **1994**, 52, 218–222. https://doi.org/https://doi.org/10.1007/BF02619095.

Pizzi, A.; Tekely, P. Mechanism of polyphenolic tannin resin hardening by hexamethylenetetramine: CP–MAS 13C–NMR. J. Appl. Polym. Sci. **1995**, 56, 1645–1650.

Pizzi, A.; Valenzuela, J.; Westermeyer, C. Low Formaldehyde Emission, Fast Pres– Sing, Pine and Pecan Tannin Adhesives for Exterior Particleboard. Holz Roh. Werkst. **1994**, 52, 311–315.

Pizzi. Wood Adhesives: Chemistry and Technology. Marcel Dekker New York, NY, USA 1983.

Prasittisopin, L.; Li, K. A new method of making particleboard with a formaldehyde–free soy–based adhesive. Compos. Part A Appl. Sci. Manuf. **2010**, 41, 1447–1453. https://doi.org/10.1016/j.compositesa.2010.06.006.

PRé Consultants (2015) SimaPro 9.5 [Computer Software]. PRé Consultants, The Netherlands.

Prendin, A.L.; Normand, S.; Carrer, M.; Bjerregaard Pedersen, N.; Matthiesen, H.; Westergaard–Nielsen, A.; Hollesen, J. Influences of summer warming and nutrient availability on Salix glauca L. growth in Greenland along an ice to sea gradient. Sci. Rep. **2022**, 12, 3077.

Qi, G.; Li, N.; Wang, D.; Sun, X. S. Physicochemical Properties of Soy Protein Adhesives Obtained by In Situ Sodium Bisulfite Modification During Acid Precipitation. **2012**, 301–312. https://doi.org/10.1007/s11746–011–1909–6.

Qiao, Z.; Gu, J.; Lv, S.; Cao, J.; Tan, H.; Zhang, Y. Preparation and Properties of Normal Temperature Cured Starch–Based Wood Adhesive. BioResources **2016**, 11 (2), 4839–4849. https://doi.org/10.15376/biores.11.2.4839–4849.

Quideau, S.; Deffieux, D.; Douat–Casassus, C.; Pouységu, L. Plant polyphenols: Chemical properties, biological activities, and synthesis. Angew. Chem. Int. **2011**, 50, 586–621.

Raj, A.; Jhariya, M.K.; Yadav, D.K.; Banerjee, A. (Eds.) Climate Change and Agroforestry Systems: Adaptation and Mitigation Strategies; CRC Press: Boca Raton, FL, USA, 2020.

Rajagopalan, N.; Bilec, M. M.; Landis, A. E. Life Cycle Assessment Evaluation of Green Product Labeling Systems for Residential Construction. **2012**, 17, 753–763. https://doi.org/10.1007/s11367–012–0416–9.

Raydan, N. D. V.; Leroyer, L.; Charrier, B.; Robles, E. Recent Advances on the Development of Protein–Based Adhesives for Wood Composite Materials—a Review. Molecules **2021**, 26 (24), 7617. https://doi.org/10.3390/molecules26247617.

Réh, R.; Krišťák, Ľ.; Sedliacˇik, J.; Bekhta, P.; Božiková, M.; Kunecová, D.; Vozárová, V.; Tudor, E.M.; Antov, P.; Savov, V. Utilization of Birch Bark as an Eco–Friendly Filler in Urea–Formaldehyde Adhesives for Plywood Manufacturing. Polymers **2021**, 13, 511. https://doi.org/10.3390/polym13040511.

Reinprecht, L. Wood Deterioration, Protection and Maintenance; John Wiley & Sons: Hoboken, NJ, USA, 2016.

Ricci, A.; Olejar, K.J.; Parpinello, G.P.; Kilmartin, P.A.; Versari, A. Application of Fourier Transform Infrared (FTIR) Spectroscopy in the Characterization of Tannins. Appl. Spectrosc. Rev. **2015,** 50, 407–442. https://doi.org/10.1080/05704928.2014.1000461.

Rinaldi, A.; Moio, L. Effect of Enological Tannin Addition on Astringency Subqualities and Phenolic Content of Red Wines. J. Sens. Stud. **2018**, 33 (3), 1–11. https://doi.org/10.1111/joss.12325.

Romppanen, S. The LULUCF Regulation : The New Role of Land and Forests in the EU Climate and Policy Framework. J. Energy Nat. Resour. Law **2020**. https://doi.org/10.1080/02646811.2020.1756622.

Rosenboom, J. G.; Langer, R.; Traverso, G. The Hidden Costs of a Plastic Planet. Nat. Rev. Mater. **2022**, 7 (2), 117–137. https://doi.org/10.1038/s41578–021–00407–8.

Rosso, M. De; Panighel, A.; Vedova, A. D.; Stella, L.; Flamini, R. Changes in Chemical Composition of a Red Wine Aged in Acacia, Cherry, Chestnut, Mulberry, and Oak Wood Barrels. J. Agric. Food Chem. **2009**, 57 (5), 1915–1920. https://doi.org/10.1021/jf803161r.

Rossouw, D. du T.; Pizzi, A.; McGillivray, G. The Kinetics of Condensation of Phenolic Polyflavonoid Tannins With Aldehydes. J. Polym. Sci. A1. **1980**, 18 (12), 3323–3343. https://doi.org/10.1002/pol.1980.170181201.

Roux, D.G. Recent advances in the chemistry and chemical utilization of the natural condensed tannins. Phytochemistry **1972**, 11, 1219–1230.

RStudio. Integrated Development Environment for R; RStudio PBC: Boston, MA, USA, 2012.

Sadat, A.; Biswas, T.; Cardoso, M. H.; Mondal, R.; Ghosh, A.; Dam, P.; Nesa, J.; Chakraborty, J.; Bhattacharjya, D.; Franco, O. L.; Gangopadhyay, D.; Mandal, A. K. Silkworm Pupae as a Future Food with Nutritional and Medicinal Benefits. Curr. Opin. Food Sci. **2022**, 44. https://doi.org/10.1016/j.cofs.2022.100818.

Sahoo, K.; Bergman, R.; Alanya–Rosenbaum, S.; Gu, H.; Liang, S. Life Cycle Assessment of Forest–Based Products: A Review. Sustain. **2019**, 11 (17), 1–30. https://doi.org/10.3390/su11174722.

Santiago–Medina, F. J.; Pizzi, A.; Abdalla, S. Hydroxymethylfurfural Hardening of Pine Tannin Wood Adhesives. J. Renew. Mater. **2017**, 5, 435–447. https://doi.org/10.7569/JRM.2017.634166.

Santoni, I.; Pizzo, B. Evaluation of Alternative Vegetable Proteins as Wood Adhesives. Ind. Crops Prod. **2013**, 45, 148–154. https://doi.org/10.1016/j.indcrop.2012.12.016.

Santos, J.; Antorrena, G.; Freire, M.S.; Pizzi, A.; González–Álvarez, J. Environmentally friendly wood adhesives based on chestnut (Castanea sativa) shell tannins. Eur. J. Wood Wood Prod. **2017**, 75, 89–100. https://doi.org/10.1007/s00107–016–1054–x.

Santos, S. C.; Costa, W. F.; Ribeiro, J. P.; Guimarães, D. O.; Ferri, P. H.; Ferreira, H. D.; Seraphin, J. C. Tannin Composition of Barbatimão Species. Fitoterapia **2002**, 73 (4), 292–299. https://doi.org/10.1016/S0367–326X(02)00081–3.

Sartori, C. J.; Mota, G. S.; Miranda, I.; Mori, F. A.; Pereira, H. Tannin Extraction and Characterization of Polar Extracts from the Barks of Two Eucalyptus Urophylla Hybrids. BioResources **2019**, 13 (3), 4820–4831. https://doi.org/10.15376/biores.13.3.4820–4831.

Sathre, R.; Connor, J. O. Meta–Analysis of Greenhouse Gas Displacement Factors of Wood Product Substitution. Environ. Sci. Policy **2010**, 13 (2), 104–114. https://doi.org/10.1016/j.envsci.2009.12.005.

Schwanninger, M.; Rodrigues, J. C.; Pereira, H.; Hinterstoisser, B. Effects of Short–Time Vibratory Ball Milling on the Shape of FT–IR Spectra of Wood and Cellulose. Vib. Spectrosc. **2004**, 36 (1), 23–40. https://doi.org/10.1016/j.vibspec.2004.02.003.

Science, W. M.; Kristak, L.; Antov, P.; Bekhta, P. Recent Progress in Ultra–Low Formaldehyde Emitting Adhesive Systems and Formaldehyde Scavengers in Wood–Based Panels : A Review. Wood Mater. Sci. Eng. **2023**, 18 (2), 763–782. https://doi.org/10.1080/17480272.2022.2056080.

Sealy–Fisher, V. J.; Pizzi, A. Increased Pine Tannins Extraction and Wood Adhesives Development by Phlobaphenes Minimization. Holz als Roh– und Werkst. **1992**, 50 (5), 212–220. https://doi.org/10.1007/BF02663290.

Sedliacˇik, J.; Bekhta, P.; Potapova, O. Technology of Low–Temperature Production of Plywood Bonded with Modified Phenol– Formaldehyde Resin. Wood Res. **2010**, 55, 123–130.

Sen, S.; Tascioglu, C.; Tırak, K. Fixation, leachability, and decay resistance of wood treated with some commercial extracts and wood preservative salts. Int. Biodeterior. Biodegrad. **2009**, 63, 135–141.

Seppepere, T.; Hernandez–Ramos, F.; Labidi, J.; Oostingh, G.J.; Bogner, B.; Petutschnigg, A.; Tondi, G. Purification of industrial tannin extract through simple solid–liquid extractions. Ind. Crop. Prod. **2019**, 139, 111502.

Sepperer, T.; Neubauer, J.; Eckardt, J.; Schnabel, T.; Petutschnigg, A.; Tondi, G. Pollutant Absorption as a Possible End–of–Life Solution for Polyphenolic Polymers. Polymers (Basel). **2019**, 11, 911. https://doi.org/10.3390/polym11050911.

Sgarbossa, A.; Boschiero, M.; Pierobon, F.; Cavalli, R.; Zanetti, M. Comparative Life Cycle Assessment of Bioenergy Production from Differentwood Pellet Supply Chains. Forests **2020**, 11, 1127. https://doi.org/10.3390/f11111127.

Shirmohammadli, Y.; Efhamisisi, D.; Pizzi, A. Tannins as a Sustainable Raw Material for Green Chemistry: A Review. Ind. Crops Prod. **2018**, 126, 316–332. https://doi.org/10.1016/j.indcrop.2018.10.034.

Shukla, S.R.; Zhang, J.; Kamdem, D.P. Pressure treatment of rubberwood (Heavea brasiliensis) with waterborne micronized copper azole: Effects on retention, copper leaching, decay resistance and mechanical properties. Constr. Build. Mater. **2019**, 216, 576–587.

Singh, A.; Yadav, R.K.; Srivastava, A. Synthesis of resole–type phenolic beads from phenol and formaldehyde by suspension polymerization technique. J. Appl. Polym. Sci. **2009**, 112, 1005–1011.

Singleton, V. L.; Orthofer, R.; Lamuela–Raventos, R. M. Analysis of Total Phenols and Other Oxidation Substrates and Antioxidants by Means of Folin–Ciocalteu Reagent. Methods Enzymol. **1999**, 299, 152–178. https://doi.org/10.1016/j.scienta.2016.11.004.

Söderholm, P. The Green Economy Transition: The Challenges of Technological Change for Sustainability. Sustain. Earth **2020**, 3 (1), 6. https://doi.org/10.1186/s42055–020–00029–y.

Soimakallio, S.; Böttcher, H.; Niemi, J.; Mosley, F.; Turunen, S.; Hennenberg, K. J.; Reise, J.; Fehrenbach, H. Closing an Open Balance: The Impact of Increased Tree Harvest on Forest Carbon. GCB Bioenergy **2022**, 14 (8), 989–1000. https://doi.org/10.1111/gcbb.12981.

Solt, P.; Konnerth, J.; Gindl–Altmutter, W.; Kantner, W.; Moser, J.; Mitter, R.; van Herwijnen, H.W.G. Technological performance of formaldehyde–free adhesive alternatives for particleboard industry. Int. J. Adhes. Adhes. **2019**, 94, 99–131.

Sommerauer, L.; Thevenon, M. F.; Petutschnigg, A.; Tondi, G. Effect of Hardening Parameters of Wood Preservatives Based on Tannin Copolymers. Holzforschung **2019**, 73 (5), 457–467. https://doi.org/10.1515/hf–2018–0130.

Soto, R.; Freer, J.; Baeza, J. Evidence of Chemical Reactions between Di– and Poly–Glycidyl Ether Resins and Tannins Isolated from Pinus Radiata D. Don Bark. Bioresour. Technol. **2005**, 96 (1), 95–101. https://doi.org/10.1016/j.biortech.2003.05.006.

Sow, C.; Riedl, B.; Blanchet, P. UV–waterborne polyurethane–acrylate nanocomposite coatings containing alumina and silica nanoparticles for wood: Mechanical, optical, and thermal properties assessment. J. Coat. Technol. Res. **2011**, 8, 211–221.

Sowunmi, S.; Ebewele, R. O.; Conner, A. H.; River, B. H. Fortified Mangrove Tannin–Based Plywood Adhesive. J. Appl. Polym. Sci. **1996**, 62 (3), 577–584. https://doi.org/10.1002/(sici)1097–4628(19961017)62:3<577::aid–app15>3.3.co;2–x.

Spierling, S.; Knüpffer, E.; Behnsen, H.; Mudersbach, M.; Krieg, H.; Springer, S.; Albrecht, S.; Herrmann, C.; Endres, H. J. Bio–Based Plastics – A Review of Environmental, Social and Economic Impact Assessments. J. Clean. Prod. **2018**, 185, 476–491. https://doi.org/10.1016/j.jclepro.2018.03.014.

Spulle, U.; Meija, A.; Kulinš, L.; Kopeika, E.; Liepa, K.H.; Šillers, H.; Zudrags, K. Influence of Hot Pressing Technological Parameters on Plywood Bending Properties. BioResources **2021**, 16, 7550–7561.

Sreeram, K.J.; Ramasami, T. Sustaining tanning process through conservation, recovery and better utilization of chromium. Resour.Conserv. Recycl. **2003**, 38, 185–212.

Stefani, P.M.; Peña, C.; Ruseckaite, R.A.; Piter, J.C.; Mondragon, I. Processing Conditions Analysis of Eucalyptus Globulus Plywood Bonded with Resol–Tannin Adhesives. Bioresour. Technol. **2008**, 99, 5977–5980. https://doi.org/10.1016/j.biortech.2007.10.013.

Sulaiman, N.S.; Hashim, R.; Amini, M.H.M.; Sulaiman, O.; Hiziroglu, S. Evaluation of the properties of particleboard made using oil palm starch modified with epichlorohydrin. BioResources **2013**, 8, 283–301. https://doi.org/10.15376/biores.8.1.283–301.

Swenberg, J. A.; Moeller, B. C.; Lu, K.; Rager, J. E.; Fry, R. C.; Starr, T. B. Formaldehyde Carcinogenicity Research: 30 Years and Counting for Mode of Action, Epidemiology, and Cancerrisk Assessment. Toxicol. Pathol. **2012**, 00, 1–9. https://doi.org/10.1177/0192623312466459.

Sylvi, D.; Ismed, I.; Merlin, S. Characteristics of Mangium (Acacia Mangium) Bark Extract with Some Extraction Time and Its Application to Cotton Fabric Dyeing. EKSAKTA **2022**, 23 (04), 329–342. https://doi.org/https://doi.org/10.24036/eksakta/vol23–iss04/362.

Szczurek, A.; Fierro, V.; Thébault, M.; Pizzi, A.; Celzard, A. Structure and Properties of Poly(Furfuryl Alcohol)–Tannin PolyHIPEs. Eur. Polym. J. **2016**, 78, 195–212. https://doi.org/10.1016/j.eurpolymj.2016.03.037.

Tahir, P.; Halip, J. A.; Lee, S. H. Tannin–Based Bioresin as Adhesives. In Lignocellulose for Future Bioeconomy; **2019**; pp 109–133. https://doi.org/10.1016/B978–0–12–816354–2.00007–4.

Tarmian, A.; Zahedi Tajrishi, I.; Oladi, R.; Efhamisisi, D. Treatability of wood for pressure treatment processes: A literature review. Eur. J. Wood Wood Prod. **2020**, 78, 635–660.

Tejado, A.; Peña, C.; Labidi, J.; Echeverria, J. M.; Mondragon, I. Physico–Chemical Characterization of Lignins from Different Sources for Use in Phenol–Formaldehyde Resin Synthesis. Bioresour. Technol. **2007**, 98 (8), 1655–1663. https://doi.org/10.1016/j.biortech.2006.05.042.

Thébault, M.; Pizzi, A.; Essawy, H. A.; Barhoum, A.; Van Assche, G. Isocyanate Free Condensed Tannin–Based Polyurethanes. Eur. Polym. J. **2015,** 67, 513–526. https://doi.org/10.1016/j.eurpolymj.2014.10.022.

Thébault, M.; Pizzi, A.; Essawy, H.A.; Barhoum, A.; Van Assche, G. Isocyanate free condensed tannin–based polyurethanes. Eur. Polym. J. **2015**, 67, 513–526.

Thébault, M.; Pizzi, A.; Santiago–Medina, F.J.; Al–Marzouki, F.M.; Abdalla, S. Isocyanate–free polyurethanes by coreaction of condensed tannins with aminated tannins. J. Renew. Mater. **2017**, 5, 21–29.

Thevenon, M.F.; Tondi, G.; Pizzi, A. High performance tannin resin–boron wood preservatives for outdoor end–uses. Eur. J. Wood Wood Prod. **2009**, 67, 89–93.

Tondi, G. Tannin–Based Copolymer Resins: Synthesis and Characterization by Solid State 13C NMR and FT–IR Spectroscopy. Polymers (Basel). **2017,** 9 (6). https://doi.org/10.3390/polym9060223.

Tondi, G.; Cefarin, N.; Sepperer, T.; D'Amico, F.; Berger, R. J. F.; Musso, M.; Birarda, G.; Reyer, A.; Schnabel, T.; Vaccari, L. Understanding the Polymerization of Polyfurfuryl Alcohol: Ring Opening and Diels–Alder Reactions. Polymers (Basel). **2019**, 11 (12), 1–15. https://doi.org/10.3390/polym11122126.

Tondi, G.; Link, M.; Kolbitsch, C.; Lesacher, R.; Petutschnigg, A. Pilot Plant Up–Scaling of Tannin Foams. Ind. Crops Prod. **2016**, 79, 211–218. https://doi.org/10.1016/j.indcrop.2015.11.013.

Tondi, G.; Palanti, S.; Wieland, S.; Thevenon, M.F.; Petutschnigg, A.; Schnabel, T. Durability of tannin–boron–treated timber. BioResources **2012**, 7, 5138–5151.

Tondi, G.; Petutschnigg, A. Middle Infrared (ATR FT–MIR) Characterization of Industrial Tannin Extracts. Ind. Crops Prod. **2015,** 65, 422–428. https://doi.org/10.1016/j.indcrop.2014.11.005.

Tondi, G.; Pizzi, A. Tannin–Based Rigid Foams: Characterization and Modification. Ind. Crops Prod. **2009**, 29 (2–3), 356–363. https://doi.org/10.1016/j.indcrop.2008.07.003.

Tondi, G.; Pizzi, A.; Olives, R. Natural Tannin–Based Rigid Foams as Insulation for Doors and Wall Panels. Maderas Cienc. y Tecnol. **2008**, 10 (3), 219–228. https://doi.org/10.4067/S0718–221X2008000300005.

Tondi, G.; Pizzi, A.; Pasch, H.; Celzard, A. Structure Degradation, Conservation and Rearrangement in the Carbonisation of Polyflavonoid Tannin/Furanic Rigid Foams – A MALDI–TOF Investigation. Polym. Degrad. Stab. **2008**, 93, 968–975. https://doi.org/10.1016/j.polymdegradstab.2008.01.024.

Tondi, G.; Schnabel, T. Bio–based polymers for engineered green materials. Polymers (Basel). **2020**, 12, 775.

Tondi, G.; Schnabel, T.; Wieland, S.; Petutschnigg, A. Surface properties of tannin treated wood during natural and artificial weathering. Int. Wood Prod. J. **2013**, 4, 150–157.

Tondi, G.; Thevenon, M. F.; Mies, B.; Standfest, G.; Petutschnigg, A.; Wieland, S. Impregnation of Scots Pine and Beech with Tannin Solutions: Effect of Viscosity and Wood Anatomy in Wood Infiltration. Wood Sci. Technol. **2013,** 47, 615–626. https://doi.org/10.1007/s00226–012–0524–5.

Tondi, G.; Wieland, S.; Wimmer, T.; Thevenon, M. F.; Pizzi, A.; Petutschnigg, A. Tannin–Boron Preservatives for Wood Buildings: Mechanical and Fire Properties. Eur. J. Wood Wood Prod. **2012**, 70 (5), 689–696. https://doi.org/10.1007/s00107–012–0603–1.

Toplak, M.; Birarda, G.; Read, S.; Sandt, C.; Rosendahl, S. M.; Vaccari, L.; Demšar, J.; Borondics, F. Infrared Orange: Connecting Hyperspectral Data with Machine Learning. Synchrotron Radiat. News **2017**, 30 (4), 40–45. https://doi.org/10.1080/08940886.2017.1338424.

Toplak, M.; Read, S. T.; Sandt, C.; Borondics, F. Quasar: Easy Machine Learning for Biospectroscopy. Cells **2021**, 10 (9), 1–10. https://doi.org/10.3390/cells10092300.

Trosa, A.; Mondovi, S. M.; Pizzi, A. Stability and Performance of Tannin–Accelerated PF Resins for Plywood. **2000**, 55 (1997), 1997.

Trosa, A.; Pizzi, A. A No–Aldehyde Emission Hardener for Tannin–Based Wood Adhesives for Exterior Panels. Holz als Roh – und Werkst. **2001**, 59 (4), 266–271. https://doi.org/10.1007/s001070100200.

UNECE/FAO. Chapter 1, Economic Overview and Policies in Forest Products – Annual Market Review 2020–2021; 2021.

United Nations. Paris Agreement to the United Nations Framework Convention on Climate Change; T.I.A.S. No. 16–1104; United Nations: San Francisco, CA, USA, 2015.

Valentini, L.; Ceccarini, M. R.; Verdejo, R.; Tondi, G.; Beccari, T. Stretchable, Bio–Compatible, Antioxidant and Self–Powering Adhesives from Soluble Silk Fibroin and Vegetal Polyphenols Exfoliated Graphite. Nanomaterials **2021**, 11 (9). https://doi.org/10.3390/nano11092352.

Valenzuela, J.; Von Leyser, E.; Pizzi, A.; Westermeyer, C.; Gorrini, B. Industrial Production of Pine Tannin–Bonded Particleboard and MDF. Eur. J. Wood Wood Prod. **2012**, 70 (5), 735–740. https://doi.org/10.1007/s00107–012–0610–2.

Valenzuela, J.; Westermeyer, C. Non–Emulsifiable, Water–Based, Mixed Diisocyanate Adhesive Systems for Exterior Plywood : Part II. Theory Application and Industrial Results. Holzforschung. **1993**, 47 (1), 68–71. https://doi.org/10.1515/hfsg.1993.47.1.68.

Vázquez, G.; Antorrena, A.; Parajó, J. C. Selection of Operational Conditions in Alkaline Lixiviation of Pinus Pinaster Bark. Holz als Roh–und Werkst. **1986**, 44 (11), 415–418. https://doi.org/10.1007/BF02609635.

Vázquez, G.; Antorrena, G.; Parajó, J. C.; Francisco, J. L. Preparation of Wood Adhesives by Polycondensation of Phenolic Acids from Pinus Pinaster Bark with Resoles. Holz als Roh– und Werkst. **1989**, 47 (12), 491–494. https://doi.org/10.1007/BF02613031.

Vázquez, G.; Fontenla, E.; Santos, J.; Freire, M. S.; González–Álvarez, J.; Antorrena, G. Antioxidant Activity and Phenolic Content of Chestnut (Castanea Sativa) Shell and Eucalyptus (Eucalyptus Globulus) Bark Extracts. Ind. Crops Prod. **2008**, 28 (3), 279–285. https://doi.org/10.1016/j.indcrop.2008.03.003.

Vázquez, G.; Pizzi, A.; Freire, M. S.; Santos, J.; Antorrena, G.; González–Álvarez, J. MALDI–TOF, HPLC–ESI–TOF and 13C–NMR Characterization of Chestnut (Castanea Sativa) Shell Tannins for Wood Adhesives. Wood Sci. Technol. **2013**, 47 (3), 523–535. https://doi.org/10.1007/s00226–012–0513–8.

Vázquez, G.; Santos, J.; Freire, M. S.; Antorrena, G.; González–Álvarez, J. DSC and DMA Study of Chestnut Shell Tannins for Their Application as Wood Adhesives without Formaldehyde Emission. J. Therm. Anal. Calorim. **2012**, 108 (2), 605–611. https://doi.org/10.1007/s10973–011–2138–9.

Vendamme, R.; Schüwer, N.; Eevers, W. Recent Synthetic Approaches and Emerging Bio–Inspired Strategies for the Development of Sustainable Pressure–Sensitive Adhesives Derived from Renewable Building Blocks. J. Appl. Polym. Sci. **2014**, 131 (17), 8379–8394. https://doi.org/10.1002/app.40669.

Vera, M.; Urbano, B.F. Tannin polymerization: An overview. Polym. Chem. **2021**, 12, 4272–4290.

Versari, A.; Du Toit, W.; Parpinello, G. P. Oenological Tannins: A Review. Aust. J. Grape Wine Res. **2013,** 19 (1), 1–10. https://doi.org/10.1111/ajgw.12002.

Vignault, A.; González–Centeno, M. R.; Pascual, O.; Gombau, J.; Jourdes, M.; Moine, V.; Iturmendi, N.; Canals, J. M.; Zamora, F.; Teissedre, P. L. Chemical Characterization, Antioxidant Properties and Oxygen Consumption Rate of 36 Commercial Oenological Tannins in a Model Wine Solution. Food Chem**. 2018**, 268, 210–219. https://doi.org/10.1016/j.foodchem.2018.06.031.

Vnučec, D.; Kutnar, A.; Goršek, A. Soy–based adhesives for wood–bonding–a review. J. Adhes. Sci. Technol. **2017**, 31, 910–931. https://doi.org/10.1080/01694243.2016.1237278.

Wang, A. Y.; Xiong, H.; Wang, Z.; Chen, L. Effects of Different Durations of Acid Hydrolysis on the Properties of Starch–Based Wood Adhesive. Int. J. Biol. Macromol. **2017**, 103, 819–828. https://doi.org/10.1016/j.ijbiomac.2017.05.102.

Wang, J.; Wu, H.; Liu, R.; Long, L.; Xu, J.; Chen, M.; Qiu, H. Preparation of a fast water–based UV cured polyurethane–acrylate wood coating and the effect of coating amount on the surface properties of oak (Quercus alba L.). Polymers **2019**, 11, 1414.

Wang, W.; Zhang, W.; Li, J. Reactivity of Larch and Valonia Tannins in Synthesis of Tannin–Formaldehyde Resins. BioResources **2016**, 11, 2256–2268. https://doi.org/10.15376/biores.11.1.2256–2268.

Wang, Y.; Wang, D.; Sun, X. S. Thermal Properties and Adhesiveness of Soy Protein Modified with Cationic Detergent. **2005**, 82 (5), 357–363.

Watrelot, A.A.; Norton, E.L. Chemistry and reactivity of tannins in vitis spp.: A review. Molecules **2020**, 25, 2110. https://doi.org/10.3390/molecules25092110.

Wawer, I.; Wolniak, M.; Paradowska, K. Solid State NMR Study of Dietary Fiber Powders from Aronia, Bilberry, Black Currant and Apple. Solid State Nucl. Magn. Reson. **2006**, 30 (2), 106–113. https://doi.org/10.1016/j.ssnmr.2006.05.001.

Wei, J.; Wei, C.; Su, L.; Fu, J.; Lv, J. Synergistic Reinforcement of Phenol–Formaldehyde Resin Composites by Poly (Hexanedithiol)/ Graphene Oxide. J. Mater. Sci. Chem. Eng. **2015**, 3, 56–70. https://doi.org/http://dx.doi.org/10.4236/msce.2015.38009.

Widsten, P.; Kandelbauer, A. Adhesion Improvement of Lignocellulosic Products by Enzymatic Pre–Treatment. **2008**, 26, 379–386. https://doi.org/10.1016/j.biotechadv.2008.04.003.

Wilts, H.; Brien, M. O. A Policy Mix for Resource Efficiency in the EU : Key Instruments , Challenges and Research Needs. Ecol. Econ. **2019,** 155, 59–69. https://doi.org/10.1016/j.ecolecon.2018.05.004.

Wong, E.D.; Zhang, M.; Wang, Q.; Kawai, S. Formation of the density profile and its effects on the properties of particleboard.Wood Sci. Technol. **1999**, 33, 327–340. https://doi.org/10.1007/s002260050119.

Xi, X.; Pizzi, A.; Frihart, C. R.; Lorenz, L.; Gerardin, C. Tannin Plywood Bioadhesives with Non–Volatile Aldehydes Generation by Specific Oxidation of Mono– and Disaccharides. Int. J. Adhes. Adhes. **2020**, 98. https://doi.org/10.1016/j.ijadhadh.2019.102499.

Xie, Y.; Fu, Q.; Wang, Q.; Xiao, Z.; Militz, H. Effects of chemical modification on the mechanical properties of wood. Eur. J. Wood Wood Prod. **2013**, 71, 401–416.

Xu, G.; Zhang, Q.; Xi, X.; Lei, H.; Cao, M.; Du, G.; Wu, Z. Tannin–Based Wood Adhesive with Good Water Resistance Crosslinked by Hexanediamine. Int. J. Biol. Macromol. **2023**, 234, 123644. https://doi.org/10.1016/j.ijbiomac.2023.123644.

Xu, Y.; Guo, L.; Zhang, H.; Zhai, H.; Ren, H. Research Status, Industrial Application Demand and Prospects of Phenolic Resin. RSC Adv. **2019**, 9, 28924–28935. https://doi.org/10.1039/c9ra06487g.

Xu, Y.; Han, Y.; Li, J.; Luo, J.; Shi, S. Q.; Li, J.; Gao, Q.; Mao, A. Research Progress of Soybean Protein Adhesive: A Review. J. Renew. Mater. **2022**, 10 (10), 2519–2541. https://doi.org/10.32604/jrm.2022.020750.

Yadav, U.S.; Kumar, H.; Mahto, V. Experimental investigation of partially hydrolysed polyacrylamide–hexamine–pyrocatechol polymer gel for permeability modification. J. Sol–Gel Sci. Technol. **2020**, 94, 335–346.

Yamaguchi, H.; Okuda, K.I. Chemically modified tannin and tannin–copper complexes as wood preservatives. Holzforschung. **1998**, 52, 596–602.

Yang, M.; Rosentrater, K. A. Life Cycle Assessment and Techno–Economic Analysis of Pressure Sensitive Bio–Adhesive Production. Energies **2019**, 12 (23). https://doi.org/10.3390/en12234502.

Yang, M.; Rosentrater, K. A. Life Cycle Assessment of Urea–Formaldehyde Adhesive and Phenol–Formaldehyde Adhesives. Environ. Process. **2020**, 7 (2), 553–561. https://doi.org/10.1007/s40710–020–00432–9.

Yao, M.; Yang, Y.; Song, J.; Yu, Y.; Jin, Y. Lignin–Based Catalysts for Chinese Fir Furfurylation to Improve Dimensional Stability and Mechanical Properties. Ind. Crops Prod. **2017**, 107 (May), 38–44. https://doi.org/10.1016/j.indcrop.2017.05.038.

Yazaki, Y.; Hillis, W. E. Molecular Size Distribution of Radiata Pine Bark Extracts and Its Effect on Properties. Holzforschung **1980**, 34 (4), 125–130. https://doi.org/10.1515/hfsg.1980.34.4.125.

Younesi–Kordkheili, H.; Pizzi, A. Ionic liquids as enhancers of urea–glyoxal panel adhesives as substitutes for urea– formaldehyde resins. Eur. J. Wood Wood Prod. **2017**, 75, 481–483. https://doi.org/10.1007/s00107–016–1116–0.

Yu, B.; Zhang, Y.; Shukla, A.; Shukla, S. S.; Dorris, K. L. The Removal of Heavy Metals from Aqueous Solutions by Sawdust Adsorption – Removal of Lead and Comparison of Its Adsorption with Copper. J. Hazard. Mater. **2001**, 84 (1), 83–94. https://doi.org/10.1016/S0304–3894(01)00198–4.

Yurtsever, M.; ¸Sengil, I.A. Biosorption of Pb (II) ions by modified quebracho tannin resin. J. Hazard Mater. **2009**, 163, 58–64.

Zanetti, M.; Causin, V.; Saini, R.; Cardin, A.; Cavalli, R. Effect of Tannin on Increasing UF Adhesive Performance at High Temperature Investigated by TMA and TGA Analysis. Eur. J. Wood Wood Prod. **2014**, 72, 385–392. https://doi.org/10.1007/s00107–014–0795–7.

Zanetti, M.; Cesprini, E.; Marangon, M.; Szczurek, A.; Tondi, G. Thermal Valorization and Elemental Composition of Industrial Tannin Extracts. Fuel **2021**, 289 (August 2020), 119907. https://doi.org/10.1016/j.fuel.2020.119907.

Zhang, J.; Long, C.; Zhang, X.; Liu, Z.; Zhang, X.; Liu, T.; Li, J.; Gao, Q. An Easy–Coating, Versatile, and Strong Soy Flour Adhesive via a Biomineralized Structure Combined with a Biomimetic Brush–like Polymer. Chem. Eng. J. **2022**, 450 (P4), 138387. https://doi.org/10.1016/j.cej.2022.138387.

Zhang, L. L.; Lin, Y. M.; Zhou, H. C.; Wei, S. D.; Chen, J. H. Condensed Tannins from Mangrove Species Kandelia Candel and Rhizophora Mangle and Their Antioxidant Activity. Molecules **2010**, 15 (1), 420–431. https://doi.org/10.3390/molecules15010420.

Zhang, Q.; Hong, J.; Zhang, T.; Tian, X.; Geng, Y.; Chen, W.; Zhai, Y.; Liu, W.; Shen, X.; Bai, Y. Environmental Footprints of Soybean Production in China. Environ. Dev. Sustain. **2023**, 25 (9), 9047–9065. https://doi.org/10.1007/s10668–022–02424–1.

Zhang, S.Y. Wood specific gravity–mechanical property relationship at species level. Wood Sci. Technol. **1997**, 31, 181–191.

Zhang, T.; Yu, C.; Yu, M.; Huang, Y.; Tan, J.; Zhang, M.; Zhu, X. Multifunctional Tannin Extract–Based Epoxy Ts Derived from Waste Bark as a Highly Toughening and Strengthening Agent for Epoxy Resin. Ind. Crop. Prod. **2022**, 176, 114255. https://doi.org/10.1016/j.indcrop.2021.114255.

Zhang, W.; Ma, Y.; Wang, C.; Li, S.; Zhang, M.; Chu, F. Preparation and Properties of Lignin – Phenol – Formaldehyde Resins Based on Different Biorefinery Residues of Agricultural Biomass. Ind. Crop. Prod. **2013**, 43, 326–333. https://doi.org/10.1016/j.indcrop.2012.07.037.

Zhang, W.; Yang, X.; Li, C.; Liang, M.; Lu, C.; Deng, Y. Mechanochemical activation of cellulose and its thermoplastic polyvinyl alcohol ecocomposites with enhanced physicochemical properties. Carbohydr. Polym. **2011**, 83, 257–263.

Zhang, Y.; Shi, R.; Xu, Y.; Chen, M.; Zhang, J.; Gao, Q.; Li, J. Developing a Stable High–Performance Soybean Meal–Based Adhesive Using a Simple High–Pressure Homogenization Technology. J. Clean. Prod. **2020**, 256, 120336. https://doi.org/10.1016/j.jclepro.2020.120336.

Zhanga, B.; Lan, K.; Harris, T.; Ashton, M.; Yao, Y. Climate–Smart Forestry through Innovative Wood Products and Commercial Afforestation and Reforestation on Marginal Land. Environ. Sci. Ecol. **2023**, 120 (23), e2221840120. https://doi.org/https://doi.org/10.1073/pnas.2221840120.

Zhao, X.; Liu, T.; Ou, R.; Hao, X.; Fan, Q.; Guo, C.; Sun, L.; Liu, Z.; Wang, Q. Fully Biobased Soy Protein Adhesives with Integrated High–Strength, Waterproof, Mildew–Resistant, and Flame–Retardant Properties. ACS Sustain. Chem. Eng. **2022**, 10 (20), 6675–6686.

Zhao, Y.; Yan, N.; Feng, M.W. Thermal degradation characteristics of phenol–formaldehyde resins derived from beetle infested pine barks. Thermochim. Acta **2013**, 555, 46–52.

Zhao, Z.; Umemura, K. Investigation of a New Natural Particleboard Adhesive Composed of Tannin and Sucrose. 2. Effect of Pressing Temperature and Time on Board Properties, and Characterization of Adhesive. BioResources **2015**, 10, 2444–2460.

Zheng, J.; Suh, S. Strategies to Reduce the Global Carbon Footprint of Plastics. Nat. Clim. Chang. **2019**, 9 (5), 374–378. https://doi.org/10.1038/s41558–019–0459–z.

Zhou, X.; Pizzi, A. Pine Tannin Based Adhesive Mixes for Plywood. Int. Wood Prod. J. **2014**, 5 (1), 27–32. https://doi.org/10.1179/2042645313Y.0000000043.

Zhou, Y.; Zeng, G.; Zhang, F.; Tang, Z.; Luo, J.; Li, K.; Li, X.; Li, J.; Shi, S. Q. Preparation of Functional Fiber Hybrid Enhanced High Strength and Multifunctional Protein Based Adhesive. Mater. Des. **2022**, 224, 111289. https://doi.org/10.1016/j.matdes.2022.111289.